Sp 1/45/v.2

NASA

SPACE SYSTEMS TECHNOLOGY MODEL

VOLUME II

Space Technology Trends and Forecasts

NEWARK PUBLIC LIBRARY
OCT 1 1980
U. S. GOVT. PUBS.
DEPOSITORY 376

May 1980

National Aeronautics and Space Administration
Office of Aeronautics and Space Technology
Code RS
NASA Headquarters
Washington, D.C. 20546

NAS 1.2:

General Introduction
Introduction to Volume II
1. Power and Electric Propulsion
Photovoltaic Energy Conversion
Space Energy Conversion and Storage
Thermal-to-Electric Energy Conversion
Power Systems
Electric Propulsion
2. Chemical Propulsion
3. Materials and Structures
4. Information Systems
Sensors
Data Processing
Communications
5. Navigation, Guidance & Control
6. Automated Operations

NASA

Space Systems Technology Model

VOLUME II: SPACE TECHNOLOGY TRENDS AND FORECASTS

May 1980

best copy available

National Aeronautics and Space Administration
Office of Aeronautics and Space Technology
Code RS
NASA Headquarters
Washington, D.C. 20546

CONTENTS

SECTION		PAGE
	GENERAL INTRODUCTION	iii
	INTRODUCTION TO VOLUME II	xv
1	POWER AND ELECTRIC PROPULSION	1-1
	1.1 Photovoltaic Energy Conversion	1-1
	1.2 Space Energy Conversion and Storage: Technical Projections	1-7
	1.3 Thermal-to-Electric Energy Conversion	1-35
	1.4 Power Systems Management and Distribution	1-50
	1.5 Electric Propulsion	1-59
2	CHEMICAL PROPULSION	2-1
3	MATERIALS AND STRUCTURES	3-1
4	INFORMATION SYSTEMS	4-1
	4.1 Sensors	4-1
	4.2 Data Processing	4-89
	4.3 Communications	4-109
5	NAVIGATION, GUIDANCE AND CONTROL	5-1
	5.1 Gyroscope	5-1
	5.2 Star Trackers	5-4
	5.3 Horizon Sensors	5-6
	5.4 Instrument Pointing Accuracy and Stability	5-8
	5.5 On-Board Estimation	5-11
6	AUTOMATED OPERATIONS	6-1
	6.1 On-Board Automation	6-1
	6.2 Automated Problem Solving	6-6
	6.3 Machine Vision	6-8

GENERAL INTRODUCTION

This document is the second issue of the Space Systems Technology Model. This issue received NASA-wide inputs and coordination; the first issue was constructed solely for OAST internal usage. This Model will be revised and published on an annual basis. It contains NASA system and program requirements, technology trends, and forecasts for space technology. The Model provides a base of information for guiding technology development for future systems and programs. It also displays the expected availability of technology improvements to enable and/or enhance future missions.

PURPOSE OF THE MODEL

The purpose of the NASA Space Systems Technology Model is to serve as a reference for: planning technology programs and options; identifying technologies required for planned and potential future missions; assessing ongoing technology programs; and providing a technology reference source for mission planning. Ascertaining technology requirements for planned and future missions assures that the focus of technology programs is coupled to the overall goals and missions of NASA.

The system technology needs and requirements presented in the Technology Model do not constitute official agency plans, but may be used in their developments. The Model is a broader menu of candidate and opportunity systems and programs for the future than current funding expectations will allow.

GENERAL DESCRIPTION

The three volumes of the Model treat systems, programs, and technology from the present to reasonable limits of projection.

Volume I contains those systems and programs which the NASA program offices endorse as being within their ten-year planning horizon.

Volume II contains trends and forecasts of space technology.

Volume III provides information about innovative systems, programs, and technology. Part A presents systems and programs which are validated by program offices, but which are either beyond the ten-year planning period or are still deemed speculative. Part B systems and programs derive from sources other than the program offices and, as such, are considered more speculative than Part A missions. Part C presents emerging technologies with little-to-no historical trend, and provides best-possible forecasts of their potential.

The information in the Model has been assembled from a variety of written and oral sources. Validated information contained in the Model has been identified by tracable, formal reference to the responsible NASA Headquarters office. The emphasis is on quantitative descriptions where possible.

The elements presented in the Model include:

1. Mission Systems. An assemblage of hardware and software, ground- or space-based, whose functions are integrated to achieve a program-level objective. Examples are Venus Orbiting Imaging Radar, Space Shuttle, and the National Oceanic Satellite System.

2. Mission Instruments. Scientific equipment for performing experimental or operational measurements which are intended for use in space. Examples are Electromagnetic Containerless Processing System, Solar Backscatter Ultraviolet Spectrometer, and Thematic Mapper.

3. Programs. Funded activities that are approved or are prospective discrete elements of the space budget. Included are: flight programs which use mission and instrument systems to conduct experiments and demonstrate capabilities in space. Examples are the Space Science Platform and the Large Space Structures System Technology and Development Plan. Investigatory programs which are nonflight specific aggregations of activities, often analytic in nature but which may contain flight elements. Examples are 30/20 GHz Wideband Communications satellite program and the National Materials Laboratory. Functional service programs which provide users with space-derived information, capabilities, or methods. An example is the Application Data Service Development program.

In summary, the items presented are the implements which NASA has or envisions to achieve the perceived goals of the civil space program. These goals are expressed in the NASA Five-Year Planning Document, published annually, and this Model serves as a supplement to the current "Five-Year Plan."

The content of the three volumes and their parts has been selected to maintain a clear distinction between different levels of planning information (see Fig. 1). The information in Volume I is for definitive programs, i.e., systems and programs which are approved, planned, or candidates for initiation within the next ten years (see Fig. 2 for definition of these categories). The information contained in Volume III, for systems and programs expected to start after ten years, can be strongly influenced by new technology. Figure 3 shows the relationship

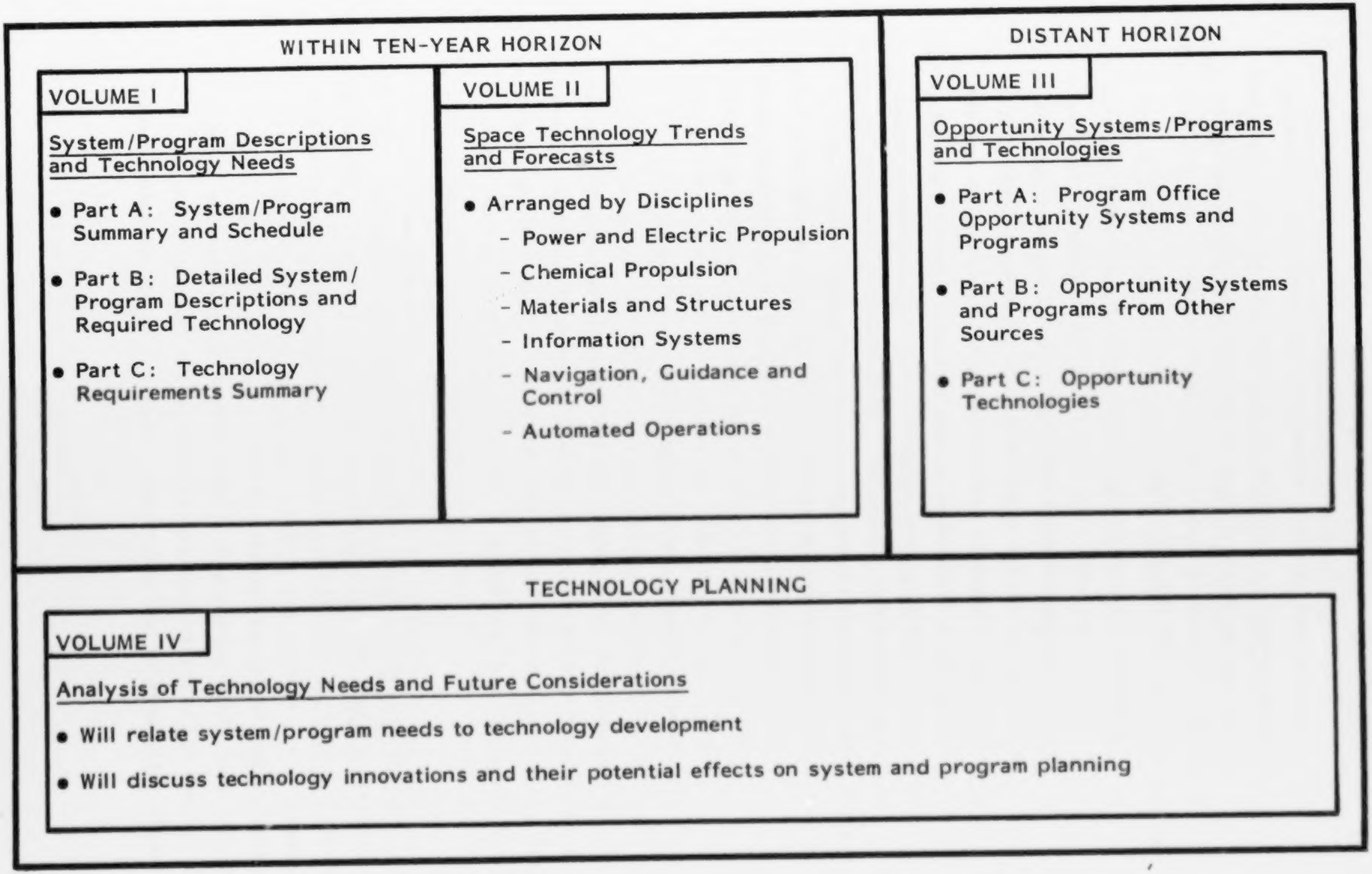

WITHIN TEN-YEAR HORIZON

VOLUME I

System/Program Descriptions and Technology Needs

- Part A: System/Program Summary and Schedule
- Part B: Detailed System/Program Descriptions and Required Technology
- Part C: Technology Requirements Summary

VOLUME II

Space Technology Trends and Forecasts

- Arranged by Disciplines
  - Power and Electric Propulsion
  - Chemical Propulsion
  - Materials and Structures
  - Information Systems
  - Navigation, Guidance and Control
  - Automated Operations

DISTANT HORIZON

VOLUME III

Opportunity Systems/Programs and Technologies

- Part A: Program Office Opportunity Systems and Programs
- Part B: Opportunity Systems and Programs from Other Sources
- Part C: Opportunity Technologies

TECHNOLOGY PLANNING

VOLUME IV

Analysis of Technology Needs and Future Considerations

- Will relate system/program needs to technology development
- Will discuss technology innovations and their potential effects on system and program planning

Figure 1. NASA Space Systems Technology Model

VOLUME I

APPROVED - A

MISSIONS WHICH HAVE BEEN FUNDED AND AUTHORIZED FOR IMPLEMENTATION.

PLANNED - P

MISSIONS DESIGNATED BY THE PROGRAM OFFICES AS POSSIBLE NEW STARTS WITHIN THE NEXT FIVE YEARS.

CANDIDATE - C

MISSIONS CONSIDERED FOR POSSIBLE INITIATION WITHIN TEN YEARS, BUT CURRENTLY NOT PLANNED AS A NEW START WITHIN THE NEXT FIVE YEARS.

VOLUME III

OPPORTUNITY - O

POTENTIAL MISSIONS FOR START BEYOND TEN YEARS AND/OR THOSE MISSIONS OF A SPECULATIVE NATURE. SUCH MISSIONS PROVIDE OPPORTUNITIES FOR TECHNOLOGY DEVELOPMENT TO SHAPE SYSTEM DESIGNS.

Figure 2. Categories of Systems and Programs

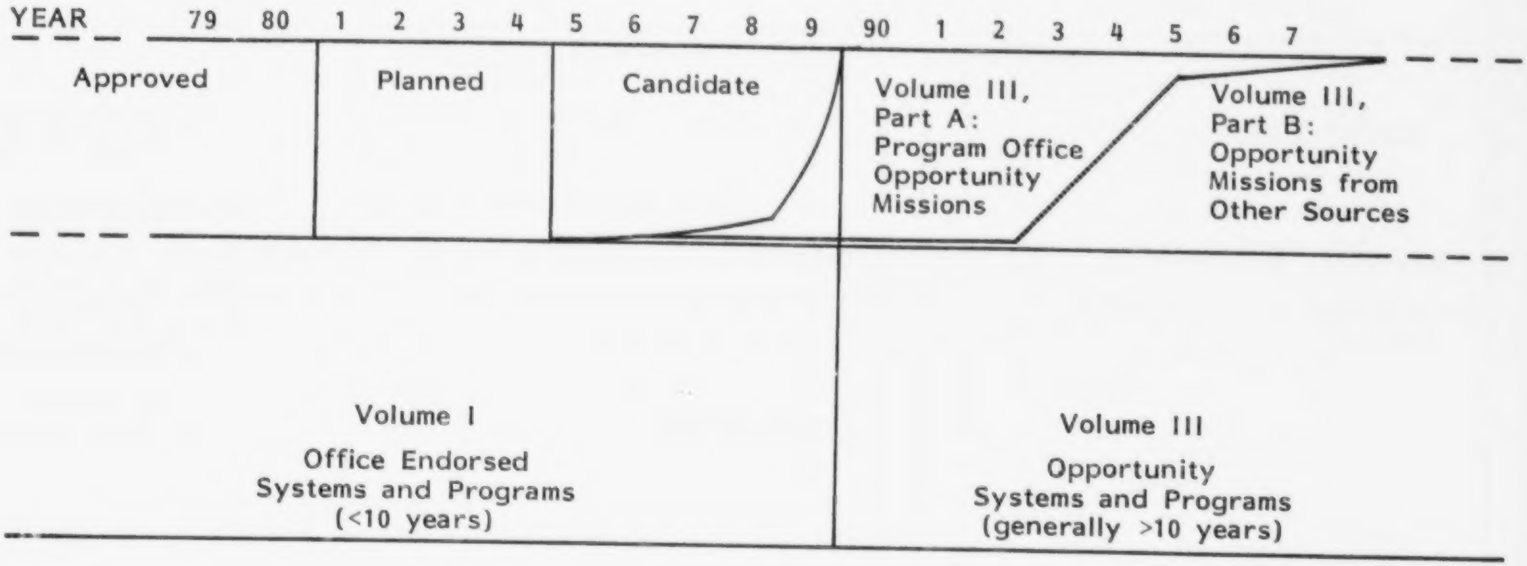
YEAR
79
80
1
2
3
4
5
6
7
8
9
90
1
2
3
4
5
6
7
Approved
Planned
Candidate
Volume III, Part A: Program Office Opportunity Missions
Volume III, Part B: Opportunity Missions from Other Sources
Volume I
Office Endorsed Systems and Programs (<10 years)
Volume III
Opportunity Systems and Programs (generally >10 years)

NOTE: Systems/programs are included in Model if flight or start is 1979 or later.

Figure 3. Model Presentation of NASA Systems and Programs

between the categories, time, and the volumes of this Model. The technology trends and forecast information has been similarly separated into two volumes. Volume II presents data for ongoing and forecastable technology developments. Volume III, Part C presents data on opportunity technologies which have no current credible system or program applications or which cannot be forecasted now.

VOLUME I

Volume I, System/Program Descriptions and Technology Needs, contains details on systems and programs endorsed by the responsible program offices for a start in the next ten years. Identification of the systems and programs and their relative time phasing was obtained from the program offices at NASA Headquarters by means of several iterated reviews over the last six months. Technical characteristics of the systems and programs were compiled to the extent available and subjected to review and validation by the responsible program offices.

The systems and programs are grouped in categories corresponding to basic NASA program areas: Planetary, Astrophysics, Solar Terrestrial, Life Sciences, Resource Observation, Global Environment, Communications, Space Transportation, Utilization of the Space Environment, and Technology Development (OAST instrument systems). They are sequenced by funding and/or development status (Fig. 2). Funded, ongoing systems and programs are designated Approved. Those identifed as possible new starts within the next five years are designated as Planned. Systems and programs identified as new starts within the present five-year plan period but considered for possible initiation within ten years are designated Candidate. Those potentially starting after ten years and/or those of a speculative nature are designated Opportunity; they are presented in Volume III.

Volume I is arranged in three parts:

Part A: System/Program Summary and Schedule

- This is a chronological list of systems and programs by program area (Planetary, Astrophysics, etc.). The list includes system/program name, status, source, start data for major effort, launch data if applicable, and primary contact for information.
- At the end of Part A, the start dates are displayed graphically by program area.

Part B: Detailed System/Program Descriptions and Required Technology

A section for each mission system or program presents technical details.

- The first page presents general information: an illustration; basic features; and narrative on objective, description, technology needs, references, and contacts.
- Following pages present technical characteristics to the extent that they are now known or relevant. A technical characteristic is generally presented as a nominal value, the degree of confidence in the value, and the state of technology readiness. Comments are provided to explain particular conditions.
- Instrument systems are presented in a format which contains name, status, carrier, physical and general properties, principal purpose and features, principal physical property measured, associated ranges and resolutions, comments, sources, and contacts. For the science programs (Planetary, Astrophysics, Solar Terrestrial, and Life Sciences) the instrument systems are not presented separately, but are grouped on a sheet with the related mission system.

Part C: Technology Requirements Summary

Values of particular technical characteristics are tabulated for all mission systems. The data are further presented versus time. Analysis of the plotted data should reveal trends in technology demanded by the aggregate of NASA mission systems and programs envisioned for the next ten years. In Volume III, Part A, the characteristics of mission systems and programs beyond ten years are added to these plots.

VOLUME II

Volume II, Space Technology Trends and Forecasts, presents data characterizing space technology developments. The present and projected status of space technology is arranged by discipline: power and electric propulsion; chemical propulsion; materials and structures, information systems; navigation, guidance and control; and automated operations. Past technology trends, state of the art, and a ten-year or more forecast of capabilities are included.

These forecasts were obtained from NASA technology development managers at Headquarters and the Centers. The technology development managers were asked to identify figures of merit for technology discipline and forecast their growth. The resulting set of forecasts in Volume II can be related in many cases to Volumes I and III system and program characteristics.

VOLUME III

Volume III, Opportunity Systems/Programs and Technologies, is divided into three parts:

- Part A: Program Office Opportunity Systems and Programs, presents technical details on systems and programs which the offices endorse but which are speculative or beyond ten years. The format is identical to Volume I, Parts B and C. These missions are called "opportunity" because there is ample time for vigorous technology development to greatly impact their form and feasibility.
- Part B: Opportunity Systems and Programs from Other Sources, presents a selection of systems and programs which cannot now be advocated by the NASA program offices for various reasons; they are too distant, too speculative in feasibility, pertinence, or utility; or too controversial.
- Part C: Opportunity Technologies, presents information on emerging technologies. Opportunity technology often provides revolutionary advances which may enable otherwise unachievable mission systems. The format is a one-page description of contacts, character, relation to mission and instrument systems and other technologies, status descriptors, and coarse forecasts.

VOLUME IV

(to be supplied at a later date)

Volume IV, Analysis of Technology Needs and Future Considerations, was to relate system and program needs to technology development and discuss technology innovations and their potential effects on mission and program planning. As of the date of this issue, Volume IV has not been produced. NASA Headquarters, supported by the Centers, is preparing technology development plans which would form the essence of this volume. Drafts of Volumes I, II, and III of the Model served as the primary basis for preparing these plans. Further evolution will lead to a presentation of technology plans in a formal Volume IV.

MODEL USE AND MAINTENANCE

The NASA Space Systems Technology Model is an outcome of the space technology program planning and implementation process. The Model is intended to be a companion to the NASA Five-Year Planning Document and will be updated annually. It is believed that the Model will improve steadily through subsequent iterations.

Requests for additional copies of the Model should be addressed to Stan Sadin, Code RS-5, NASA Headquarters, Washington, DC 20546. Comments and suggestions for additional information to be included in future updates should be sent to the same address.

ACKNOWLEDGMENTS

This Model is the product of support from many organizations and individuals. An acknowledgment of the contributors appears at the end of this volume.

William J Cuneo Jr

William J. Cuneo, Jr.
Model Coordinator
OAST/RS

S R Sadin

Stan R. Sadin
Deputy Director,
Program Development
OAST/RS

INTRODUCTION TO VOLUME II

Volume II, Space Technology Trends and Forecasts, presents trends and forecasts for a number of critical, quantitative parameters of figures of merit, which may be used to characterize technological capabilities in the major discipline areas of space technology. The trends are based on historical data, and the forecasts represent the considered concensus opinions of knowledgeable experts in NASA Centers and Headquarters who are active contributors in their respective fields.

The major discipline areas included in this volume are:

- 1 Power and Electric Propulsion
    - 1.1 Photovoltaic Energy Conversion
    - 1.2 Space Energy Conversion and Storage
    - 1.3 Space Power Reactor/Conversion Technology
    - 1.4 Power Systems Management and Distribution
    - 1.5 Electric Propulsion
- 2 Chemical Propulsion
- 3 Materials and Structures
- 4 Information Systems
    - 4.1 Sensors
    - 4.2 Data Processing
    - 4.3 Communications
- 5 Navigation, Guidance and Control
- 6 Automated Operations

For the most part, the trends and forecasts presented here consist of a graphical display for each relevant figure of merit, accompanied by a descriptive narrative which explains the rationale and assumptions behind the forecast. This material is generally preceded by introductory remarks, an explanation of the figure of merit chosen to characterize the technology, a summary of the present state of that technology, and where appropriate, explanations of the goals and objectives of NASA and other technology development programs.

The graphical displays were prepared against the following guidelines and definitions.

- They should show a development trend with a discrete value for present capability.
- Where deemed feasible, they show a "most probable" forecast line (assuming sustained current level-of-effort funding, except where otherwise noted by the contributor), bracketed by a range of optimistic and pessimistic views of future progress, as defined by the contributor.
- Where used, "technology readiness date" is defined as the year the technology would be accepted for use in Phase B planning. Nominally, the technology would be expected to be demonstrated to the required capability level five years before the anticipated launch date of the mission.

The narrative material is intended to substantiate the forecasts by citing ongoing development programs, proposed enhancements, goals, objectives, and schedules for NASA research and technology development, other agencies, and the private sector. Attempts have been made to present and discuss discrete forecasts for the year 1990 for each figure of merit. Technology readiness levels, as defined on the opposite page, are used to define the degree of development being forecast. When a technology readiness level is not identified, "Level 7" technology readiness is to be understood.

Material was solicited from the expert contributors against the aforementioned guidelines. However, little attempt was made during the editorial process to confine the authors to this particular framework. Thus, there may be individual departures from this format, depending on the nature of the materials being discussed and the individual contributor's presentation styles.

The material presented herein has been subjected to review by the contributor's professional peers. However, the speculative nature of underlying assumptions behind and inherent uncertainty of such forecasts should be kept in mind by the users of this document.

TECHNOLOGY READINESS LEVELS

LEVEL 1	BASIC PRINCIPLES OBSERVED AND REPORTED
LEVEL 2	CONCEPTUAL DESIGN FORMULATED
LEVEL 3	CONCEPTUAL DESIGN TESTED ANALYTICALLY OR EXPERIMENTALLY
LEVEL 4	CRITICAL FUNCTION/CHARACTERISTIC DEMONSTRATION
LEVEL 5	COMPONENT/BREADBOARD TESTED IN RELEVANT ENVIRONMENT
LEVEL 6	PROTOTYPE/ENGINEERING MODEL TESTED IN RELEVANT ENVIRONMENT
LEVEL 7	ENGINEERING MODEL TESTED IN SPACE

ACKNOWLEDGMENTS

The following NASA Headquarters personnel coordinated the preparation of the technology trends and forecasts in their respective discipline areas:

1.	Power and Electric Propulsion	J. P. Mullin
2.	Chemical Propulsion	F. W. Stephenson
3.	Materials and Structures	W. A. Brainard
4.	Information Systems	
	Sensors	B. Rubin
	Data Processing and Communications	L. B. Holcomb
5.	Navigation, Guidance and Control	W. B. Gevarter
6.	Automated Operations	W. B. Gevarter

The technical experts at NASA's field centers who furnished the actual trends and forecasts presented in this volume are too numerous to delineate here, but by-line credit has been given when possible.

R. W. Riebling served as overall coordinator and editor of this volume.

FIGURES

NO. PAGE

1.1 Specific Power of Solar Arrays 1-3

1.2 Specific Cost of Solar Arrays 1-4

1.3 Design Life of Solar Arrays 1-6

1.4 Primary Battery Storage Capacity 1-11

1.5 Primary Battery Design Life 1-15

1.6 Secondary Battery Cycle Life at Various Temperatures - Ni/Cd Cell (Low Earth Orbit) 1-17

1.7 Secondary Batteries Design Life (Low Earth Orbit) 1-19

1.8 Battery Design Life (Geosynchronous Orbit) 1-20

1.9 Secondary Battery Specific Cost 1-22

1.10 Fuel Cell Specific Cost 1-28

1.11 Fuel Cell Power Level 1-29

1.12 Fuel Cell Specific Power 1-30

1.13 Fuel Cell Design Life 1-31

1.14 Fuel Cell Electrolyzer Storage Capacity 1-32

1.15 Fuel Cell Electrolyzer Design Life 1-33

1.16 Fuel Cell Electrolyzer Specific Cost 1-34

1.17 Power Levels for Electric Propulsion 1-36

1.18 Specific Power, Nuclear Thermal-to-Electric Energy Conversion 1-39

1.19 Design Life, Nuclear Thermal-to-Electric Energy Conversion 1-40

1.20 Expected Specific Power of Radioisotope Generators for Space Power 1-45

1.21 Expected Efficiency of Radiosotope Generators for Space Power 1-46

1.22 Lifetime Requirements for Space Power Missions 1-47

1.23 Projected Space Power Demand 1-51

FIGURES (Cont.)

NO.		PAGE
1.24	Power Distribution Voltage	1-54
1.25	Power Distribution Mass vs. Systems Voltage	1-55
1.26	Power Management System Voltage Dependent Costs (High-Frequency AC Distribution, "Mil Grade" Components)	1-56
1.27	Power Management System, Frequency-Dependent Costs (High-Frequency AC Distribution, "Mil Grade Components)	1-58
1.28	Specific Impulse vs. Thrust	1-60
1.29	Specific Mass for Solar Array; Thruster and Power Processor; Complete Solar Electric Propulsion Stage	1-69
1.30	Mass as a Function of Specific Impulse	1-71
1.31	Power/Thrust vs. Specific Impulse	1-73
2.1	Energy Conversion Efficiency (I_s) of Chemical Rocket Engines	2-3
2.2	Chemical Rocket Engine Service Life	2-4
2.3	Chemical Booster Rocket	2-5
2.4	Earth-to-Orbit Transportation Costs	2-6
3.1	Estimated Erectable Spacecraft Capability Using One Shuttle Flight	3-3
3.2	Maximum Usable Non-Metallic Service Temperature	3-4
3.3	Maximum Service Temperatures for Metals	3-6
3.4	Composites - Space Environment Lifetime of Resin Matrix	3-7
3.5	Strength-to-Mass Ratio for Graphite/Polyimide Materials	3-9
3.6	Strength-to-Mass Ratio for Composite Tension Panels	3-11
3.7	Dynamic Loads Analysis Costs	3-13
3.8	Temperature and Heat Rejection Capability of Thermal Protection Systems	3-16
4.1	Narrowband UV Laser Pulse Energy	4-4

FIGURES (Cont.)

NO.		PAGE
4.2	Electric Efficiency of UV Gas Lasers	4-5
4.3	Wavelength Coverage of UV Lasers	4-7
4.4	Peak Power of Dye Lasers	4-10
4.5	RMS Range Accuracy of Centimeter Accuracy Space-Based Laser Ranging	4-13
4.6	Transmitter Prime Power of Computed-Accuracy Space-Based Laser Ranging	4-15
4.7	Spectral Resolution of Submillimeter-Wave Heterodyne Radiometer	4-19
4.8	Noise Temperature of Submillimeter-Wave Heterodyne Radiometer	4-20
4.9	Antenna Beamwidth	4-23
4.10	Radiometer Receiver Weight	4-24
4.11	Receiver Input Power	4-26
4.12	Specific Cost	4-27
4.13	Infrared Detection Sensitivity at 100 μm	4-29
4.14	Spaceborne Passive Microwave Sounder Resolution Trends	4-32
4.15	Spaceborne Passive Multifaction Microwave Imager Resolution Trends	4-34
4.16	Antenna Size Versus Spatial Resolution	4-35
4.17	Radiometer Sensitivity vs. Crosstrack Spatial Resolution	4-36
4.18	Schematic Representation of Advanced Mapping Spectrometer	4-38
4.19	Infrared Remote Sensing Required Detectivity as a Function of Wavelength (AMS 1985 Requirements)	4-43
4.20	Infrared Detector Array Performance	4-44
4.21	Performance of Radiative Cooler	4-45
4.22	Development of Lightweight Optics	4-46

FIGURES (Cont.)

NO.		PAGE
4.23	Instrument Data Rate for Planetary Spacecraft	4-47
4.24	Single-Mode Power of Lead Salt Lasers	4-51
4.25	Operating Temperature of Lead Salt Lasers	4-52
4.26	Bandwidth and Heterodyne Quantum Efficiency of 8-12 μm HgCdTe Photomixers	4-53
4.27	Spectral Response of HgCdTe Photomixers	4-54
4.28	Technology Development--Infrared Imaging InSb and HgCdTe CCIRID-Monolithic Linear Arrays	4-58
4.29	Monolithic InSb and HgCdTe Linear Arrays	4-59
4.30	Monolithic InSb and HgCdTe Array Sensitivity	4-60
4.31	Monolithic Linear Arrays--Spectral Range	4-62
4.32	Performance Growth	4-70
4.33	Hybrid Thermal IR/CCD Arrays, Cost Per Detector Element	4-72
4.34	Cooling Requirements	4-73
4.35	Reliability	4-74
4.36	5-m Wavelength Heterodyne Radiometer Noise Temperature	4-77
4.37	1-mm Wavelength Heterodyne Radiometer Noise Temperature	4-78
4.38	0.5-mm Wavelength Heterodyne Radiometer Noise Temperature	4-80
4.39	0.1-mm Wavelength Heterodyne Radiometer Noise Temperature	4-81
4.40	Wide Swath Radar Technology	4-85
4.41	Multi-Frequency SAR Operation	4-86
4.42	SAR Amplitude Precision/Accuracy	4-88
4.43	Performance of Spaceborne Computers	4-93
4.44	Performance of Spaceborne Computers Per Kilogram	4-94

FIGURES (Cont.)

NO.		PAGE
4.45	Performance of Spaceborne Computers Per Watt	4-95
4.46	Capacity of Spaceborne Mass Storage Systems	4-98
4.47	Transfer Rate of Spaceborne Mass Storage Systems	4-99
4.48	Processor Performance	4-103
4.49	Ground Processing Costs	4-104
4.50	Processor Throughput	4-105
4.51	On-Line Auxiliary Storage Capacity	4-107
4.52	High-Speed Data Buffering	4-108
4.53	Protected Communications Market Demand and Satellite Capacity Versus Time	4-110
4.54	Antennas Operating Frequency	4-118
4.55	Antennas - Number of Beams	4-119
4.56	Antennas - Reflector Size	4-121
4.57	20-GHz GaAs FET Power Per Chip	4-123
4.58	GaAs FET LNA Noise Figure at 30 GHz	4-125
4.59	Microwave Amplifier Operating Frequency	4-127
4.60	Microwave Amplifier Efficiency	4-128
4.61	Microwave Amplifer Life	4-130
4.62	Microwave Amplifier Output Power Versus Frequency	4-131
4.63	Electron Guns - Cathode Emission	4-134
4.64	Cathode Lifetime	4-136
4.65	Secondary Yield	4-137
4.66	Equivalent Data Rate at Jupiter	4-140
4.67	Output Power in Space-to-Space Communications	4-145

FIGURES (Cont.)

NO.		PAGE
4.68	Power Conversion Efficiency in Space-to-Space Communications	4-147
5.1	Gyro Drift	5-2
5.2	Gyro Lifetime	5-3
5.3	Star Tracker Pointing Accuracy	5-5
5.4	Horizon Sensor Angular Error	5-7
5.5	Instrument Pointing Stability	5-9
5.6	Instrument Pointing Control Accuracy (Stellar Reference)	5-10
5.7	On-Board Estimator Capacity	5-12
6.1	Number of Processors On-Board Spacecraft	6-2
6.2	Image Processing Speed for 400 x 400 Pixels	6-3
6.3	On-Board Processor Speed of Operation	6-4
6.4	Total On-Board Core Memory	6-5
6.5	Problem Complexity vs. Solution Time	6-7

ACRONYMS

AMO	air mass zero (solar cells)
AMS	advanced mapping spectrometer
ASAR	advanced synthetic aperture radar
ASPS	annular suspension and pointing system
ATS	applications technology satellite
AU	astronomical unit; the mean earth-sun distance
BAC	Boeing Aircraft Company
BOL	beginning of life
CASTS	composites for advanced space transportation systems
CCD	charged-coupled device
CCIRID	charged-coupled infrared imaging device
CTD	charged-transfer device
CVD	chemical vapor deposition
CW	continuous wave
DDS	distributed data system
DIAL	differential absorption lidar
DoD	Department of Defense
DOD	depth of discharge (batteries)
DSN	deep space network
DSRV	deep submergence rescue vehicle
EOL	end of life
FDM	frequency division multiplexing
FET	field effect transistor
FOV	field of view
GE	General Electric

ACRONYMS (Cont.)

GEO	geosynchronous earth orbit
GLL	Galileo mission
GSFC	Goddard Space Flight Center
IF	intermediate frequency
IFOV	instantaneous field of view
IMC	image motion compensation
IMPATT	impact avalanche and transit time (diode)
IR	infrared
IRAS	infrared astronomical satellite
ISPM	international solar polar mission
IUS	inertial upper stage
LAMMR	large antenna multifrequency microwave radiometer
LEO	low earth orbit
LHS	laser heterodyne spectrometer
LO	local oscillator
LNA	low noise amplifier
LSI	large scale integration
LSST	large space systems technology
MDP	master data processing
MIC	microwave integrated circuit
MIS	metal insulator semiconductor
MNOS	metal nitride oxide semiconductor
MOPS	millions of operations per second
MOSFET	metal oxide-silicon field-effect transistor
MPP	massively parallel processor

ACRONYMS (Cont.)

MSFC	Marshall Space Flight Center
NEEDS	NASA end-to-end data system
NEP	nuclear electric propulsion
NIMS	near-infrared mapping spectrometer
NOAA	National Oceanic and Atmospheric Administration
NOSS	National Oceanic Satellite System
OAST	Office of Aeronautics and Space Technology
OEX	orbiter experiment
OSTA	Office of Space and Terrestrial Applications
OTV	orbit transfer vehicle
OSTDS	Office of Space Tracking and Data Systems
PC	photoconducting
PPTS	precision pointing and tracking system
R&D	research and development
RSI	reusable surface insulation
RT&E	research, technology and engineering
RTG	radioisotope thermoelectric generator
RTOP	research and technology operating plan
SAR	synthetic aperture radar
SEP	solar electric propulsion
SIR-A	Shuttle imaging radar "A"
SMMR	scanning multichannel microwave radiometer
SMMW	submillimeter wave
SPE	solid polymer electrolyte (fuel cells)
SRT	supporting research and technology

ACRONYMS (Cont.)

SSME	space shuttle main engine
STS	space transportation system
TDI	time delay and integration
TDM	time division multiplexing
TPS	thermal protection system
TWT	traveling wave tube
UV	ultraviolet
VLSI	very large scale integration
VOIR	Venus Orbiter Imaging Radar

1 POWER AND ELECTRIC PROPULSION

1.1 PHOTOVOLTAIC ENERGY CONVERSION

Solar Array (W. A. Hasbach, Jet Propulsion Laboratory)

Solar array technology is being advanced in several areas. OAST R&T development programs are directed at increasing the level of electric power available while reducing the specific costs. The technologies to accomplish these goals are in the areas of: reduced specific mass and volume; increased efficiency of solar conversion components; and increased operating life of cells and arrays. Weight reduction for deployable structures is under development using composite materials and flexible array blankets.

Although silicon cell technology may be approaching the practical limits of efficiency ($\sim$18%), major efforts in silicon research are being directed towards ultrathin ($\leq$50 μm) cells possessing efficiencies nearly as great as devices of conventional thickness ($\geq$200 μm). Ultrathin silicon cell research should offer opportunity for greatly improved resistance to radiation. Another approach that could provide substantial improvement in effective radiation resistance involves the development of techniques to rejuvenate cells by in-situ annealing. Present power output of silicon cells degrades by 25% from beginning of life (BOL) levels in 7 to 10 years for spacecraft in high earth orbits (GEO). Restoration of close to original capability would reduce size and weight penalties for long-duration missions.

Gallium arsenide cell technology is being developed to utilize its efficiency and reduced susceptibility to radiation damage. Ultrathin ($\leq$50 μm) approaches to gallium arsenide such as chemical vapor deposition (CVD) technology would provide very high efficiency ($\sim$20% air mass zero, AMO) and excellent radiation resistance ($\sim$10% reduction in BOL after 10 years). Development of multiple bandgap technology cell designs permitting 30% conversion efficiency would offer significant improvement in array power output and/or mass reduction. These developments coupled with encapsulation technology, which offers an economical, low-mass alternative to cover glasses, would improve array performance dramatically.

OAST is currently funding programs in thin cell technology, encapsulation techniques, GaAs cell development, multiple bandgap technology, radiation-resistant cells, and blanket and array designs that minimize structure weight and subsystem costs. Breakthroughs in these development programs, particularly in the multiple bandgap cells, would significantly enhance the expected capabilities.

Specific power, specific cost, and design life were the parameters chosen to describe the evolution of solar array technology. Technology readiness dates shown represent Level 6 state of development.

Specific Power (Fig. 1.1). Array specific power output has improved from 5.7 W/kg capability for Skylab to the current state-of-the-art capability of 30 W/kg.

Solar electric propulsion (SEP) capability (1985) is forecast to be about 66 W/kg. Improvements in ultrathin cell (silicon or gallium arsenide) efficiency and radiation resistance along with the development of lightweight structures should boost specific power higher than 120 W/kg by 1990. Technology breakthroughs in solar cells now being tested in the laboratory coupled with concentrator-enhanced solar array developments could increase capabilities by 1990 to greater than 200-250 W/kg. Gains to several times that level might be possible in the middle 1990s if all the possible developments now foreseen were to reach maturation.

Specific Costs (Fig. 1.2). Specific costs of current solar arrays are approximately \$600/W. Higher power arrays such as SEP ($\sim$25 kW) which allow the use of semi-automated assembly processes and standardized cells, covers, and interconnects could reduce those costs to \$250-300/W. Further reductions in cost are expected to come from the use of larger area solar cells. At this time, a number of approaches to low cost

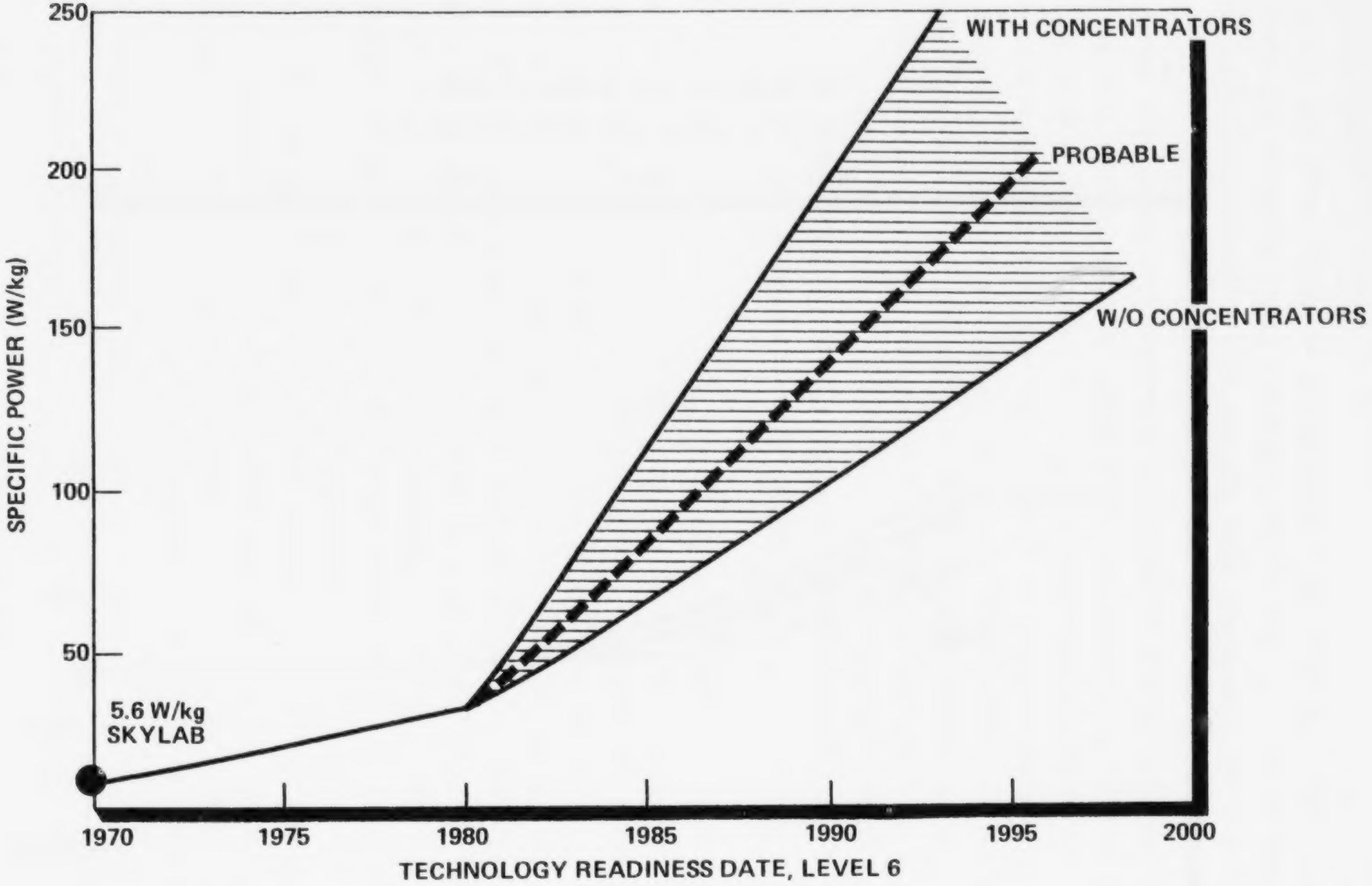

Figure 1.1. Specific Power of Solar Arrays

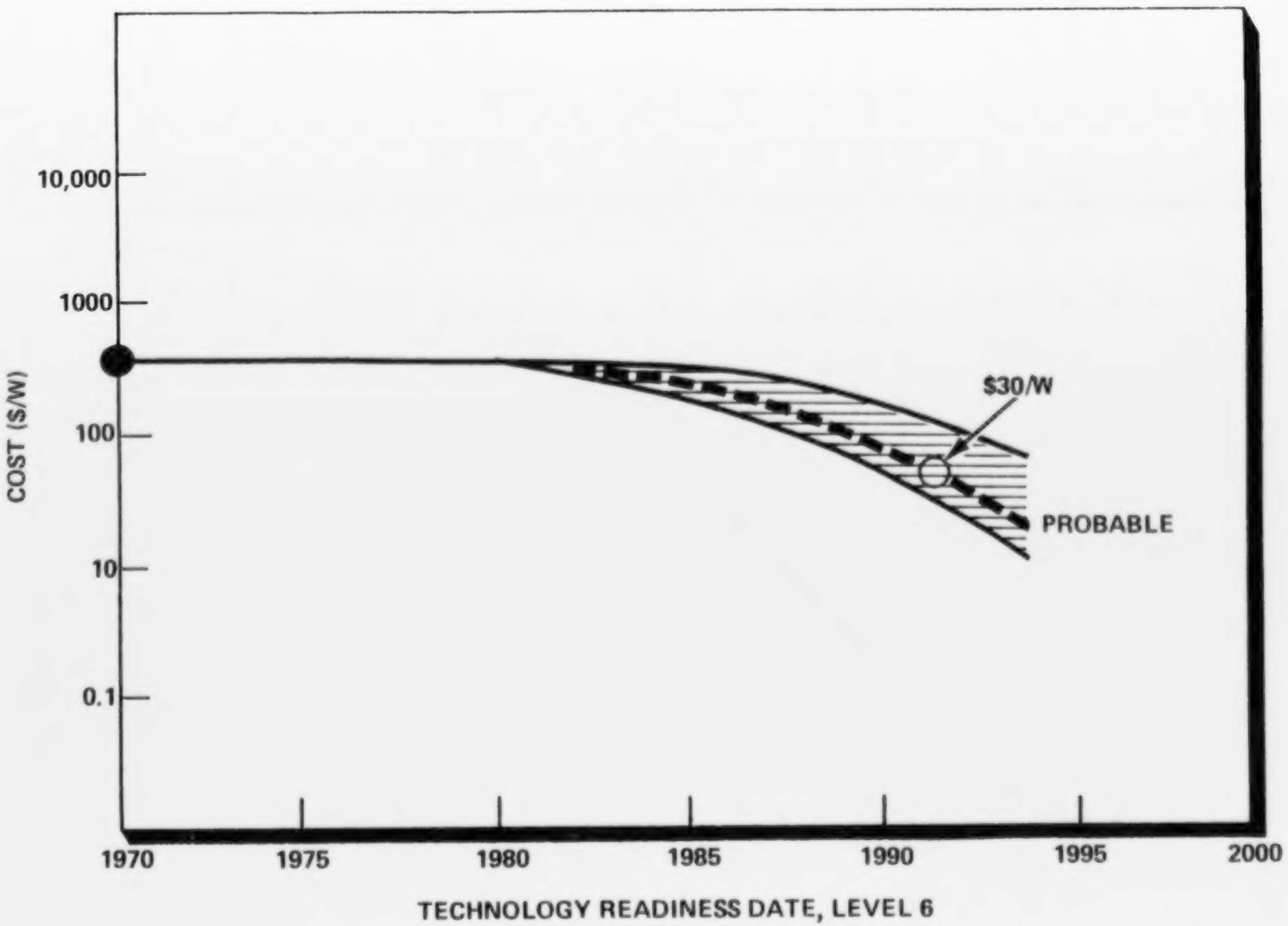

Figure 1.2. Specific Cost of Solar Arrays

blanket and array design to achieve less than $30/W for large scale solar arrays are presently being evaluated. While the lead role in reducing solar cell costs resides with the DOE, NASA continually monitors that effort for developments of potential benefit to space cells. That promise does exist as demonstrated by recent work which suggests that lower cost silicon material developed for terrestrial use may be indistinguishable in performance from space quality single crystal material. Gallium arsenide cells, although projected to be more expensive than silicon, can operate at higher temperatures allowing the utilization of solar concentrators. Through the use of low-cost concentration systems gallium arsenide arrays with fewer and more efficient solar cells have the potential for significant cost reductions. Further radical reductions in array costs would be predicated on substantial revision of methods of procuring and of operational procedure.

Design Life (Fig. 1.3). A good figure of merit for solar array operating life is the power per unit area delivered after a specific mission duration. Silicon cells now produce over 50% more power per unit area after 7 years in GEO than they did in 1970 (17 mW/cm^2 vs. 11 mW/cm^2). Optimistically, if in-situ annealing proves feasible, design life could be extended indefinitely by 1990. This technology development would effectively eliminate the solar array as a critical, constraining spacecraft component for long-duration missions. Other approaches to reduce radiation damage are also being pursued in the event annealing proves impractical. This work should increase power output to beyond 20 mW/cm^2 by 1990. Expressed another way, one current target of the OAST program is to reduce output power loss to less than 15% after 10 years in GEO. For purposes of the projection of Fig. 1.3, design life terminates when output power degrades to 75% beginning of life power for a GEO mission.

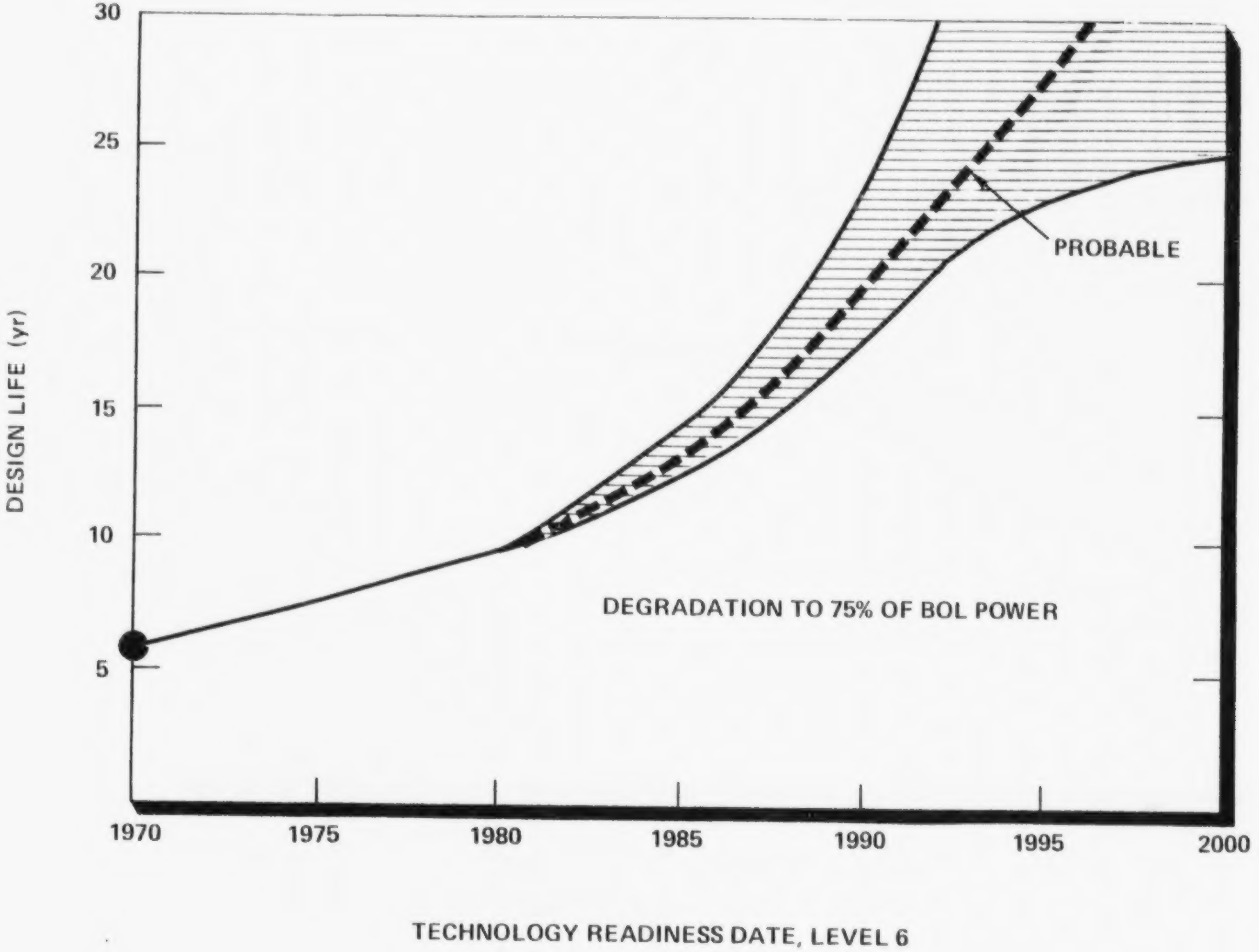

Figure 1.3. Design Life of Solar Arrays

1.2 SPACE ENERGY CONVERSION AND STORAGE: TECHNOLOGY PROJECTIONS

I. Stein, Jet Propulsion Laboratory
and
J. S. Fordyce, Lewis Research Center

1.2.1 Batteries

Several government agencies and private contractors are developing primary and rechargeable or secondary electrochemical storage batteries with the goal of achieving low-cost, long-life, and high-energy density per unit weight. However, many of the systems are not compatible with the space environment or NASA's requirements. Among the potential systems are the alkali metal high-energy couples under development since the late 60s, which for brevity will all be lumped together as Na/X, Li/X. This designation actually includes a wide range of low- and high-temperature alkali metal concepts with different positive electrodes, X. At this time, a very substantial effort is being expended on their development.

Four systems, nickel-cadmium (Ni/Cd), nickel-hydrogen (Ni/H_2), and the Na/X, Li/X high-energy group are the most promising in relation to future space needs. However, it appears that, in order for the sodium and lithium systems to become usable and reliable storage batteries, particularly high-rate secondaries, significant resources must be spent to bring them to reality within the next 20 years. A significant effort is necessary to bring Ni/H_2 to the level of technical development of the Ni/Cd system technology. For long life and low cost, Ni/Cd must still be considered seriously. Ni/H_2 appears to have potential for geosynchronous and possibly low earth orbit, but this will only become evident in the near future when a broader data base is accumulated. The alkali metal systems are potentially lightweight but not necessarily low cost or long lived.

During the first two decades of the space era, Ag/Zn was the most common primary battery, although the majority of orbiting spacecraft contained Ni/Cd secondary batteries as their energy storage system. The choice of this electrochemical system over others was based primarily on the following factors:

(a) High cycle capability
(b) Simple charge control requirements
(c) Reasonable specific energy
(d) Good reliability

During the late 50s and early 60s there was a considerable effort put into the development of the Ni/Cd system. The driving force for this effort was caused by the increased mission requirements placed on the orbiting spacecraft. Six-month mission goals quickly developed into four year missions as success followed success. Spacecraft became "operational" vehicles rather than scientific experiments, and the requirements on the energy storage system forced development to the present state of the art.

During the decade 1957-1967, the development efforts for Ni/Cd systems concentrated on the following areas:

(a) Terminal seal
(b) Separator
(c) Design parameters, such as negative-to-positive capacity ratio
(d) Cell pressure

Successful development work in these areas resulted in considerable and significant improvement in the Ni/Cd system. At the same time that this development was proceeding, many life cycling programs were being conducted in order to establish a credible data base which would be used in both life predictions and the associated reliability factors.

The Ni/Cd battery system has become sophisticated because the required data base was developed. The effort included:

(a) Continued development of nickel electrodes which led to new impregnation techniques, and in turn, resulted in superior electrodes.

(b) Power system designers learned to operate within the constraints of the Ni/Cd system, and thus the life cycling results of the batteries improved significantly.

(c) Cell manufacturers improved their quality control significantly because of the various pressures imposed on them by the Government agencies.

(d) Users have learned techniques of extending the service life of the Ni/Cd batteries by various techniques, i.e., deep discharge reconditioning, low temperature operation.

In the late 60s, initial development was begun on the secondary Ni/H_2 cell, which combined the best electrodes known to electrochemical conversion system developers with respect to rate and cycle life capability. This system has continued to evolve and is rapidly gaining acceptance among the space community for flight application. It offers higher energy density and long life at deep depths of discharge.

Since 1970, important progress has been made in the field of energy storage. This is attributed to discovery of novel methods of utilizing the high-energy alkali metals, both sodium and lithium, in both primary and secondary systems. At the present time, a great deal of work is in progress to develop practical cells based on these high-energy anodes.

The important parameters which characterize space batteries are storage capacity and design life. Storage capacity is a measure of the battery's energy density and is expressed in terms of watt-hours/kilogram. Design life is the number of years the battery can operate continuously within the required voltage limits in the case of rechargeable or secondary systems, and the number of years a battery can be stored and still deliver full capacity in the case of primary systems. When defining the design life, the type of cycling regime and the orbit are usually described. Costs also become increasingly important as total storage capacities increase to the level of many tens of kilowatt hours and larger.

1.2.1.1 Storage Capacity

Primaries. The silver-zinc (Ag/Zn) system is the most common primary battery is use. It can now deliver about 150 W-h/kg depending upon the application. Some improvement can be expected. Over the past several years, lithium primaries based on SO_2 and $SOCl_2$ have been developed. Of these, the $SOCl_2$ system is likely to find the most space application. Figure 1.4 displays the projections. It shows a forecast of the specific energy density of primary batteries utilized for space application through the 1980s. It is expected that the specific energy density of the $Li/SOCl_2$ battery will increase from 150 to 300 W-h/kg by the late 1980s.

Secondaries. Projections of the storage capacities of the system of interest have not changed considerably over the years. The largest gains should be possible in the more energetic systems such as Li/X and Na/X with modest gains still possible in the Ni/H_2 and Ni/Cd systems.

The Na and Li systems should improve with more development. Improvements in materials, packaging, and operating techniques should all raise the storage capacity. Without improvements in these areas only modest gains will result, due to the need to reduce depth of discharge (DOD) to achieve greater life.

The Ni/Cd and Ni/H_2 system will achieve modest gains from packaging and electrode improvements, and extensive effort will be needed to realize significant advances. To meet NASA's projected capacity requirements, a change from Ni/Cd to Ni/H_2 and finally to high-energy systems is likely. It is expected that the high-energy systems will increase from 40 to 250 W-h/kg over the next two decades.

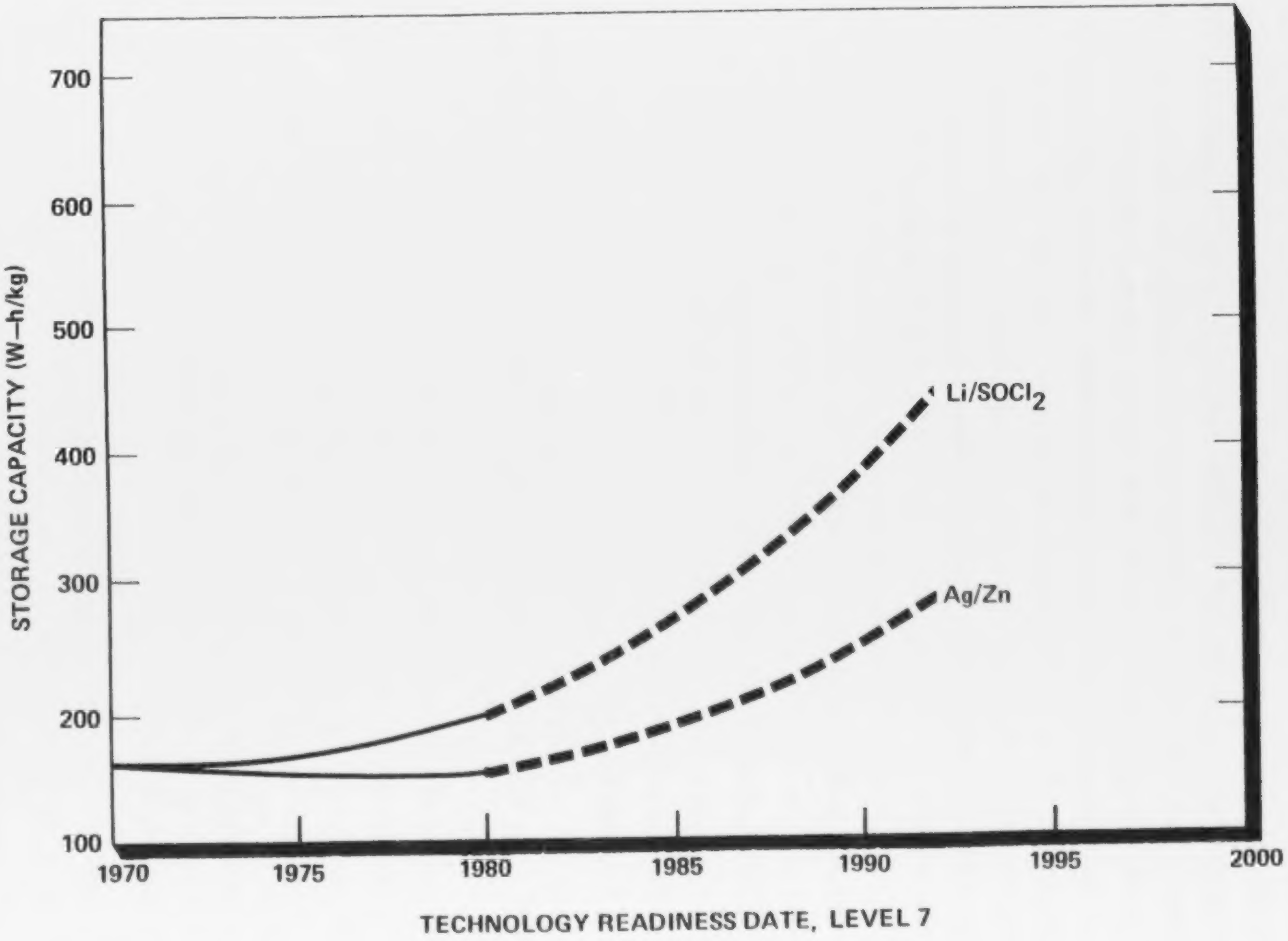

Figure 1.4. Primary Battery Storage Capacity

Ni/Cd. In order to determine the improvements possible in an existing system such as Ni/Cd, a base point must be established; unfortunately this base is a function of usage. A standard GE 20 cell used in many flight programs weighs 950 g and delivers a minimum of 24 A-h at an average of approximately 1.2 V. This results in a cell capability of 30.3 W/kg. In terms of a packaged battery, using standard packaging techniques, this figure is reduced to 24.3 W-h/kg packaged specific energy density. For a low earth orbit in general the depth of discharge has been restricted to 20% for missions exceeding 1 yr, and thus the useful energy density of a Ni/Cd battery is 4.9 W-h/kg. However, in the case of a geosynchronous orbit, where the same battery can perform at a 60% depth of discharge, the useful energy density is 14.6 W-h/kg. Ni/Cd batteries which are used in planetary missions are also considered to have a useful energy density approximately 60% of the battery output, and thus it is similar to the case of the geosynchronous orbit. We can establish three base points of reference for useful energy density:

Low Earth Orbit: 4.9 W-h/kg
Geosynchronous Orbit: 14.6 W-h/kg
Planetary Mission: 14.6 W-h/kg

In order to improve this state of the art, the following steps can be taken:

1. Reduce the cell weight by reducing the mass of the cell case walls.
2. Reduce the battery assembly structural weight from 25% of cell weight toward a goal of 5%.
3. Change the plate manufacturing process to improve the sintered nickel plate, and the utilization of the active materials.
4. Improve the utilization by application of reconditioning techniques.
5. Improve the life predictability.

Lightweight flight-battery design is being developed to take care of items 1 and 2. It is estimated that overall battery energy density can be increased from the present 24.3 W-h/kg to 40 W-h/kg within about 2 yr with these improvements. Reconditioning techniques will most likely gain widespread acceptance over the next few years, and this technique will increase the useful depth of discharge in geosynchronous orbit regimes from 60% to 80%. We can also expect the present 20% depth of discharge for low earth orbit regimes to increase to approximately 40% within the next few years. Thus, the immediate forecast for useful specific energy for the Ni/Cd system within a 2-3 yr period is as shown below. The 1982 estimates appear to be close to the practical upper limit of Ni/Cd capability.

	Present (W-h/kg)	1982 (W-h/kg)
Low Earth Orbit	4.9	16.0
Geosynchronous Orbit	14.6	32.0

Ni/H_2. Continued progress is being made with the Ni/H_2 cell. The packaged energy density is presently about 45 W-h/kg, for systems utilizing 50 A-h Ni/H_2 cells. This figure may be improved when much larger cells are designed and utilized. It is obvious that, unless the Ni/H_2 system improves its rated energy density, it holds little weight advantage over the forthcoming Ni/Cd systems for geosynchronous orbit regimes. However, it is forecast that this new system will be able to utilize about 60% of its specific energy during a low earth orbit regime, and thus would present a significant weight gain over the 1982 Ni/Cd useful specific energy. Thus, the useful specific energy for the Ni/H_2 packaged system by 1982 is expected to be:

Low Earth Orbit: 31.5 W-h/kg
Geosynchronous Orbit: 36.0 W-h/kg

It is also forecast that the Ni/H_2 system will inherently have even better reliability than the Ni/Cd system, and it also will be a more "forgiving" system with simpler system requirements.

Na/X, Li/X--High-Energy Systems. Among the candidate systems in this group are ambient temperature organic electrolyte lithium/transition metal dichalcogenide (e.g., TiS_2) cells, moderate-temperature (100-170°C) sodium/dichalcogenide (e.g., TiS_3, VS_3) cells with solid electrolyte containment of the liquid negative, and the high-temperature molten salt batteries (350-400°C) using sodium/sulfur (several configurations under development) and lithium/iron sulfide. Extensive work in the high-temperature concepts for terrestrial applications has 200 W-h/kg as the goal for 1989 (Ref. 5) load leveling applications.

These systems range in energy density from 60 to 150 W-h/kg at the present time. It is anticipated that this can improve to a range of 100-250 W-h/kg in the future. These systems will produce energy storage sufficient to meet NASA requirements near the end of the century. Considerable effort is necessary to realize these goals. Not enough is known of the systems to predict the best applications for this technology. Significant advances must be made in many key components to provide reliable unattended operation suitable for space application. So far, most development has been performed only at the single cell level and projections have been made on this basis rather than projected for usage in battery systems.

1.2.1.2 Design Life

Primaries. The silver-zinc (Ag/Zn) system has a maximum design life of about five years or less depending on the conditions. Not much improvement is expected. For the $Li/SOCl_2$ system, improvements in separators and stability characteristics of the depolarizing electrolyte should provide improvement. Figure 1.5 displays the projections. It gives a forecast for the design life of primary space application batteries. It is expected that the life will be increased from about 3 to 10 yr by the late 1980s.

Secondaries. The only system with any demonstrated life is the Ni/Cd in both LEO and GEO applications. Many feel that the Ni/H_2 is capable of better performance in terms of life. The system appears to

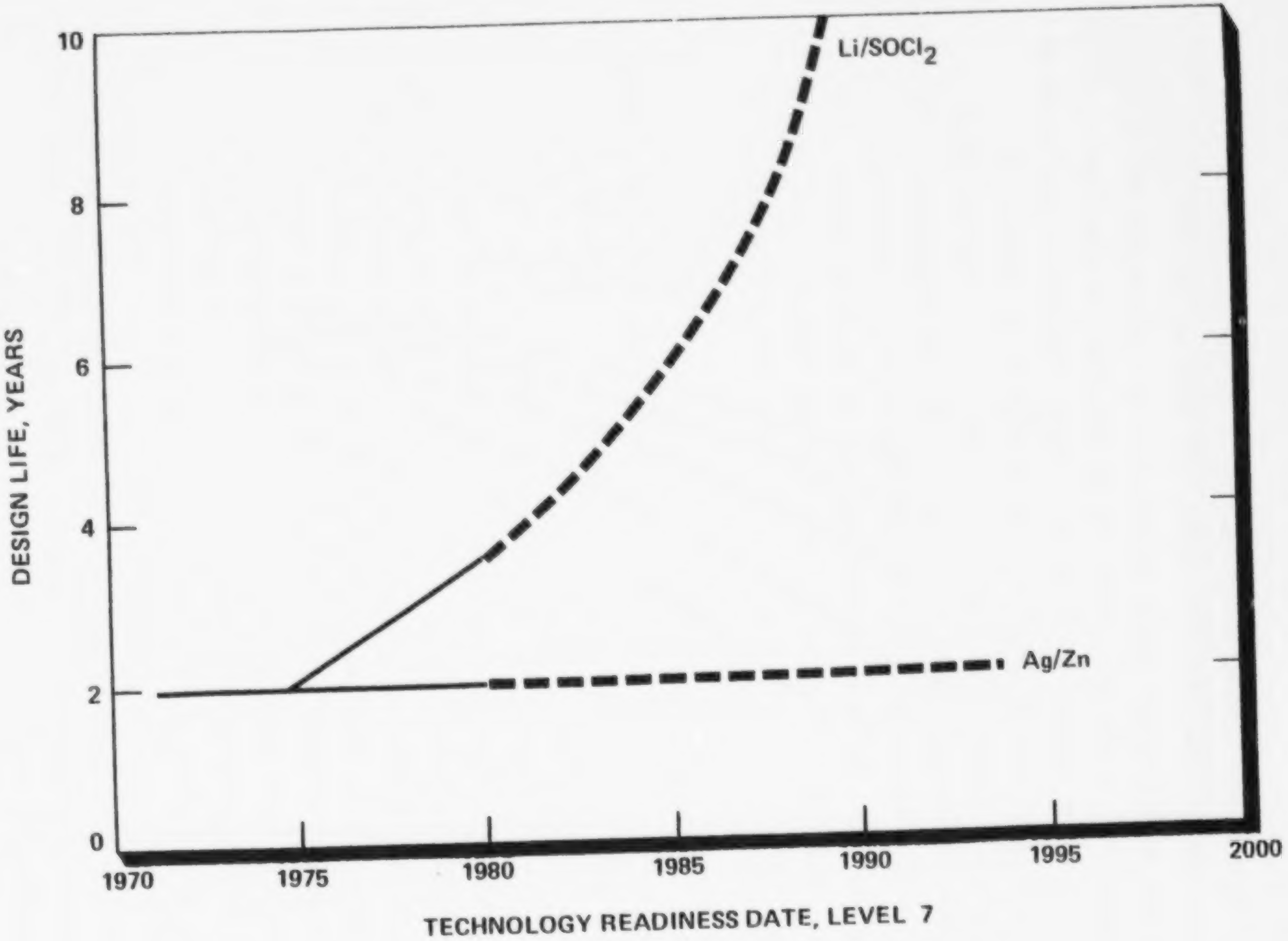

Figure 1.5. Primary Battery Design Life

work well in GEO with less of a probability in LEO. However, these systems appear to be the only two systems that will give up to 10+ years of service within the next 20 years.

The high-energy systems do not appear to be able to perform well for long periods of time, and this capability does not appear to be forthcoming in the near future. These systems will be lightweight but relatively short-lived in the near term. It is not expected that low-temperature lithium systems will last any longer than silver-zinc although they will be lighter. The high-temperature systems are plagued by materials and control problems, and results reported in the literature present activated lives of 4 to 25 months, but not as batteries. Most of the cells have small capacities (25-40 A-h). When cells are made into batteries lives decrease dramatically due to cell variations. It is difficult to predict when and if these systems will find use, but it is felt that they will not be available for space use in the next 10-15 years.

Figures 1.6, 1.7, and 1.8 display the projections of the life parameters: cell mean cycle life, design life at low earth orbit, and geosynchronous.

Variation in performance can be expected depending on the use in either LEO or GEO. Therefore, the curves reflect activated life and the time frame within which these systems can be expected to operate. Not enough is known in the high-energy systems of the relation of a small number of deep cycles (800) over a long period of time or a large number of shallow cycles over the same period. It will take dramatic breakthroughs to bring these systems to a point where they can operate safely and reliably as a battery for long periods of time with no maintenance.

Figure 1.6 describes the present state of the art for the Ni/Cd system in low earth orbit applications. It shows the cell mean cycle life as a function of depth of discharge and operating temperature, and the figure is included to emphasize the importance of temperature and

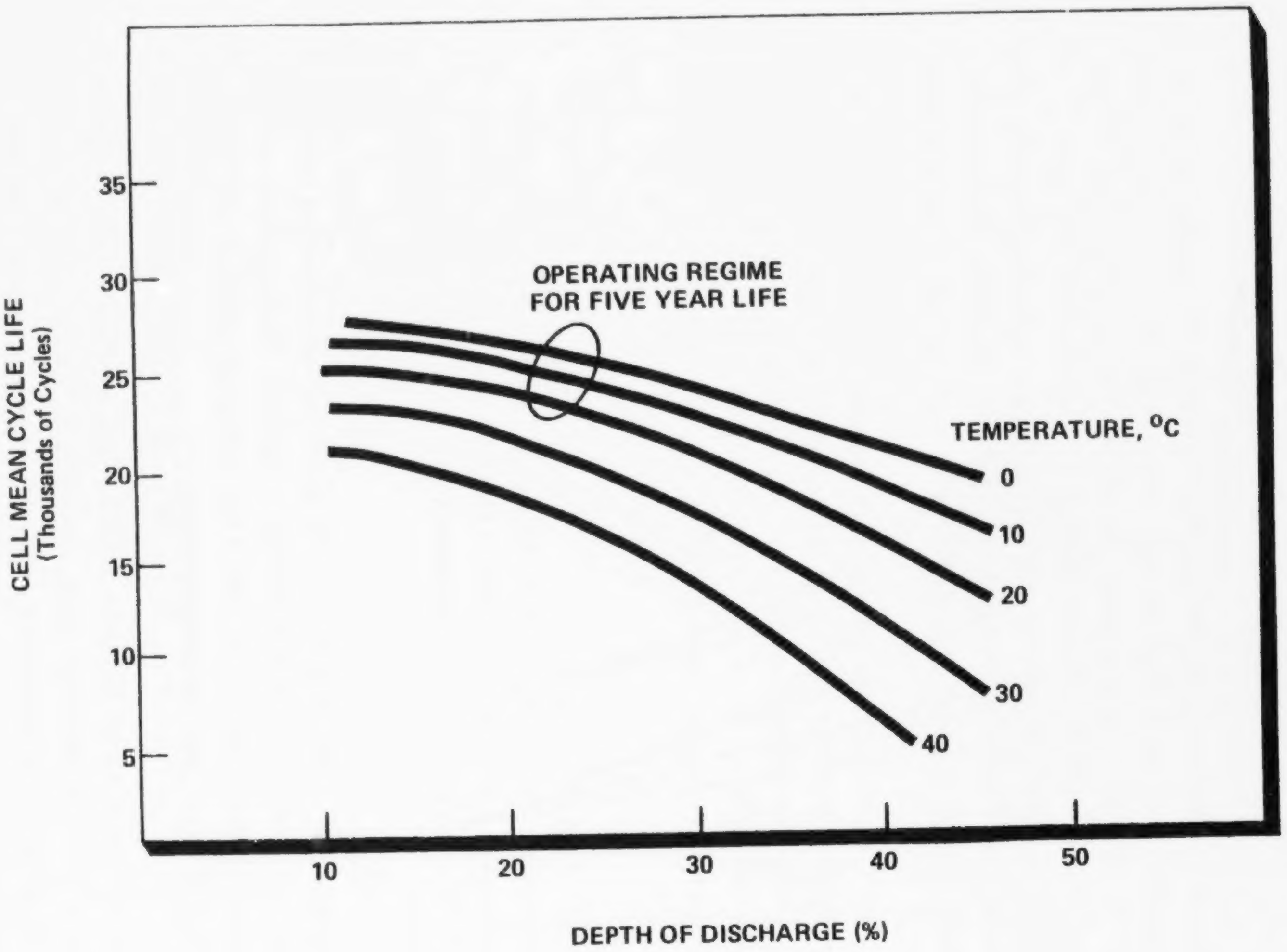

Figure 1.6. Secondary Battery Cycle Life at Various Temperatures – Ni/Cd (Low Earth Orbit)

and depth of discharge for this type of application. This type of curve is further influenced by cell reliability factors at the various depths of discharge and temperatures, and makes the present choice of 20% depth of discharge at temperatures between 0°C and 20°C obligatory for 5 yr of life.

Figure 1.7 projects the design life forecast for the Ni/Cd, Ni/H_2 and high-energy systems. For the high energy systems, life is shown over a range of depths of discharge in the low earth orbit regime. It shows the trends to longer life overall. At the same DOD for 1980 batteries, life will increase in the future while at increasing DODs they will maintain relatively the same life. As noted earlier, considerable uncertainty exists for Ni/H_2 particularly as data is yet to be developed.

Figure 1.8 projects the design life forecast for the Ni/Cd and Ni/H_2 system at 60-80% depth of discharge and in geosynchronous orbit regime. It shows a significant improvement from the present 5-yr life to 10-yr life by the mid 1980s. While not reflected on the plot it is to be noted that appreciable uncertainty exists for the Ni/H_2 system at this time.

1.2.1.3 Cost ($/kW-h)

Primaries. The major space application for primary cells is in manned spacecraft auxiliary power and planetary probe batteries. Cost is not a particularly important parameter for these applications and is not projected.

Secondaries. Cost is difficult to project when comparing known systems vs. systems in early development. However, the consensus is that all systems will decrease in cost omitting inflation ($/kW-h) due to increases in life, use, and DOD developments.

Ni/H_2 is expected to decrease in cost because it is now a handmade cell. Moving it from the model shop, a dedicated manufacturer and the learning curve should decrease its cost. It does not appear that the

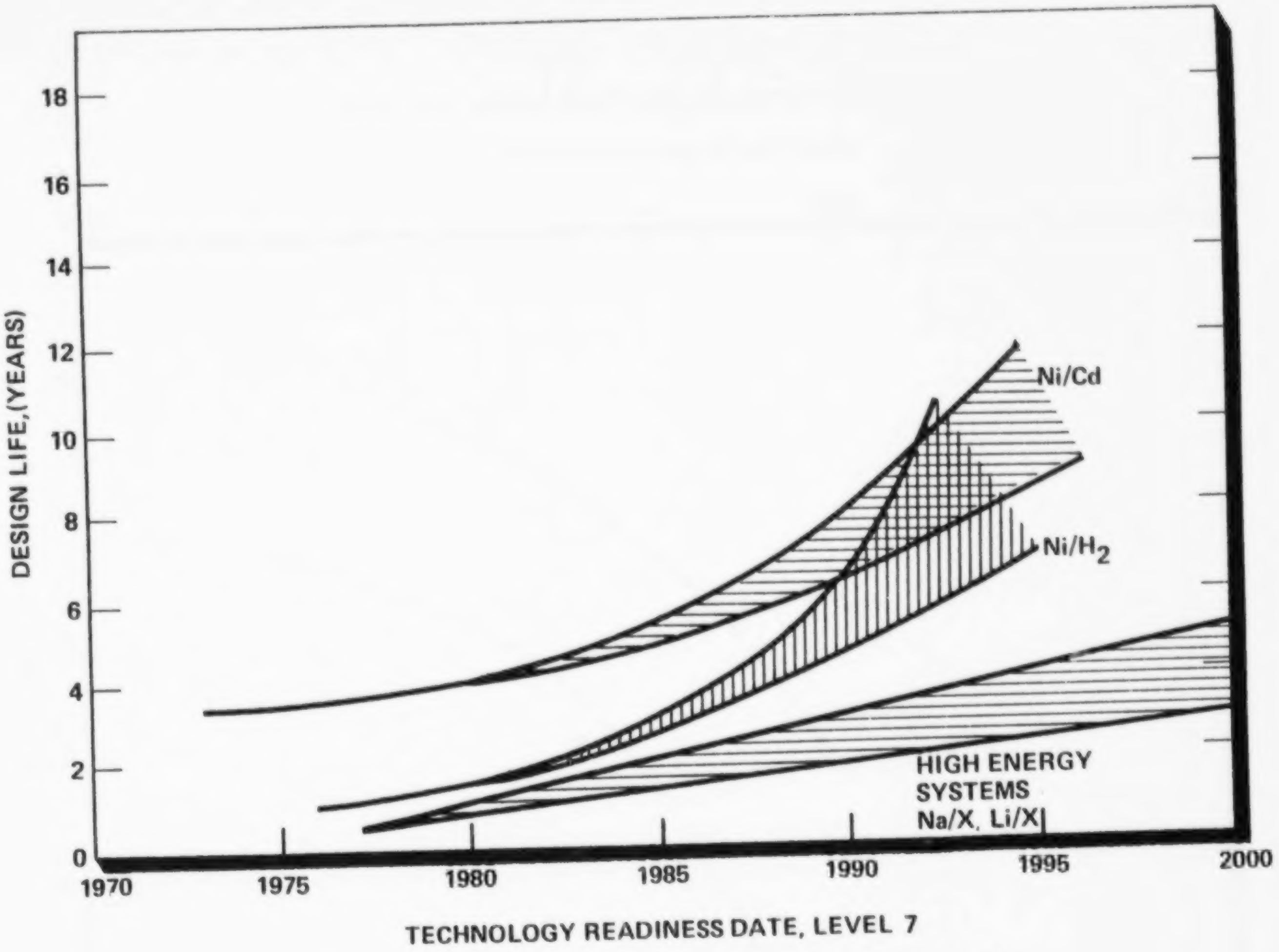

Figure 1.7. Secondary Batteries Design Life (Low Earth Orbit)

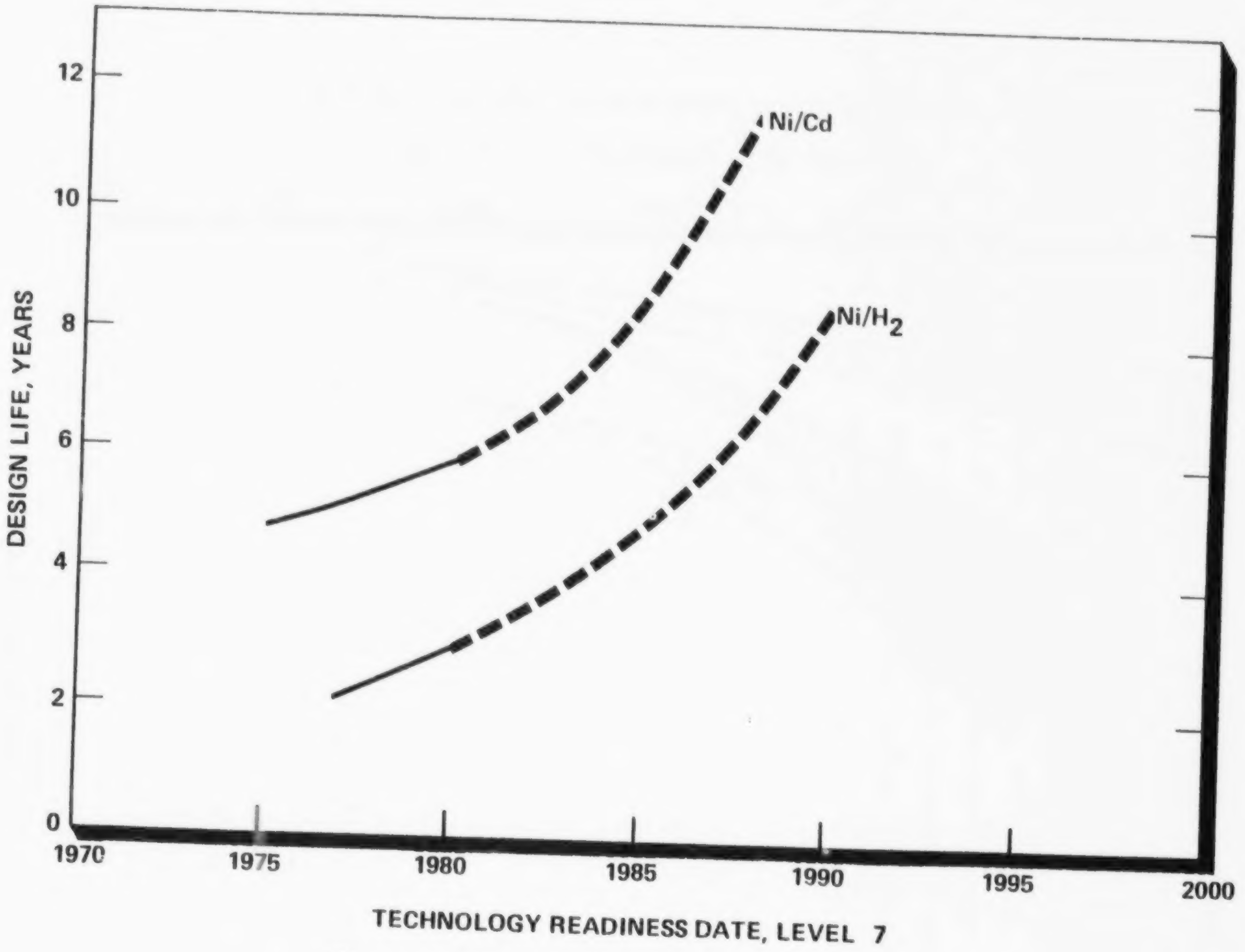

Figure 1.8. Battery Design Life (Geosynchronous Orbit)

system will become a high-volume product; therefore, it is expected to remain relatively costly. The high-energy systems are costly, but published projections show dramatic decreases dependent on mass production. However, the space cell will still be more costly than its terrestrial counterpart by 2.5-10 times, depending on capacity and extent of use. Figure 1.9 provides a projection.

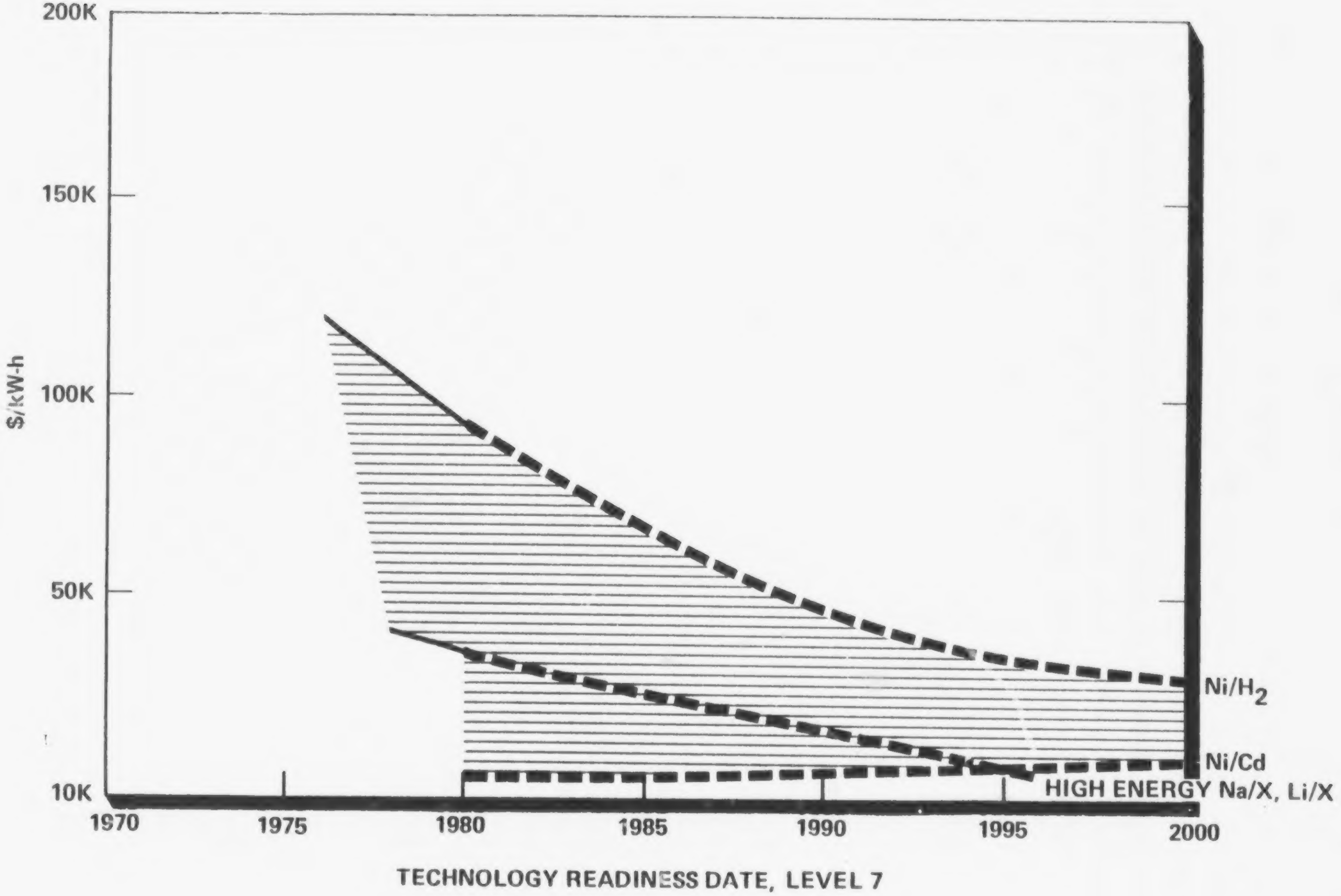

Figure 1.9. Secondary Battery Specific Cost

References

1. Energy Storage Systems for Automobile Propulsion, VCRL-52303, 15 December 1977, Contract W7405-Eng 8, Lawrence Livermore Laboratory.

2. A Collection of Technical Papers - AIAA/NASA Conference on Advanced Technology for Future Space Systems, 8-10 May 1979.

3. L. W. Sifer and W. J. Billerbeck, Synchronous Orbit Power Needs, NASA Technical Memo 80280, April 1979.

4. Future Orbital Power Systems Technology Requirements, NASA Conference Publication 2058, Symposium held at LeRC, 31 May-1 June 1978.

5. DOE Battery and Electrochemical Contractors Conference Publication, Volume II, 10-12 December 1979, held at Arlington, Virginia.

1.2.2 Fuel Cells

Fuel cells are presently used as power sources for the Shuttle and are envisioned as auxiliary power sources for orbital transfer vehicles (OTVs). Fuel cells integrated with an electrolyzer unit present attractive weight savings for low earth orbiting (LEO) satellites requiring multikilowatt energy storage.[1] Applicable parameters for the fuel cell power generation application are specific cost ($/We), power level (kW), specific power (W/kg), and design life. For the fuel cell-electrolyzer units for energy storage, the useful parameters are storage capacity (W-h/kg), design life (h), and specific cost ($/kW-h).

The present state-of-the-art space technology is exemplified by the alkaline electrolyte Shuttle Orbiter fuel cells, the lightweight fuel cell stack developed for future OTV applications developed by United Technologies Corporation and the solid polymer electrolyte (SPE) orbiter demonstration units, and SPE electrolysis units developed by General Electric. The orbiter fuel cell is at a flight readiness level; the lightweight OTV stack initial developmental testing is to begin in early 1980. Cost estimates are very nebulous. A study recently initiated[2] should help provide these figures, but no data are available as yet. However, orbiter fuel cells were built for delivery several years ago[3] at $40/W, and a lightweight stack could probably be built now for that figure. The orbiter stack operating on dedicated cryogenic reactants H_2 and O_2 was designed for a peak power of 12 kW with brief overloads to 15 kW and an average of 4.5 kW; however, the average load has now been pushed up to ~7 kW. The lightweight OTV stack is designed to use propellant-grade H_2 and O_2 reactants at a maximum power of 3.5 kW with an average load of 2.2 kW. The other large alkaline fuel cells built have been for Deep Submergence Rescue Vehicles (DSRV) and have had power levels of

---

[1] J. B. Trout, "Energy Storage for Low Earth Orbit Operations at High Power," Proceedings of AIAA/NASA Conference on Advanced Technology for Future Space Systems, 8-10 May 1979, Hampton Virginia.

[2] Energy Storage Subsystem Study, PRC Systems Service Company, Huntsville, Alabama, Contract NAS3-21962, (initiated 1 November 1979).

[3] R. E. Martin, United Technologies, Project Review, 30 January 1979.

20-35 kW. Specific power of these units is ~110 W/kg for the Shuttle fuel cell and ~150 W/kg for the lightweight OTV stack. These figures represent weights of the stack and accessories without power conditioning or gas supplies. Design life for the Shuttle power plant is 5000 h and for the OTV power plant 2500 h. The only present funding for development of space fuel cells (both SPE and alkaline) is found in the OAST 7-yr fuel cell-electrolyzer program being conducted by the Johnson Space Center and Lewis Research Center.

Terrestrial fuel cell systems are under development by the Department of Energy, Electric Power Research Institute, Gas Research Institute, and the Tennessee Valley Authority. The phosphoric acid system is the early entry with prototype modules from 40 kW to 10 MW to be ready for commercial entry be 1986. Technical feasibility units are going on test in 1980. By the early 1990s, the molten carbonate fuel cell for base load and cogeneration use in the megawatt to hundreds of megawatt size may be ready. The solid oxide electrolyte fuel cell may be available by the year 2000. It is uncertain what role, if any, these terrestrial fuel cell systems will play in future space activities but they illustrate the technological potential and offer potentially low-cost power generation at high efficiency.

The technology of combining fuel cells with electrolyzer units as an integrated system for energy storage is in the early development stage. Subscale units are currently being tested or about to be tested under LEO conditions, but a full breadboard model of the integrated system (6-7.5 kW) will not be tested for about 2 yr. Maximum power capability in LEO would probably be ~15 kW by 1985. Design life of the individual units at present could be estimated at 5000 h with possible improvement to 10,000-20,000 h by 1985.

A study has recently been completed[1] aimed at optimizing operating conditions, i.e., the pressures, temperatures, etc., of the various subsystems in order to minimize total weight of a storage system based on the SPE fuel cell and electrolyzer. Figures for alkaline components would probably be similar. From this study, a 35-100 kW system would weigh 35 kg/kW. This includes the recycling gas and water supplies, heat management, and the increase in the size of the solar array required due to the lower efficiency (20% less) of the fuel cell electrolyzer system compared to a battery system. To compare storage capacities for an individual orbit as is done for battery storage systems, with 0.6 h for the dark portion of each orbit, the result is 35 kg/0.6 kW-h, or 17 W-h/kg. If we consider only the weight of the fuel cell + electrolyzer units + gas storage without the thermal management and additional solar array penalty, we have a delivered storage capacity of 50 W-h/kg.

---

[1] Electrochemical Cell Technology for Orbital Energy Storage, General Electric Company, Direct Energy Conversion Programs, Wilmington, Massachusetts, Contract NAS3-15831, Monthly Report #4, 10 September 1979 (summary report in preparation).

Costs can only be estimated based on the present technology, and to facilitate comparison with the battery system only the storage components which would be replaced are included. Using the orbiter fuel cell cost of $40K/kW, the cost of the fuel cell-electrolyzer system would be about $100K/kW. If we estimate the life of present components to be about 1 yr, the total specific cost is $28.5/kW-h and the specific cost per orbit is $167K/kW-h. For comparison: commercial systems for terrestrial application cost approximately $350/kW when mass produced. The studies now underway[1] should give a better estimate of these costs.

It should be emphasized that both the estimates of total specific cost ($/kW-h) and total storage capacity (W-h/kg) are based on only modest improvements in the life of the components. A doubling of life would double the total storage capacity and halve the total specific cost. Increases in efficiency, pressure, and temperature of operation would also improve these figures. The conditions of the LEO orbit enter into the above calculations, which were done assuming a light-to-dark ratio of 3/2.

---

[1] Trout, op. cit.

The present state-of-the-art data and future trends are summarized in Figs. 1.10 through 1.13 for fuel cells and Figs. 1.14 through 1.16 for fuel cell-electrolyzer storage systems. Steady advances in technology are assumed. The earliest technology readiness date for the fuel cell electrolyzer system is shown as 1983 at the completion of the planned breadboard test. Specific costs for fuel cell electrolyzers are assumed to decrease as the size and number of units produced increases. Based on the GE study[1] which concluded that major reduction in weights of the fuel cell electrolyzer units and accessories were unlikely, a relatively slow increase is postulated in specific storage capacity per orbit as seen in Fig. 1.14.

It should be emphasized that the data base for space fuel cells and electrolyzers is very meager. The number of units and tests planned in the near future may not be sufficient to give reliable projections for a number of years.

---

[1] GE Monthly Report #4, op. cit.

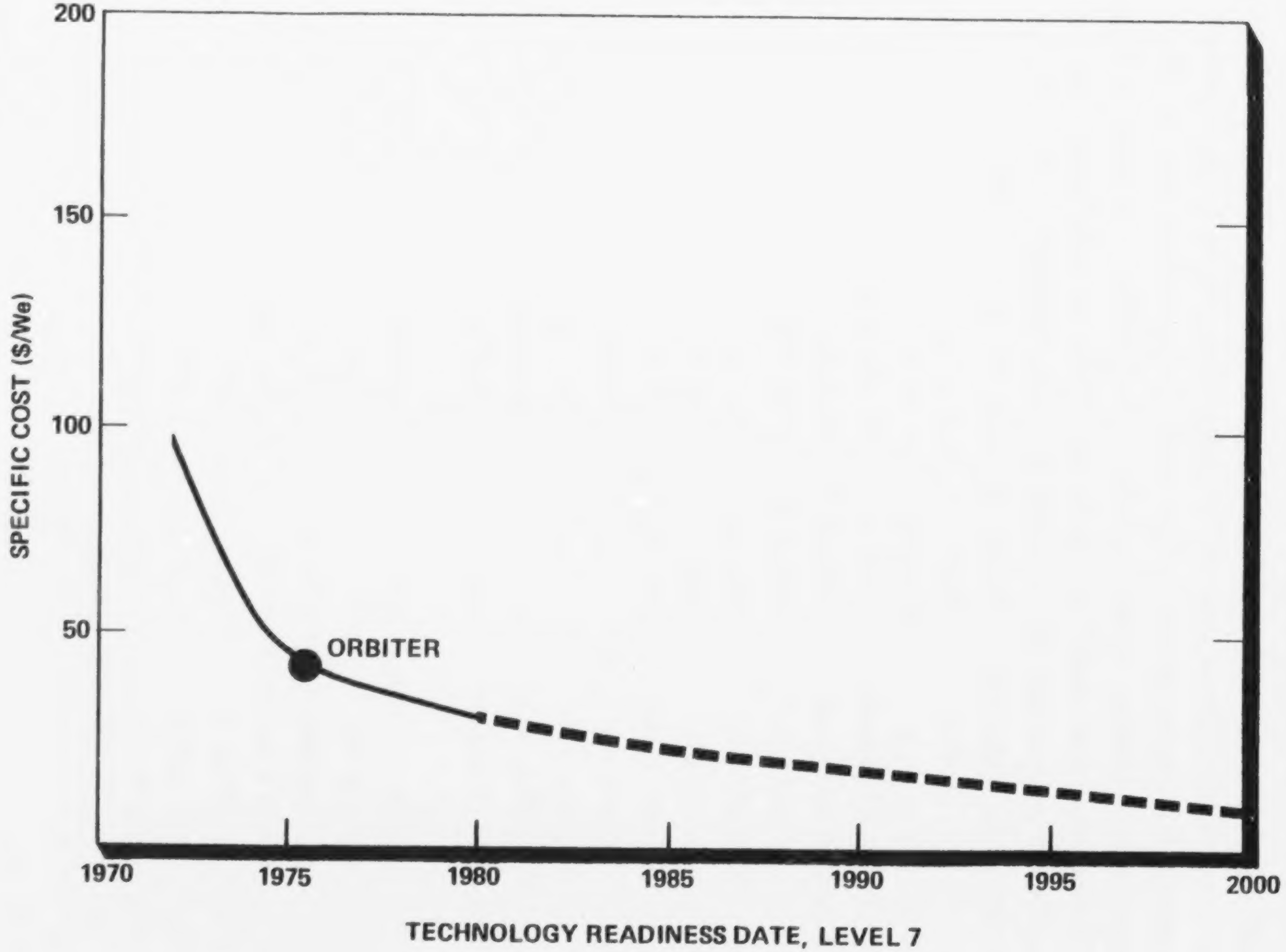

Figure 1.10. Fuel Cell Specific Cost

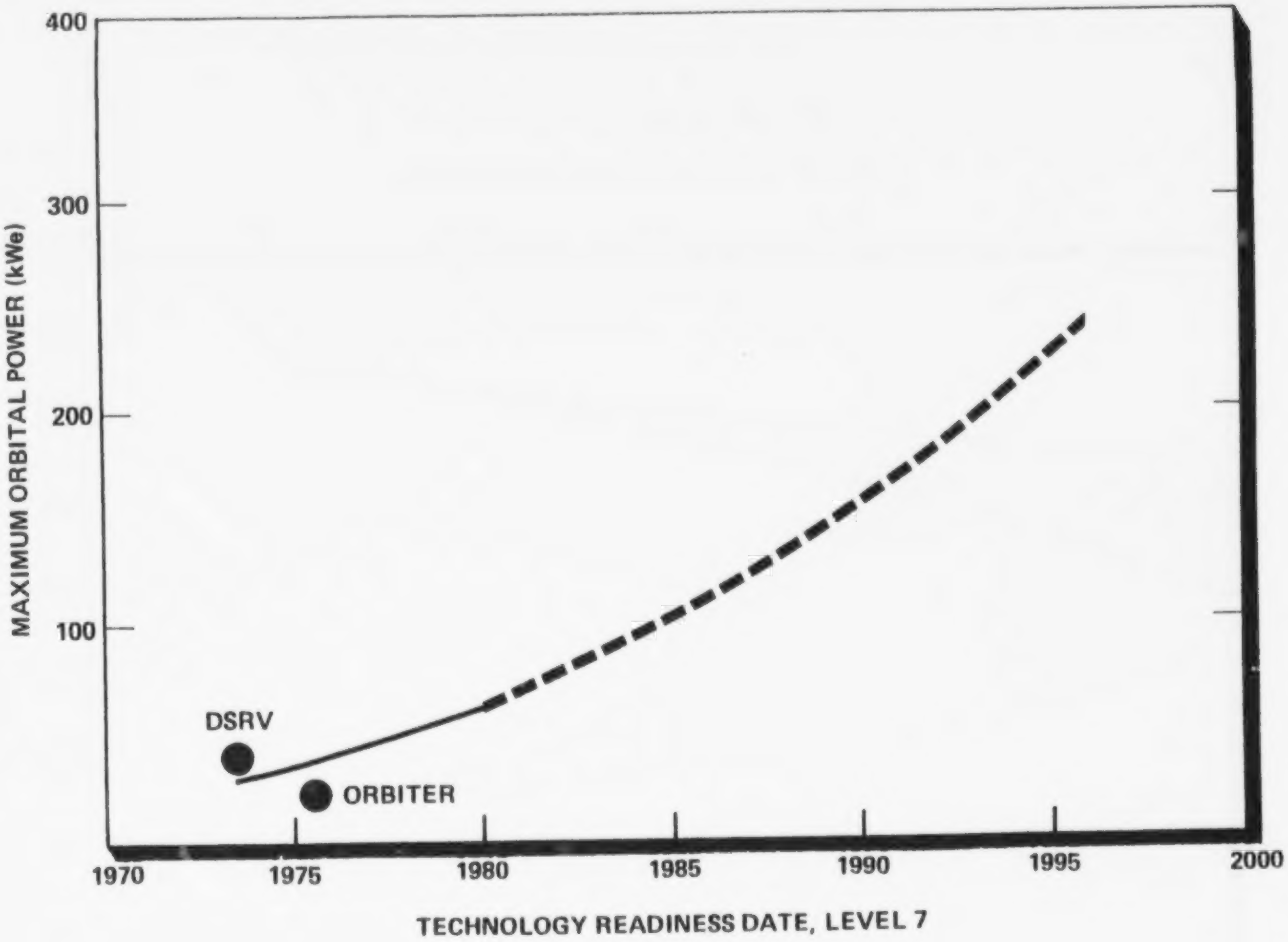

Figure 1.11. Fuel Cell Power Level

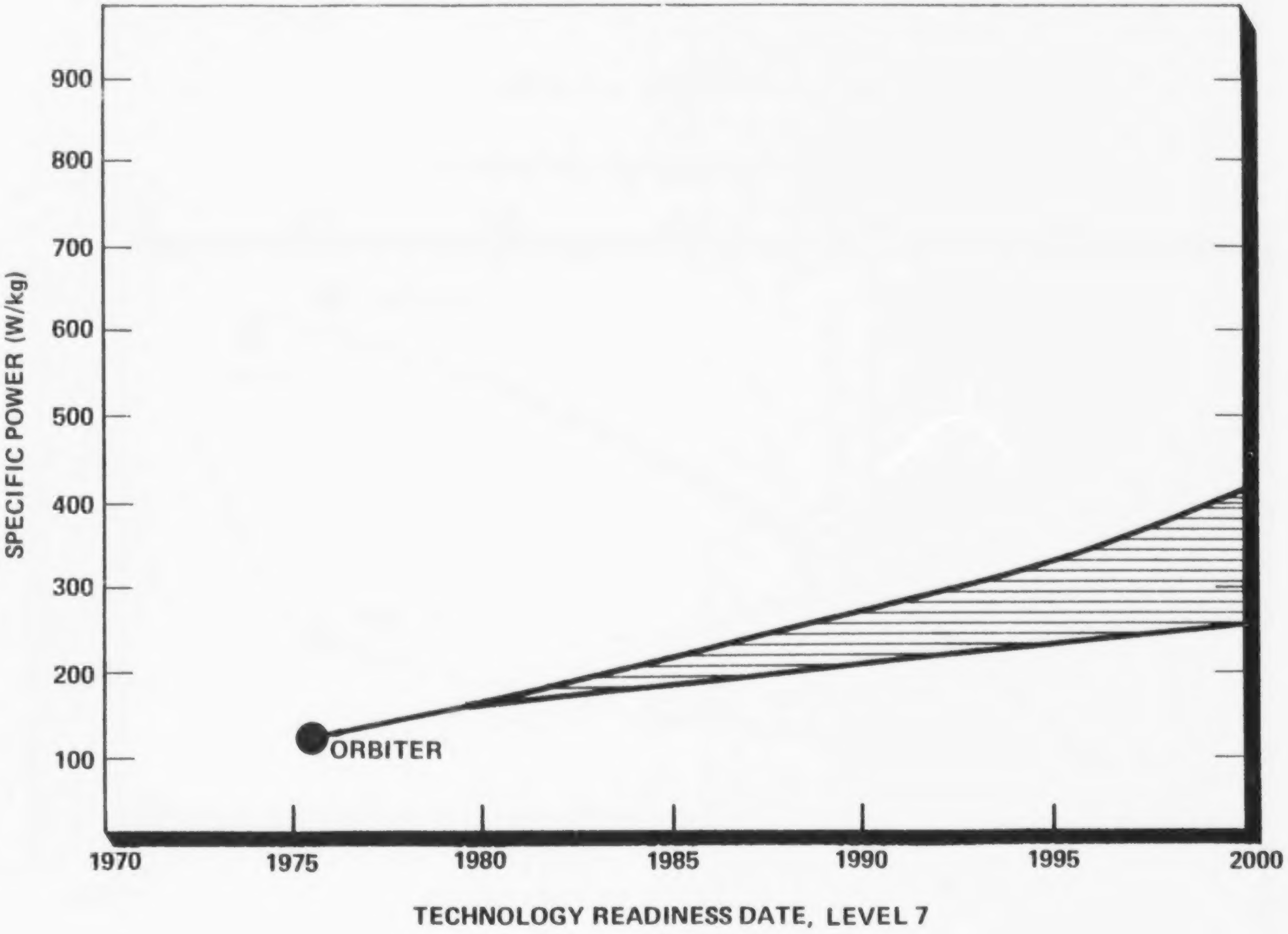

Figure 1.12. Fuel Cell Specific Power

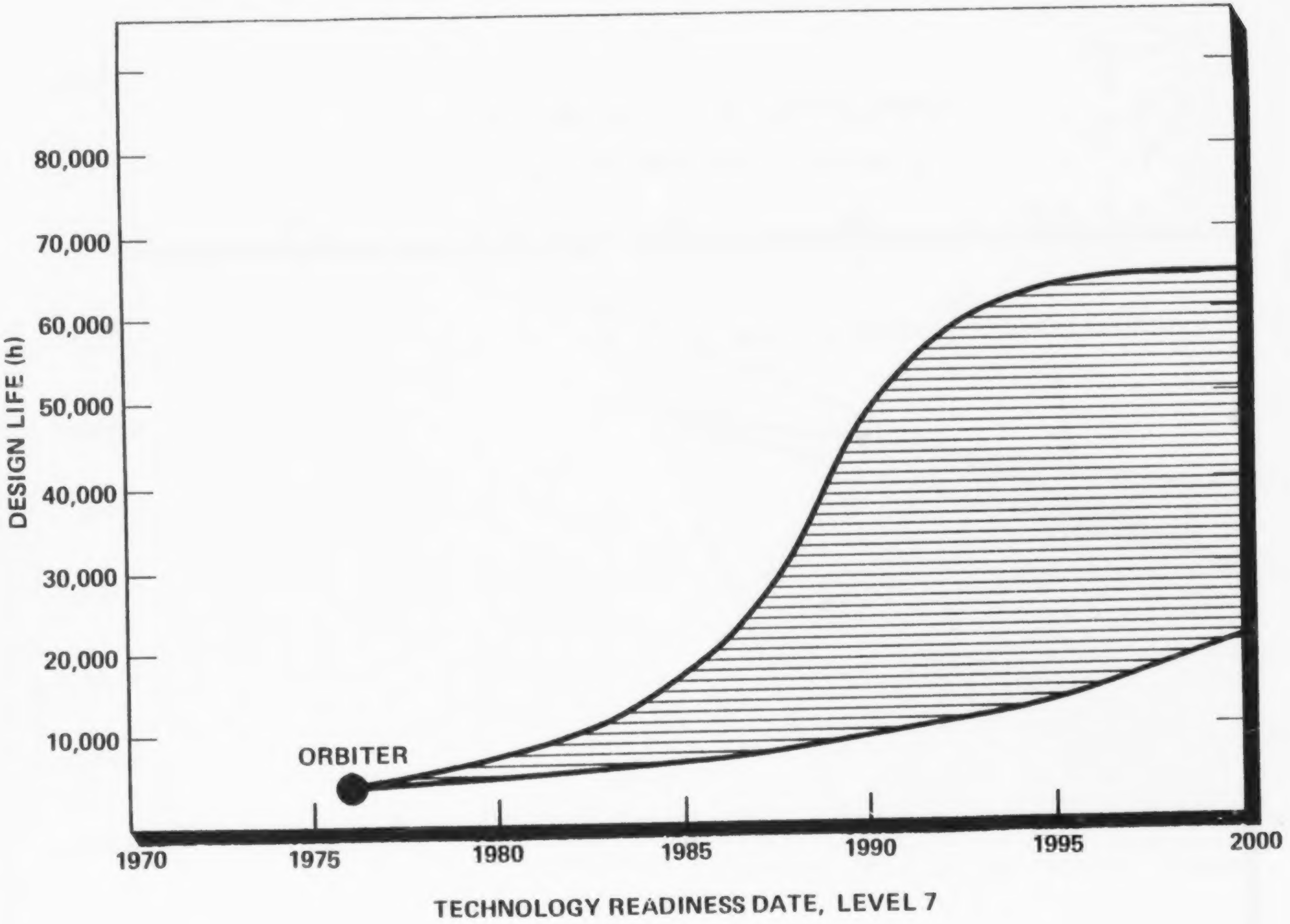

Figure 1.13. Fuel Cell Design Life

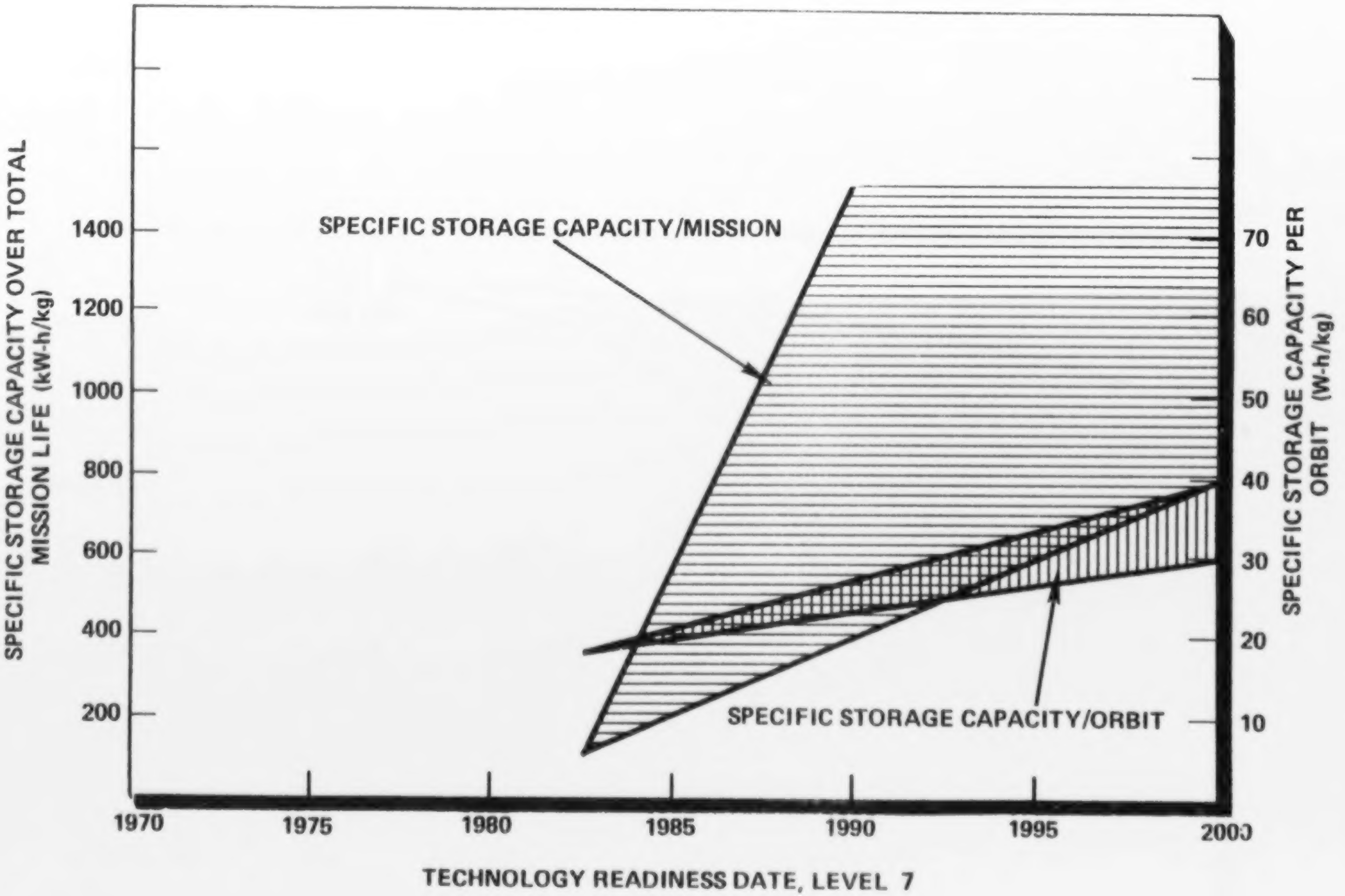

Figure 1.14. Fuel Cell Electrolyzer Storage Capacity

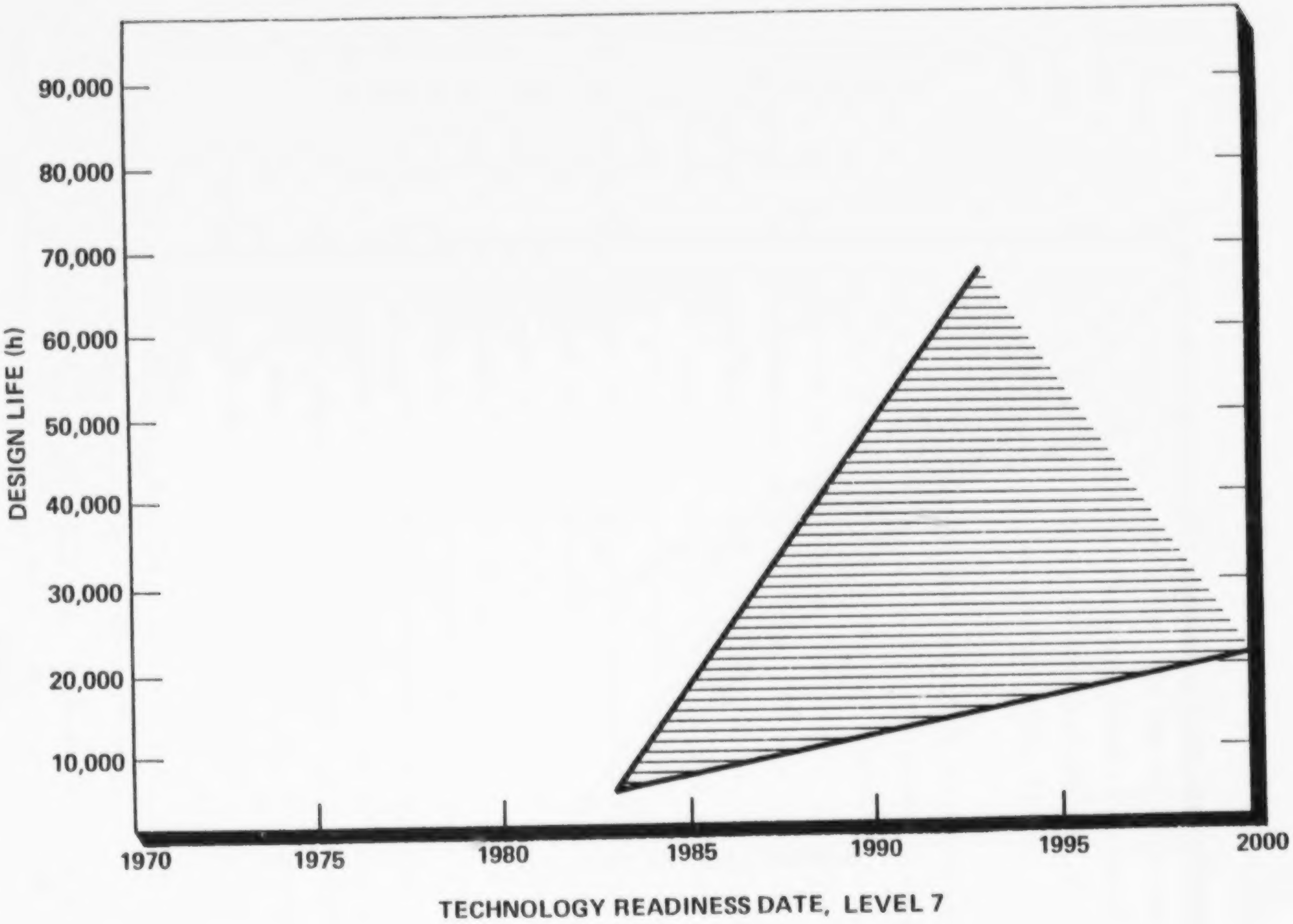

Figure 1.15. Fuel Cell Electrolyzer Design Life

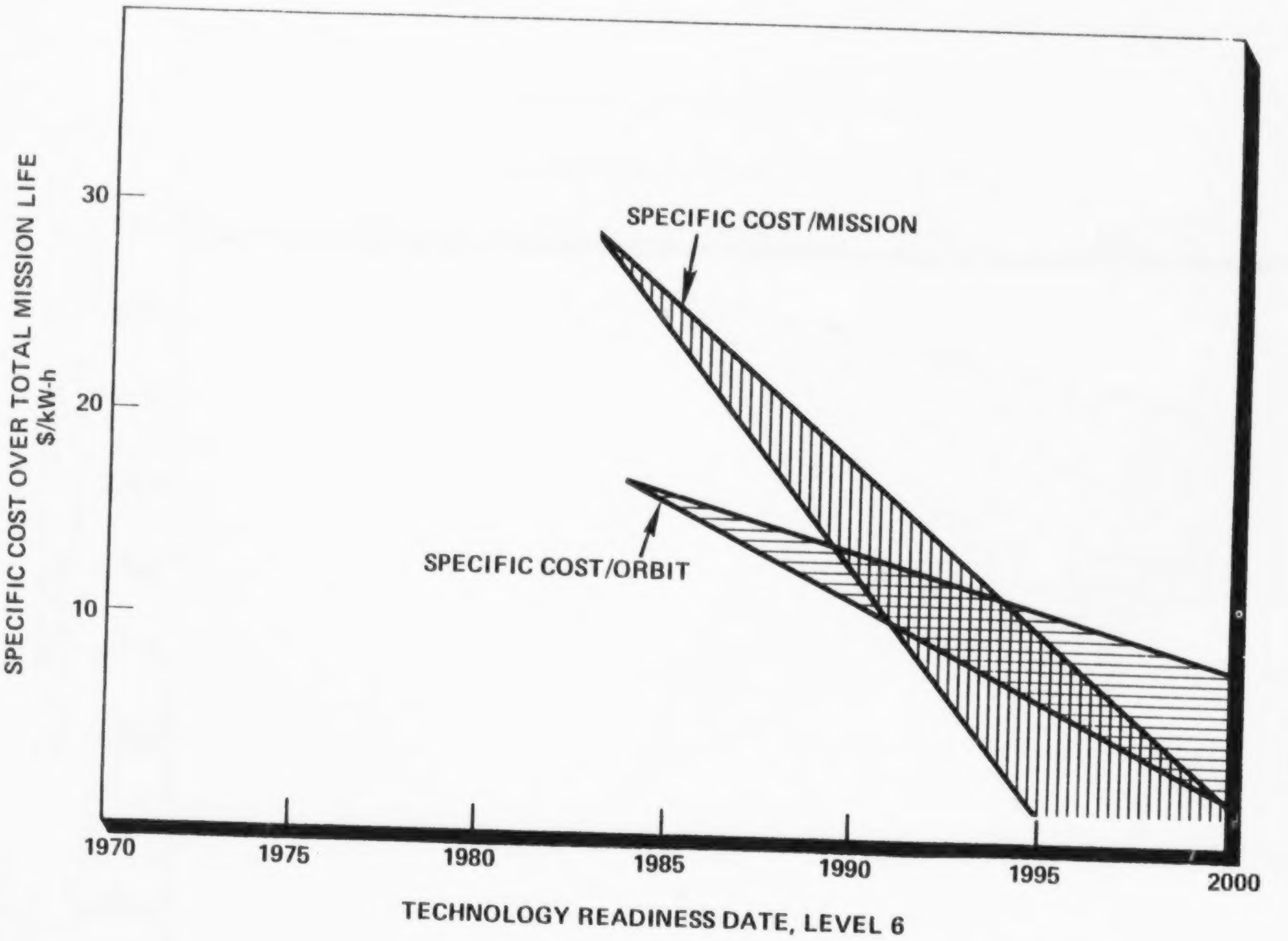

Figure 1.16. Fuel Cell Electrolyzer Specific Cost

1.3 THERMAL-TO-ELECTRIC CONVERSION

J. F. Mondt, Jet Propulsion Laboratory
B. J. Rock, Department of Energy

1.3.1 Space Power Reactor/Conversion Technology (J. F. Mondt, JPL; B. J. Rock, DOE)

Considerable past effort has been devoted to research on Rankine and Brayton cycle dynamic conversion systems. At the present time, emphasis is being placed on thermionic and thermoelectric conversion targeted at NASA nuclear electric propulsion applications and expected military and civil high orbit space power needs in the 1990s.

The NASA/JPL R&T development programs are directed at technology to raise the level of electric power available while reducing mass and volume, improving the efficiency of thermionic and thermoelectric converters, and increasing the lifetime of the converter components. The thermionic converter technology is approaching 12% efficiency at 1650 K emitter temperature. Efforts in thermionic research are being directed at improving efficiency and power density at 1650 K emitter temperature. Emitter and collector material screening effort is being conducted to select the materials for the converter. The screening is based on actual power performance data and electrode efficiency from operating converters. Development of thermoelectric materials with higher operating temperatures than 1300 K is also being investigated. The lanthanum, chromium, sulfide, selenide materials appear promising up to 1500 K. Silicon carbide is also possible for up to 1650 K. Development of thermoelectric materials or thermionic electrodes with 12 to 15% conversion efficiency would make an attractive 100-kWe nuclear power subsystem for low-thrust electric propulsion engines to be used for unmanned scientific exploration of our solar system and beyond.

Power Level (Fig. 1.17). For the outer planet missions, the maximum payload per single shuttle launch can be delivered by the maximum power system that will fit in the shuttle. At an assumed 15% system conversion efficiency, and a heat rejection temperature of 950 K, the maximum power nuclear electric propulsion (NEP) system is about 400 kWe. With this NEP, it is possible to deliver large payloads to circular

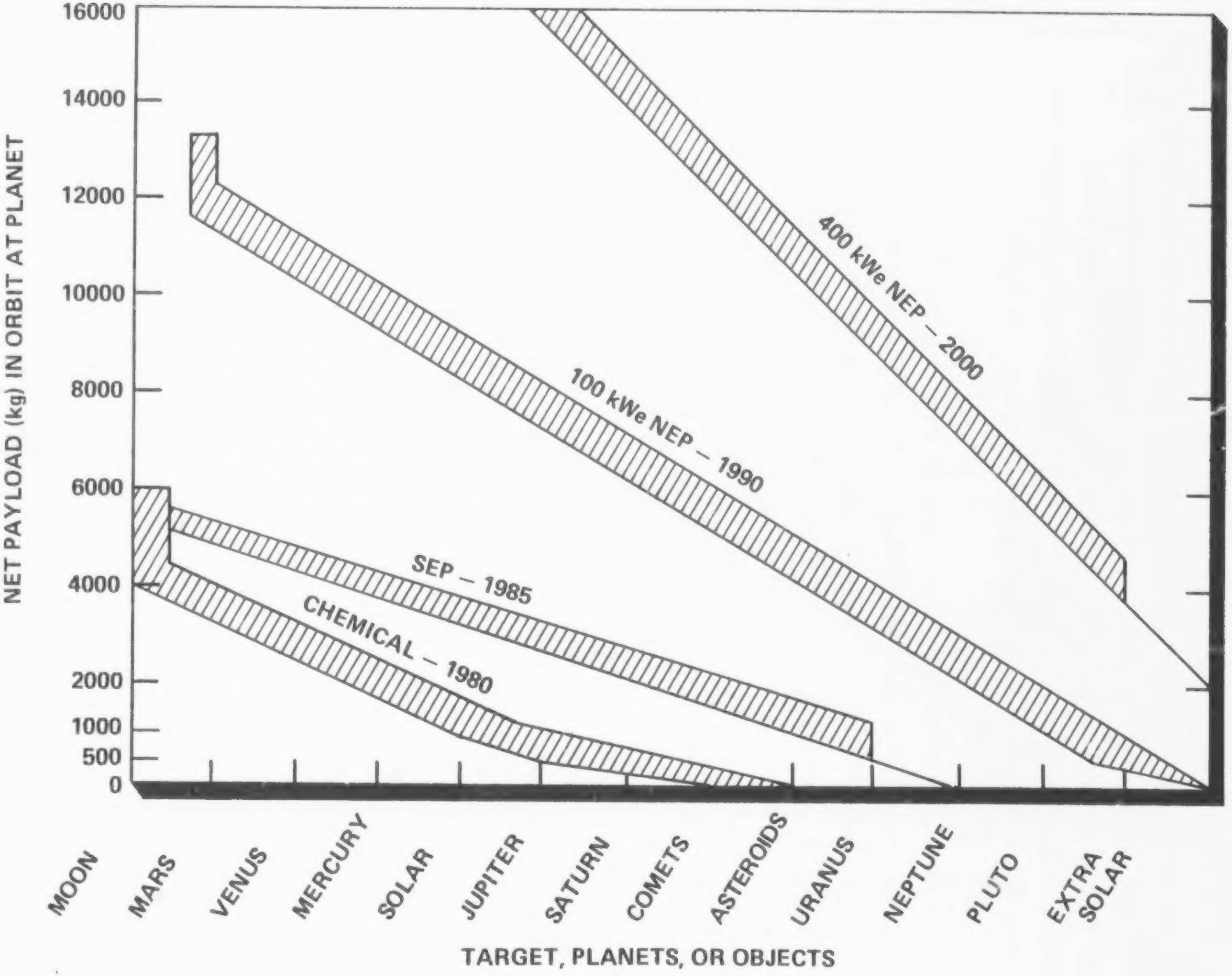

Figure 1.17. Power Levels for Electric Propulsion

orbits of any planet in the solar system with 10-yr mission times or less. Several future military and civil space applications require long life space power systems in the 10-100 kWe range. Since this requirement can be met with low power and low temperature, near term thermoelectric technology is expected to be adequate.

The electric propulsion missions can use the 100-kWe NEP system combined with a chemical stage in one shuttle launch to deliver 1000-8000 kg payloads to the outer planets. The chemical stage would boost the NEP stage and payload to high earth orbit or earth escape. Then the NEP stage would be used beyond earth escape to propel the payload to the target planet. This also allows starting the nuclear reactor in high earth orbit or after earth escape. The early reactor systems could be developed, tested, and used in space without nuclear radiation hazards to the earth. The 100-kWe system can also be used as a single stage from shuttle orbit, without the chemical stage, to deliver larger payloads to the outer planets, or larger payloads to GEO. Therefore, the first nuclear electric power system could be developed at the 100-kWe power level and used for both electric propulsion missions and other missions requiring 10-100 kWe of power in space.

DOE has a two million dollar a year Space Reactor (SPAR) Electric Power Supply Program in which components for a 10-to-100 kWe space nuclear reactor electrical power plant are being designed, fabricated and tested. Such a power plant will consist of: (1) a nuclear reactor for generator heat, including heat pipes for transferring the energy from the reactor to the power conversion equipment; (2) a radiation shield to attenuate radiation to an acceptable level for the payload; (3) thermoelectric (TE) converters to convert heat to electricity; and (4) a radiator for rejecting waste heat to space.

The present design calls for the following characteristics.

POWER PLANT CHARACTERISTICS AT 100 kWe

Efficiency (%)		9
Power (kW_t)		1110
Reactor temp (K)		1400
Radiator power (kW_t)		1010
Shield half angle (deg)		30
Mass (kg)		1755
Reactor	400	
Shield	380	
Converter	285	
Radiator	530	
Structure	160	

Specific Power (Fig. 1.18). The specific power of these nuclear electric systems is based on calculations since none of these systems has been built to date. However, using the present flight-qualified silicon-germanium thermoelectric material and existing reactor and heat-pipe technology, the calculated specific power is about 33 W/kg at the 100-kWe power level. Probable improvements in the thermoelectric materials or thermionics increase the calculated specific power to about 50 W/kg at 100 kWe. Optimistically, if the thermoelectric or thermionic materials now being developed in the laboratory work as predicted, the capability of a 100-kWe system could be 65 W/kg. Using these same materials at the 500-kWe level would result in a power system with a 100 W/kg capability.

Design Life (Fig. 1.19). Design life is defined for purposes of this discussion as the time from mission start to the time when the power output level from the power subsystem has decreased by 20% from its initial power. The thermoelectric materials on Voyager are designed for a 5-yr lifetime and have operated for 3 yr with little degradation in power. Thermionic converters have operated for 5 yr without degradation or failure at a higher temperature than required for this application. The limiting life component at the higher temperature is probably the nuclear reactor fuel element. The goals and component designs are all based on 10-yr lifetimes for electric propulsion.

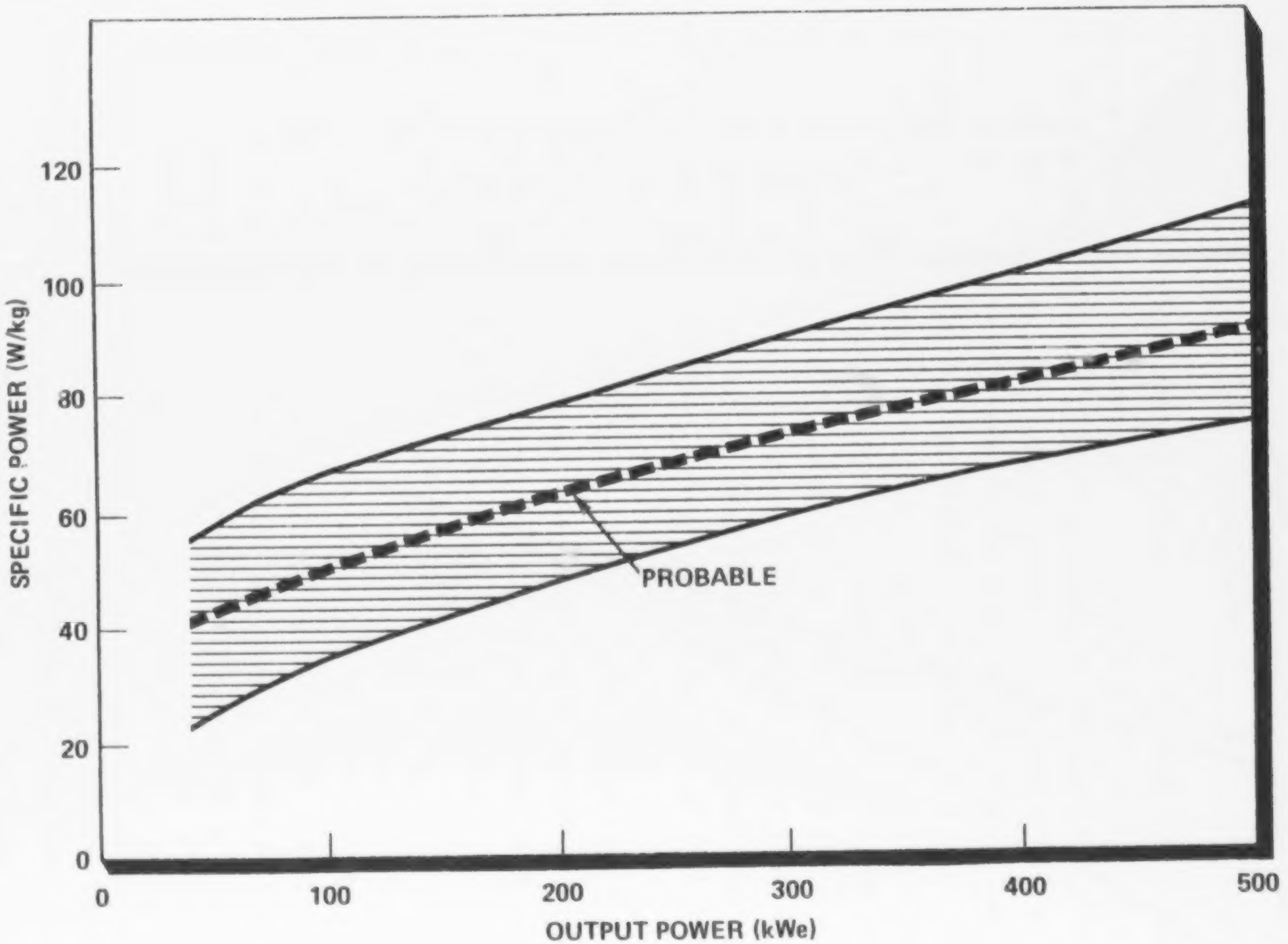

Figure 1.18. Specific Power, Nuclear Thermal-to-Electric Energy Conversion

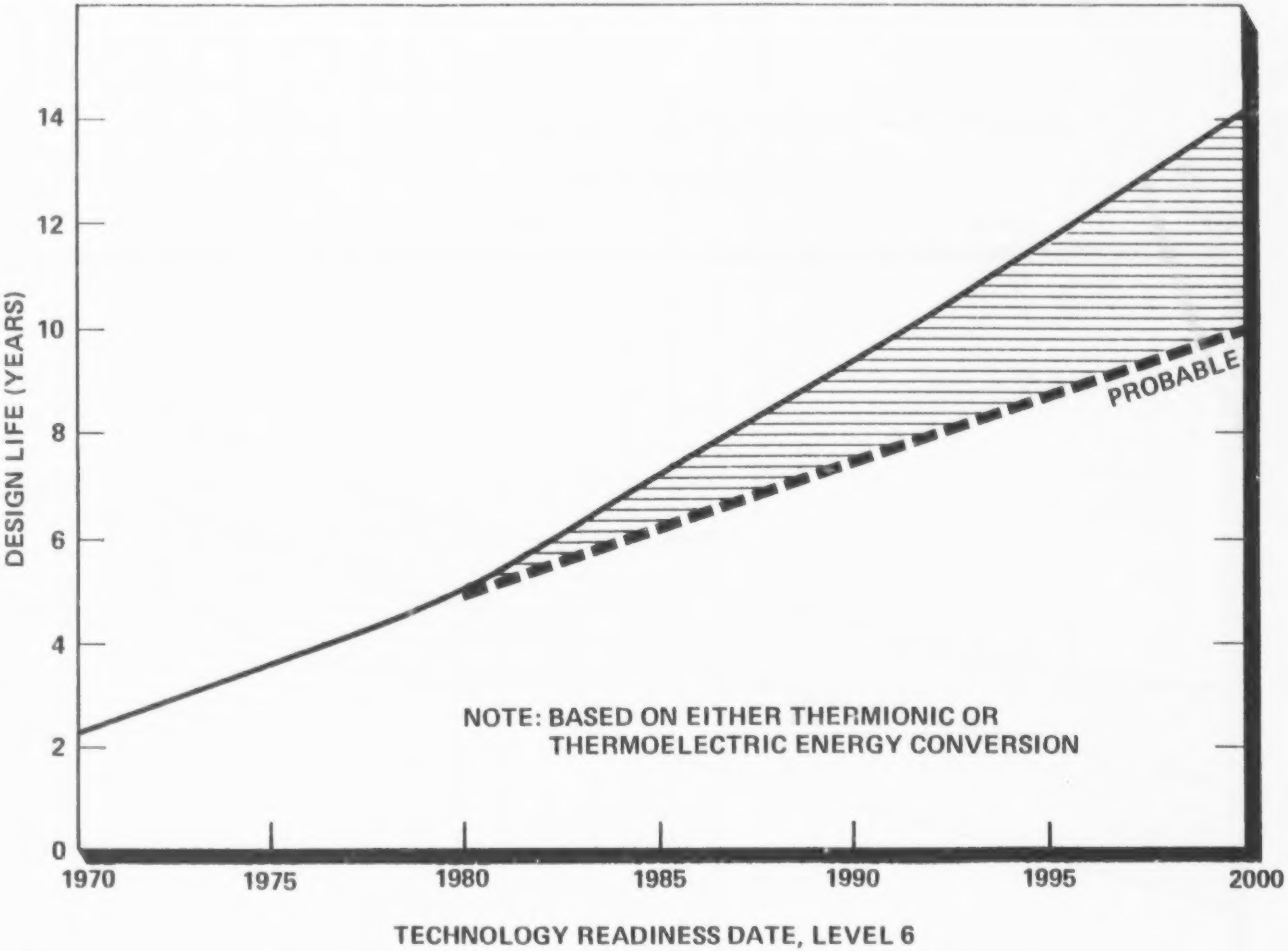

Figure 1.19. Design Life, Nuclear Thermal-to-Electric Energy Conversion

1.3.2 Radiosotope Generators (RTGs & Dynamic Systems)

Advances in RTG technology are measured by three major parameters: increased energy conversion efficiency, higher specific power, and longer lifetimes at the optimum performance level.

Increasing the conversion efficiency is possible through the development of thermoelectric materials exhibiting higher figure of merit (z) as well as increasing the operating temperature difference. A maximum temperature is set by the isotope fuel capability. This is currently 373 K, higher than the thermoelectric material capability. Therefore, the RTG performance can be improved by developing a thermoelectric material with a higher temperature capability, and this is being investigated in the present NASA technology program. A higher temperature material operating at temperatures below its capability can operate for longer lifetimes. Increases in specific power are also possible through the development and use of low density thermal insulation and the use of high strength, low weight structural members such as carbon alloys.

The RTG technology being developed and supported by DOE is concentrating on the fuel, fuel capsule, and thermal electric conversion technologies. The NASA R&T program is directed primarily at improving the conversion efficiency of the thermoelectric materials through increased figures of merit and operating temperatures.

In the thermoelectric materials area, DOE has a 1.5 million dollar thermoelectric program in FY 80 to develop higher efficiency thermoelectric materials by developing new materials, by improving standard materials through modifications such as alloying and by segmenting new materials with existing standard materials.

There are presently three major and three supportive ongoing thermoelectric materials development projects managed by the Power Systems Section of the Advanced Nuclear Systems and Projects Division of DOE. The ongoing projects are:

- 3M - This project utilizes pressure contacted selenide thermoelectrics, the P-leg is Cu_2 Ag Se and the N-leg is Nd Se_x. A thermoelectric material conversion efficiency of 10.5% at the T_H of 850°C is the goal.

- General Atomic - This project utilizes selenide thermoelectric materials segmented with various standard, state-of-the-art thermoelectric materials. The resulting bonded legs will be used in a radiation coupled TRANSIT type converter design. Very light weight as well as high conversion efficiency is the objective sought.

- Syncal - This project is based on bonded silicon-germanium couples in a radiation cooled configuration. The silicon-germanium is modified by the addition of gallium phosphide for the purpose of reducing thermal conductivity and thereby increasing conversion efficiency. A thermoelectric materials efficiency of at least 9.5% in a proven couple configuration at the T_H of 1000°C is the goal.

- Teledyne Energy Systems - This effort is to investigate the fabrication of segmented selenide-TAGS thermoelectric P-type legs.

- Ames Laboratory (Iowa State University) - This work is to investigate the rare earth sulfides and selenides as potential thermoelectric materials. The investigations focus on the method of preparation, electrical, and thermal properties and thermal stability.

- Jet Propulsion Laboratory (JPL) - The objective of this work is to evaluate thermoelectric technology by:

(1) Conducting experimental tests on materials, couples, and modules produced by other contractors to confirm thermoelectric characteristics, thermophysical properties, and long-term stability; and

(2) Conducting long-term life test of electrically heated thermoelectric generators.

A list of calculated RTG parameters based on the segmented selenide thermoelectrics with a hot junction temperature of 750°C and a cold junction temperature of 139°C are as follows:

REFERENCE DESIGN TABLE 1 SUMMARY

Material	
P leg	$(Cu,Ag)_2Se/(BiSb)_2Te_3$
N leg	$GdSe_{1.5}/PbTe$
T_H	750°C
T_C	139°C
Number of couples	748
Number of circuits	4
Voltage/Couple	0.156 V
Electric Power	286 W
Thermal Power	2750 W
System Efficiency (BOL)	10.4%
Voltage	30.8 V
Generator size	
Diameter	26 in
Length	30 in
Generator weight	84.3 lb
Fuel	PuO_2
Fuel form design	GPHS
Design lifetime	5 yr
Specific power (BOL)	3.39 W/lb

The use of selenides, when segmented with other thermoelectric materials, appears to have promise of obtaining higher performance without pushing the temperature limits. It is anticipated that generators of even higher specific power will evolve using this or other advanced technology as a basis.

The specific power for RTGs has increased from 2W/kg for missions during the 1960s and early 1970s to 4 W/kg for the Voyager mission (Fig. 1.20). The specific power for Galileo is 4 W/kg (same RTG as on Voyager). The specific power for the international solar polar mission (ISPM) is 5 W/kg. These are lower than projected since the selenide technology failed to meet its anticipated capabilities. The future projections and goals are based on the successful development of the advanced sulfide thermoelectric materials. Higher specific power levels than those projected are potentially possible only through increasing the isotope heat source temperature capability. Such changes are, however, largely constrained by radiation shielding and safety requirements.

The system conversion efficiency of RTGs has steadily improved (Fig. 1.21). The improvements are due to material advances as well as increased operating temperatures. The future projections and goals are predicated on the development of new thermoelectric materials such as the sulfide system.

The technology goals are 9% system efficiency by 1985, which assumes an improved silicon germanium alloy operating between 1300 K hot junction and 425 K cold junction temperatures. It is projected to have a 15% system efficiency by 1990, with a new thermoelectric material operating between 1375 K (present isotope heat source capability) and 425 K cold junction temperature.

The design life for RTGs is usually dictated by the specific mission requirement. The degradation in output power for any RTG will be determined by the thermal power decay rate of the radiosotope fuel (half power after 87 yr for Pu 238). Many of the RTGs used in the mission shown on the graph of Fig. 1.22 have operated considerably longer than

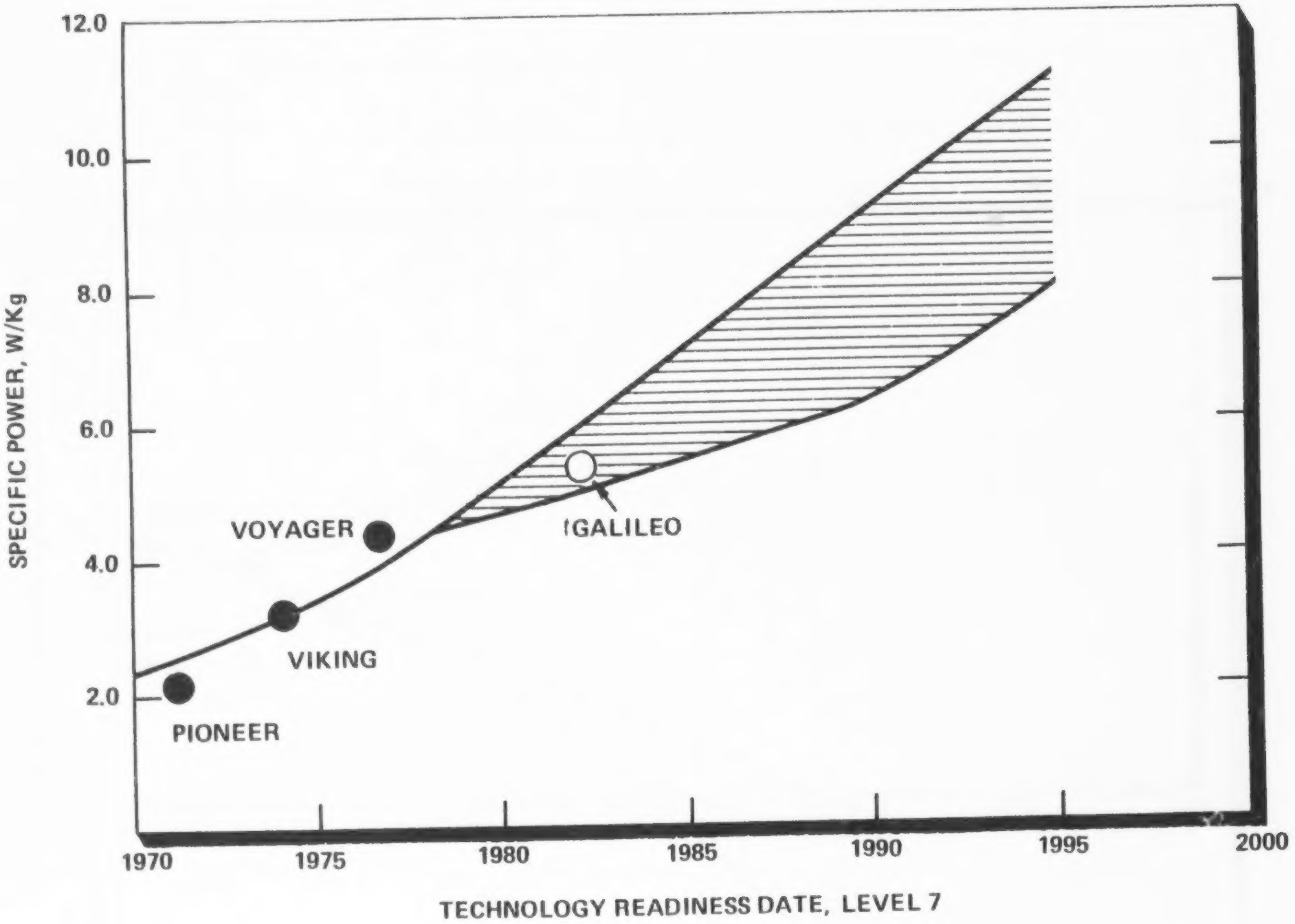

Figure 1.20. Expected Specific Power of Radioisotope Generators for Space Power

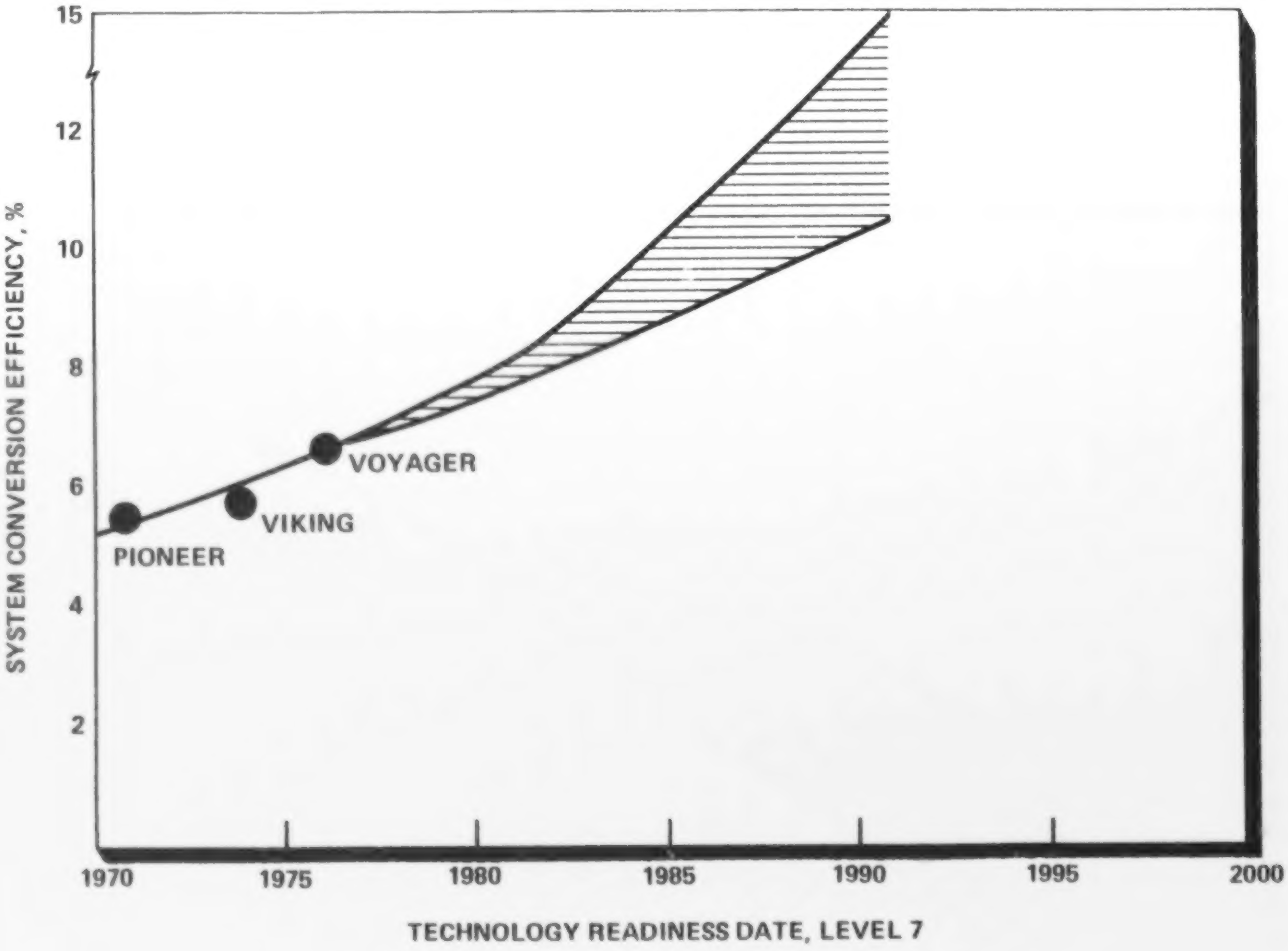

Figure 1.21. Expected Efficiency of Radioisotope Generators for Space Power

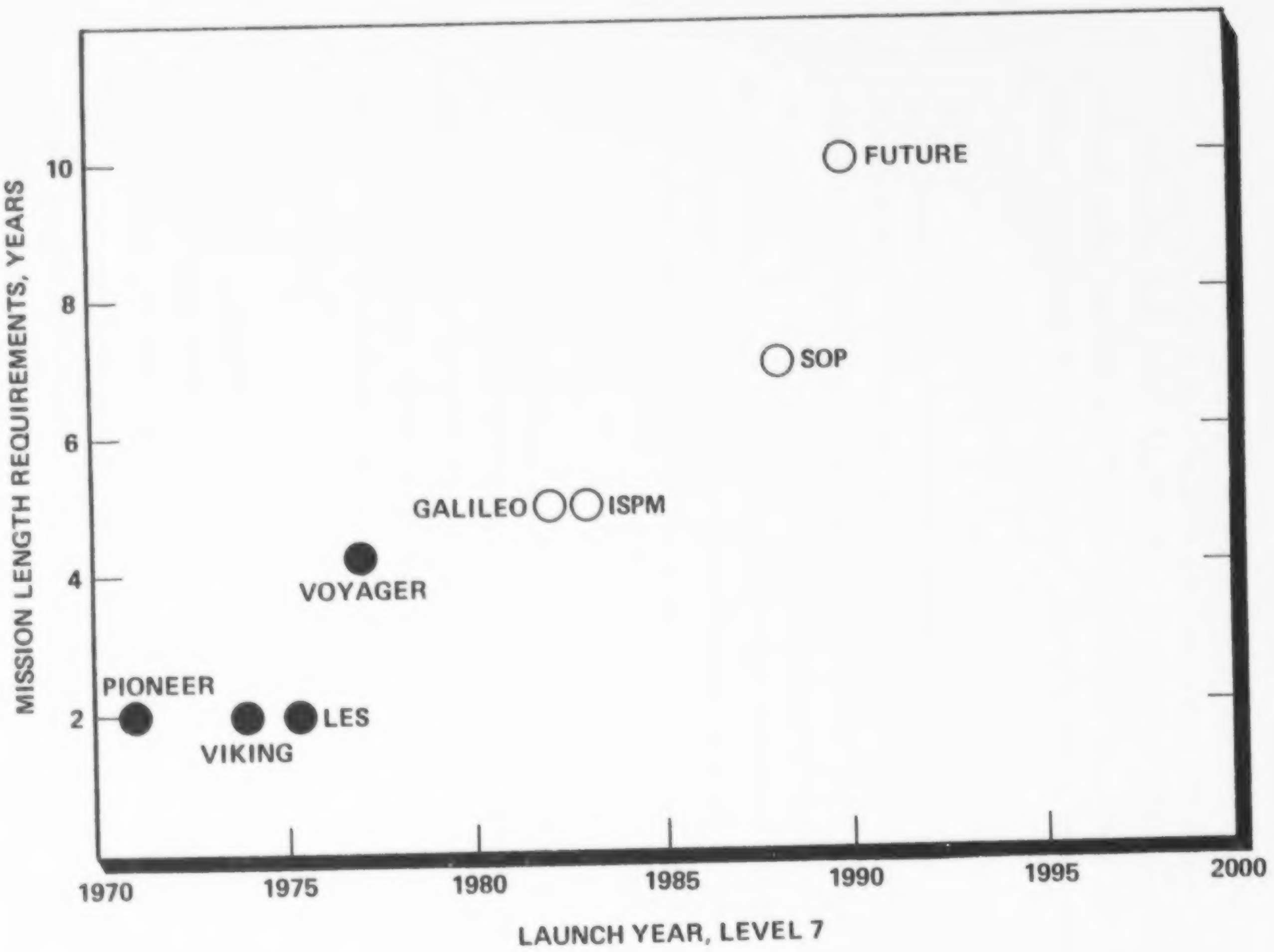

Figure 1.22. Lifetime Requirements for Space Power Missions

their original design life requirements. For most application, thermoelectrics can be designed to match the isotope fuel lifetime, but only at the expense of specific power and efficiency, simply by decreasing the operating temperatures. The operating lifetime of a given RTG is directly related to the hot junction operating temperature. Higher temperatures reduce RTG lifetimes due to higher material sublimation rates, diffusion rates, interaction rates, etc. A design life of 10 yr, as shown on the graph, is based RTGs designed for maximum specific power and efficiency, with a 20% reduction in power out at the end of the 10-yr life.

The specific cost of RTGs cannot be realistically assessed at present. In part, this is due to uncertainties in government-controlled fuel costs as well as developmental costs (which are primarily funded by DOE). Per interagency agreement, NASA traditionally uses the first RTGs for any mission free of cost and pays for the use of any additional ones. The cost of the RTGs that NASA buys is based on the total DOE development costs divided by the total number of flight type RTGs that DOE produced during development.

Considerable past effort was expended by both NASA and DOE to develop the technology for dynamic isotope power systems at power levels ranging up to 10 kW. Both Brayton and organic Rankine cycles were pursued. In the face of an expected near term military flight requirement, the organic Rankine system was selected for further technology verification in a DOE program.

The Department of Energy has also funded application studies for assessing the integration of the organic Rankine power system into various potential DOD spacecraft missions. These studies indicate that the pumped liquid loop feature of the Organic Rankine Dynamic Isotope Power System (DIPS) can offer significant protection of a satellite against certain hostile threats. This is in addition to its other inherent attributes such as:

- Increased user power
- Extended mission duration
- Improved orbit prediction
- Spacecraft thermal control enhancement
- Orbit/orientation insensitivity

The current Department of Energy program (two million dollars in FY 80) is planned to be completed on 1 October 1980. The flight system objectives are defined as follows:

Power	1.3 kWe
Voltage	28 V DC
Lifetime	10 yr
Reliability	0.95
Weight	≤450 lb for a non-integrated system - includes power conversion system, heat source assemblies with isotope and space radiator

1.4 POWER SYSTEMS MANAGEMENT AND DISTRIBUTION

W. R. Hudson, NASA Headquarters

The power systems management and distribution technology program is advancing on a broad front to provide the basic technical understanding necessary to assure environmental compatibility and to control the generation and distribution of energy in future space systems. The program seeks to develop critical components, circuits, and subsystems which permit the simultaneous achievements of low-cost, high-power space energy systems. The interaction of the space plasma environment with high voltage systems, spacecraft, and large space structures is also being investigated. To date NASA has launched individual spacecraft with at most a few kilowatts of power-generating capability. The cumulative total solar power generating capability launched to date is approximately 100 kW. There are many missions on the planning horizon (just beyond the 5-yr plan) that require large increments in space power. Figure 1.23 depicts the two classes of demand that were identified in the 1979 space power cross-cut study. The historical average cost of space energy systems has been very high: in the range of $1000/kW-h. For the projected missions to be feasible, unit energy costs must be reduced by a factor of 10 to 100.

A key element of future high power space systems is the development of components such as power transistors, switches, and capacitors. The recent development of high-voltage switching transistors in the range of 600 V and 100 A is a good example. This program is continuing and doubling of both the voltage and the current is projected by the end of FY 1983.

Another example is the heat-pipe-cooled transformer. At higher power levels, heat-pipe-cooled components have the potential for greatly reducing mass, increasing operating life, and raising the upper limit of power handling capability. For a 2.4-kW heat-pipe-cooled transformer, 40% less mass was required than a standard conduction-cooled transformer. It also operated at 20°C lower mean winding temperature, and lower temperature implies longer operating life.

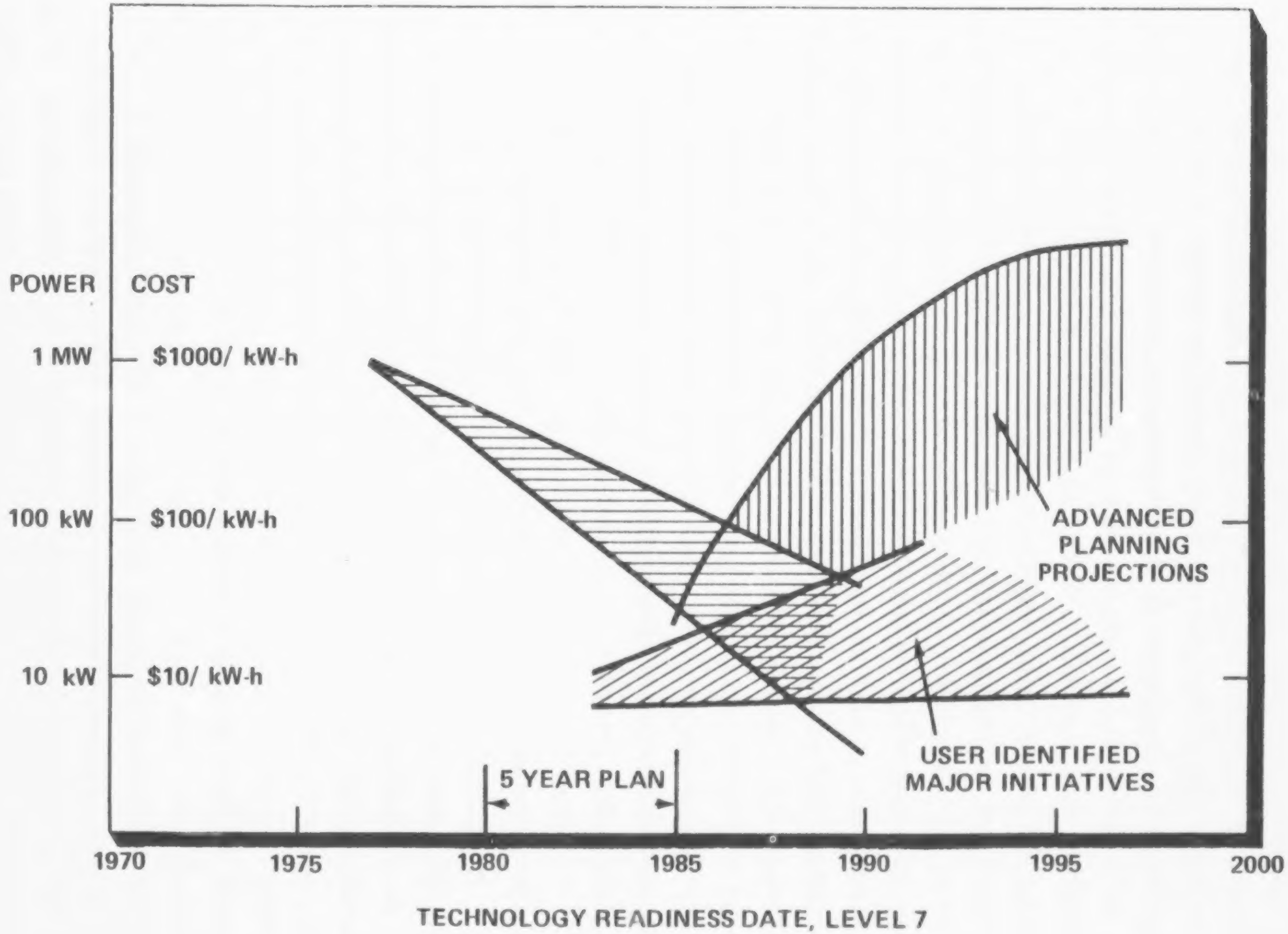

Figure 1.23. Projected Space Power Demand

These are just two examples of component technology programs. Other areas include lightweight, high voltage capacitors, solid-state switch gear, power MOSFETs, and rotary power transfer devices.

An important subelement of the power system management area is high-power circuit technology. This area includes circuits for power inverters and converters. A program goal of 1 kg/kW for high-power conversion equipment has been set. Three basic types of inverters and converters are presently being explored: the series-resonant inverter, the capacitor diode voltage multiplier, and the conventional converter.

Future missions will require the capability of a spacecraft power system to automatically perform monitoring, computation, command, and control functions without the need for ground intervention. Future outer planetary exploration missions will result in long round-trip signal time delaying or preventing proper power system management from earth. Fabrication of an automated power systems management breadboard has been completed and it is currently undergoing functional verification tests at the Jet Propulsion Laboratory. The objective of the effort is to demonstrate the capability of a spacecraft power system to automatically perform monitoring, computational, command and control functions.

For missions in hostile environments special power systems may be required. An orbiter of Mercury is one such mission. Because silicon solar cell technology is not viable in the expected high-temperature environment, solar thermoelectric generators are being examined as a possible power source. Current designs under study would provide 350 W at 0.45 A with an area of 3.24 m^2 and a mass of 19.8 kg.

Environmental interaction is also part of the power management and distributions program. This includes efforts in spacecraft charging and in the interaction of high voltage systems with the ambient space plasma environment.

The present distribution voltage (Fig. 1.24) for the Shuttle Orbiter is 28 V. The major driver for distribution voltage is the conductor weight required to carry high currents. Figure 1.25 shows the strong inverse dependency of power distribution weight on voltage for a 130-kW system. To be feasible, the distribution voltage must be in the vicinity of 300 V. Note the relative insensitivity of power conditioning and switch gear mass to system voltage.

Any prediction of future distribution voltage is then almost predetermined by the system power level and size (length of conductor runs). Up to 1-kW power levels, 28-V distribution is practical. At 10-kW levels, it becomes necessary to increase the voltage to 120 V (about household levels). In like manner, at 100-kW power level the voltage increases to 300 V and at 1 MW it increases further to 1000 V. The NASA program to develop components and circuits has focused technology development on these three voltage levels. One further consideration is that between 500 V and 1000 V the interactions of high-voltage systems with the space plasma become a concern at low altitudes (relatively high plasma densities).

There are two basic power distribution systems under study for power distribution on multi-hundred kilowatt systems: AC and DC. On a life-cycle cost basis, the two approaches are approximately equal; the AC costs are projected at $0.32/kW-h, and the DC costs are $0.40/kW-h. For comparison purposes, the power management system for Halley Class solar electric propulsion system was $32/kW-h.

As discussed in a previous paragraph, bus weights are a strong inverse function of voltage. Therefore, it follows that transportation-to-orbit costs decrease with voltage. As shown in Fig. 1.26, the hardware costs rise slowly as voltage increase. In addition, efficiencies improve and component losses are reduced, thereby reducing the cost of solar array components and batteries. Figure 1.26 also shows that the function has a broad minimum for multi-hundred kilowatt systems, and a voltage of 1000 V seems like a good number for further development work.

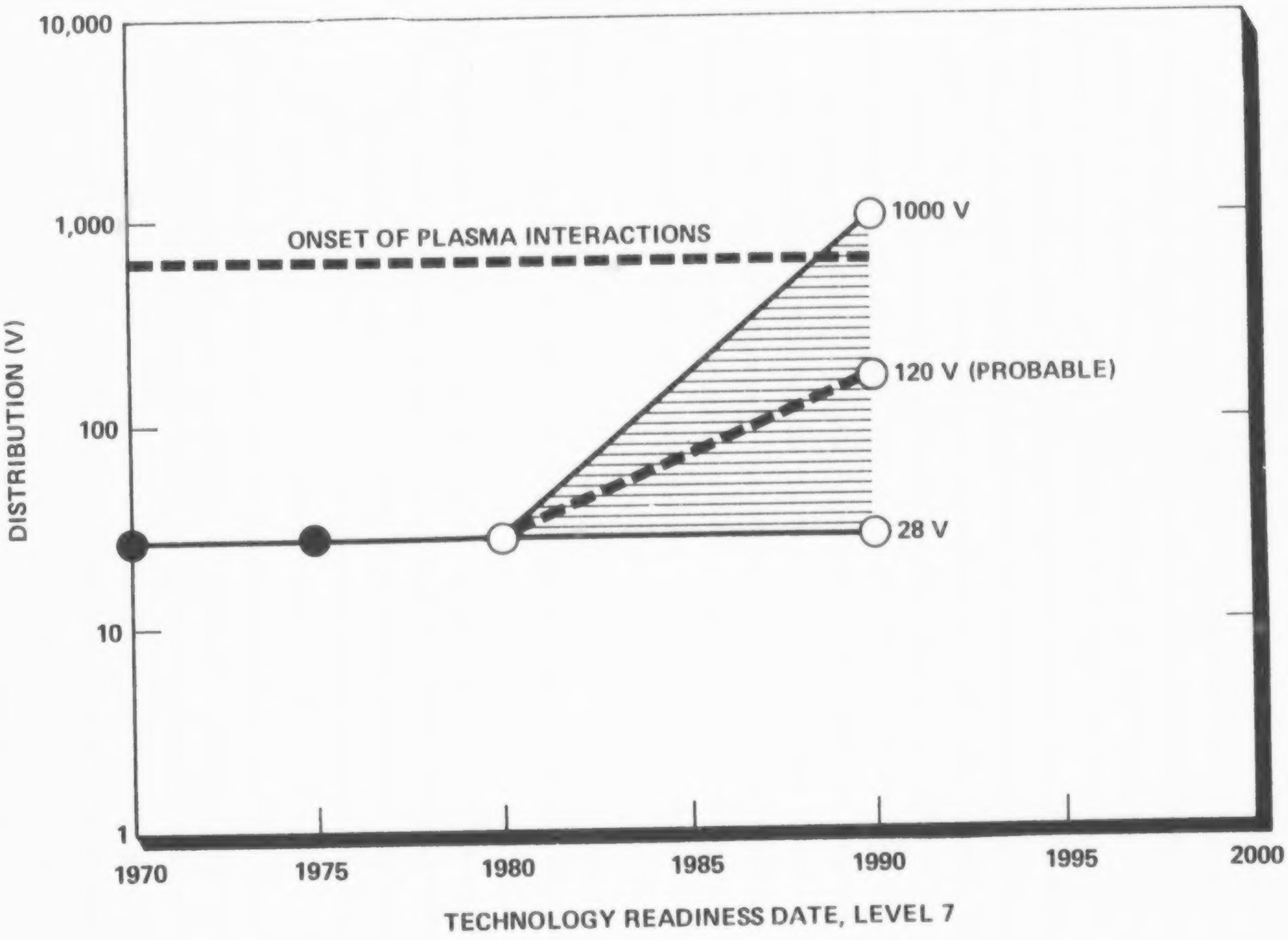

Figure 1.24. Power Distribution Voltage

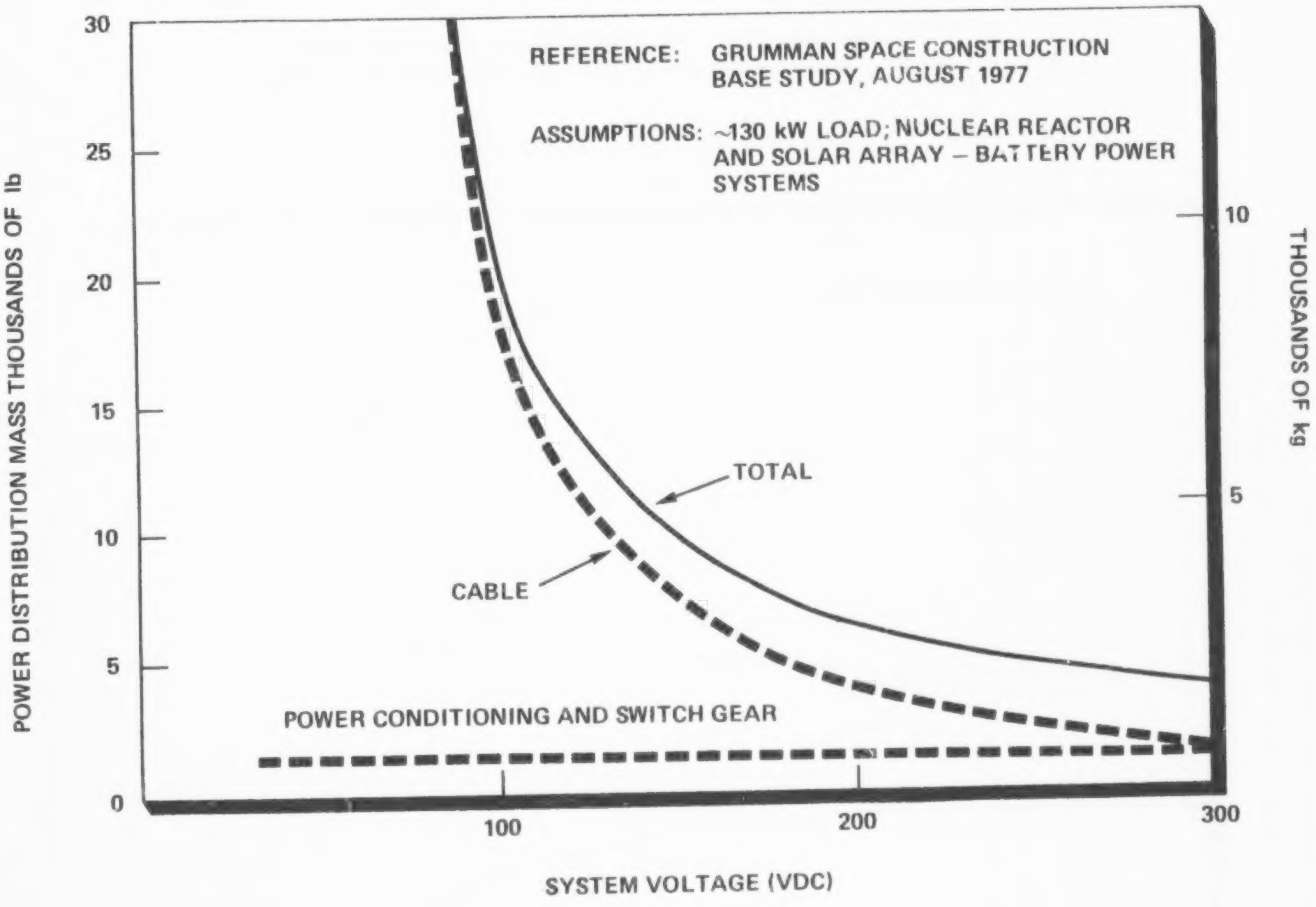

Figure 1.25. Power Distribution Mass vs. System Voltage

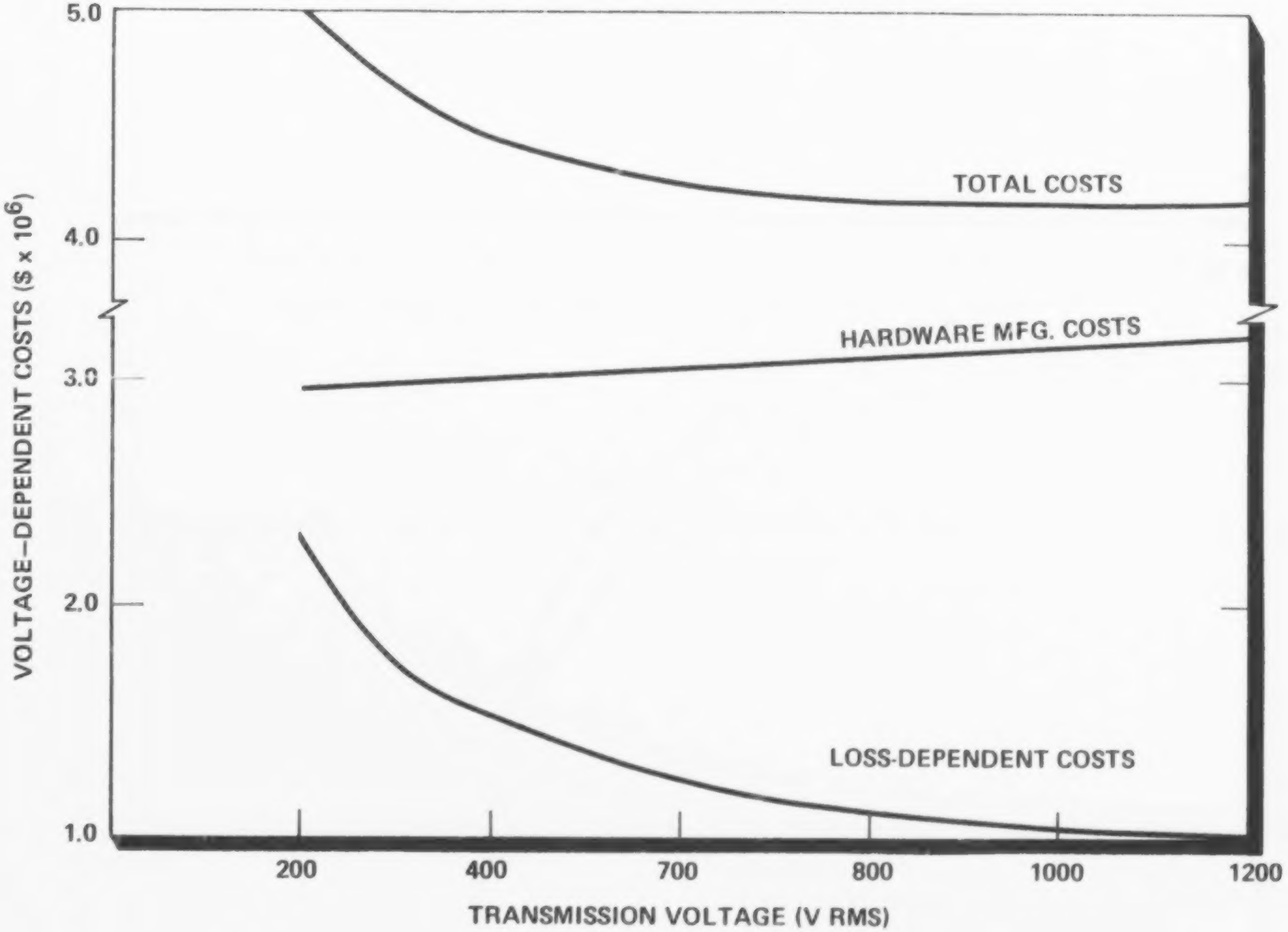

Figure 1.26. Power Management System Voltage Dependent Costs
(High-Frequency AC Distribution, "Mil. Grade" Components)

Another important parameter for power management cost is the transmission frequency. Figure 1.27 shows the hardware cost and transportation-to-orbit cost as a function of frequency. Production cost initially decreases with frequency and then rises due to special high frequency consideration in the construction cost. Weight and transportation costs decrease rapidly with increasing frequency. It has been determined that maintenance costs are not significant. As can be seen from the curve, the most effective frequency lies between 20 and 26 kHz. Human engineering considerations require that frequencies be above the audible range (20 kHz has been established as the minimum allowable frequency).

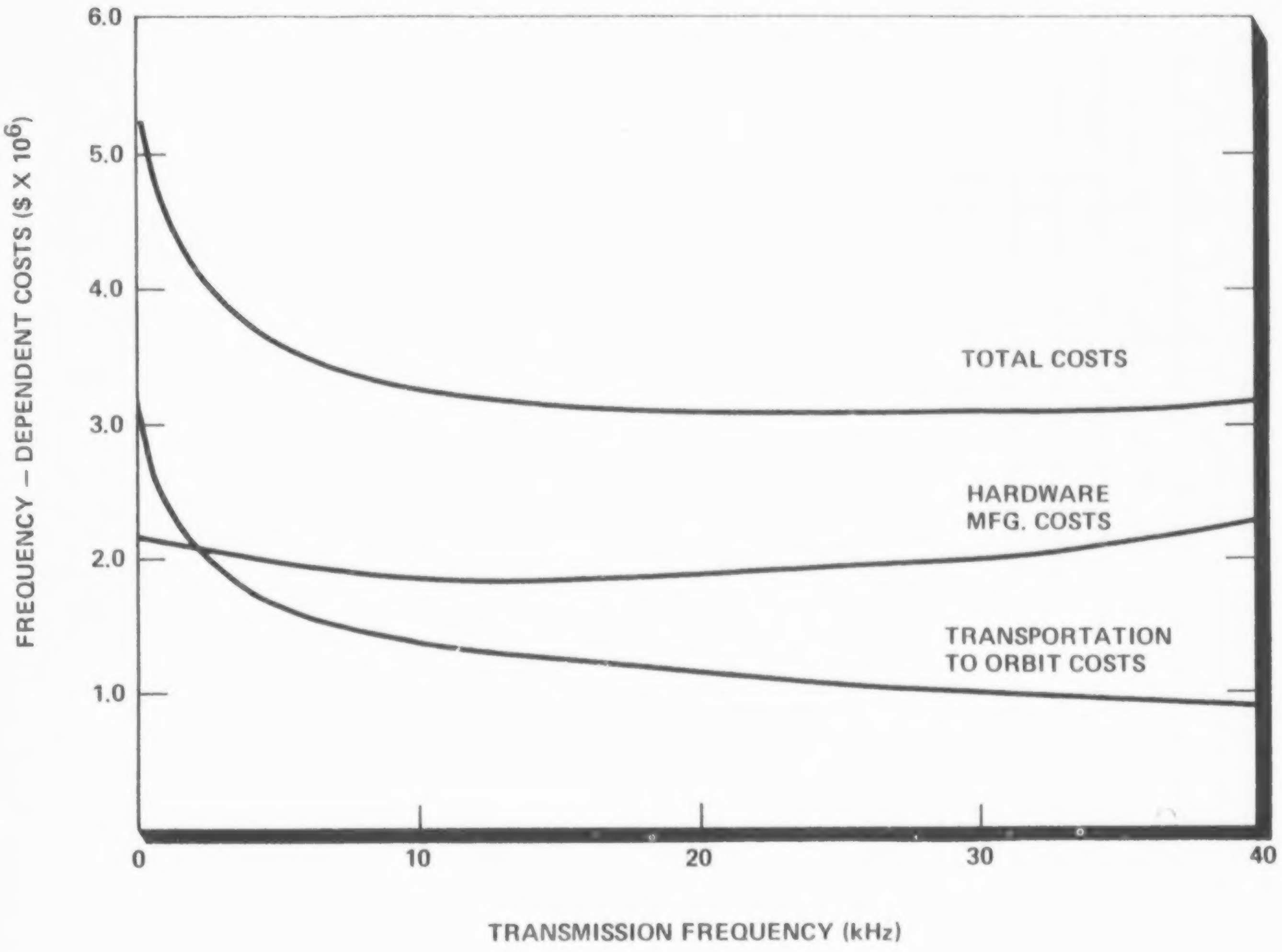

Figure 1.27. Power Management System, Frequency-Dependent Costs
(High-Frequency, AC Distribution, "mil. grade" Components)

1.5 ELECTRIC PROPULSION

Wayne Hudson, NASA Headquarters

The NASA Electric Propulsion Research and Technology program is directed toward providing the technology base to meet the nation's future needs in the area of low thrust, high specific impulse propulsion.[1-5]

For the energetic mission[6-9] included in NASA's plan for exploring the solar system an electric propulsion system (Fig. 1.28) will be needed to augment the Shuttle-IUS Space Transportation System. Some of the missions under study include: comet and asteroid rendezvous, Saturn orbiter with probes, Mercury orbiter, and Mars surface sample return. Detailed mission analysis has shown that electric propulsion is readily able to provide larger payloads, shorter trip times, more mission flexibility (i.e., launch any year to Jupiter) and less complicated trajectories (i.e., no gravity assists for Mercury orbiter).

Studies have also demonstrated that solar array power can be constructively utilized after the propulsive portion of a mission has been completed. For example, on planetary orbiter missions, the array power capability (anywhere from 1 kW to 100 kW) could be used for radar systems, laser systems, and increased communications capability.[10]

Earth orbital mission studies have identified several potential uses of electric propulsion. The one millipound auxiliary thruster has been developed specifically to demonstrate the technology for north-south stationkeeping of geosynchronous satellites. The longer the operation life of the satellite (the greater the total impulse), the greater the savings in propellant mass that can be realized from using electric propulsion. For example, on a five-year stationkeeping mission, the use of auxiliary electric propulsion can provide 15-20% of the total spacecraft mass for extra payload. Another auxiliary propulsion application of ion thrusters could be to provide orbital control of future sun-synchronous satellites (i.e., the next generation Landsat). In this application the orbital control function consists of either maintaining a

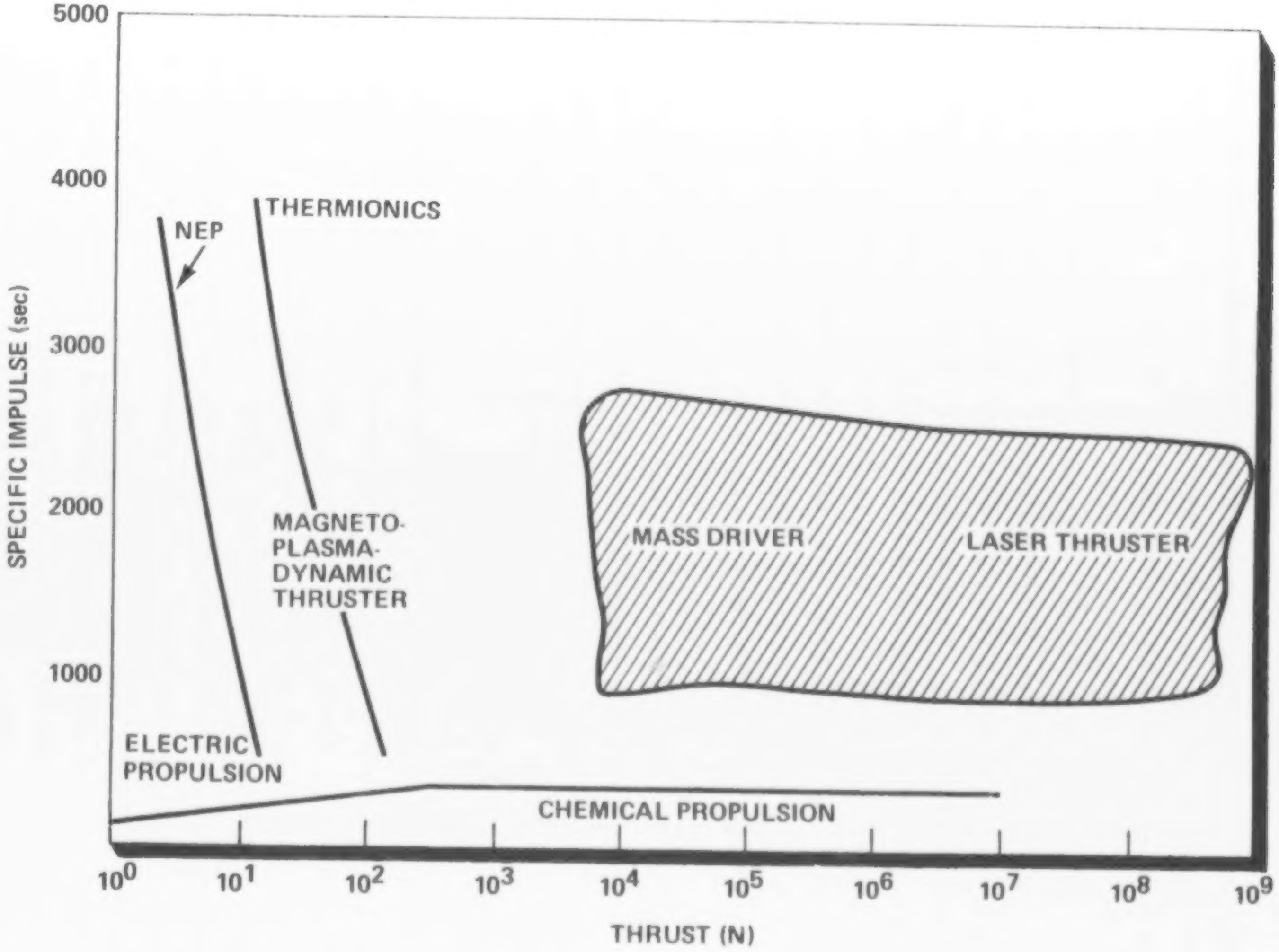

Figure 1.28. Specific Impulse vs. Thrust

precise sun-synchronous orbit or programming an orbit change. The onboard solar array power required for electric propulsion might also be used to advantage for earth orbital applications. A second generation Landsat that utilized a multikilowatt solar array would have its capabilities enhanced considerably.

In addition, larger ion thruster systems have been studied for orbital transfer of large payloads or very lightweight structures. The more efficient utilization of propellant that results from high specific impulse of electric propulsion represents a major logistics benefit for any earth orbital scenario that requires large amounts of propellant transported to orbit. Although NASA's large space systems program is in the embryonic stages, it might well require electric propulsion for orbital transfer of large delicate structures and for on-orbit stationkeeping and attitude control.

1.5.1 Program Status

At this point in time, the one millipound auxiliary thruster is midway through the fabrication of flight hardware. The NASA Office of Space Transportation has initiated the Phase B for the development of a solar electric propulsion stage. Within the technology program we have initiated an ion thruster extended performance effort: to expand the specific impulse operation range, to increase thrust to mass, and to operate efficiently with inert gases. The preliminary technology steps are being taken to eventually develop nuclear electric propulsion. Advance propulsion concepts such as the magnetoplasmadynamic (MPD) thruster and the mass driver are being evaluated.

Auxiliary Thruster

The objective of the auxiliary propulsion technology program is to develop a prototypical one millipound electron bombardment thrust system and subject it to flight qualification level testing. Since the last Electric Propulsion meeting, the launch date for Air Force Space Test Program P80-1 mission has slipped to mid 1982 because of delays in the prime experiment. The ion thruster system, however, will be delivered in November of 1980.

The ion thruster flight package consists of two thruster subsystems and a diagnostics instrument subsystem. The 8-cm thrusters operate at a specific impulse of 3000 s, require 180 W, weigh 26 kg, and develop a thrust of 1 mlb. One thruster will operate cyclically to demonstrate the durability of the subsystem over a simulated 7-yr north-south stationkeeping mission on a typical geosynchronous satellite. The other thruster will be used for special purpose testing.

Primary Thruster

The objective of the solar electric propulsion base-line program is to demonstrate the technology readiness of high specific impulse (3000 s) ion thruster propulsion by the end of 1980.

During 1979, both ion thrusters and power processing units were fabricated and acceptance tested. Currently, they are being assembled into the bimodular thrust subsystem (BIMOD). The BIMOD consists of two thrusters, two power processors, thruster gimbals, and a heat pipe thermal rejection system.

The principal tasks associated with the base-line technology program include a mission profile life test, a thruster endurance test, power processor development, and thrust subsystem module development.

Magnetoplasmadynamic Accelerator

Three years ago a thorough evaluation of the quasi-steady state MPD was initiated to evaluate the viability of this technology for future orbital transfer vehicles and interplanetary transportation. Although the physics associated with the MPD is somewhat more complicated than that associated with electron bombardment thrusters, the MPD offers the potential of higher thrust density and increased power processing simplicity. The thrust per unit exhaust area is 10^4 times greater than the bombardment thruster. As a result the MPD could replace an array of ion thrusters. Inherently, the MPD technology is predicted to perform better at higher power levels and at somewhat lower specific impulses. Instead of twelve power supplies, the MPD will require only two or three. Furthermore, the MPD has no requirement for neutralization such as the bombardment thruster. Two important problem areas that need to be addressed in the quasi-steady state MPD are the appropriate electrical pulse formation and the necessary propellant pulse control.

The 1981 goals of the program are to determine if the recent breakthrough in the understanding of the fundamental physical mechanisms of the MPD can be manifested in thruster performance and life. Continuing fundamental research at Princeton University projects thruster efficiencies up to 50% at specific impulses in the range of 1000-5000 s. The evaluation program is being carried out at Princeton University under the technical cognizance of the Jet Propulsion Laboratory. A thrust stand for the performance characterization is currently being constructed. The thrust stand will be capable of time resolved (<100 msec resolution) measurements of thrust.

Nuclear Electric Propulsion

Nuclear electric propulsion (NEP) is a significant option for future transportation in the solar system. It has the potential for constant power independent of solar intensity, it is inherently a long life technology, it does not suffer from radiation damage, nor does it require ancillary energy storage systems or precision solar tracking systems. NEP will eventually be needed by NASA to successfully complete the intensive study of the outer planets of the solar system. It also would have many advantages as a future orbital transfer system. The nuclear reactor that would be developed for NEP would have many other applications such as: earth orbital platforms, lunar and planetary bases, and planetary orbital research stations.

The principal components of a NEP system are the reactor, the thermal-to-electric conversion system, and the electric thrusters. Some work is being done in each of these areas. The thruster technology program is described in detail elsewhere and the overall systems studies have been initiated at the Jet Propulsion Laboratory.

The nuclear reactor technology that would provide the basis of NEP is under development by Los Alamos Scientific Laboratory under funding and management of the Department of Energy. The present reactor design is 1.2 MW thermal, heat pipe cooled system capable of 100-250 kW of electrical power. The design calls for a reactor about 0.5 m in diameter and 0.5 m long. Approximately 90 molybdenum/lithium heat pipes are used to carry heat to the thermal-to-electric conversion system which is mounted on the heat pipes external to the reactor. The reactor fuel is UO_2. The major design limit is the maximum operating temperature of the reactor. At temperatures of about 1350 K the fuel swelling is estimated to be only a few percent. Above this temperature fuel swelling is known to increase but insufficient data exists to make an accurate projection. If as a result the first space reactor is designed to operate at about 1350 K, the major options for conversion technology would be Brayton and thermoelectrics. The lower operating temperatures have an impact on system efficiency and mass. As discussed earlier, this area is under study to determine which conversion technologies should be pursued to provide NASA with the earliest NEP capability.

Mass Driver

The evaluation of critical technologies associated with the mass driver has also been initiated. It could be used to return carefully chosen asteroids to earth orbit. Another potential use is as a lunar-surface-based material launcher. Subsequently, the materials would be collected at one of the points in space where the gravitational forces of the earth and moon cancel each other out. A large scale space development such as a space colony or a solar power satellite would have to be planned before the mass driver becomes energetically favorable.

A 2.5 m long mass driver is currently being constructed at Princeton University. This system has all the major components of a planned space system such as a cryogenic service station and the pulse drive circuits. The mass driver is of axial geometry with equal length sections of acceleration and deceleration, each containing 59 drive coils, 13 cm in diameter. Intermediate energy storage is provided by capacitors with two phases operating in quadrature. The drive coils are individually energized through SCRs with timing supplied by position sensing optical detectors. The mass carrying bucket includes two superconducting magnetic field intensities. Magnetic flight is generated by eddy current repulsion from six aluminum guide strips that line the mass driver tube.

Nominal acceleration is projected to be 5000 m/s^2 giving a maximum bucket velocity of 112 m/s. In 1981, the length of the system will be increased to 10 m and critical scaling parameters will be determined.

Laser Propulsion

The concept of laser propulsion compares favorably with other advanced concepts for transfer of large payloads at relatively low cost. Laser radiation can heat an expellant to much higher temperatures than can be achieved with either chemical or nuclear reactions. Typical systems can attain specific impulses of 1000 s or greater. The laser propulsion system becomes viable when a space-based laser power transmission system becomes operational and when there is a requirement for orbital transfer of large payloads. Its advantage is gained from the fact that it can be very lightweight since the power generation part of the system is not included in the vehicle. A potentially important advance was achieved during 1979 with the demonstration of a laser sustained plasma in pure hydrogen.

1.5.2 Trends and Forecasts

Figure 1.28 shows the specific impulse--thrust parameter space of interest. At low specific impulse (below 500 s) chemical propulsion systems are capable of providing practically any thrust level. Conversely, at low thrusts (below a few pounds) electric propulsion systems can operate over a wide band of specific impulses above 1000 s. Given the current systems, the choices are between high thrust chemical thrust systems which provide short trip times and the high payload to propulsion system mass ratios of the high specific impulse systems. Very significant

best copy available

benefits would result from systems that have the advantages of both high thrust and high specific impulse. The direction of our advanced propulsion technology program is toward these benefits.

1.5.3 Space Propulsion Depends on Energy Sources

In the near term most space power will be supplied by chemical reactions and photovoltaics. As stated earlier in the next few years we will demonstrate high power (10 kW) arrays with specific powers of 66 W/kg. By the year 2000 photovoltaic systems should easily achieve specific powers of >200 W/kg and perhaps as much as 1000 W/kg. Table 1 shows some other on-board energy sources compared to hydrogen-oxygen. The future propulsion circa 2000 and beyond may very well depend on breakthroughs in the technologies associated with these types of energy sources. Suppose metallic hydrogen can be created and is stable. Suppose large space-based high power laser systems become a reality. Suppose a discovery is made which greatly increases the amount of antimatter that can be created and stored. In each case, space propulsion technology would be revolutionized. In the next few years we will be examining some new advanced concepts and re-examining some old ones.

TABLE 1

ON-BOARD ENERGY SOURCES

Type	Maximum Theoretical Energy per Mass (J/kg)
Chemical (O_2-H_2)	1.5×10^7
Free Radical ($H+H \rightarrow H_2$)	2.2×10^8
Nuclear Fission	8.2×10^{13}
Nuclear Fusion	3.9×10^{14}
Matter-Antimatter	6.3×10^{16}

In the near term, enhanced propulsion capability will be provided by the considerable growth potential inherent in ion bombardment thrusters.

Thruster performance can be extended to higher specific impulse, higher thrust, and higher power levels. NASA currently has an active technology program to do this. The program goals include doubling the thrust-to-power ratio of the thruster to 20 mlb/kW, characterizing the performance over the 1400-1500 s specific impulse range, decreasing the specific mass to 15 kg/kW and the flight test of direct drive.

The power processor currently in the final stages of development testing was designed to thruster requirements specified in the early 1970s. The thruster power processor interface requirements accommodated a broad spectrum of electric propulsion missions. The resultant power processor design allows greater thruster flexibility, but results in increased power processor complexity--12 supplies, 4000 parts, and a component mass of over 17 kg. The technology thrust in this area is to greatly reduce the complexity of the power processor and interface with the thruster. So far, it has been shown that the discharge supply can be used to power the cathode tip heater, cathode and main isolator heaters, and the cathode keeper functions. The program is currently examining the impact of eliminating the magnetic baffle supply. These power processor alternatives are all being tested with thrusters for stability and control of operation. Three grid beam extraction systems have been under study in the technology program for over a year. The constant ground plane created by the third grid essentially lacks the plasma sheaths in position and eliminates defocusing particularly at low net accelerating voltages. Thirty-centimeter ion thrusters have operated at beam currents of 6 A for short periods of time and for prolonged periods at 3 A. Preliminary results on the 3 A life test showed a lower internal thruster erosion rate than 2 A operation. This result may be explained by the lower discharge voltages at higher beam currents.

To put the technology trends in perspective, it is convenient to break an electric propulsion system down into the three specific functions of energy conversion, power processing, and electric thruster. Electric energy is created by some energy conversion system. First generation electric propulsion systems use photovoltaics; later systems may use nuclear reactors. Next, this electrical energy is converted by the power processor into the set of currents and voltages required by the thruster. Finally, the thruster converts electrical energy into thrust energy. The critical parameters are specific mass and thrust power.

The SEP array as an energy converter has considerable growth potential. If the SEP solar array blanket is replaced with 2 mil, 14% efficient cells, and 2 mil cover glasses, the specific power would increase to 122 W/kg. This corresponds to the present level of 15 kg/kW and the future projection of about 5 kg/kW. Alternately, if concentrators with a 3.2 concentration ratio were added to the SEP array, the specific power of the base-line system would be increased to 120 W/kg. Additional cost benefits accrue from both changes, since either higher efficiencies or concentration would reduce the number of cells which in turn would reduce the cost. Furthermore, if thin high efficiency solar cells are combined with concentrators, specific power greater than 200 W/kg is achievable. More long-range solar array performance extensions may be realized from technologies such as continuously variable concentration ratios, high voltage solar arrays, and advanced cells. For the ion thruster and power processor, the present specific mass is 35 kg/kW and the projection is for 10-20 kg/kW over the next 10 to 20 years. Trends and forecasts for these functions are shown in Fig. 1.29 along with the total for the solar electric propulsion stage.

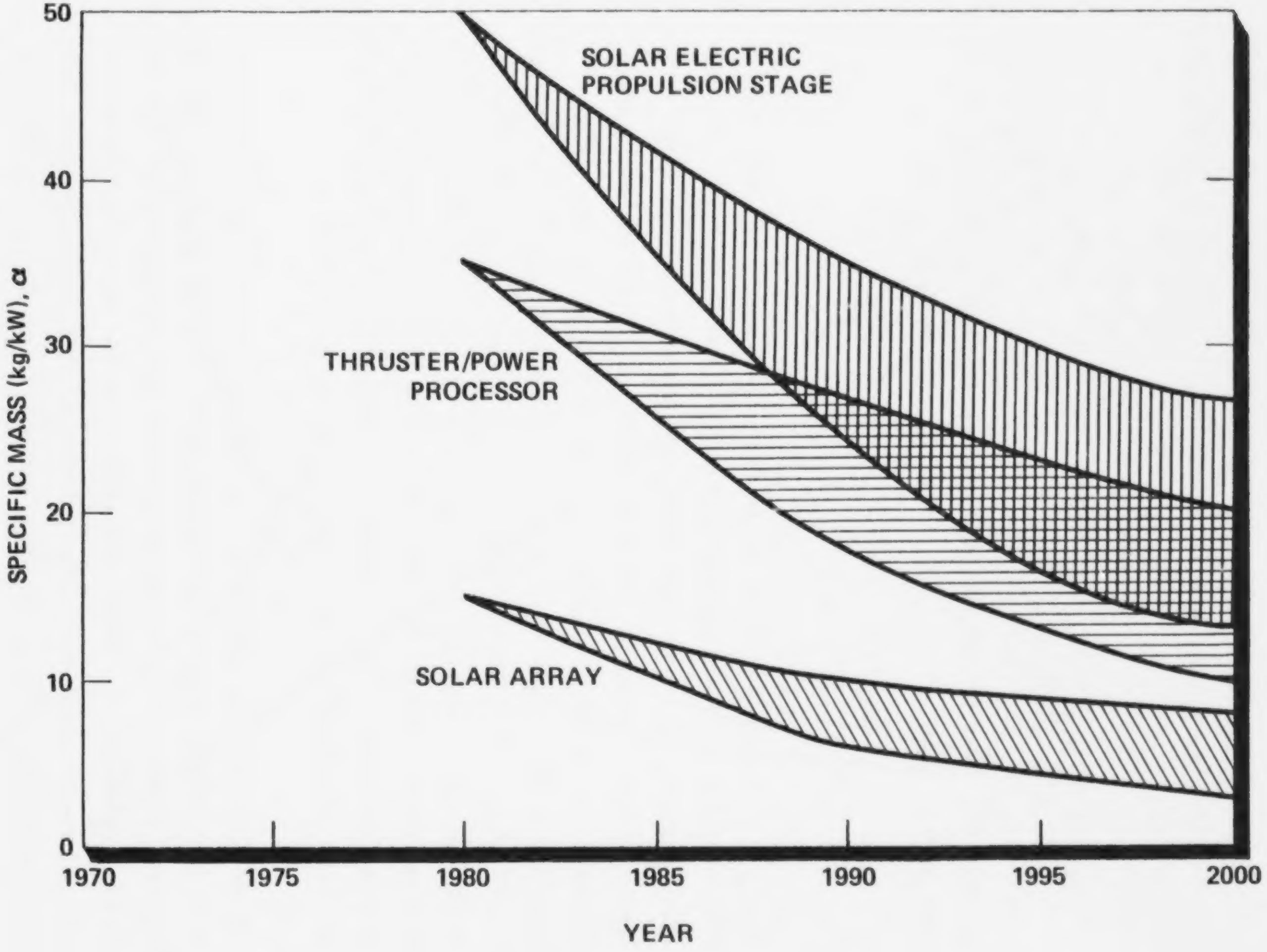

TECHNOLOGY READINESS DATE, LEVEL 6

Figure 1.29. Specific Mass for Solar Array; Thruster and Power Processor; Complete Solar Electric Propulsion Stage

The impact of these projected improvements in specific mass are best shown by a plot of total system mass versus specific impulse. For example, on a mission of given thrusting time, t, performed at a constant thrust, T, the total propellant mass, M_p, is inversely proportional to the exhaust velocity, V_e, or specific impulse, I_s, where g_o is the gravitational constant.

$$M_p = \frac{Tt}{V_e} = \frac{Tt}{I_s g_o}$$

Assuming that the mass of the propulsion system, M_s, is linearly dependent on the power, then

$$M_s = \alpha P = \frac{\alpha g_o T I_s}{2\eta}$$

The term α is the specific mass, η is the efficiency, and the calculation is bounded by assuming 100% efficiency of the conversion of power to thrust. Figure 1.30 shows how these two mass components combine for propulsion systems of specific mass 50 kg/kW and 20 kg/kW, assuming a constant thrust of 1 N for 15,000 hr. One newton is on the order of the thrust for a SEPS stage and the life of the base-line thruster system is 15,000 hr. For particular missions a line of constant mass represents the payload capability of the earth-to-orbit and earth escape propulsion systems. The much lower total mass curve for the 20 kg/kW specific mass represents the potential of thousands of kilograms of payload reduction or greater science payload at earth escape.

The second critical parameter for electric propulsion systems is efficiency with which input power can be converted to thrust. Starting with the input power to the power processor, the efficiency is the product of the efficiencies of the power processor and the electric thruster. The power processor efficiency is currently at 89%, a few percent improvement may be achieved by replacing the silicon control rectifiers with transistors, but beyond that not much further gain can be expected for ion bombardment thrusters. The thruster component of efficiency offers

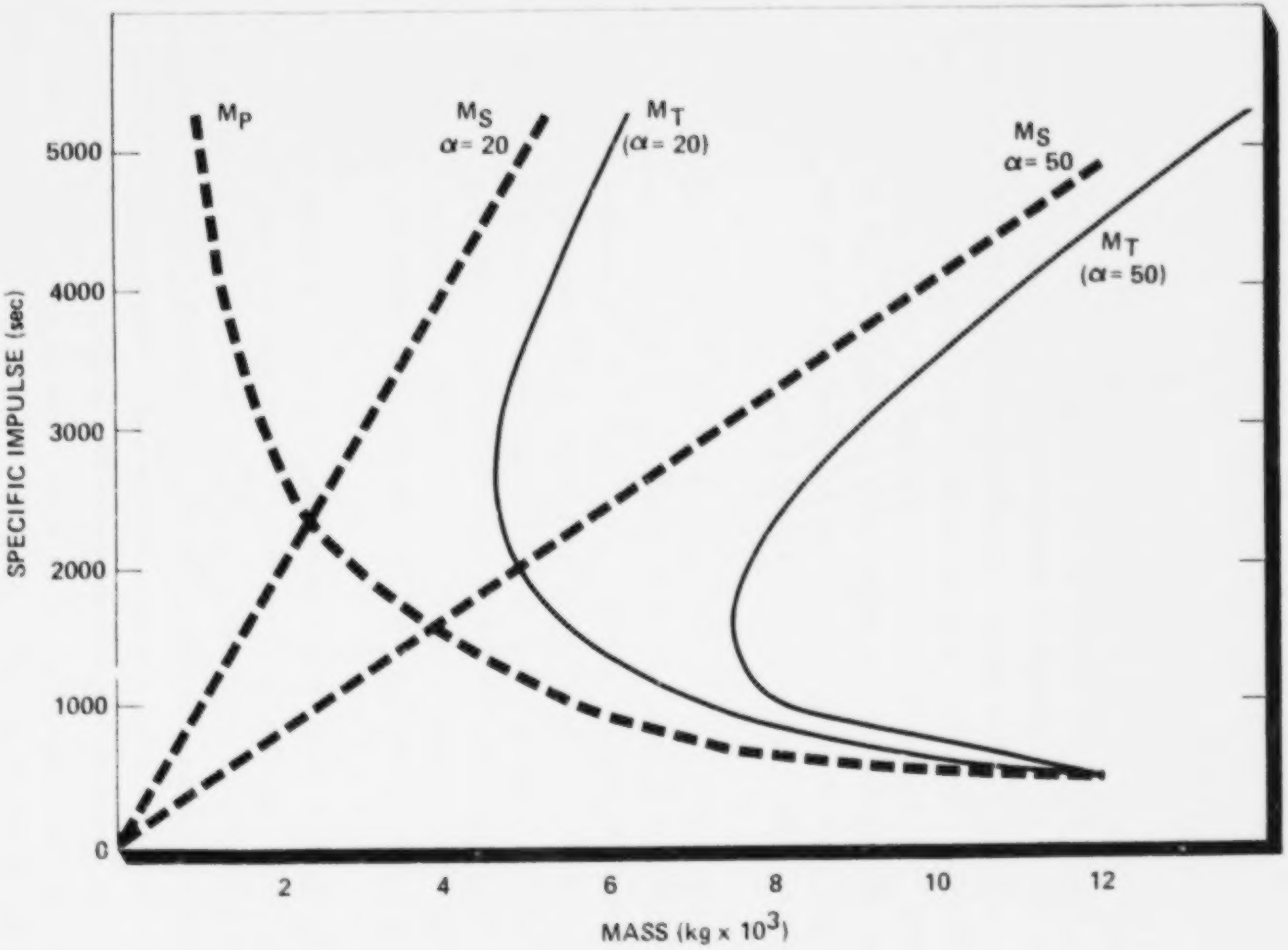

Figure 1.30. Mass as a Function of Specific Impulse

more potential for improvement. It can be thought of as the percent of the input power that manifests itself in the thruster beam. In terms of the thruster physics more insight is gained by examining the efficiency expressed as a power-to-thrust ratio, P/T. This ratio can be shown to be

$$P/T = \frac{g_o I_s}{2} + \frac{\varepsilon}{(m_i g/e) I_s}$$

where ε is the discharge losses in eV/ion, m_i is the mass of the accelerated ion, and e is the charge on an electron.[11] The equation is plotted in Fig. 1.31 for a 30-cm mercury thruster operating with discharge losses of 250 eV/ion. The first term represents the power in the ion beam and the second term represents the power required to ionize the propellant. Although this represents the predominant percentage of the power, small amounts are used for neutralizing the ion beam, operating the gimbals, and energizing the logic and control circuits.

As shown in Fig. 1.31, the curve falls off sharply from the ordinate, passes through a minimum, and then approaches asymptotically to the line corresponding to 100% efficiency. To the left of the minimum the second term of equation dominates, implying low efficiency because a large proportion of the power is going into creating ions. To the right of the minimum the first term, the power to produce thrust, dominates and the efficiency of converting power to thrust is high. The operating point of the base-line 30-cm diameter thruster (SEPS) is shown for reference.

The electric propulsion technology development program is directed toward inert gas thrusters and toward lower specific impulses. Inert gas thrusters will be required for any large scale application in earth orbit because of environmental concerns. Low specific impulse is also desirable for minimizing orbital transfer time. That this is true can be seen from the first term of the power-to-thrust ratio equation above. Given the practical situation of an upper bound on the available power, the maximum thrust is inversely proportional to trip time. At low specific impulse, it is very important to address technologies of lowering

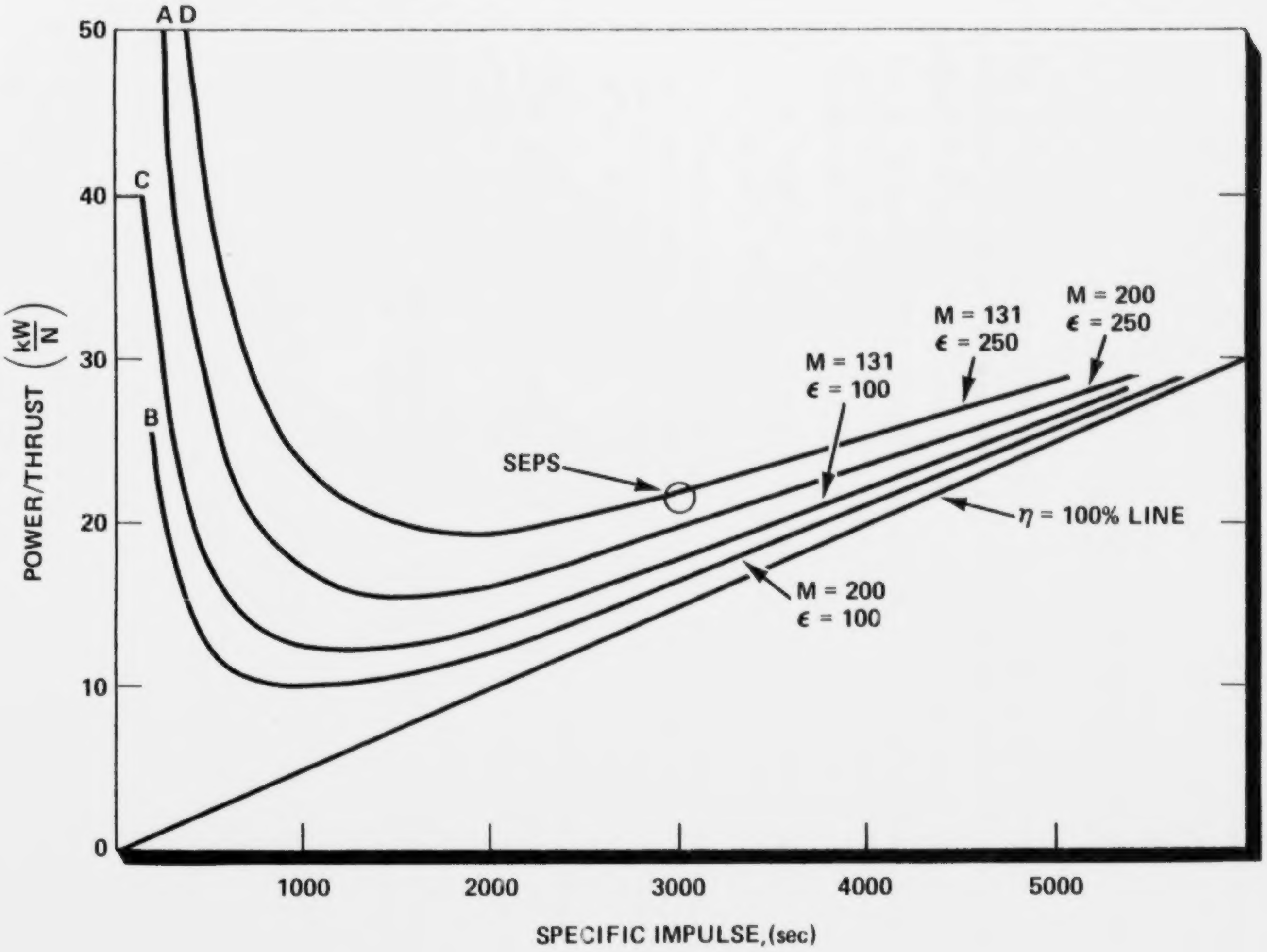

Figure 1.31. Power/Thrust vs. Specific Impulse

the energy required to create ions, e. The impact can be seen by comparing curve A with B and C with D in Fig. 1.31. The effect of changing from mercury propellant to xenon is shown by comparing curve A with D and B with C. At specific impulse of 1000 s, the penalty for using xenon instead of mercury is 2.5 kW/N at $\varepsilon = 100$ eV/ion and 6.4 kW/N at $\varepsilon = 250$ eV/ion. The benefit of reducing discharge losses from 250 eV/ion to 100 eV/ion is 7.2 kW/N for mercury and 11 kW/N for xenon.

By 1982, we should be able to achieve performance of mercury thrusters near the curve B values at specific impulses between 1000 s and 2000 s. The performance shown by curve D will be achieved by 1985. The further improvement from curve D to C may be possible by 1990.

REFERENCES

1 James Lazar, "Electric Propulsion Status and Development Plans," AIAA No. 73-1143, AIAA 10th Electric Propulsion Conference, November 1973.

2 W. R. Hudson and R. C. Finke, "NASA Electric Propulsion Program," AIAA No. 76-1068, AIAA 12th International Electric Propulsion Conference, November 1976.

3 W. R. Hudson, "NASA Electric Propulsion Program," AIAA No. 78-711, AIAA/DGLR 13th International Electric Propulsion Conference, April 1978.

4 W. R. Hudson, "NASA Electric Propulsion Technology Program," AIAA No. 79-2118, AIAA/DGLR 14th International Electric Propulsion Conference, October 1979.

5 W. R. Hudson and R. C. Finke, "Electric Propulsion Circa 2000," AIAA No. 80-0912, Global Technology 2000 Conference, Baltimore, Maryland, May 1980.

6 K. L. Atkins, "Mission Applications of Electric Propulsion," AIAA No. 74-1085, AIAA/SAE 10th Propulsion Conference, October 1974.

7 K. L. Atkins and J. H. Duxbury, "Solar Electric Propulsion Mission and Spacecraft Capabilities for Outer Planet Exploration," AIAA/AGU Conference on the Exploration of the Outer Planets, September 1975.

8 K. L. Atkins and C. G. Sauer, "Solar Electric Propulsion Combined with Earth Gravity Assist: A New Potential for Planetary Exploration," AIAA No. 76-807, AIAA/AAS Astrodynamics Conference, August 1976.

9 K. L. Atkins, "Ion Drive: A Step Toward 'Star Trek'," AIAA No. 76-1069, AIAA 12th International Electric Propulsion Conference, November 1976.

10 H. M. Kavanagh, Solar Electric Propulsion Vehicle: What Science Could Do With Large Amounts of Power, JPL No. 660-66, August 1977.

11 G. R. Brewer, Ion Propulsion Technology and Applications, Gorbon and Breach, p 76, 1970.

blank page

2 CHEMICAL PROPULSION

F. W. Stephenson, NASA-Headquarters

Chemical propulsion technology is being advanced in the areas of higher performance, longer service life, and lower weight in order to increase vehicle and spacecraft capability and to reduce overall vehicle and mission costs. Efforts are directed specifically at the technology for fully reusable propulsion for earth-to-orbit and orbital transfer vehicles; high-performance, low-thrust propulsion for the low acceleration orbital transfer of large space structures; and long-life, on-board propulsion for planetary orbiters, landers, and launchers.

In the area of space transportation, increased engine performance reduces the amount of propellants required to deliver a given payload and also reduces the size and cost of the vehicle performing the mission. Longer engine service life reduces vehicle operations costs, and lighter weight engines tend to improve center of gravity location and alleviate flight-control problems, particularly for winged vehicles.

For planetary missions, increased spacecraft propulsion performance has a significant impact on reducing the earth launch capability required to accomplish the mission. This can greatly reduce overall mission costs and in some cases enables a mission to be accomplished with an existing launch capability. Long life is a necessity since the spacecraft propulsion systems generally must operate away from earth periodically for up to 10 years.

Trends and forecasts for advanced chemical propulsion systems are discussed below. Parameters chosen to describe the evolution of this technology include energy-conversion efficiency, engine service life, engine thrust-to-weight ratio, and the effects of advanced propulsion on earth-to-orbit transportation costs. Technology readiness dates shown represent a Level 6 state of development.

Rocket Engine Energy Conversion Efficiency (Fig. 2.1). Significant gains are projected for the conversion of heat energy to kinetic energy (specific impulse) in rocket engines. Earth-to-orbit (booster) engines, such as the Shuttle main engine, currently average about 75% efficiency while operating from sea level to vacuum conditions. This should increase to at least 80% by 1990. Smaller but still significant gains are anticipated for upper stage and spacecraft engines. Since these engines operate only in a vacuum and their performance is not degraded by ambient pressure forces, their conversion efficiency is always considerably higher than that achieved by booster engines.

Chemical Rocket Engine Lifetime (Fig. 2.2). In the past, rocket engine operational life was measured in minutes, since space transportation consisted of expendable launch vehicles. With the advent of reusable engines for the Space Shuttle, service life began to be measured in hours between major overhauls. The Shuttle main engine has a specified life of 7.5 h. With a strong technology program in reusable engines, service life should reach at least 100 h with minimum servicing and maintenance requirements. This will include at least 500 mission operations as compared to the current 55 missions specified for the Shuttle main engine.

Chemical Rocket Engine Thrust-to-Weight Ratio (Fig. 2.3). Space vehicles are in general extremely tail heavy, which moves the center of gravity toward the rear and creates control problems, particularly with winged vehicles like the Shuttle Orbiter. A major contributor to this problem are the rocket engines located at the tail of any space vehicle. Lower engine weight for a given thrust level would greatly alleviate the control problem. Projections for earth-to-orbit (booster) engine thrust-to-weight ratio improvements show an increase from the current 90-100 level to 130 or more by 1990.

Earth-to-Orbit Transportation Costs (Fig. 2.4). The propulsion technologies leading to the above projections are primarily aimed at greatly reducing the costs of doing business in space while accomplishing a broader spectrum of space missions in a routine manner. The Space

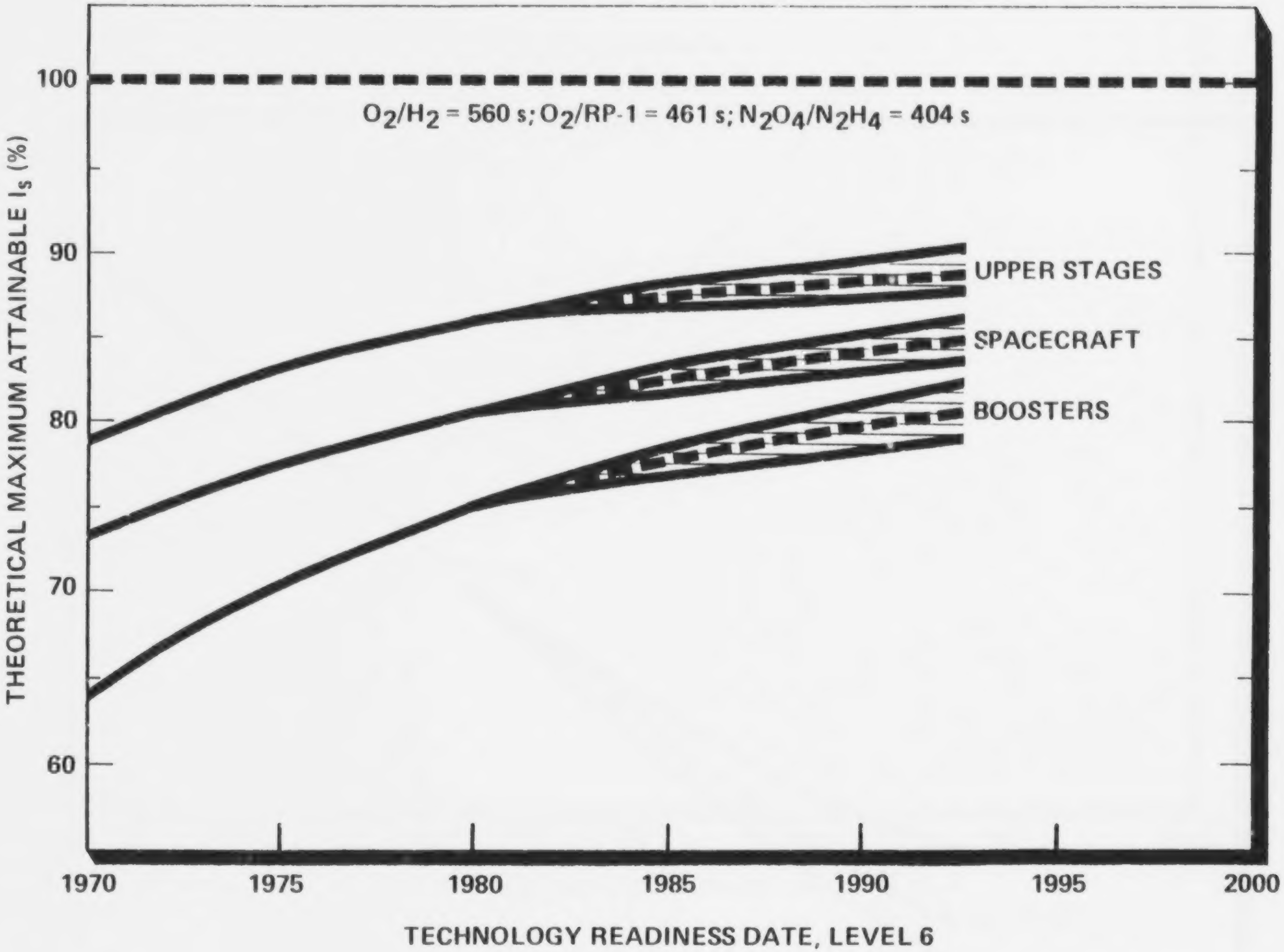

Figure 2.1. Energy Conversion Efficiency (I_s) of Chemical Rocket Engines

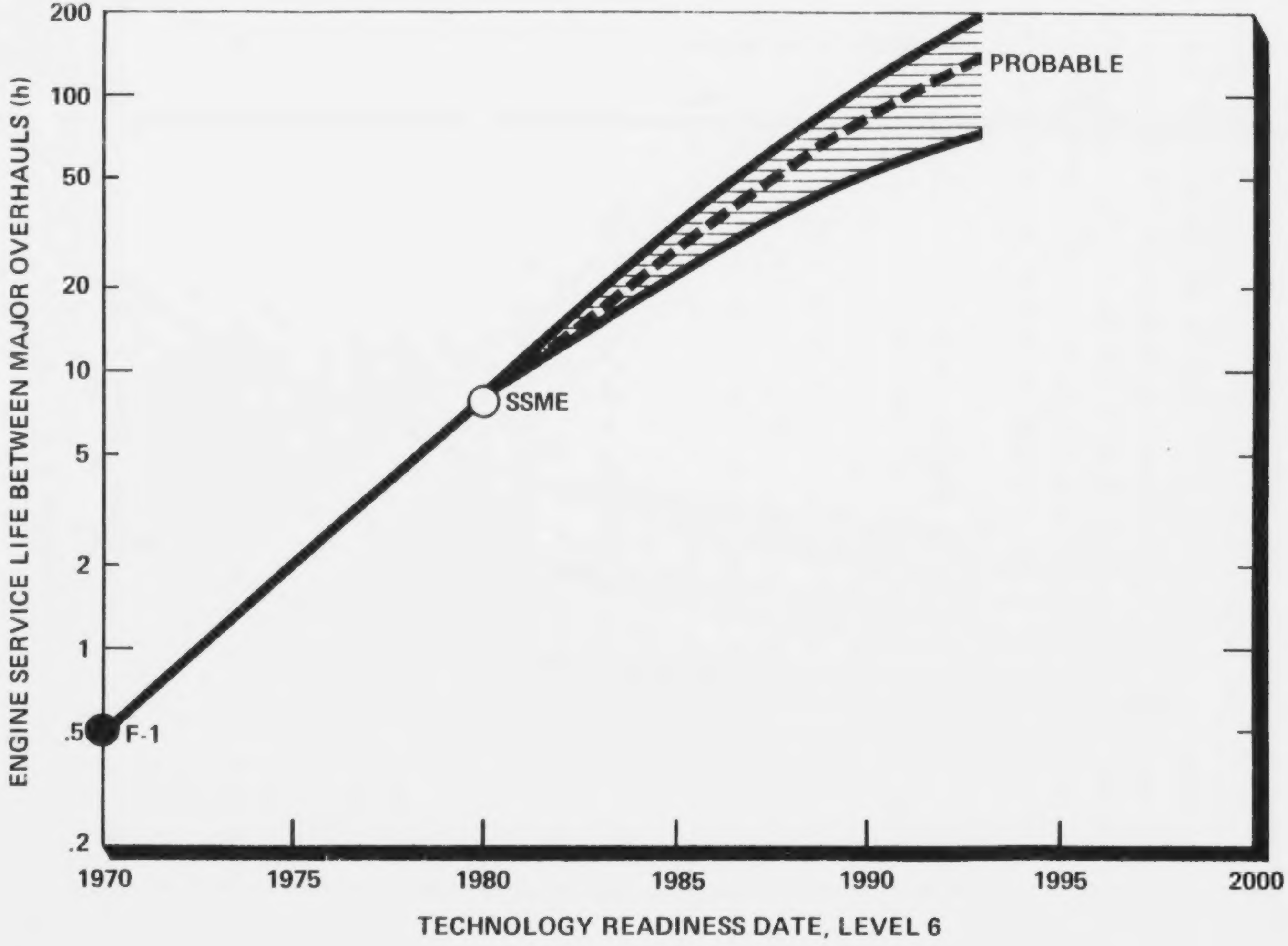

Figure 2.2. Chemical Rocket Engine Service Life

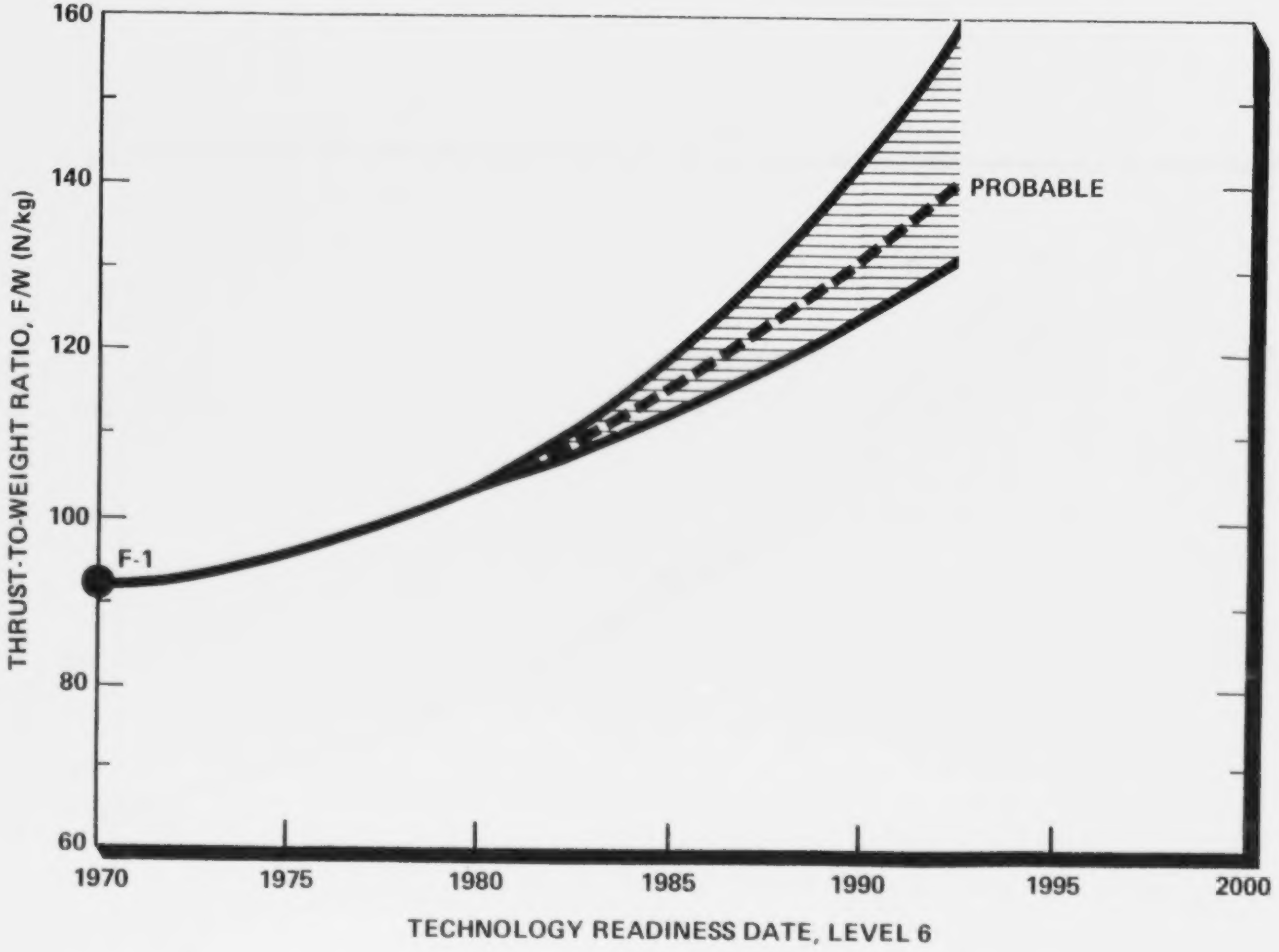

Figure 2.3. Chemical Booster Rocket

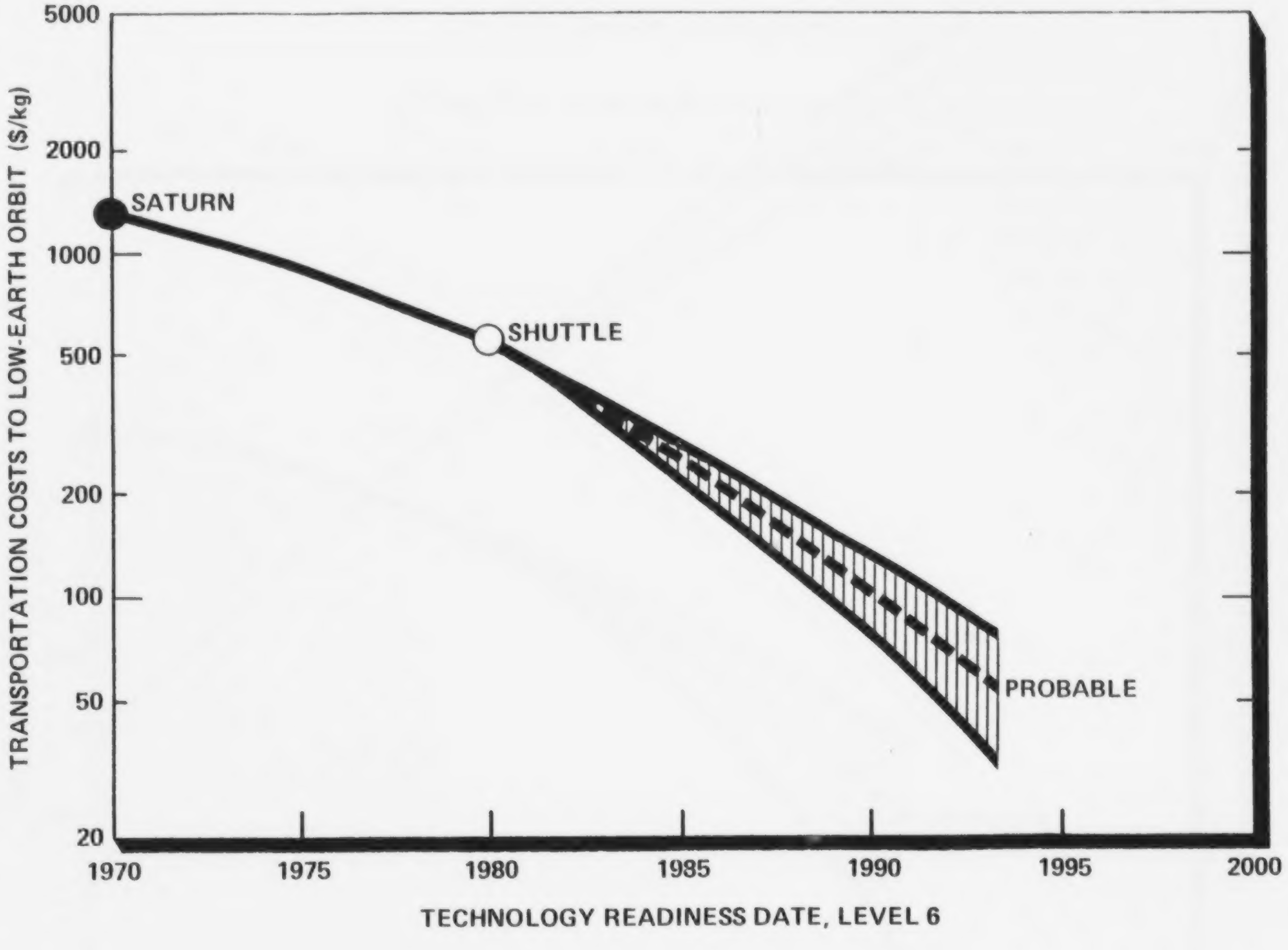

Figure 2.4. Earth-to-Orbit Transportation Costs

Shuttle has begun the evolution of space transportation, leading ultimately to a fully reusable low-cost system. Cost projections show a decrease from the current Shuttle cost of $600/kg to a level of approximately $100/kg by 1990.

blank page

3 MATERIALS AND STRUCTURES

W. A. Brainard, NASA-Headquarters

R&T program areas provide the advanced materials and structures technology that will make future space transportation systems (STS) and spacecraft feasible by significantly improving performance, durability, and cost effectiveness. The major objectives are to develop the materials for spacecraft structures, thermal protection systems, and propulsion and power systems. Structures technology is developed to provide concepts and materials application for large space structural systems and advanced STS. This technology encompasses both design and analysis together with the predictive technique required for verification of structural dynamics and acoustic response.

Specific directions in materials include continuing basic research as well as more generic oriented activity. Fundamental physics and chemistry studies in material science provides the means to better understand and predict materials behavior. Work on materials for advanced space transportation systems continues to focus on composite materials such as the fiber/resin and metal matrix systems, and their preparation and characterization. Additional efforts involve space environmental effects on composites and metallic superalloys and the development of bearings, seals, and lubricants for advanced STS.

Specific directions in the structures R&T are on the concepts, design, assembly, deployment, control, and dynamics of space structures. Activity will focus on predicting and controlling the response of payloads and deployed structures, such as antennas or platforms, to the space vehicle dynamics and space environment. Development of computer analysis and optimization codes for design and static/dynamic response will continue. Work on high-temperature structures will involve thermal protection systems (TPS) for planetary entry and advanced STS, with metallic TPS concepts receiving specific attention. The aerothermal loading of structures will be investigated from both predictive and experimental points of view.

Erectable Spacecraft Capability (Fig. 3.1). Erectable element (nestable column) technology is relatively mature due to past and ongoing R&D efforts. The major future thrust in this area is defining man's capability and role in the assembly process. Based on the current understanding of man's productivity and the state of the art for erectable element technology, an astronaut assembled platform capability of 100-200 m could be demonstrated by 1985 using one Shuttle flight. Ongoing and planned efforts for large space systems technology (LSST) in the development of automated assembly methods are expected to demonstrate concept viability (ground tests) by 1985, clearing the way for a flight experiment to demonstrate an automatically assembled platform capability of 300-500 m by 1990 using one Shuttle flight.

Maximum Usable Non-Metallic Service Temperature (Fig. 3.2). Polyimide matrix composite materials offer the most potential for increasing the maximum service temperature from the current state-of-the-art value of 450 K to perhaps as high as 720 K by 1990. R&D on graphite/polyimide composites under the CASTS project will demonstrate Level 4 technology readiness for service temperatures to 590 K by 1983.

Utilization of hybrid polyimide matrix composites are forecast to provide moderate increases in service temperature that will reach 648 K by 1990. The hybrid will probably consist of outer plies of condensation-cure polyimide and inner plies of addition-cure polyimides. Optimistically, technology breakthroughs in manufacture of condensation-cure polyimide structures could increase the service temperature to 720 K by 1990.

Upper bounds on maximum service temperature are based on service life that does not exceed 125 h. Structural applications requiring significantly longer service life may be limited to service temperatures indicated by the lower bound. The lower bound for 1000 h service is forecast to be 575 K in 1990.

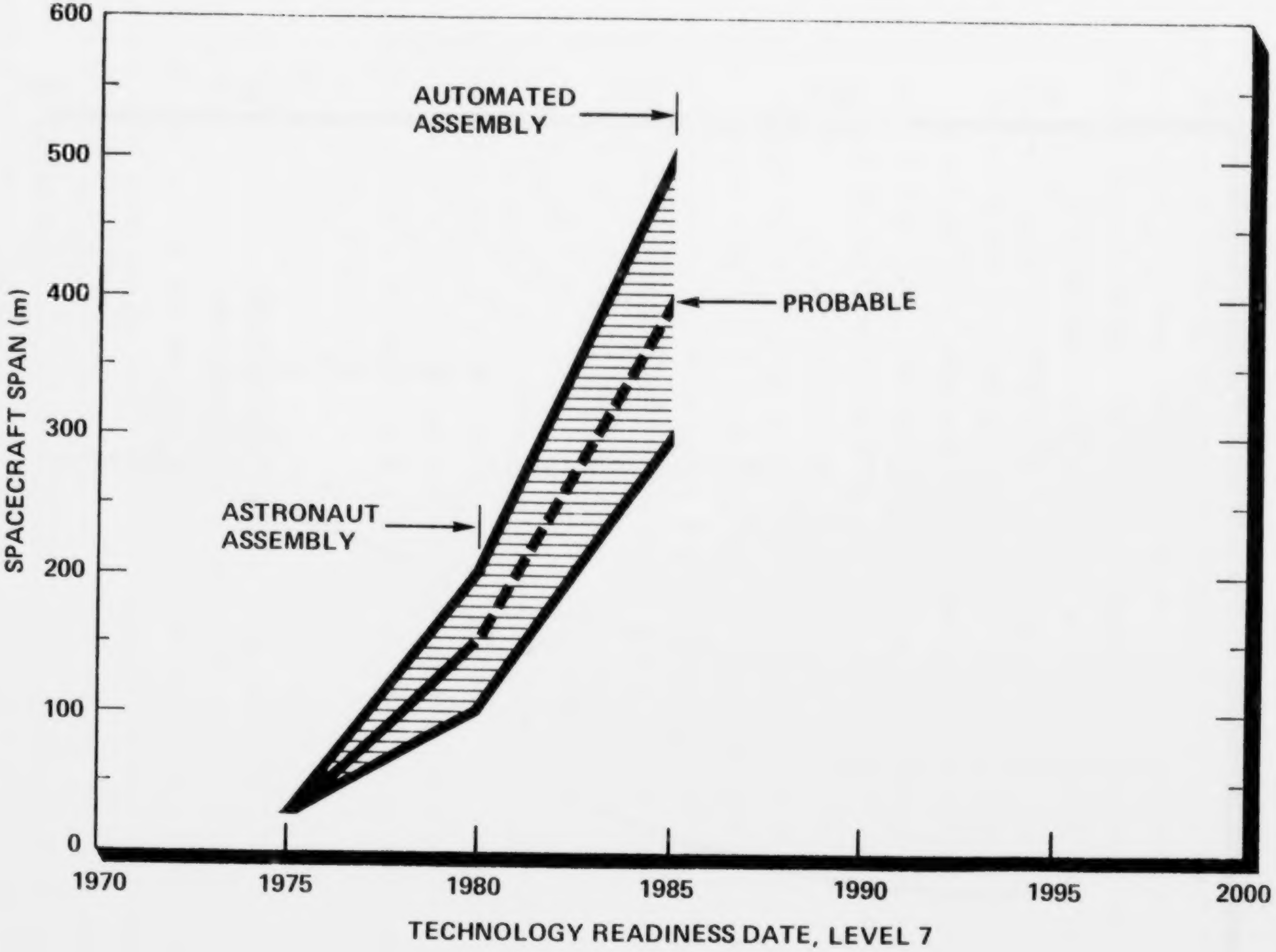

Figure 3.1. Estimated Erectable Spacecraft Capability Using One Shuttle Flight

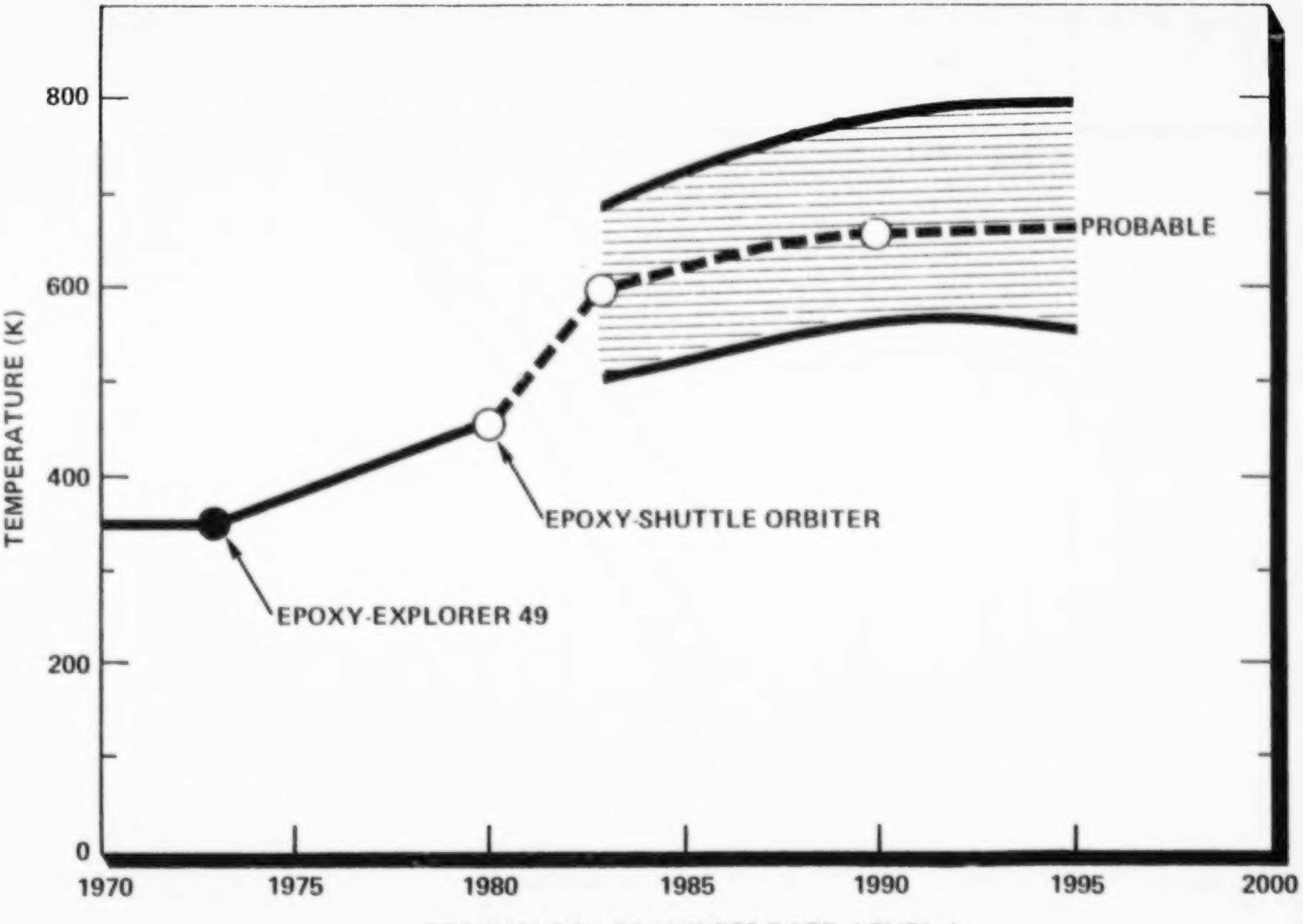

Figure 3.2. Maximum Usable Non-Metallic Service Temperature

Maximum Usable Metallic Service Temperature (Fig. 3.3). This forecast treats the maximum service temperature for metals expected to be available for 500 mission application to entry vehicles. Important increases in the maximum use temperature of low-density, high-strength alloys including aluminum and titanium alloys and superalloys are expected but are not examined here. Coated columbium is the structural metal having the highest use temperature for entry applications in the foreseeable future. This material has not been demonstrated in engineering components in space, but sufficient research and development are in hand to give very high confidence that the material can be used at temperatures up to 1350 K. No flight experience can be obtained in the 1980s unless an OEX experiment is conducted, and such an experiment is not currently planned. However, such an experiment would be expected to show 1600 K capability.

The use temperatures of columbium in air is limited by loss of the coating. While 1600 K is probably the maximum temperature for extended service in air with the current coating, development of an HfO_2 SiO_2 coating is possible and an optimum coating of this type could lead to service temperatures up to 2200 K.

Currently, maximum service temperature is not viewed as the major materials problem for future transportation systems, and essentially no research is being done to extend the service temperature capability of refractory metals. Therefore, the most probable maximum service temperature for metals is 1600 K.

Resin Matrix Composites Space Environment Lifetime (Fig. 3.4). Because of the long times involved and the rapid changes in materials, candidate materials for any application are unlikely ever to have space-demonstrated lifetime for the duration of the application. Selection must be made on the basis of accelerated ground tests. By 1970, ground tests had shown that, except for possible surface problems, several polymers which are candidate matrix materials should survive 10 years in GEO with no substantial degradation of mechanical properties. Surface coatings, which may be required for thermal control as well as for radiation protection, are not included in this forecast.

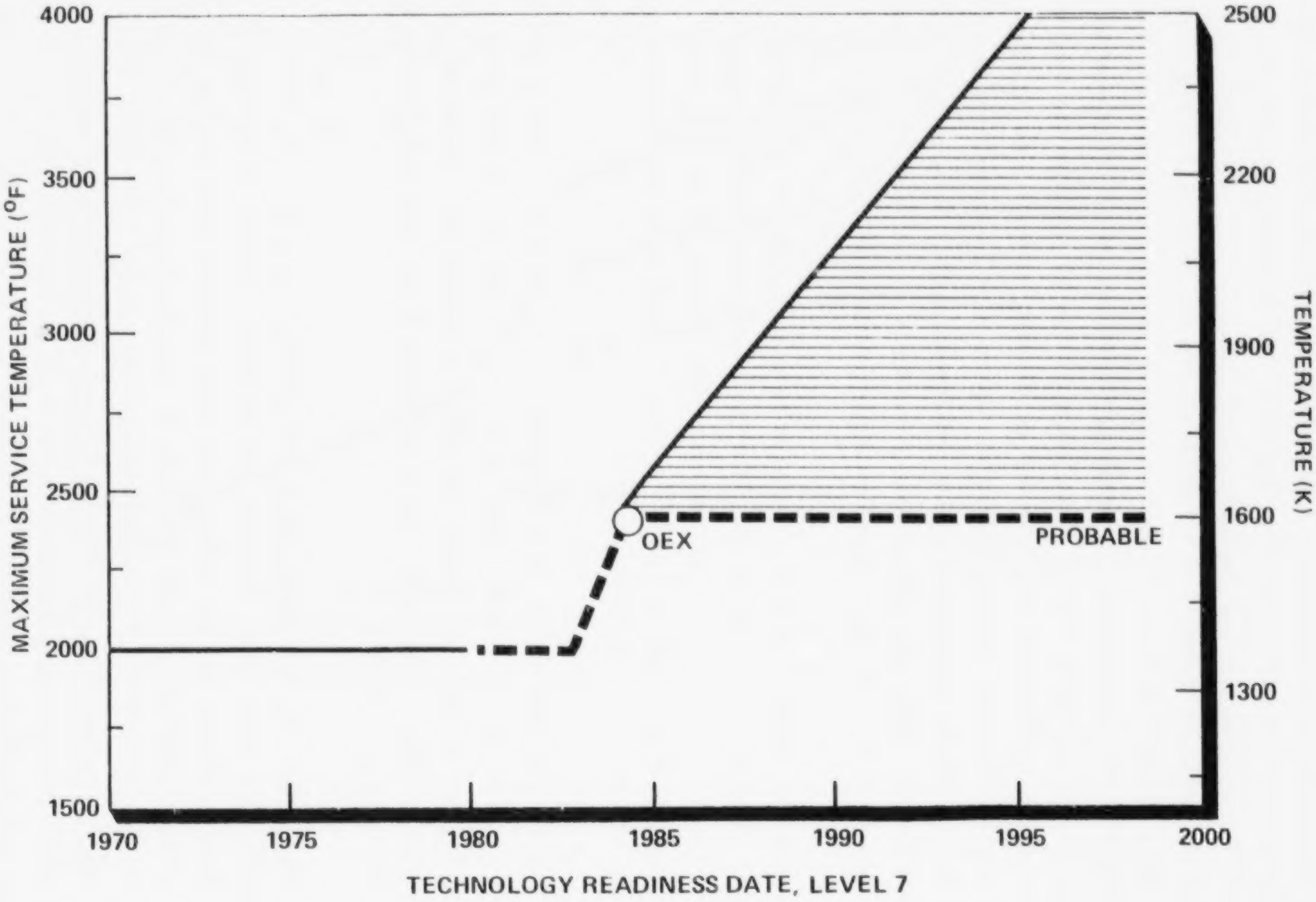

Figure 3.3 Maximum Service Temperatures for Metals

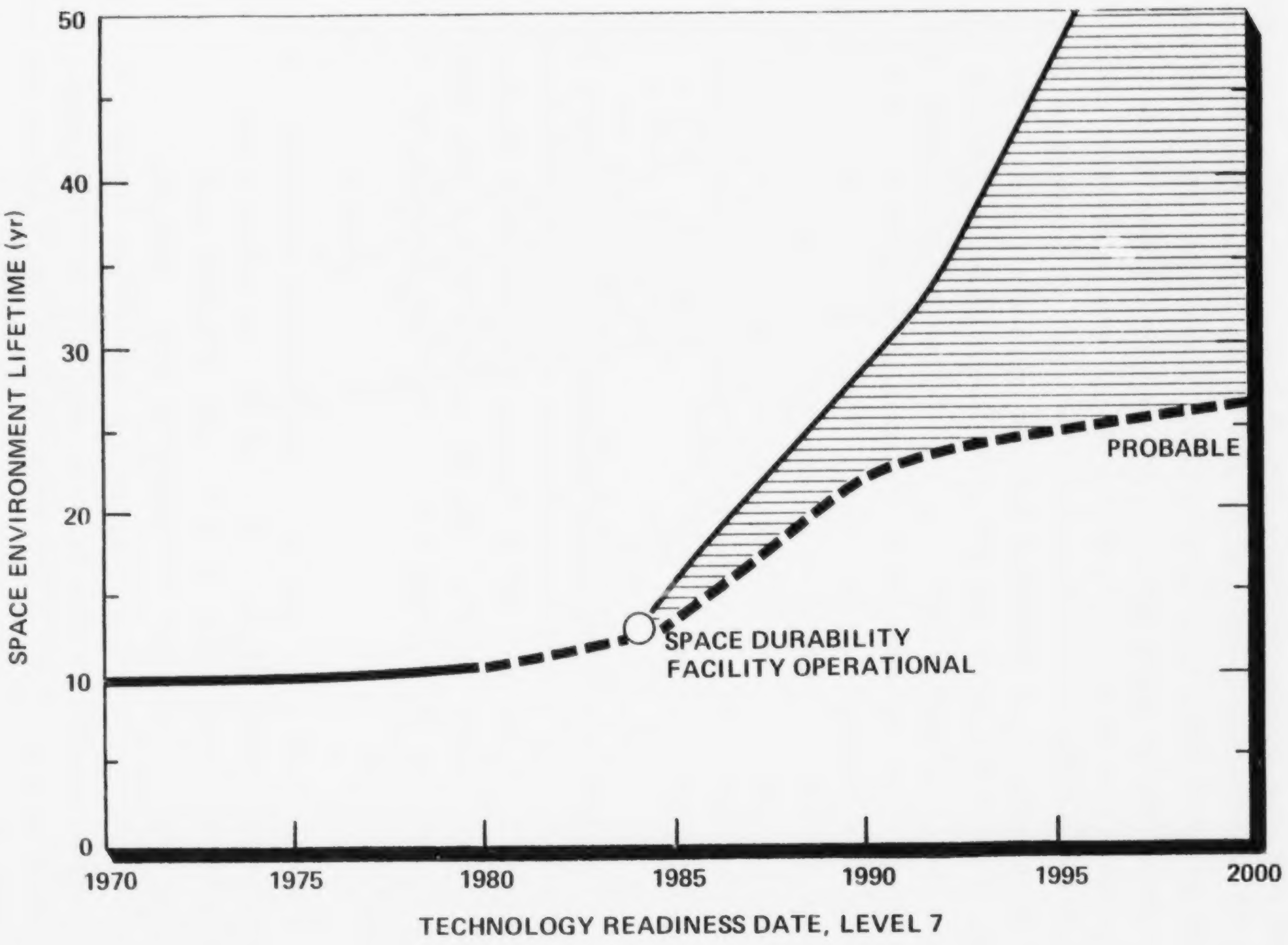

Figure 3.4. Composites – Space Enviroment Lifetime of Resin Matrix

Little progress has been made in this area since 1970. However, renewed support for research on space durability of composite materials will provide a much better definition of lifetime by 1990. Progress should be particularly rapid after 1984 if the Langley Research Center proposal for a Space Durability Facility is approved. Materials suitable for use as matrix resins should be demonstrated to have at least a 25-year lifetime. This demonstration will be based upon accelerated ground tests which are designed and interpreted in the light of fundamental theories of the interaction of materials with the space environment. Current results show that, after the radiation dose absorbed in 30 years' exposure, epoxy materials begin to suffer serious degradation of physical and mechanical properties. However, several classes of polymers which are more stable under radiation already exist. These radiation-resistant polymers, including aromatic-aliphatic hydrocarbons such as Paralene, aromatic-aliphatic polyesters, and heteroaromatic polymers such as Pyrrone, tend to be more difficult to process, but processing properties can be improved through further research.

Strength-to-Mass Ratio for Graphite/Polyimide (Fig. 3.5). The maximum attainable strength-to-mass ratio for undamaged graphite/polyimide composites is expected to remain constant at a value near 280,000 N•m/kg over the next decade and is plotted as the upper bound. R&D under the CASTS project has demonstrated Level 3 technology readiness for the undamaged composite.

Influence of flaws such as notches or slits, degradation due to moisture and thermal exposure, and tolerance for impact damage can reduce the usable strength-to-mass ratio for some polyimide matrix composites to less than one-half their as-fabricated value. Utilization of hybrid polyimide matrix composites and maturity in knowledge on the effect of flaws offer the potential to increase the usable strength-to-mass ratio to perhaps as high as 75 to 85% of the value for the as-fabricated material; thus a value of 225,000 N•m/kg is forecast for 1990.

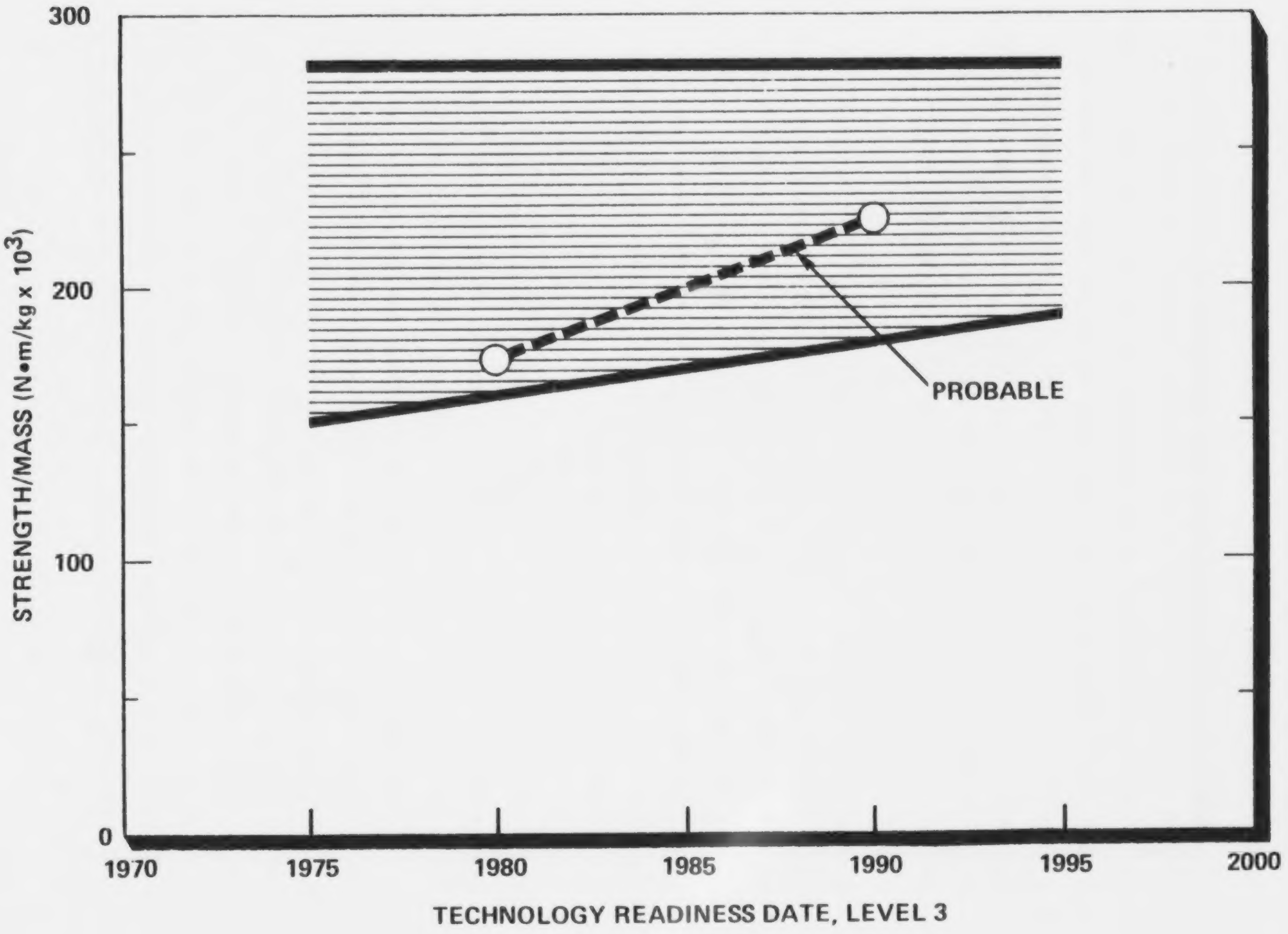

Figure 3.5. Strength-to-Mass Ratio for Graphite/Polyimide Materials

Strength-to-Weight Ratios of Tension Panels (Fig. 3.6). The strength-to-weight ratio (structural efficiency) of composite materials in general use for tension loads has increased since 1970 because stronger graphite fibers have replaced denser boron. The ratios shown in the figure are for quasi-isotropic laminates; for other laminates the ratio rises roughly in proportion to the proportion of 0° fibers. Today, allowable design values are somewhat lower than shown because the strength of manufactured panels varies from batch to batch, and this variation must be considered in the design of structures. An average value for the strength-weight ratio, without reduction for variability, is about 3×10^{-6} N•m/kg. With expected improvements in fiber manufacture and in quality control, the ratio can be expected to rise to about 4.5×10^{-6} N•m/kg by 1990.

An optimistic forecast is that improvements in fiber manufacture such as the development of ways to alleviate the high residual stresses that result from fiber creation, or a breakthrough to a stronger and lighter fiber, could raise the ratio to about 7×10^{-6} N•m/kg. Conservatively, in 1990 the strength-weight ratio will be at the same level as in 1980, at 3×10^{-6} N•m/kg. But the confidence in quality control will probably be higher and variability lower.

The strength of fiber-reinforced composite tension panels is sensitive to damage. The sensitivity can be characterized by the loss of strength due to a slit cut in the panel center; the strength falls if the slit is lengthened. Research has shown that buffer strips and stringers can inhibit unstable flaw growth. Experiments on small panels show that 60% of the undamaged strength-weight ratio can be retained. By 1990, the strength retention, on a weight-efficiency basis, can be expected to rise to 75%. The optimistic residual strength value of panels is about 85%. This upper value is limited by the weight added by the buffer strips. The lower bound, at 60% strength/weight retention, is for substantial damage characterized by a 300-mm slit. Again, weight must be added for buffer strips.

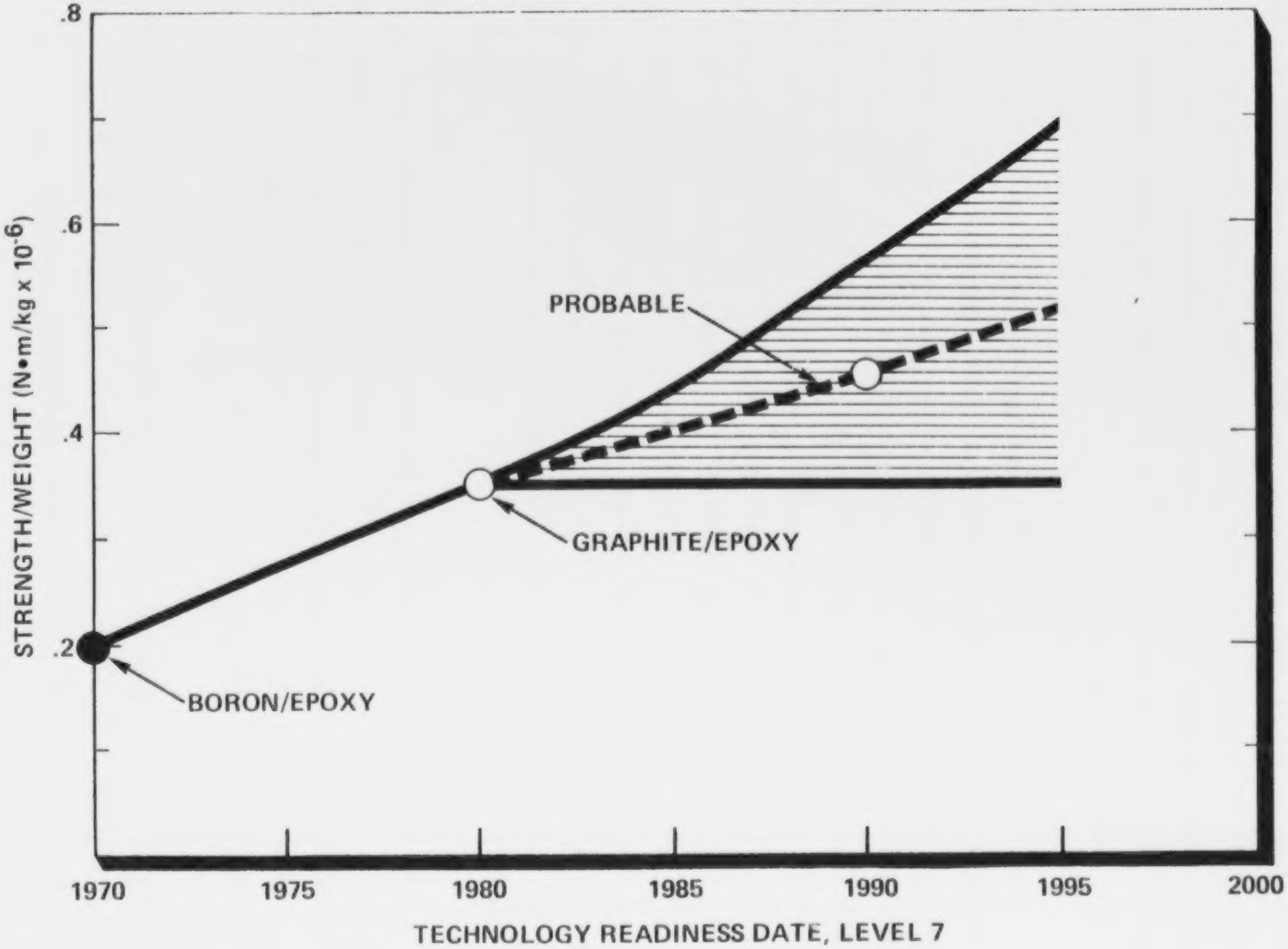

Figure 3.6. Strength-to-Mass Ratio for Composite Tension Panels

Trends and Forecasts in Payload Dynamic Load Prediction (Fig. 3.7). The data presented relates the effectiveness of analytical tools used to predict dynamic loads to the cost of such analyses. The effectiveness of the tools can be measured by several parameters such as ratio of structural weight to total payload weight, calendar time to complete analyses, accuracy of the analyses (or ratio of predicted to actual flight loads). Cost includes manpower levels and computer expenditures. A reduction in calendar time for the completion of a loads analysis cycle results in cost and weight savings to a project.

With the advent of computer tools and with a better understanding of the environment through the availability of flight data, the ratio of structural weight to total spacecraft weight was decreased by increasing the analytical effort and hence the cost. This was the trend in the 1960s for the Surveyor and Mariner spacecraft. As the analytical tools were further improved, the Viking spacecraft was designed to transient loads analysis. This required a thorough knowledge of the forcing functions derived from in-flight measurements of previously flown space vehicles. While this approach led to a lightweight structure, it was expensive. In order to reduce cost, a method for obtaining the upper bound of the dynamic loads was developed. This Shock Spectra/Impedance method was used for Voyager, resulting in a somewhat heavier structural weight at an appreciable reduction in cost.

Although the above trends are for expendable boosters, similar trends are expected for the STS. The frequency of the STS flights and the variety of payloads necessitates cost-effective dynamic-load prediction methods. The methodology to be used for a particular payload will be determined by size, complexity, and cost of the payload.

The parameter selected for characterization of the dynamic load prediction technology is total analysis cost for expensive, high-reliability payloads, of the type characterized below.

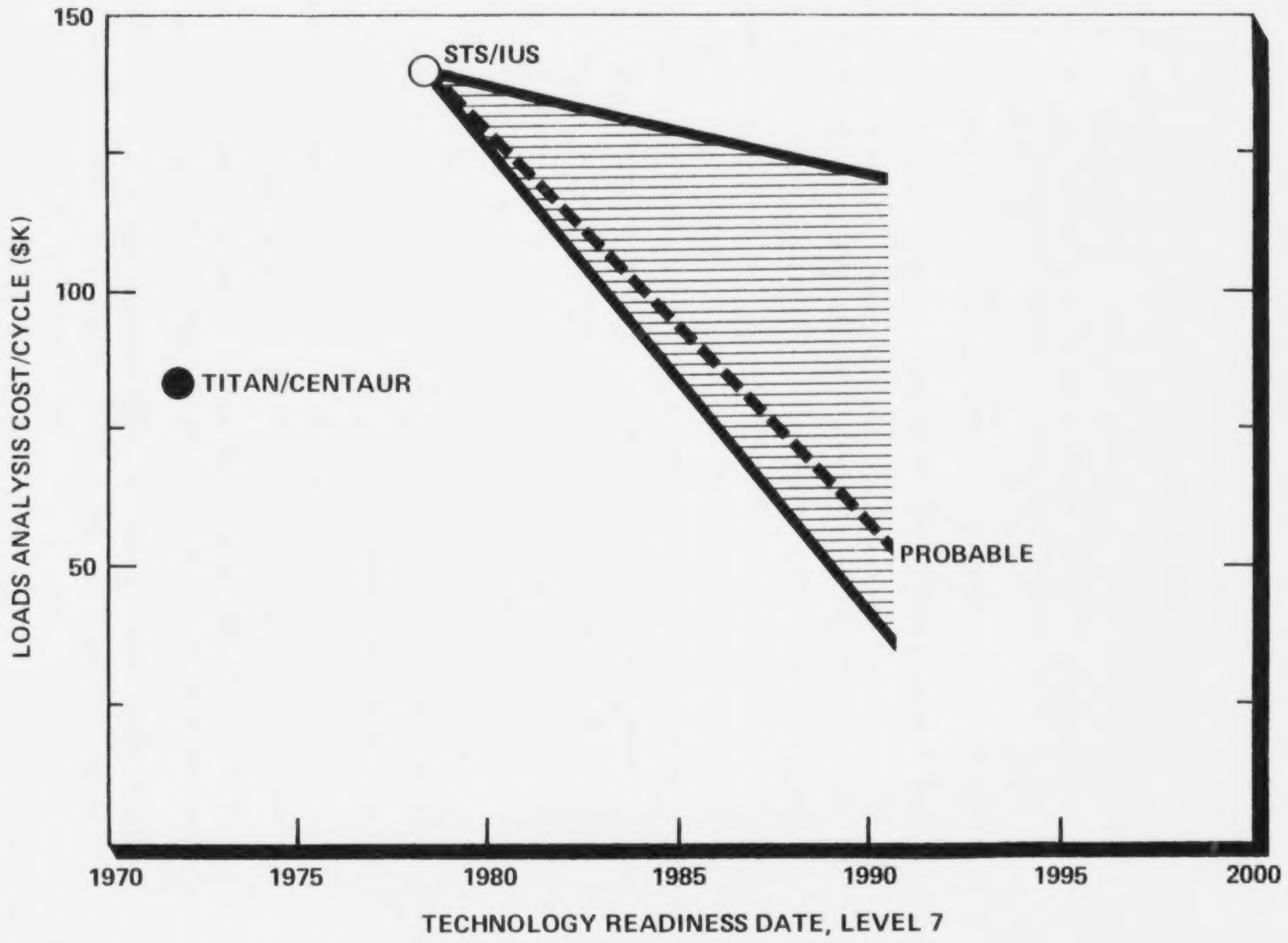

Figure 3.7. Dynamic Loads Analysis Costs

Cost	Highly expensive, large cost penalty for structural failure, detailed loads analysis justified.
Size	Large payload/orbiter dynamic interactions, may effect orbiter/external tank dynamics at launch.
Criticality	Critical launch windows, no retrieve/repair capability, single backup spacecraft.
Examples	Planetary missions, comet rendezvous, out-of-ecliptic.

The projections for the total loads analysis cost, exclusive of model development and inclusive of manpower and computer expenditure, is shown in Fig. 3.7, the projected loads analysis cost/cycle in thousands of dollars. The approximate cost of an STS/IUS (inertial upper stage) loads analysis cycle is currently estimated at $140K. This compares to a Titan/Centaur loads analysis cost of $80K, uninflated for the 1970-1975 time period. This figure shows that the current STS/IUS system transient analysis is more expensive than the Titan/Centaur analyses performed for Viking. This is mainly due to the complexities of the STS and the IUS models. The projected trend is to reduce the payload system transient loads analysis cost to at least the Tital/Centaur level by 1985. This is to be accomplished by:

1. Utilizing flight data from DATE to enhance forcing functions and improve the validity of the dynamic models, hence increase reliability of the analysis process and reduce the size of the dynamic models.
2. Using upper bound loads analysis methods for preliminary design to reduce conservatism of loads prediction.

3. Using simplified in-house transient analysis capability to decouple the loads analysis process from the launch vehicle, thus decreasing the calendar time for a loads cycle.

4. Using mode elimination methods such as are proposed by BAC in the calculation of the transient responses.

5. Taking advantage of computer developments in reducing computation costs.

All of the above are currently under development. The proposed simplified transient analysis methods have been developed at JPL and are currently being applied to the international solar polar mission (ISPM). The Generalized Shock Spectra method, currently being used to obtain design loads for the Galileo mission (GLL) and ISPM, is being modified to reduce its conservatism. This method has so far proved to be very cost effective. It is believed that the loads analyses costs can be reduced by 50% by the year 1990 if potential cost savings due to a shorter calendar time for the loads cycles are included. Such reduction prevents redesign of structure, which is costly.

A level of technology readiness does not apply to this forecast. Technology readiness in this forecast is defined as having the required software available and its accuracy and cost checked against system loads analysis data.

Temperature Capability and Heat Rejection (Fig. 3.8). The ceramic reusable surface insulation (RSI) now being used on the Space Shuttle Orbiter was originally developed for a maximum use temperature of 1530 K for 100 flights. Subsequent aeroheating updates have raised the requirement in some cases to above 1750 K. Improved materials and shorter life requirements have resulted in the adequate projected materials that have surface temperature capabilities above 1900 K with improved mechanical properties and durability. Ceramic materials with temperature capabilities

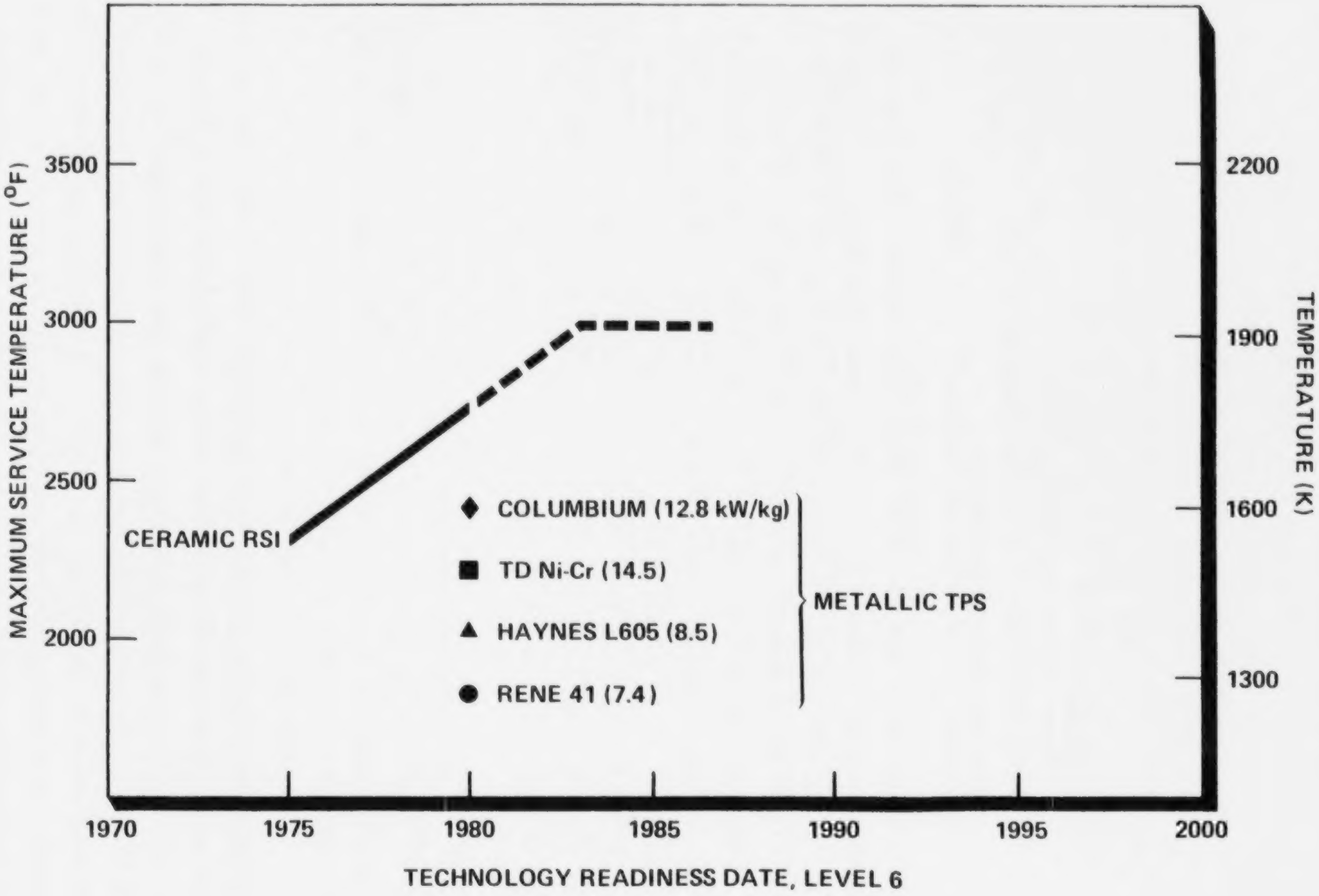

Figure 3.8. Temperature and Heat Rejection Capability of Thermal Protection Systems

above 1900 K and having mechanical properties superior by at least a factor of 2 over those currently being used on the Space Shuttle Orbiter are forecast by 1983. This forecast is based on expected improvement from further development of a family of fiber-fiber composite rigid insulation materials that have recently been invented at Ames. It is expected that improved materials will come from incorporation of new ceramic fibers being developed under NASA sponsorship and advanced bonding concepts now under study.

Metallic TPSs are little influenced by the structural and life constraints since the TPS serves a thermal function and does not carry primary structural loads. The data points in Fig. 3.8 show the maximum service temperature for four metallic TPSs and their current heat rejections per unit mass. The columbium TPS represents the maximum temperature limit for passive metallic TPS. The driver for metallic TPS technology is weight reduction. New design concepts are being developed to increase the power dissipation per unit mass. The past 10-year period has seen gains between 20-50% in kW/kg for René 41, Haynes L605, and TD Ni-Cr TPS.

Liquid metal (sodium) heat pipes have been used as a device to reduce leading edge temperatures for Shuttle application to a range that is compatible with superalloy construction. For this application, which involves nonuniform heating with a peak value of approximately 292 kW/m^2 and a surface temperature of approximately 1250 K, the heat rejection factor is approximately 1.4 kW/kg. Recent analytical studies indicate that the mass, which is governed primarily by structural consideration, can be reduced approximately 40%, increasing the heat rejection factor to approximately 2.5 kW/kg.

The current capability of thermal control materials for satellites operating in near-earth orbit and for spacecraft during interplanetary flight is approximately one earth sun. This is defined at 1.38 kW/m^2. The current thermal control coatings are pigments suspended in an organic binder. Other more refractory materials such as silica have been used for satellite thermal control in special applications.

Thermal control capability is forecast to be over 2500 earth suns (3450 kW/m^2) in 1982. The driver for this technology development is the requirement to provide thermal shielding for payloads near the sun. New approaches for thermal control differ from the traditional approach in that more refractory materials such as graphite or carbon-carbon are employed; these operate at higher temperatures than were previously attained. In addition, there is a small amount of mass loss from the shield during exposure.

The problem of protecting the payload from the heat shield remains since at elevated temperatures the heat shield itself radiates a considerable amount of energy. This protection is achieved by a configuration which enables the payload to reflect the thermal radiation emitted from the heat shield. The main advantage of this scheme is that the payload reflectors never have to face the sun; hence their reflectivity will not be degraded by damaging ultraviolet or particle radiation.

The current configuration attempts to minimize outgassing of the heat shield. Not much increase in capability beyond the 2500 earth suns can be anticipated by 1990 unless a material much more refractory than graphite is developed.

4 INFORMATION SYSTEMS

4.1 SENSORS

4.1.1 Ultraviolet-Visible Laser Remote Sensing (J. Laudenslager, JPL)

Active laser remote sensing of atmospheric transport phenomena, aerosols, and chemical species is a rapidly developing technology. Currently, IR lasers are used mostly for these remote sensing applications because IR laser technology is already highly developed. Fluorescence backscattering detection of chemical species in the atmosphere is a very sensitive technique suitable for detection of even trace molecules; however, fluorescence detection of atoms and molecules required narrow-frequency tunable laser sources in the ultraviolet or visible wavelength regions where laser technology is not as advanced.

Active laser remote sensing of species in the ultraviolet requires that this laser technology be developed at least to the present capabilities of IR lasers. Other technology items associated with UV laser sensing such as optics, detectors, electric power supplies, and data processing capabilities are similar to those already used for IR or visible dye laser sensing and do not need as much development as the UV laser technology itself. The three key parameters for UV laser technology which must be advanced before these lasers can be utilized efficiently in remote detection of chemical species are: laser pulse energy, laser efficiency, and laser wavelength coverage.

The emergence of efficient high-energy pulsed UV laser sources is very recent, since 1975. Although UV laser technology has not as yet been developed to the level of IR lasers, there do not appear to be any fundamental limitations which would prevent the rapid development of UV gas lasers.

Pulsed gas discharge lasers operating in the UV-visible regions are being developed under OAST R&T programs for specific remote sensing applications. Similar gas lasers are also being developed at other federally funded research laboratories for a variety of high-power applications such as isotope separation, laser fusion, and underwater communications. These latter applications require very high average power laser sources (>1 kW) or very high energies per pulse (>1 kJ); NASA's remote sensing requirements for UV lasers are: low average power (1 to 10 W), modest output pulse energies (0.1 to 2 J), narrowband laser operation which is tunable on and off a chemical species absorption line, narrow laser temporal pulsewidths (1 to 50 ns) for high-resolution ranging, and good electrical efficiency (>1%).

The most efficient UV gas lasers at present are the rare gas halide excimer lasers. These electric discharge gas lasers are compact, have been operated at 1% electrical efficiencies, and have shown promise for even higher efficiencies. Pulse energies greater than 1 J have been obtained from these lasers, and they are capable of high repetition rate operation if the gas is recirculated. A variety of excimer lasers which can be tuned across a bandwidth of about 1 nm are available covering a variety of wavelength regions throughout the UV, and it is also possible to operate these excimer lasers under narrow-bandwidth conditions (<0.01 Å). The ability to control the output characteristics of excimer lasers such as pulsewidth, energy per pulse, repetition rate, bandwidth, and wavelength and still have good efficiencies makes these lasers ideal for remote sensing applications.

Except for a ruby laser on Apollo 17, no laser has been flown on NASA earth-orbiting or planetary spacecraft. Visible solid-state and dye lasers have been proposed for manned spaceflight on the shuttle in the 1980s, but dye lasers do not have the pulse energy or lifetime capabilities of gas excimer lasers when the dye is frequency doubled to operate in the ultraviolet. Future remote sensing applications for any laser on a planetary spacecraft are a long-lead-time technology item. Ultraviolet laser remote sensing from an aircraft, balloon, or shuttleborne platform, however, is a highly probable near-term application which would make a significant impact on NASA programs dealing with earth's upper atmosphere. A compacted laboratory version of a UV laser can be flown on a manned aircraft or shuttle platform; however, a laser remote sensing experiment from a balloon platform requires considerable more effort since a balloon platform is unmanned and it does not have as large a power source. Technology readiness dates shown represent level 3 state of development for the UV laser sensing technology at this time.

Narrowband UV Laser Pulse Energy (Fig. 4.1). The pulse energy needed from a UV laser used for active remote sensing of chemical species depends on the laser linewidth compared to the species absorption linewidth and the altitude ranging distance. Only several hundred millijoules per pulse should be needed for a UV laser operating from a balloon platform, but more than 1 J per pulse may be required for the same laser from the orbital altitudes of the shuttle.

Rare gas halide excimer lasers operate in the range of 0.1 to 1.0 J broadband, and these points are represented on the graph in Fig. 4.1. Rare gas halide lasers operated in an oscillator-amplifier arrangement to control the frequency and frequency width still operate with the same output energy capabilities. With continued research support, it should be possible to build a UV laser system which can be operated narrowbanded and can be tuned over a limited wavelength region while still maintaining good electrical efficiency and high pulse energy (1 J).

Ratio of Electrical to Laser Output Efficiency (Fig. 4.2). The electrical efficiency of a gas discharge laser is the ratio of laser output energy per pulse over the stored electrical energy contained in the main discharge storage capacitor. Other electrical power consumption comes from filament heaters for thyratron switches, circulating pumps for the gas, and any cooling needed for laser components. Electric discharge rare gas halide lasers have inherent efficiencies of laser output to electrical discharge energy deposited in the gas of 15%; transmission line efficiencies for these lasers have been has high as 2.7%, but overall wall-plug efficiencies are typically 1%. With more development and proper design, the overall wall-plug efficiencies should be made to approach the intrinsic 2.7% electrical efficiency, but major breakthroughs in discharge technology would be needed to approach the theoretical 15% efficiency.

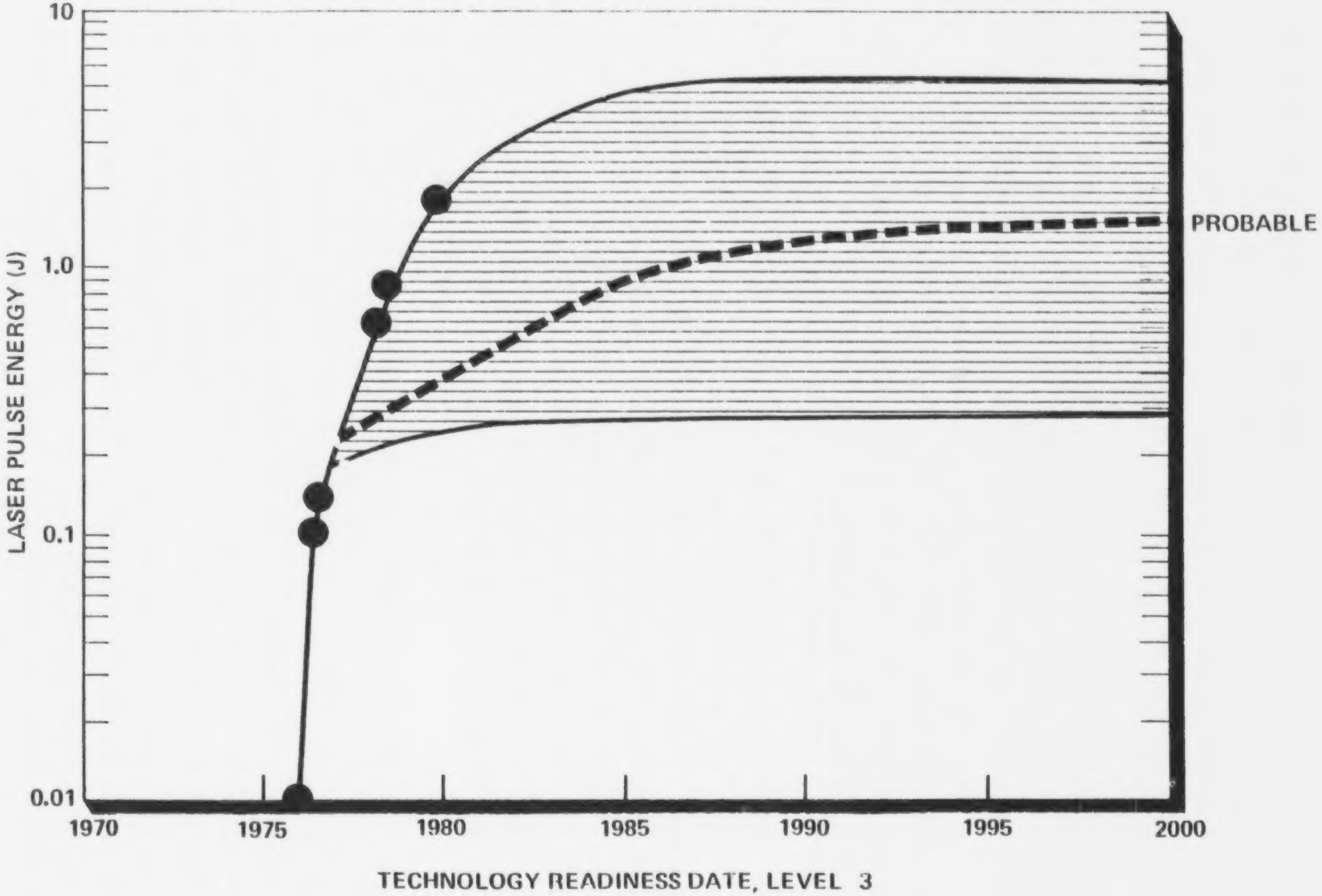

Figure 4.1. Narrowband UV Laser Pulse Energy

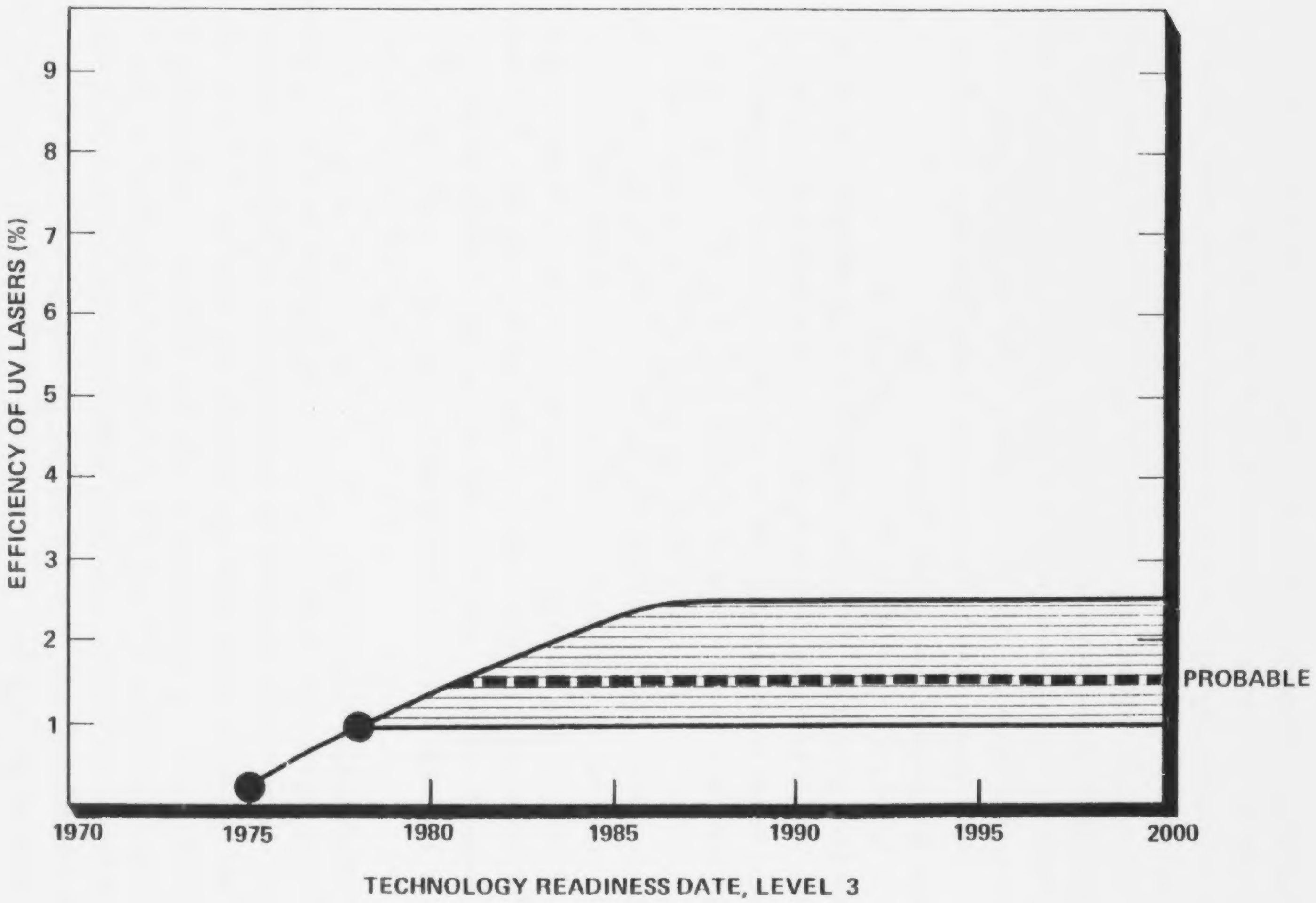

Figure 4.2. Electric Efficiency of UV Gas Lasers

Wavelength Coverage of UV Lasers (Fig. 4.3). There are a variety of rare gas halide excimer lasers which cover various small wavelength regions throughout the UV. A list of excimer lasers and their central wavelengths follows: ArF at 193 nm, KrCl at 222 nm, KrF at 249 nm, XeBr at 282 nm, XeCl at 308 nm, and XeF at 351 nm. Each of the lasers can be tuned through a wavelength region of about 1 to 2 nm. Other gas discharge lasers are being discovered which fall in various regions in the UV, such as ClF laser at 285 nm, Cl_2 laser at 256 nm, and F_2 laser at 157 nm. These lasers operate on molecular transitions and, therefore, they also are tunable over narrow ranges.

Because this class of lasers operates at high energies per pulse (see Fig. 4.1), efficient frequency-shifting techniques such as the stimulated Raman effect can be used to provide narrowband wavelength coverage throughout most of the UV.

In the near term, UV-visible lasers will be developed which can be directly tuned to match resonant lines and absorption features of a number of atmospheric species. This will allow a systems demonstration of the UV laser sensing technology to be implemented rapidly. With continued research support, rapid coverage of the entire UV wavelength region by gas lasers should be realizable.

4.1.2 High Peak Power Dye Lasers

Our understanding of the chemistry of the atmosphere will ultimately depend on our ability to measure the concentrations of the more important atomic and molecular constituents as functions of altitude and local time on a global basis. Global spatially resolved data can only be obtained using a pulsed active probe combined with a range-gated receiver and operated from a spacecraft. To probe deeper into the atmosphere, the emitted wavelengths must be within one of the atmospheric windows such as the visible-near ultraviolet band. Furthermore, due to the variety of constituents, it is desirable that the active probe be tunable over a wide frequency range. Receiver signal-to-noise considerations dictate high output energies for long-range probes.

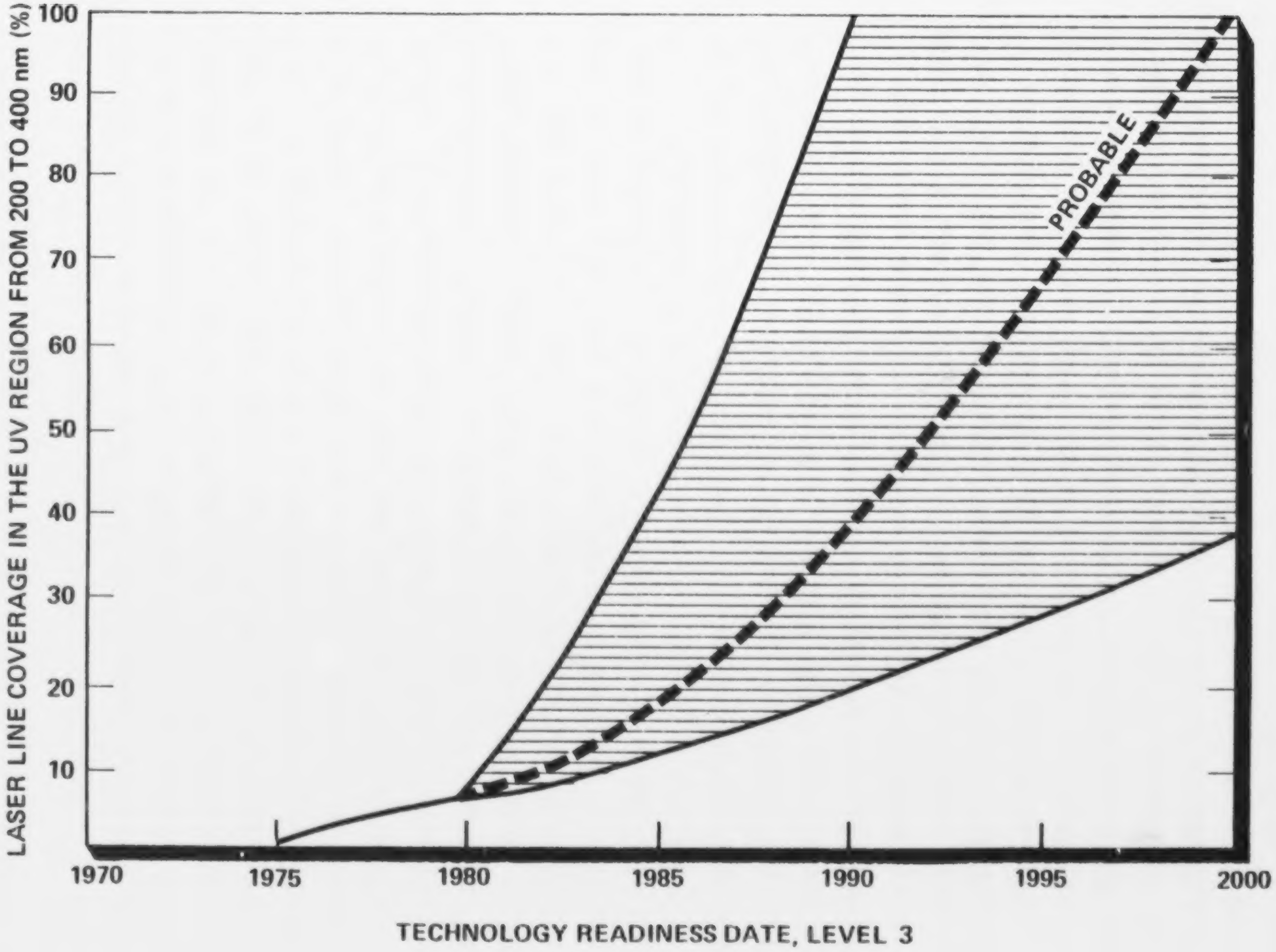

Figure 4.3. Wavelength Coverage of UV Lasers

Dye lasers are tunable over a fairly wide wavelength range (typically a few hundred angstroms), and multiple dyes can readily cover the full visible spectrum. Through the use of nonlinear frequency-doubling techniques, the range of emission can be extended throughout the near UV where useful scattering and electronic absorption and fluorescence experiments can be performed. The efficiency of the UV generation process, and hence the sensitivity of the lidar instrument, increases quadratically with the peak power of the dye laser pulse. High peak power also opens the door to next-generation two-photon lidar systems. Such systems would permit excitation of electronic levels in atomic and molecular species which cannot be reached by a single photon because (1) no laser source of the higher energy photon exists or (2) strong atmospheric attenuation makes the spatial region of interest inaccessible to the photon. Clearly then, peak power, defined as the dye laser energy divided by the pulsewidth, is the relevant parameter for characterizing the technology.

The development of dye lasers has generally proceeded along two different lines. High-energy flashlamp-pumped dye lasers with an output energy of 400 J (1) or average powers of up to 100 W (2) have been developed. These lasers typically emit over a broad wavelength band (several angstroms) and are characterized by relatively long pulsewidths (300 ns to 1 ms). On the other hand, spectrally-narrowed (10^{-3} to 10^{-1} Å) and short-pulse (10^{-3} to 10 ns) dye laser oscillators pumped by external lasers have been developed for high-resolution and time-resolved spectroscopic applications. Depending on the degree of spectal narrowing and pulsewidth and the power of the pulsed pump laser, the dye output energies can vary over a wide range (10^{-9} to 10^{-1} J). In short, the two physical quantities, energy and pulsewidth, which combine to give us the relevant parameter peak power, have been optimized via two diverging technological approaches.

---

[1] "Laser Monitoring of the Atmosphere," E. D. Hinkley, ed., in Topics in Applied Physics, Vol. 14, 1976.

[2] "Shuttle Atmospheric LIDAR Multi-User Instrument System," R. K. Seals, Jr., and J. F. Kibler, ed., NASA Document, Langley Research Center.

Under OAST sponsorship, an attempt is being made to combine the spectral purity and short pulsewidth of the low-energy, laser-pumped dye oscillator with the high output energy power capabilities of flashlam pumped systems. The technique being employed is injection-locked regenerative amplification in a flashlamp-pumped dye amplifier of a spectrally narrow short pulse from a low-energy oscillator. It is anticipated that the output energy attainable from the flashlamp-pumped system will not degrade significantly from the long-pulse value, while the pulsewidth will decrease by several orders of magnitude. This will result in a corresponding increase in peak power. This is the parameter that best describes the evolution of this technology.

Peak Power (Fig. 4.4). In 1970, short-pulse narrowband operation of dye lasers was generally achieved using pulsed nitrogen pump lasers and typically provided peak powers in the 40-kW range. The replacement of the nitrogen laser by high-power frequency-doubled, Q-switched Nd:YAG lasers as the pump source led to vastly improved dye output energies in certain dyes such as Rhodamine 6G. Current technology permits peak power generation on the order of 6 MW in narrowband operation. Approximately the same peak power is obtained if one considers high-power Q-switched laser pumping of a short-pulse (10 ns) dye laser system or alternatively a CW laser injection-locked, flashlamp-pumped, long-pulse (1 μs) dye system. By 1981, we project an increase to the 10-MW to 30-MW range resulting from the injection of a 10-ns pulse into a regenerative, flashlamp-pumped, dye laser amplifier. Incorporation of a mode-locked dye laser oscillator generating 100-ps pulses is expected to push the peak power into the 1 to 3 GW range by 1983. Amplifier design improvements will increase the peak power to 10 GW by 1985. By 1990, utilization of the full bandwidth potential of the laser dye will provide seed pulsewidths in the 1 to 10 ps range and peak powers in excess of 100 GW. At these levels, optical damage will be a severe limitation which will limit the future growth in peak power.

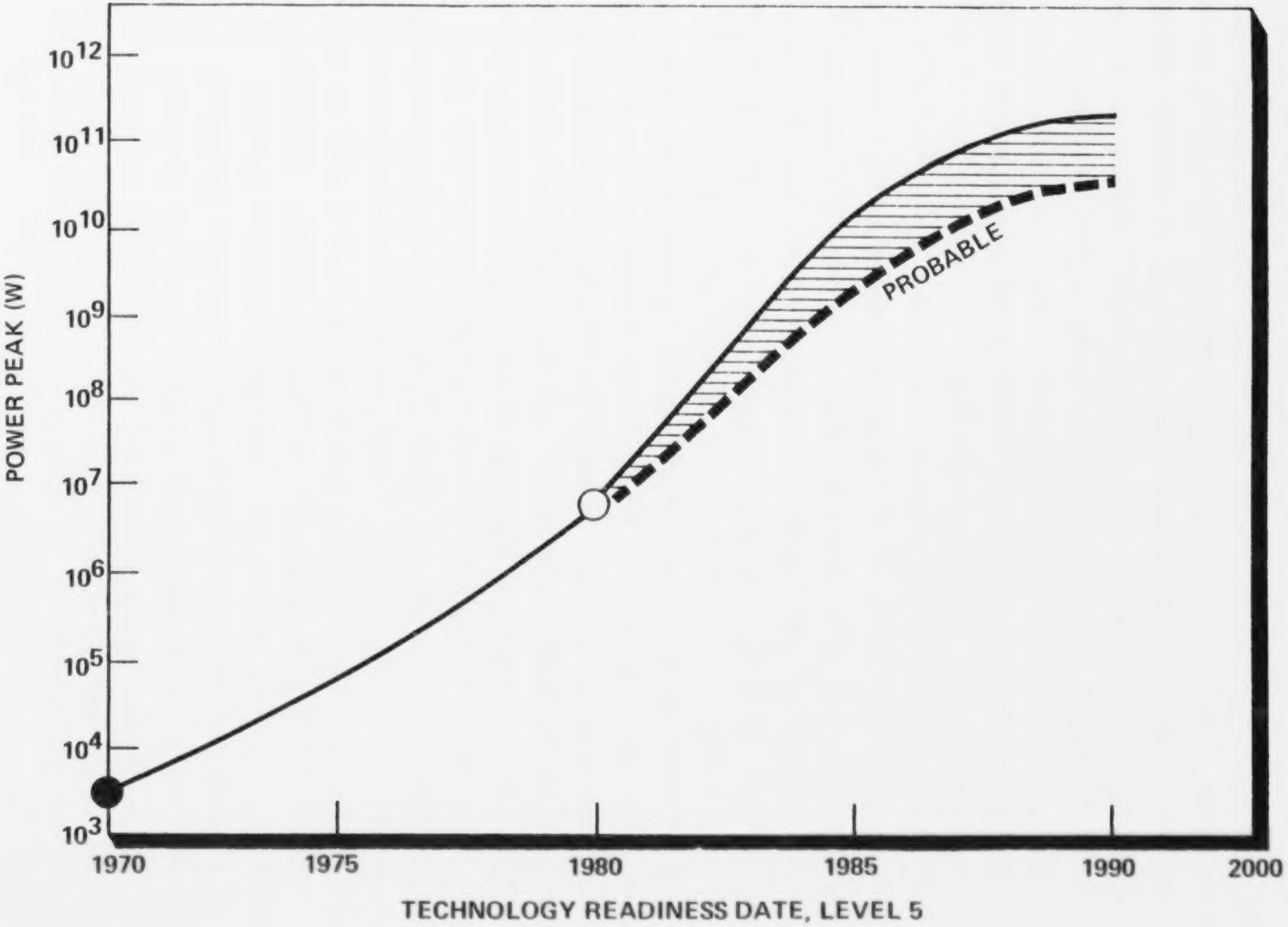

Figure 4.4 Peak Power of Dye Lasers

4.1.3 Active Sensors: Centimeter Accuracy Spacebased Laser Ranging Systems

A space-based laser ranging system capable of ranging to ground targets with centimeter accuracies has application in a variety of geophysics programs. Such a system can monitor the very slow relative motions between the tectonic plates which make up the earth's surface and possibly permit the prediction of major earthquakes. It can provide worldwide geodetic surveys and refine out models of the earth's geopotential with a precision never before realized. By combining the ranging function with altimetry, the system can better define its own orbit and simultaneously provide accurate measurements of ice and snow topography and the volumetric fluctuations in the earth's ice sheets. Because the system is space-based, it can monitor thousands of earth-based points over the period of several orbits, thereby providing considerably more geophysical data and at a cost greatly reduced relative to a large, ground-based network equipped with computers, tracking telescopes, laser transmitters, high-performance clocks and receivers, safety equipment, and necessary personnel.

A centimeter-accuracy space-based laser ranging system consists of many high-technology subsystems. The development and/or testing of these subsystems has been and is currently being funded by OAST. This includes the development of (1) a prototype flight model of a 100-ps pulsed laser transmitter; (2) a "coarse" ranging receiver consisting primarily of a high-performance photomultiplier tube, constant fraction discriminator, and epoch timer; (3) a 10-ps resolution circular-scan streak tube which serves as a range vernier for the "coarse" receiver; (4) a high-speed microcontroller and pointing system for rapidly acquiring and interrogating different ground-based targets; and (5) computer software development for the acquisition, tracking, and ranging functions. Although various technological parameters could be defined for each of these subsystems, the RMS range accuracy to a fixed retroreflector target summarizes the transmitter and receiver performance in a meaningful way. A second important parameter for the space-based application is transmitter prime power, which has been reduced significantly over the past few years as a result of OAST-funded research.

The accuracy of ground-based laser ranging systems has improved dramatically since their introduction in 1964, when few meter accuracies were typically obtained with Q-switched ruby transmitters. By 1975, the range errors were reduced to the 5 to 10 cm level with the introduction of cavity-dumped ruby laser transmitters and improved receiver techniques. Recent experiments using subnanosecond pulsed Nd:YAG lasers suggest the possibility of range accuracies to a few millimeters, which more than satisfies anticipated near-term geophysical requirements.

The development of flight-qualified laser transmitters and range receivers has typically lagged several years behind the introduction of similar ground-based hardware. The impetus for flight qualification of laser ranging systems has, for the most part, come from the military, which has been primarily interested in their use as laser range finders and designators for "smart" weapons. The rather loose accuracy requirements for these applications have been fairly well satisfied by the older, but reliable, Q-switched laser technology, and there has been only a limited military effort, primarily in the Nd:YAG laser communications area, to develop subnanosecond pulsed laser technology for space use. Under OAST sponsorship, the lessons learned from military hardware development are being combined with appropriate new technology to produce more rugged, compact, and prime power conserving subnanosecond laser ranging components for eventual spacecraft use. The parameters which we have chosen to represent the technology, RMS range accuracy and prime power, are discussed below.

RMS Range Accuracy of Flight Systems (Fig. 4.5). The first laser to fly in space on a limited-duration mission was the Apollo 11 altimeter, which utilized a Q-switched ruby laser transmitter and provided range resolution at the 1-m level in 1969. Subsequent development of range finders by the military resulted in 10 to 20 cm accuracies from a com-

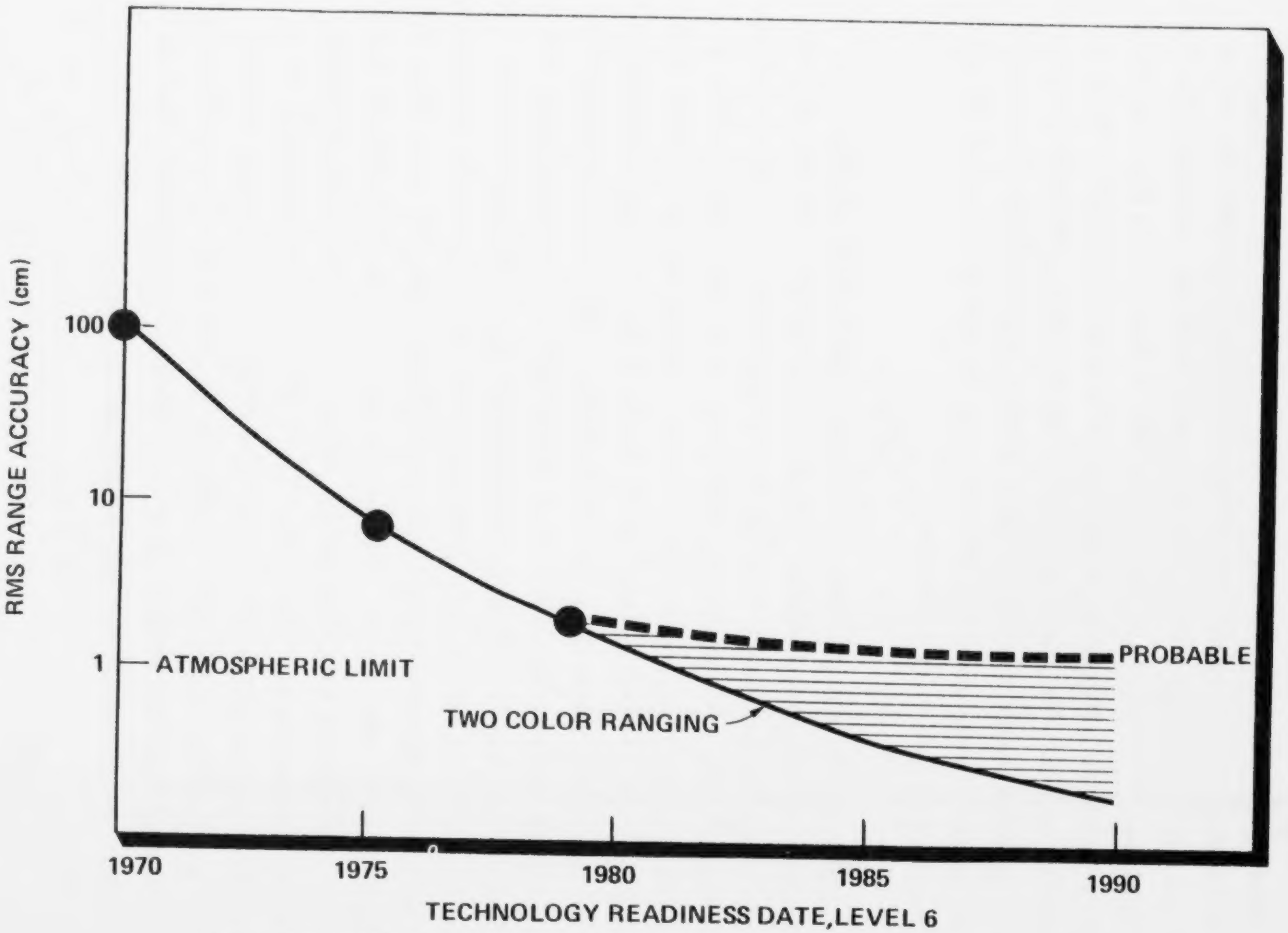

Figure 4.5. RMS Range Accuracy of Centimeter Accuracy Space-Based Laser Ranging

pact, flight-qualified package. Recent experiments indicate that, as a result of component development carried out under OAST sponsorship, the ranging instrumentation will no longer be the dominant error mechanism in the absolute range measurement. The dominant error sources will be the atmospheric refractive index contribution over the range link and retroreflector target signature effects. Current atmospheric models based on surface temperature, pressure, and humidity measurements limit the absolute range accuracy to 1 or 2 cm. A dual wavelength capability could with modest effort, be added to the present package to more accurately account for the atmospheric correction. Combined with improved retroreflector target designs, such a system could potentially provide range accuracies of a few millimeters and information on surface temperature and pressure profiles.

Prime Power Requirements for Subnanosecond Pulse Lasers (Fig. 4.6). First-generation, ground-based, subnanosecond pulsed systems used CW-pumped, model-locked laser oscillators to generate a 150-MHz pulse train from which pulses were selected at a 10-Hz rate and injected into a flashlamp-pumped regenerative amplifier. The low-energy (1 mJ), low-repetition-rate (10 Hz) output pulse train from this system was obtained at the expense of about 4 kW of prime power. The pulse was further amplified by successive single-pass amplifiers each consuming an additional 200 W of prime power. Techniques developed under OAST sponsorship have allowed us to replace the oscillator/regenerative amplifier combination by a single flashlamp-pumped laser oscillator consuming less than 100 W of prime power. The use of double-pass rather than single-pass amplifiers reduces the pumping requirements of later flashlamp-pumped amplifier stages by approximately one-half. The total power consumption of the transmitter prototype is presently less than 400 W although the upgraded engineering model will consume about 600 W due to an additional single-pass amplifier stage. Future prime power reductions will be relatively modest and due primarily to improvements in power-supply efficiency.

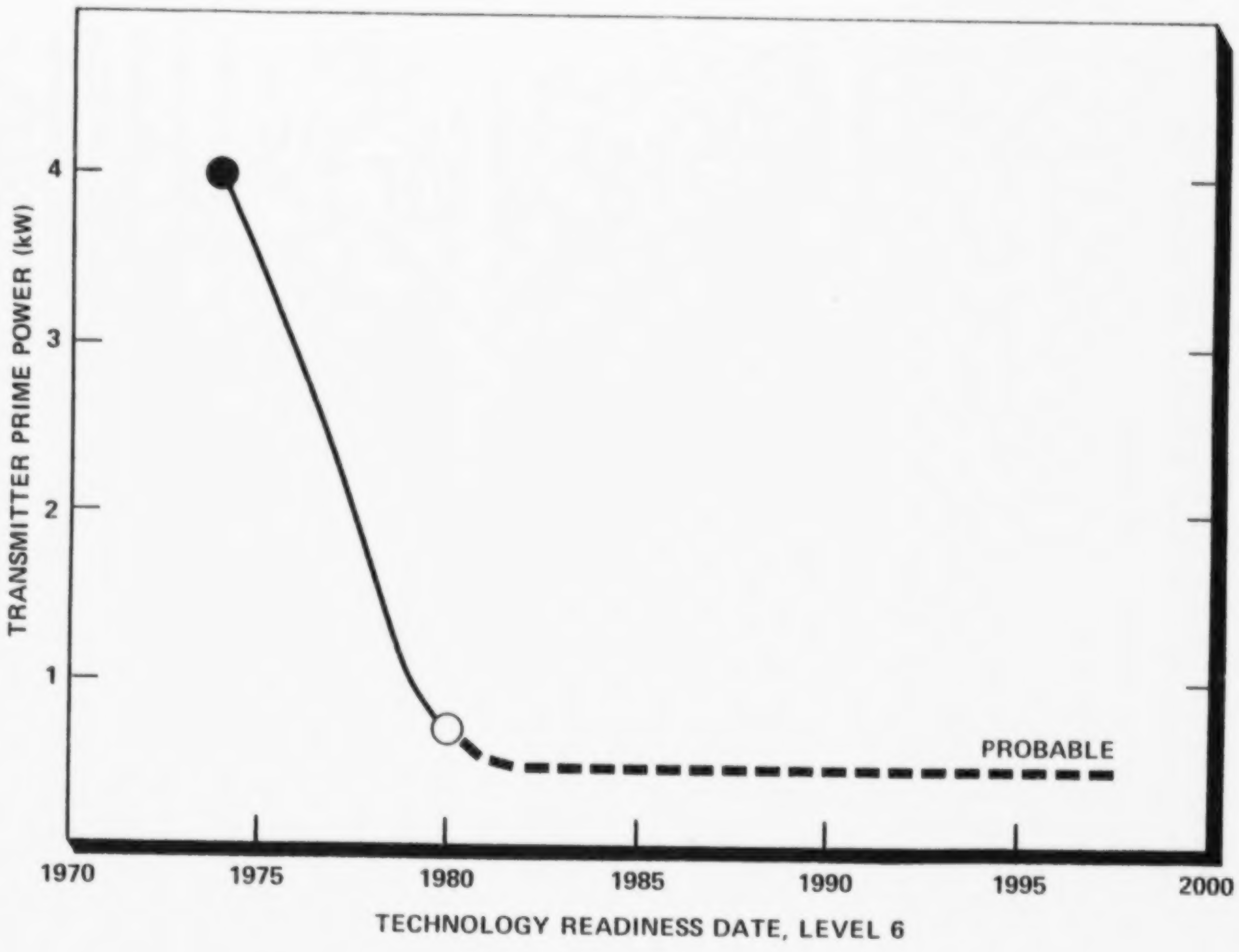

Figure 4.6. Transmitter Prime Power of Computed-Accuracy Space-Based Laser Ranging

4.1.4 IR Sensors: Submillimeter Wave Heterodyne Radiometer

Molecular species present in planetary atmospheres (including the earth) and the interstellar medium generally have strong rotational transitions in the far infrared and submillimeter wave spectrum between 0.1 and 1.2 mm. Transmissions from these molecules can provide new information regarding the chemistry and kinematics of the atmosphere or interstellar medium. High-resolution spectral analysis can be useful in identifying the emitting molecules and defining their kinematics or environment through precise measurement of the wavelength and careful analysis of the line shape. The ability to measure the signal strength of each transition accurately allows one to calculate the population density of each species.

In the submillimeter range, the limiting noise source is the thermal noise rather than quantum noise as in the infrared and optical spectrum. The receiver sensitivity can therefore be described by a noise temperature as in the microwave region. For typical bandwidths, the noise spectrum can be considered white, and the familiar linear relation between noise power, P, and system temperature, T_s, holds; i.e., $P = kT_sB$, where k is Boltzmann's constant and B is the final system bandwidth. The system temperature therefore describes the noise power level at the receiver output without signal at its input and constitutes the receiver sensitivity limit for time-varying signals. Radiometric signals, however, can be considered constant over relatively long periods of time. This makes the application of time-averaging measurement techniques possible. For an integration time τ, the minimum detectable signal power (in the temperature treatment) is given by

$$\Delta T = \frac{\alpha T_s}{\sqrt{B\tau}}$$

where α depends on the receiving technique and typically has values in the range 2 to 5. The quantity ΔT is related to the ability of the system to resolve the strength of the radiated signal (and hence, constituent concentrations). Another important parameter from a spectroscopic standpoint is clearly the spectral resolution (or final receiver bandwidth B). As can be seen from the above equation, the signal resolution ΔT depends on the spectral resolution and the integration time τ, both of which will be chosen according to the requirements of the particular experiment. We therefore choose as our relevant technological parameters the spectral resolution B and the product αT_s.

Prior to the introduction of heterodyne techniques to the submillimeter spectrum, spectroscopy used direct detection techniques. The principal elements in a direct detection system include a light-collecting telescope, a scanning interferometer for spectral narrowing and wavelength selection, and a square-law detector. Practical considerations limited the spectral resolution, determined solely by the fineness of the interferometer, to 0.005 cm^{-1} or 150 MHz. Transition linewidths are typically a few megahertz wide, and the emission lines of atmospheric constituents can be separated by as little as 5 MHz. Thus, direct detection schemes are simply incapable of identifying individual constituents and determining line-shape parameters. For detection bandwidths in excess of 1 GHz, state-of-the-art liquid-helium-cooled Ge:Ga bolometers can provide higher detection sensitivities than heterodyne systems. For limited bandwidths, however, as required for spectroscopy applications, heterodyne systems are clearly superior in sensitivity.

Under OAST sponsorship, a 1-MHz resolution submillimeter wave (SMMW) heterodyne radiometer is nearing completion. Incoming submillimeter wave radiation is mixed with the output of a frequency-stabilized SMMW local-oscillator laser via a diplexer and focused onto a Schottky diode mixer. The resulting intermediate-frequency (IF) spectrum is mixed with the output of an X-band oscillator to generate a second IF band, which is spectrally resolved to 1 MHz by a microwave receiver. The spectral resolution is set by the microwave filter bandwidth in the back end of the receiver and does not represent a performance limit. The ultimate spectral resolution is set by the SMMW laser stability, which has been measured to be 14 kHz, but there does not appear to be a need for such high resolution at this time. Signal-strength sensitivity is currently limited by the effective system noise temperature of 10,000 K. Future improvements to the design of the receiver front end are expected to dramatically reduce the system noise temperature.

Spectral Resolution or Bandwidth (Fig. 4.7). Prior to about 1970, direct detection schemes could resolve spectral detail to about 1 GHz. Improvements in interferometer design reduced this value to about 150 MHz by 1977. In 1980, heterodyne methods have sharpened the resolution to 1 MHz, and a resolution of 14 kHz seems readily achievable by 1985 if one intermittently interrupts data-taking to calibrate the local-oscillator wavelength. With further improvements to the stability of the submillimeter-wave local-oscillator laser, the resolution can probably be increased to 3 kHz by 1990, but there does not appear to be a motivation for doing so at this time. Thus the "probable" curve levels off at about 300 kHz in 1985. The curves correspond to a Level 5 stage of development.

Time-Averaged Sensitivity or Effective System Noise Temperature (Fig. 4.8). The time-averaged sensitivity depends on the system noise temperature T_s, the receiver bandwidth, B, and the integration time, τ. Spectroscopic applications suggest that we assume $B = 1$ MHz as a relevant bandwidth and, for purposes of comparison, we will assume $\tau = 1$ s. Our plot begins in 1980 since, prior to that time, 1-MHz spectral resolution had not been achieved in the submillimeter-wave region. Current estimates of the product αT_s are in the range 20,000 K and 50,000 K. Improvements to the front-end mixer design, such as the replacement of the Schottky diode by an array to reduce the field of view and reducing the effective noise temperature of the Schottky mount, should decrease the parameter value to the 6,000 to 15,000 K level by 1985. Further improvements to the receiver back end are expected to reduce the αT_s product to the 2000-5000 K range by 1990. The curves correspond to a Level 5 stage of development.

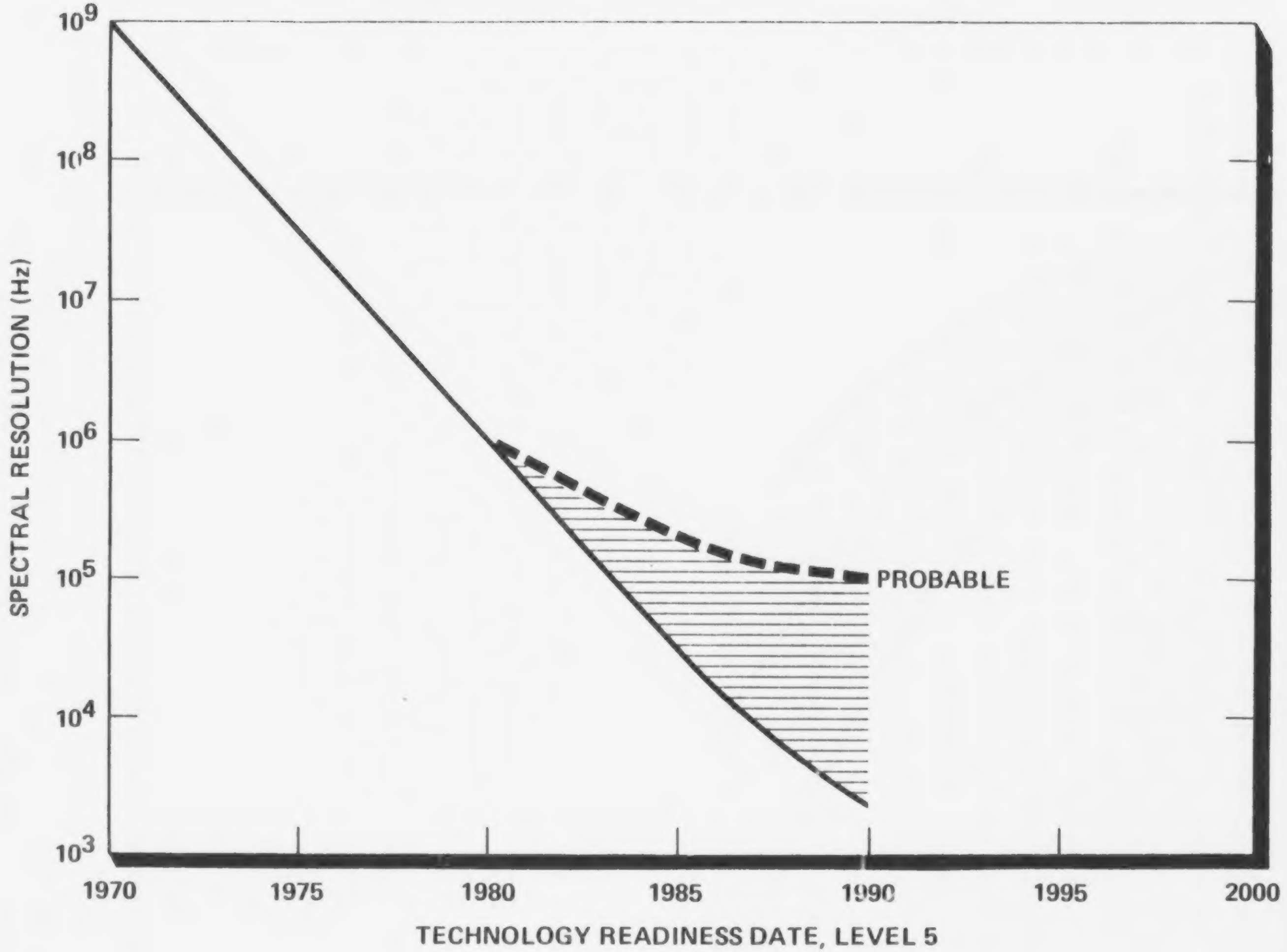

Figure 4.7. Spectral Resolution of Submillimeter-Wave Heterodyne Radiometer

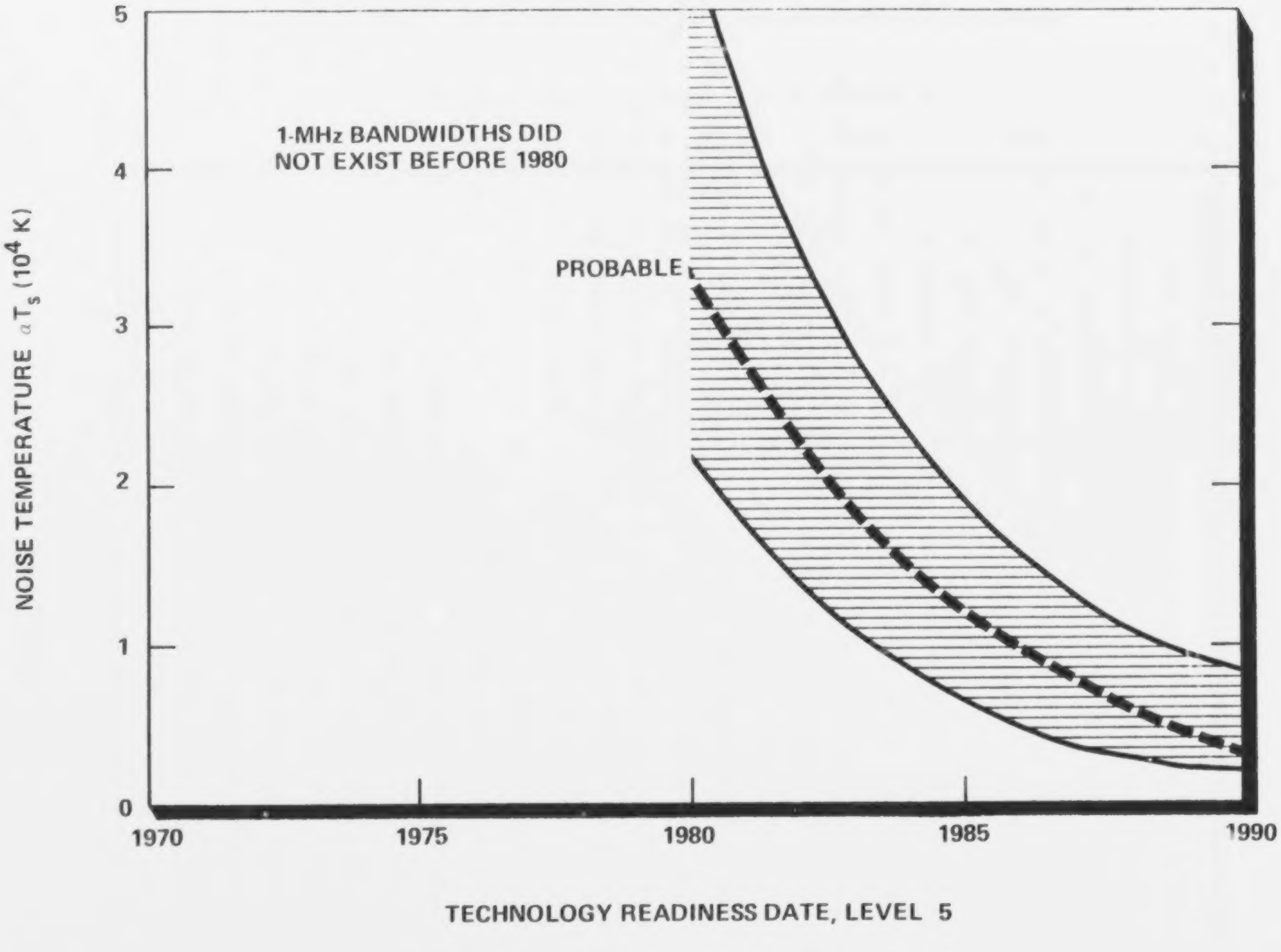

Figure 4.8. Noise Temperature of Submillimeter-Wave Heterodyne Radiometer

4.1.5 Microwave Radiometry (C. T. Swift, NASA-Langley)

Future high-resolution microwave systems for the remote sensing of the earth from space will require large antennas and 200-300 identical receivers in order to successfully accommodate the missions. Although the antenna size question is peripherally addressed for the purpose of forecasting, the bulk of this material focuses on the required receiver technology in the areas of weight, power consumption, and cost.

When the space shuttle becomes operational, NASA will have the capability of frequently launching several tens of thousands of pounds into low-earth orbit. Recognizing this capability, OAST established a large space-structures program as a means to continue to exploit the space environment. Of all the structures considered, large space antennas received high priority because of their utility in communications and high-resolution remote sensing of the earth. With regard to remote sensing, there is no doubt that antennas of the order of 100 m in diameter operating in the 10-20 cm microwave band will achieve spatial resolutions approaching 1 km from low-earth orbit. Unfortunately, conventional radiometry utilizing only one receiver in a cross-track scanning mode will not generate the imagery and coverage that the users of such data require. The difficulties are (1) it is prohibitive to move such a large antenna at the required scan rate and (2) there is insufficient integration time available to collect accurate contiguous measurements while scanning.

The scanning problem associated with large space structures has required a fresh approach to passive microwave remote sensing of the earth. The concept developed at Langley consists of arraying 200-300 identical microwave radiometers in the focal plane of the antenna along a line perpendicular to the orbital path. Neighboring radiometers will then view adjacent contiguous pixels, generating a cross-track image swath. The image is then filled by the forward motion of the spacecraft. The advantages of this concept are that no mechanical scanning of the antenna is required and the fixed, but squinted, receiver beams provide both swath width and sufficient integration time for accurate measurements of geophysical parameters.

Although the concept will work on paper, challenging demands are placed upon technology. First of all, large antennas are required to achieve the desired spatial resolutions. OAST is currently sponsoring an activity to explore technology areas such as structures, dynamics, and electromagnetics needed to produce a high-quality, cost-effective large antenna that is suitable for remote sensing and other applications. Second, the large number of required receivers built with 1977 technology will place a severe strain on delivery cost, power consumption, and weight of the end product (the manufacturing of 200-300 identical receivers and spares). OAST is currently funding an effort to address this second challenge. Breakthroughs are expected in the design and fabrication of front-end units that will reduce weight and power consumption, yet maintain the stability needed to perform accurate measurements of geophysical observables. Several prototype units will be built and evaluated in a level 6 aircraft field program.

Antenna Beamwidth (Fig. 4.9). This figure shows the expected decrease in antenna beamwidth that will be expected for L-band radiometers. Although it would be highly desirable to plot improved spatial resolution vs. time, this is not possible because the relevant platform examples cited in the figure require various orbital altitudes, which impacts the resultant resolution.

The figure does, however, generally reflect improved spatial resolution vs. time. For example, the 300-km orbit of Skylab resulted in a footprint of approximately 80 km. The high-resolution radiometer placed in the same orbit would give a footprint of approximately 0.8 km, which is within the design target of 1 km.

Radiometer Receiver Weight (Fig. 4.10). This figure shows the weight of a single radiometer (f $\leq$ 6.6 GHz) vs. time. The three points on the curves are actual weights for the case of the Seasat C-band SMMR, and tight estimates for the proposed Nimbus G S-band and VOIR (Venus Orbiting Imaging Radar) L-band radiometers. We note from the figure that some modest weight reduction was achieved in the five years from

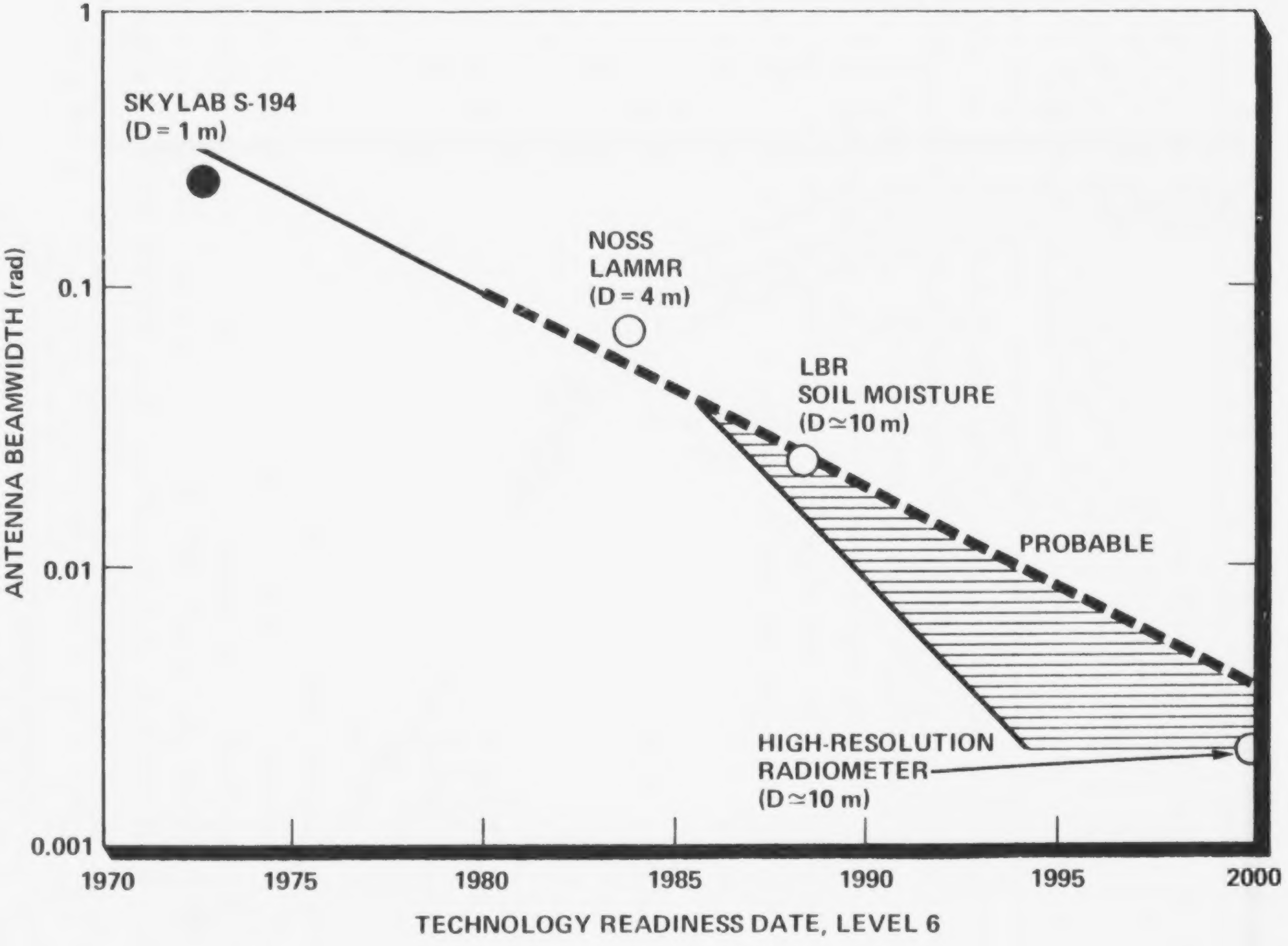

Figure 4.9. Antenna Beamwidth

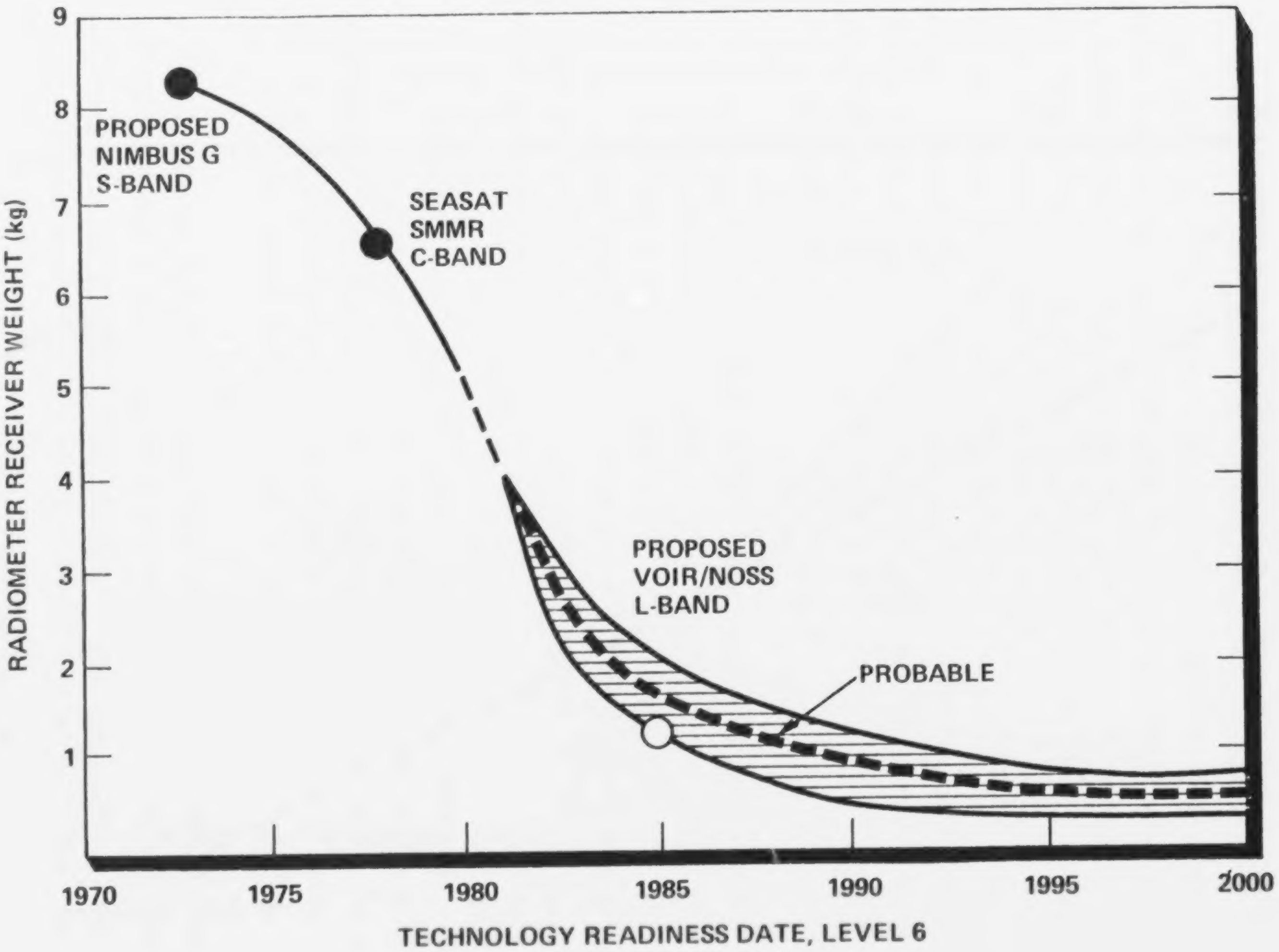

Figure 4.10. Radiometer Receiver Weight

Nimbus to Seasat due to a natural evolution of technology. As a direct result of the OAST R&T program, a reduction in size by a factor >5 will occur for units built in the 1985 time frame. When this technology is applied to the high-resolution microwave system, a weight reduction of approximately 1600 kg will have been realized. This reduced loading will also propagate a significant weight saving throughout the entire structural system.

Receiver Input Power (Fig. 4.11). This figure shows reduction in the required radiometer receiver input power vs. time. As before, the points on the curve represent either an actual consumption of power, or those based on hard estimates. A rather substantial drop in input power was realized between 1973 and 1975 as a result of improved efficiency in solid-state devices. A further reduction by a factor of 2 is expected by 1985 as a direct result of OAST microwave R&T. Future reductions will require developing means to improve internal thermal stability with less required raw input power.

Specific Cost (Fig. 4.12). This figure shows the anticipated cost per unit vs. time as expressed in 1979 dollars. Again, the data was extracted from the Nimbus G and the VOIR proposals. This figure clearly indicates that only a modest saving is realized if one of a kind is built. If the units are built in lots of 100, substantial savings in cost will occur for several reasons. First, the cost of supporting checkout equipment is specific for all radiometers; hence, the capital investment charge per unit becomes quite small. Second, the devices being built under OAST R&T incorporate microwave integrated circuits rather than discrete components as proposed for the Nimbus G experiment. There is much less labor associated with the production of integrated circuits compared to connecting discrete components; hence, cost savings. Finally, the large number of units will require a limited production-line mode of fabrication, with obvious labor and cost savings.

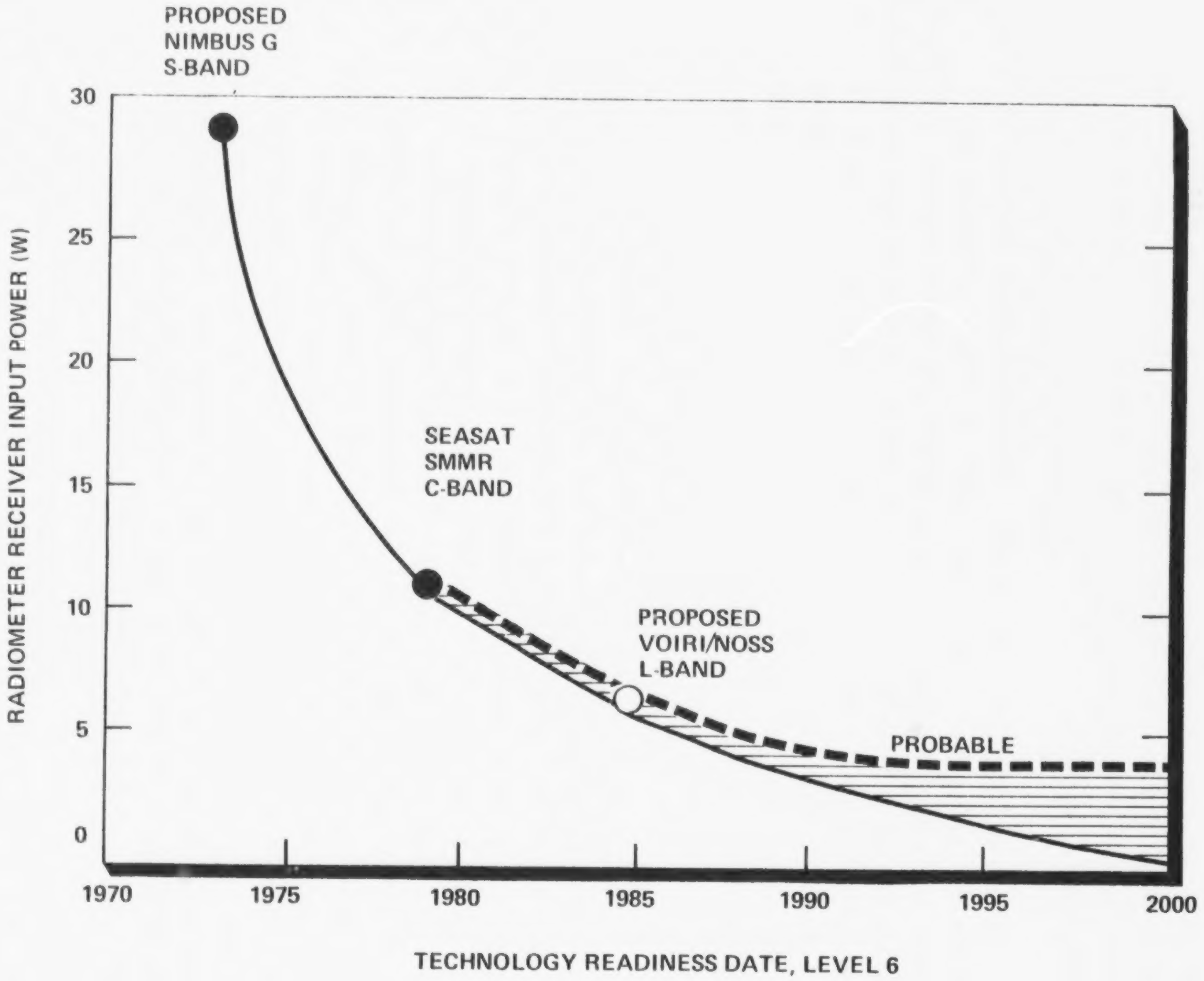

Figure 4.11. Receiver Input Power

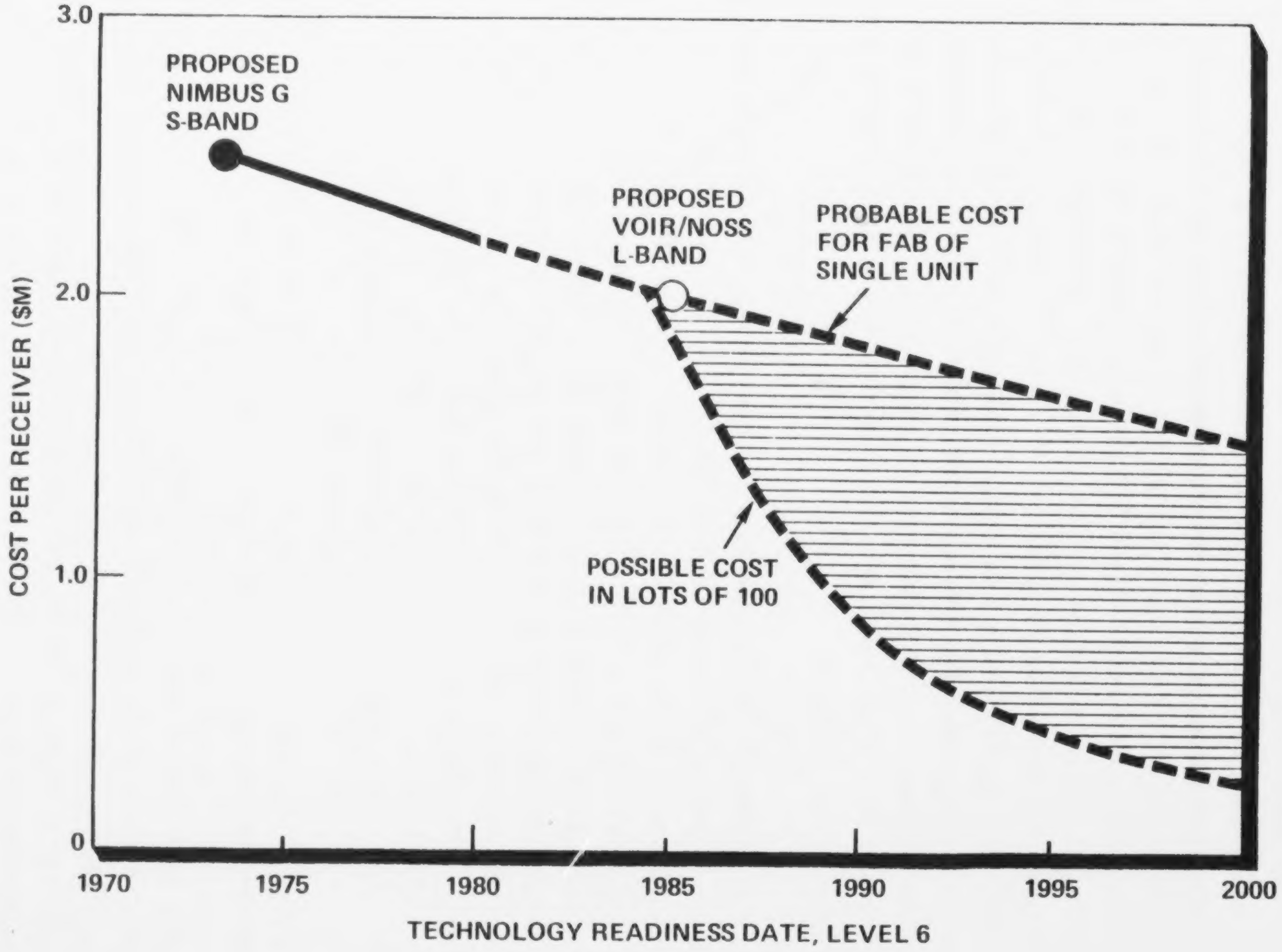

Figure 4.12. Specific Cost

4.1.6 Long-Wavelength Infrared Detection (C. R. McCreight, Ames Research Center)

The sensitivity of 100-μm infrared detectors is the characteristic that makes them most useful in low-background astronomical applications. Figure 4.13 shows the trend in noise-equivalent power (NEP), the limiting power on the detector for which signal and noise are equal, for Ge:Ga photoconductive detectors. These devices are currently the most sensitive for broadband detection at this wavelength. Performance of discrete Ge:Ga detectors is shown for the past 15 years.[1-5] The experience gained in the Infrared Astronomical Satellite (IRAS) project has helped push the sensitivity of these discrete detectors to near astrophysical (zodiacal background) limits. Continuing work on these devices is needed to improve their production yield and fundamental understanding of their performance characteristics.

The prospect of significantly improved sensitivity comes through the integrated array concept. High-density, multielement arrays of Ge:Ga detectors can be coupled to cryogenic silicon charge-coupled-device (CCD) multiplexers to allow integration and multiplexing of signals on the focal plane. Sensitivity improvements are expected through the low-noise readout which becomes possible, and the parallel sampling of the scene (in this case, NEP improves as $\sqrt{N}$, where N is the number of detectors). Projections of sensitivity were made using the relationship

$$\mathrm{NEP} = \frac{en}{R}(2/Nt_i)^{1/2}$$

where e is the electronic charge, n is the number of RMS equivalent noise carriers per readout, R is the detector responsivity, and t_i is the

---

[1] W. J. Moore and H. Shenker, Infrared Physics 5, 99, 1969.

[2] P. D. Feldman and D. P. McNutt, Applied Optics 8, 2205, 1969.

[3] W. J. Moore, NASA CR-137, 892, March 1976.

[4] P. R. Bratt and N. N. Lewis, NASA CR-152, 046, October 1977.

[5] Experimental device produced by E. E. Haller, Lawrence Berkeley Laboratory, August 1978.

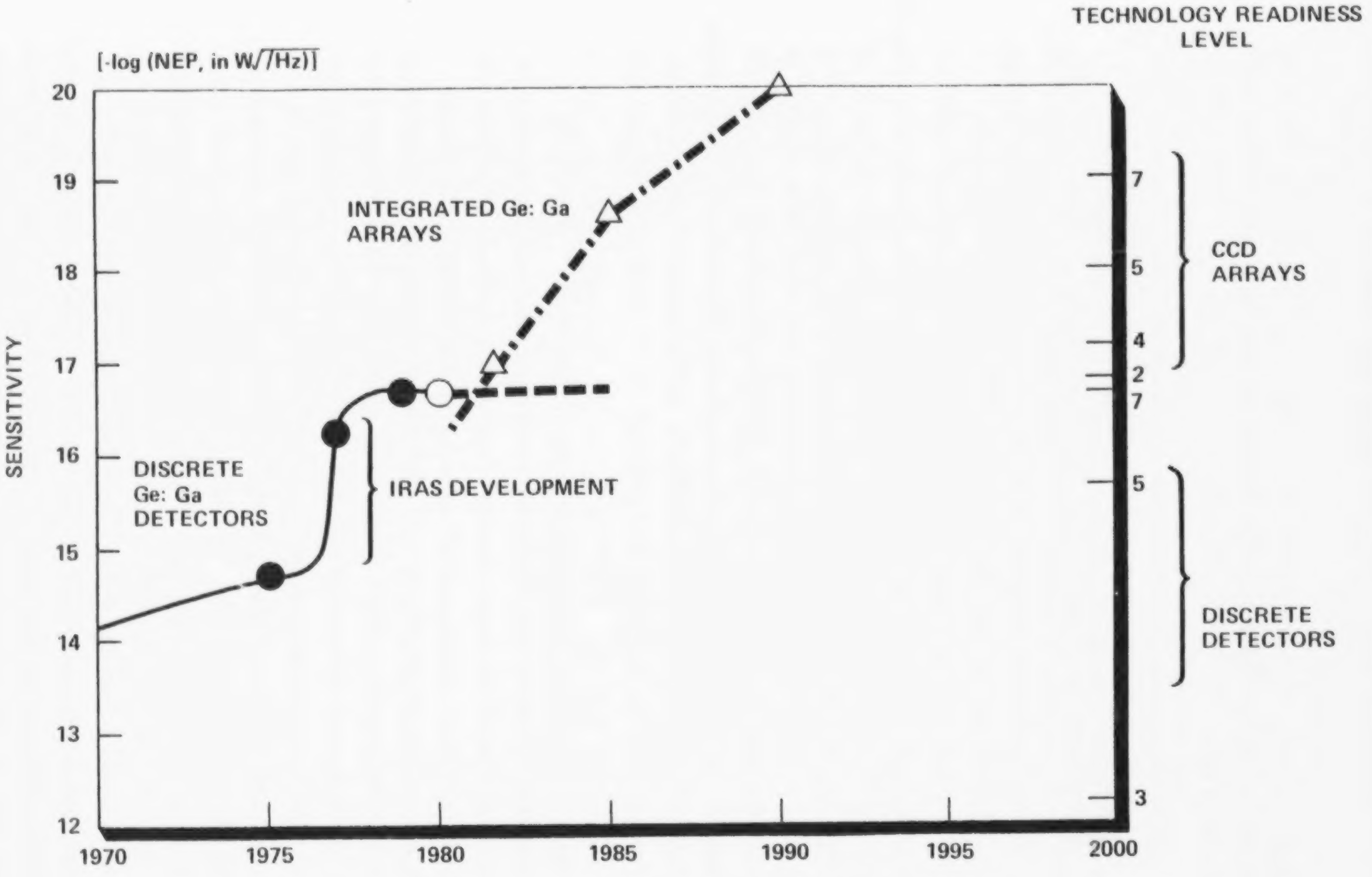

Figure 4.13. Infrared Detection Sensitivity at 100 μm

integration time. It is expected in a "realistic" sense that the array parameters shown in the following tabulation will be available in the given time frame.

Year	Number of Array Elements	Responsivity (A/W)	RMS Noise Carriers (electrons)	Maximum Integration Time (s)	NEP (W/√Hz)
1983	50	8	800	0.1	10^{-17}
1985	50	15	500	1	10^{-18}
1990	500	15	250	10	5×10^{-20}

A conceptual array design effort will be carried out in FY80. It is expected that ongoing work on discrete Ge:Ga detectors will contribute significantly to array prototype efforts, and that operational devices will be available in three or four years.

4.1.7 Microwave Sensor Technology Trends

Microwave remote sensing system technology is being exploited in several disciplines to sense atmospheric, ocean, ice, and land environmental conditions. Both passive radiometric and active radar systems have been used in experimental satellites such as Skylab, Nimbus, Tiros, and Seasat to demonstrate the feasibility of providing useful environmental measurements of ocean windspeed and temperature, ice-pack concentrations, polar ice types, water vapor, precipitation, and atmospheric temperature profiles. These experimental satellite systems have limited the antenna aperture sizes and number of channels because of limited volume, weight, and power. This has limited the spatial resolution, accuracy, and measurement objectives of these early microwave sensing systems. The Shuttle era has opened the door to larger, more complex microwave sensing systems to improve the accuracy and timeliness of those environmental measurements which can meet the NOAA and DoD weather and ocean forecasting services requirements. These new microwave systems require new antenna, receiver, and transmitter technology covering the entire microwave spectrum from 1 GHz to over 200 GHz.

During the past five years, passive radiometer system technology and particularly millimeter wave receivers in the 100-GHz to 200-GHz range for microwave sounders and large scanning antennas 1 to 100 GHz (4 to 10 m diameter apertures) have been emphasized by the OAST Multifunction Microwaves RTOP. In the future, high-resolution multibeam combined active and passive system technology will be the major thrust in the program. Antenna systems capable of multibeam operation in both active and passive modes become imperative to achieve spatial resolutions of 1 km to 2 km IFOV with adequate sensitivities to map the environmental parameters. These large antenna system structures will be required to maintain very tight tolerances on the reflector and array elements in order to achieve antenna beam efficiencies of 90% as required to accurately measure the environmental parameters.

The Large Antenna Multifrequency Microwave Radiometer (LAMMR) concepts and systems designs developed by OAST over the past two years have led to the LAMMR being selected as the major new sensor development for the National Oceanic Satellite System (NOSS) scheduled for launch in 1986. This sensor with some modifications will be the workhorse operational multifunction microwave sensor during the 1980s. The applications of this microwave imager in the various spectral bands with spatial resolution trends are shown in Fig. 4.14. The most significant LAMMR modifications in the late 1980s and 1990s will require adding 15-GHz and 30-GHz radar channels for quantitative precipitation measurements over land with profile range gating capability.

The microwave sounder is a second class of scanning multichannel microwave sensors which make measurements on the wings of the atmospheric absorption lines to provide profiles of temperature and water vapor with altitude. The 60-GHz temperature sounders (four channels) have been

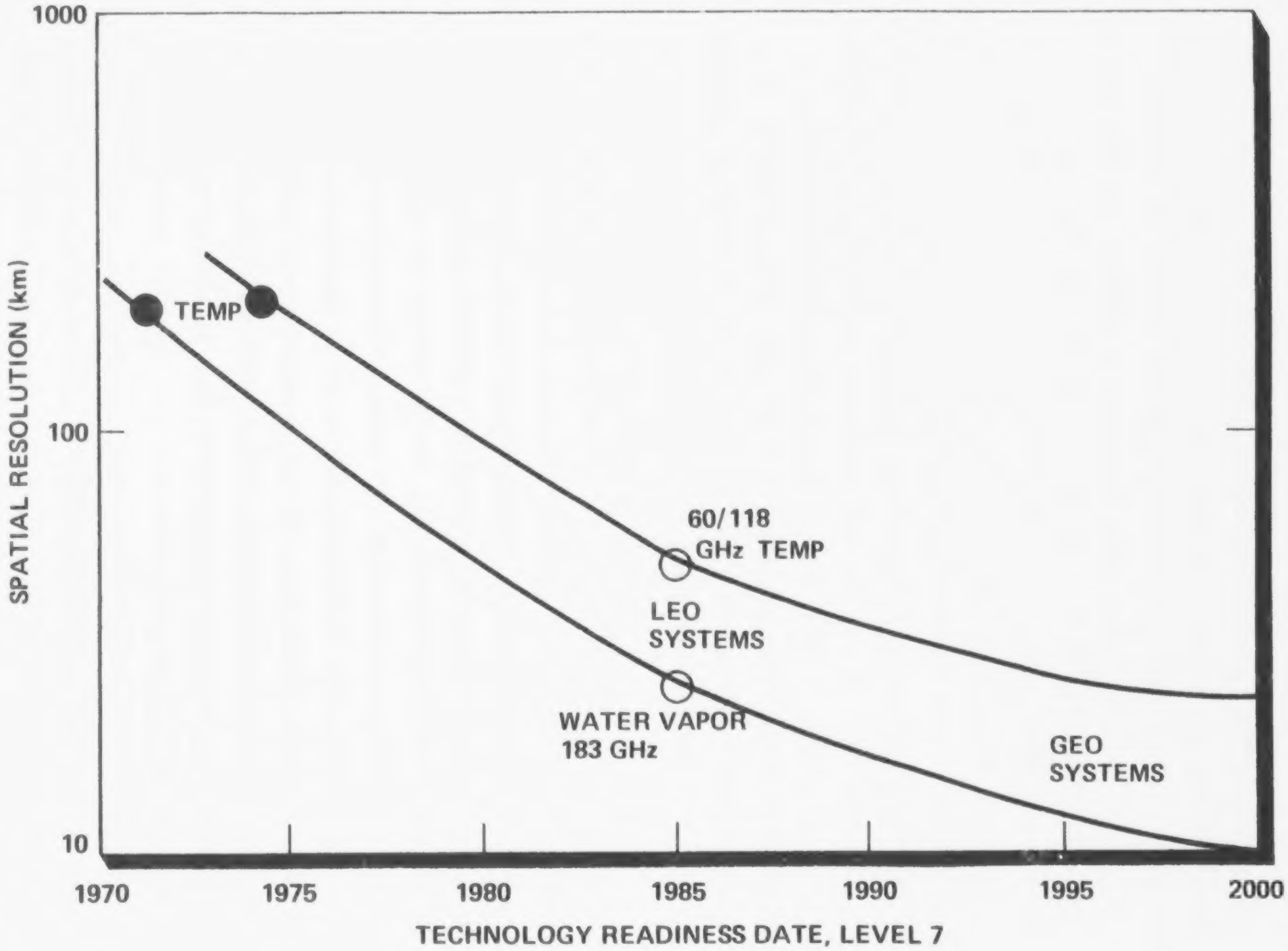

Figure 4.14. Spaceborne Passive Microwave Sounder Resolution Trends

flown on Nimbus and now Tiros-N since 1972, and the Air Force has recently launched a ten-channel 60-GHz sounder on its Defense Meterological Satellite. The spatial resolution of these early temperature sounders has been in the 200-km range, and recent meterological grid model changes with increased measurement accuracy have led to 50-km IFOV designs being proposed for the mid-1980 low earth orbiting (LEO) systems. These new systems have also incorporated the 183-GHz water vapor sounding channels to explore this new measurement capability. The development of millimeter wave technology by OAST has been instrumental in developing the first ground-based and aircraft water vapor sounders using this 183-GHz band. Figure 4.15 shows these spatial resolution trends for the LEO systems and also points out the long-range plans to place these sounders in geosnychronous orbit to improve the temporal sampling of this important forecast data. Figure 4.16 shows the relative sizes of the antennas required to meet the spatial resolution objectives of multifunction microwave sensors using real-aperture radiometer and radar techniques. To approach the 30-m to 100-m resolution domain, synthetic-aperture radar was flown on Seasat-A, but the synthetic radiometer systems techniques are in the very early conceptual study stages. During the next several years real-aperture techniques will be developed for the 1-km to 10-km resolution requirements until synthetic-aperture radiometer techniques are proven feasible for environmental measurements. Figure 4.17 shows the need for multibeam radiometer antenna systems in order to achieve the 1-km to 6-km resolutions with adequate temperature sensitivity. This multibeam requirement is present in advanced radar systems as well. The most simple radar system for LAMMR will require a two-beam antenna to accommodate the time delay between transmitting and receiving with the antenna scanning at 1 RPS. The 1986 LAMMR imaging system has reached the limit of single beam scanning systems with a reasonable swath. Advanced multibeam torus or spherical reflector approaches will be required to approach the 1-2 km resolutions in the late 1990s.

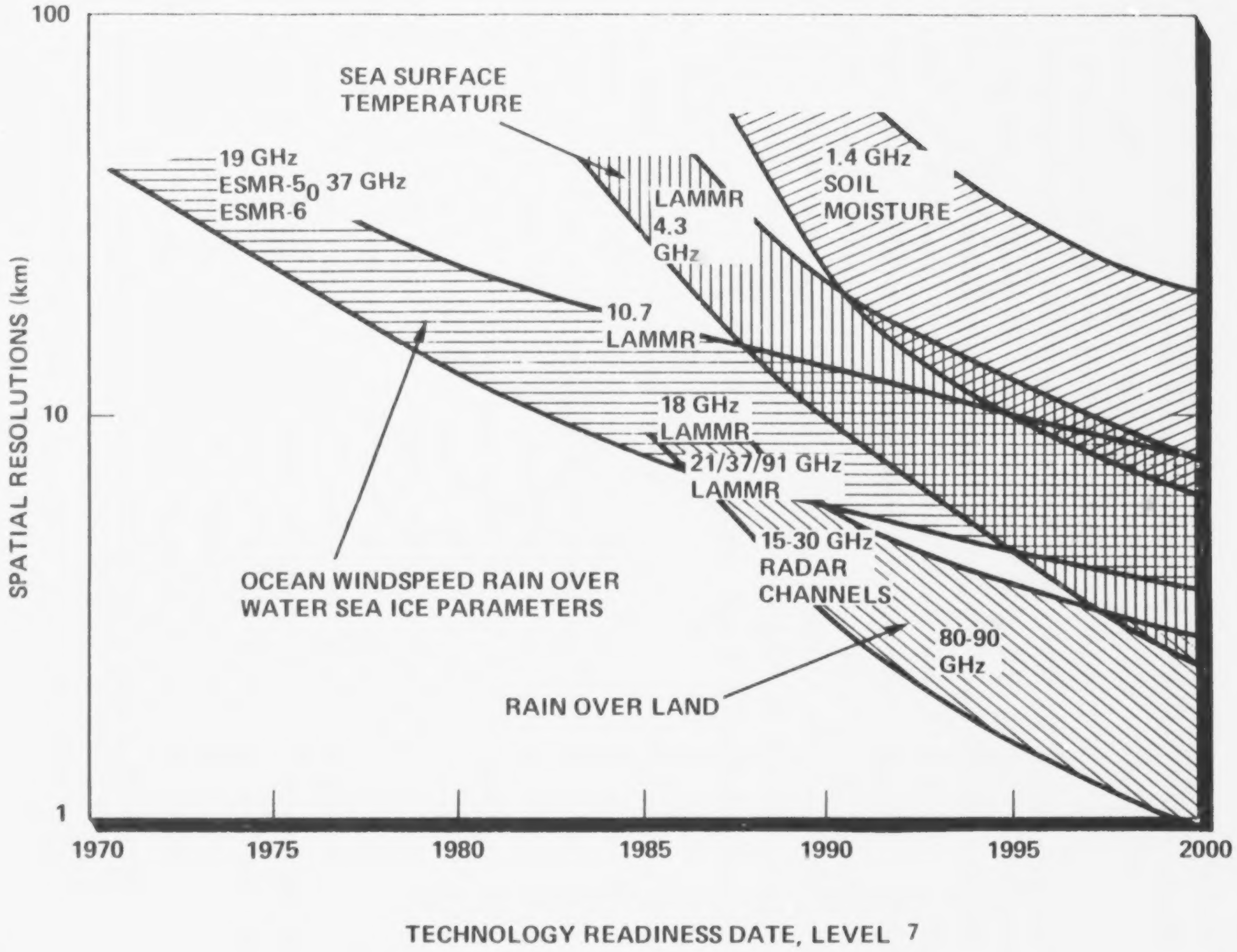

Figure 4.15, Spaceborne Passive Multifaction Microwave Imager Resolution Trends

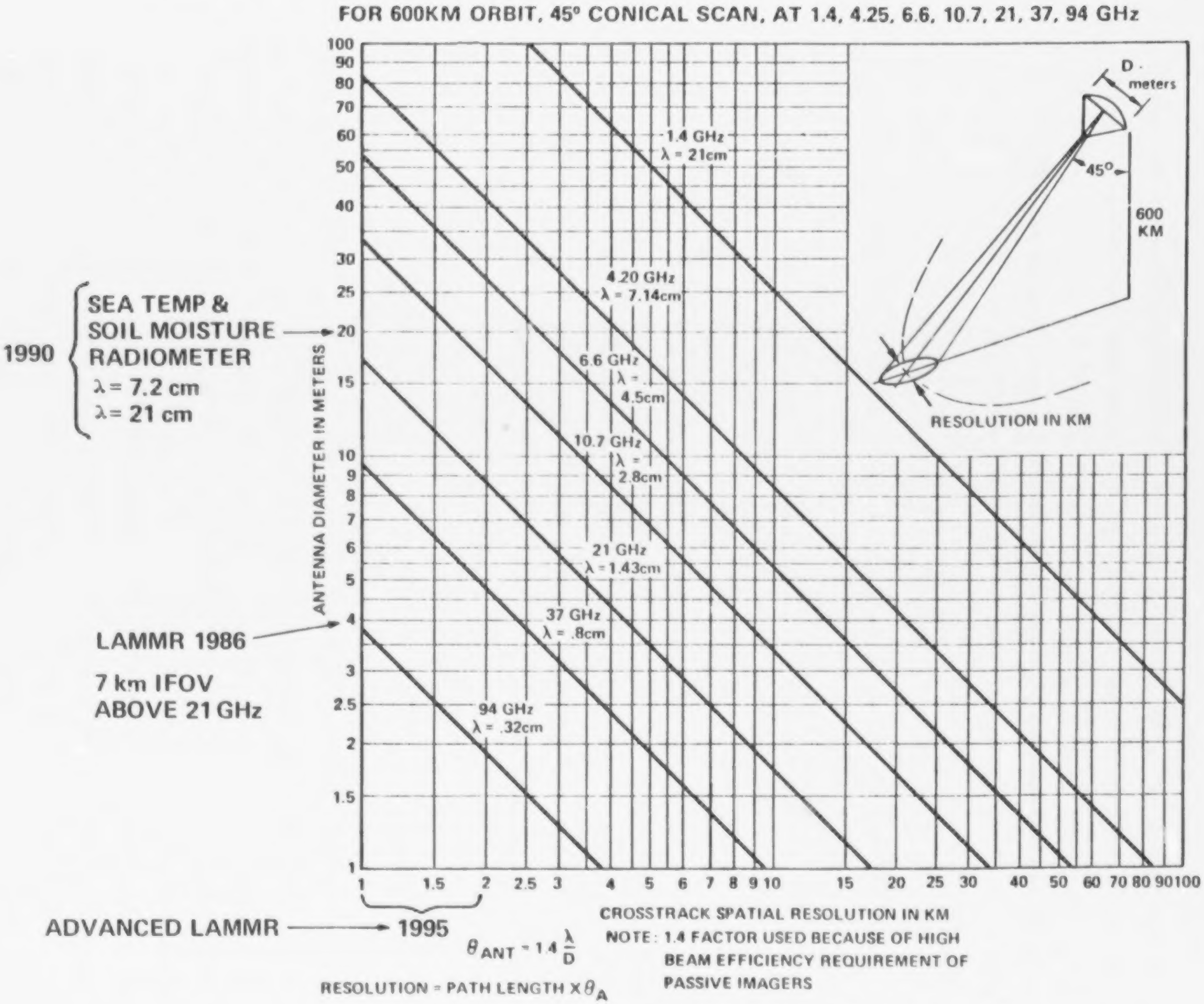

Figure 4.16. Antenna Size Versus Spatial Resolution

EXAMPLE: ±45° CONICAL SCAN, 1000°K = Ts, BW = 500MHz ORBIT 600Km,
SWATH 1330Km, K = 2° (DICKE) n = NUMBER OF BEAMS

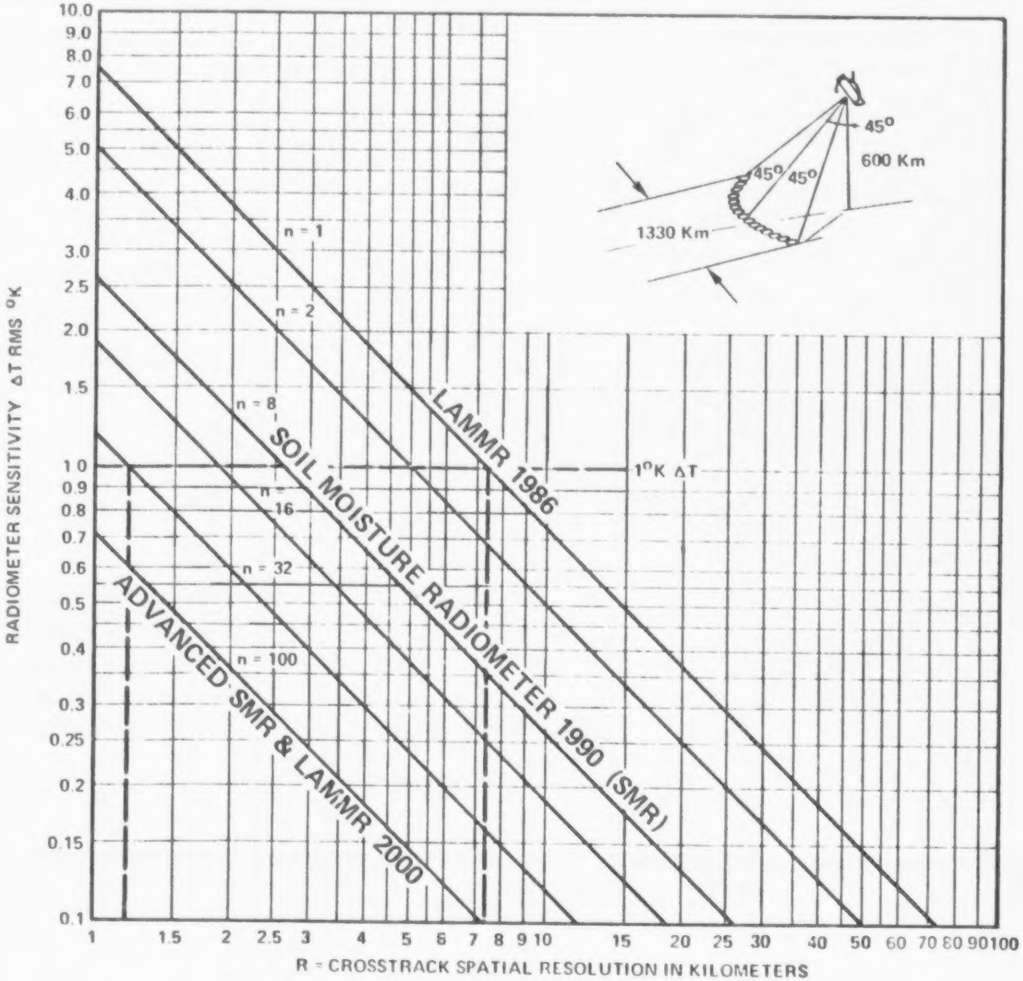

Figure 4.17. Radiometer Sensitivity vs. Crosstrack Spatial Resolution

4.1.8 Infrared Remote Sensing for Planetary Missions (J. B. Wellman, Jet Propulsion Laboratory)

The improvements in capability for remote sensing of planetary surfaces and atmospheres resulting from progress in detector array technology, cryogenic systems, advanced optics, and improved data processing and transmission are forecast. The major thrust of this projection deals with detector arrays; however, because infrared instrument performance is determined primarily by the interrelationships of these four factors it is necessary to address them simultaneously in assessing the benefits to be derived from detector array development. Although a variety of instrument types with differing experiment objectives are under consideration, they share a common dependence on the four technological areas mentioned; therefore, we have chosen to develop the forecast around a single instrument configuration--the mapping spectrometer--and to establish two benchmarks. The first is the Galileo near-infrared mapping spectrometer (NIMS); its development is sufficiently mature so that we can describe its performance with confidence. The NIMS benchmark, for Level 6 (i.e., engineering model), represents 1980 technology. The second benchmark is provided by the advanced mapping spectrometer (AMS)--an instrument concept developed for outer planet missions of the late 1980s. We forecast that the AMS will reach technology readiness Level 6 in 1985. Our projections to 1990 are then obtained by extrapolation.

Spectral mapping is the simultaneous acquisition of spatially and spectrally resolved data as indicated schematically in Fig. 4.18. The radiation from the scene is imaged upon the spectrometer slit. The spectrometer section of the instrument preserves the spatial image quality and disperses the spectrum in an orthogonal direction such that an image of the object line is formed at each of a number of wavelengths in the focal plane. By proper location of an area array detector in the focal plane, the spectral and spatial information is collected and read out. This process is repeated as the field of view sweeps over the target body, either from relative spacecraft-planet motion (pushbroom imaging) or from a scanning motion of the instrument platform.

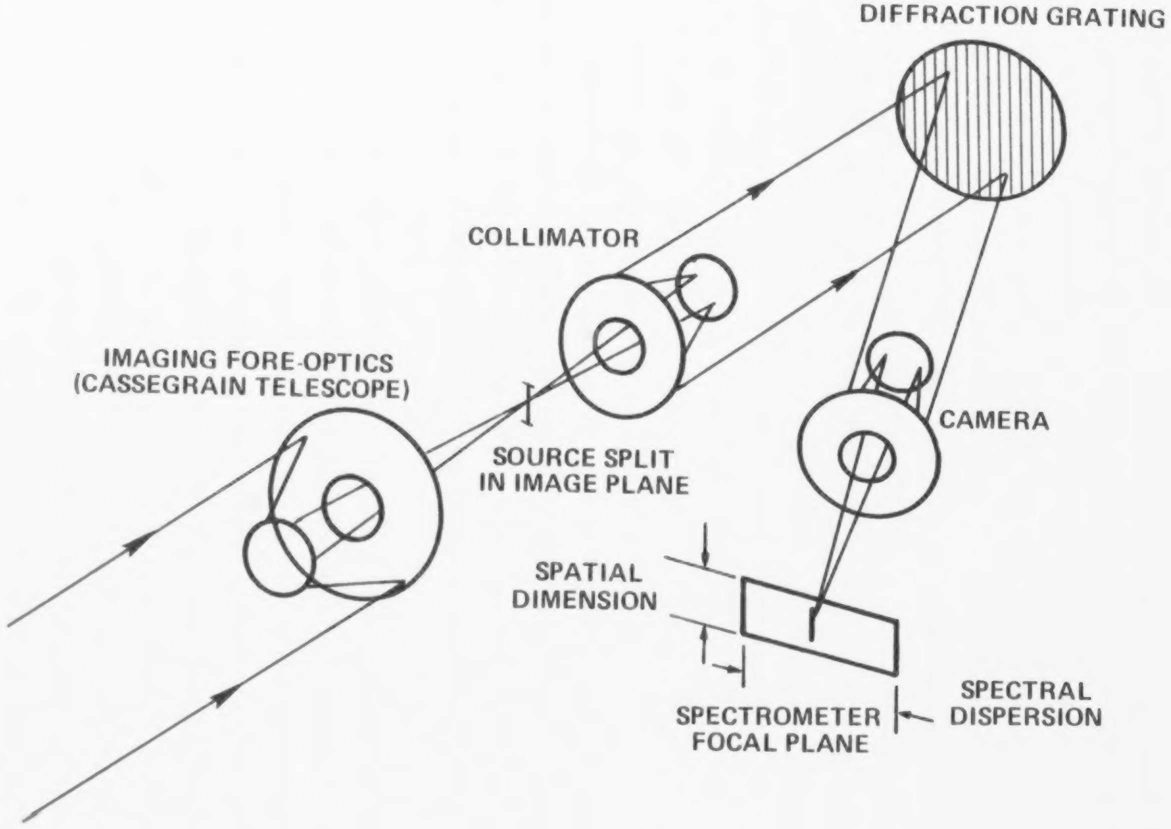
DIFFRACTION GRATING
COLLIMATOR
IMAGING FORE-OPTICS
(CASSEGRAIN TELESCOPE)
CAMERA
SOURCE SPLIT
IN IMAGE PLANE
SPATIAL
DIMENSION
SPECTRAL
DISPERSION
SPECTROMETER
FOCAL PLANE

Figure 4.18. Schematic Representation of Advanced Mapping Spectrometer

Infrared area arrays suitable for use in the NIMS were not sufficiently advanced to meet the performance requirements or to be qualified for space flight in time for the original January 1982 launch. A simpler focal plane covering the spectral range 0.6 to 5.2 μm was designed, consisting of 15 indium antimonide photodiodes and 2 silicon photodiodes. First-order considerations suggest that filling the focal plane by means of detector arrays would provide a more efficient instrument; that is, virtually all of the energy reaching the focal plane would be collected, resulting in an improvement in signal-to-noise ratio which scales with the square root of the number of detector elements. For the focal plane arrays, the relevant figure of merit is the product of the average detector D* and the square root of the number of detector elements on the focal plane. All detector data are given for a wavelength of 5 μm; however, scaling curves are provided to cover the wavelength range from 0.1 to 100 μm.

Key to IR system performance are the instrument housing and detector temperatures. The Galileo NIMS instrument is cooled radiatively to 160 K, and a two-stage radiator cools the focal plane to 80 K. Improved radiative coolers may be possible; however, with the severe weight constraints mentioned earlier, it does not seem reasonable to expect an improvement of more than 10 K, resulting in focal plane temperatures of 70 K. It is implicitly assumed that the focal plane power dissipation is small compared to parasitic sources.

The constraints imposed by the spacecraft on an instrument design are developed using the Galileo mission as a point of departure. Several assumptions are required in extrapolating from that base. The launch vehicle for a Saturn mission in 1987 will be the Space Transportation Shuttle System (Shuttle) and an upper stage carried in the payload bay. The Galileo mission has shown that weight limitations are severe. It is assumed that payload weight for the Saturn mission will be tightly constrained. A growth in the aperture for the advanced mapping spectrometer (AMS) is projected based on the development and utilization of lightweight optics, resulting in an instrument aperture of about 33 cm (1-m focal length f/3 optical system).

Two trends in the data rate from planetary spacecraft have been observed. First, the total data rate (normalized to a common spacecraft-earth range) have been increasing with time. This growth can be expected to continue based on technological developments both in spacecraft transmitting equipment and in receiving equipment, especially larger antennas. Second, the fraction of the telemetry stream occupied by visual imaging has been declining. With the demonstrated utility of infrared mapping instruments, it is reasonable to assume that an advanced mapping spectrometer would occupy a significant share of the total telemetry bandwidth. Furthermore, the use of data compression and advanced coding of data is assumed, resulting in a raw data rate allocation for the instrument in the neighborhood of 10^5 bits/s.

The IR detector array technology is approaching a crossroads. Both NASA and military operational instrumentation now utilize focal planes with a number of discrete detectors, each with a dedicated preamplifier and signal chain. The use of charged-transfer device (CTD) technology to multiplex a large number of elements into an integrated array has been demonstrated by several manufacturers. Hybrid integrated arrays utilize a silicon CCD to store and transfer the signal charge generated in an array of photodiodes. These hybrids take advantage of the relatively mature silicon CCD technology but face the difficult challenge of interfacing an array of photodiodes made in an IR detecting material with the silicon chip. Another approach is the monolithic array in which the photodiodes and the CCD are developed within the same material. The problem of interconnections is relieved; however, the new problem of manufacturing CCDs in materials which are poorly understood must be faced.

The multiplex advantage, which scales as the square root of the number of detector elements, is offset by the additional noise introduced by the multiplexing circuitry. Only when this noise source is sufficiently controlled will integrated arrays supersede the present discrete detector approach. Although progress is encouraging, that point has not been reached. We project that it will be reached within the next few years.

A large number of programs for integrated detector array development are under way, sponsored both by the military and NASA. The military programs are more extensive, both in number and in dollars; however, they fail to address certain requirements of the NASA community. Current efforts span a broad range of techniques and include many parallel efforts. The primary goal of all of these programs is to realize the multiplex advantage within the specialized constraints of specific missions. Because of the importance of mission-specific requirements, NASA's participation in this development is essential.

With the rationale described above, the instrument parameters for the two benchmark instruments and a projection of 1990 are given in Table 4.1. The detector D* values are given at 5 μm. A curve showing the required D* for the entire spectral range representing a constant signal-to-noise performance for the AMS instrument (1985) is given in Fig. 4.19. The D* projections have been analyzed.[1,2] The assumptions for detector temperature, optics parameters, and data rate are just that--reasonable assumptions--and should be compared to forecasts from other discipline areas, recognizing that the constraints to planetary missions must be taken into account.

---

[1] J. B. Wellman, "Infrared Focal Planes for Planetary Missions," Paper No. 203-14, Proceedings of the Society of Photo-Optical Instrumentation Engineers, 23rd Annual Symposium, San Diego, California, August 27-30, 1979 (in press).

[2] J. B. Wellman, "Infrared Focal Plane Arrays for Planetary Missions: A Prospectus," Proceedings of the 5th International Conference on Charge Coupled Devices, Edinburgh, UK, September 12-14, 1979.

TABLE 4.1

DEFINITION OF BENCHMARK INSTRUMENTS, PLANETARY INFRARED REMOTE SENSING

Parameter	NIMS (1980)	AMS (1985)	Extrapolation (1990)
Detector D* at 5 μm ($cm \cdot Hz^{1/2} \cdot W^{-1}$)	2×10^{13}	2×10^{13}	1×10^{14}
Number of Elements	17	128^2	128^2
Detector Product N · D*	8.2×10^{13}	2.8×10^{15}	1.3×10^{16}
Detector Temperature (K)	80	70	60
Instrument Temperature (K)	160	150	150
Optics Focal Length (m)	0.4	1.0	1.0
Optics Diameter (cm)	23	33	50
Data Rate (bits/s)	11×10^3	10^5	10^6

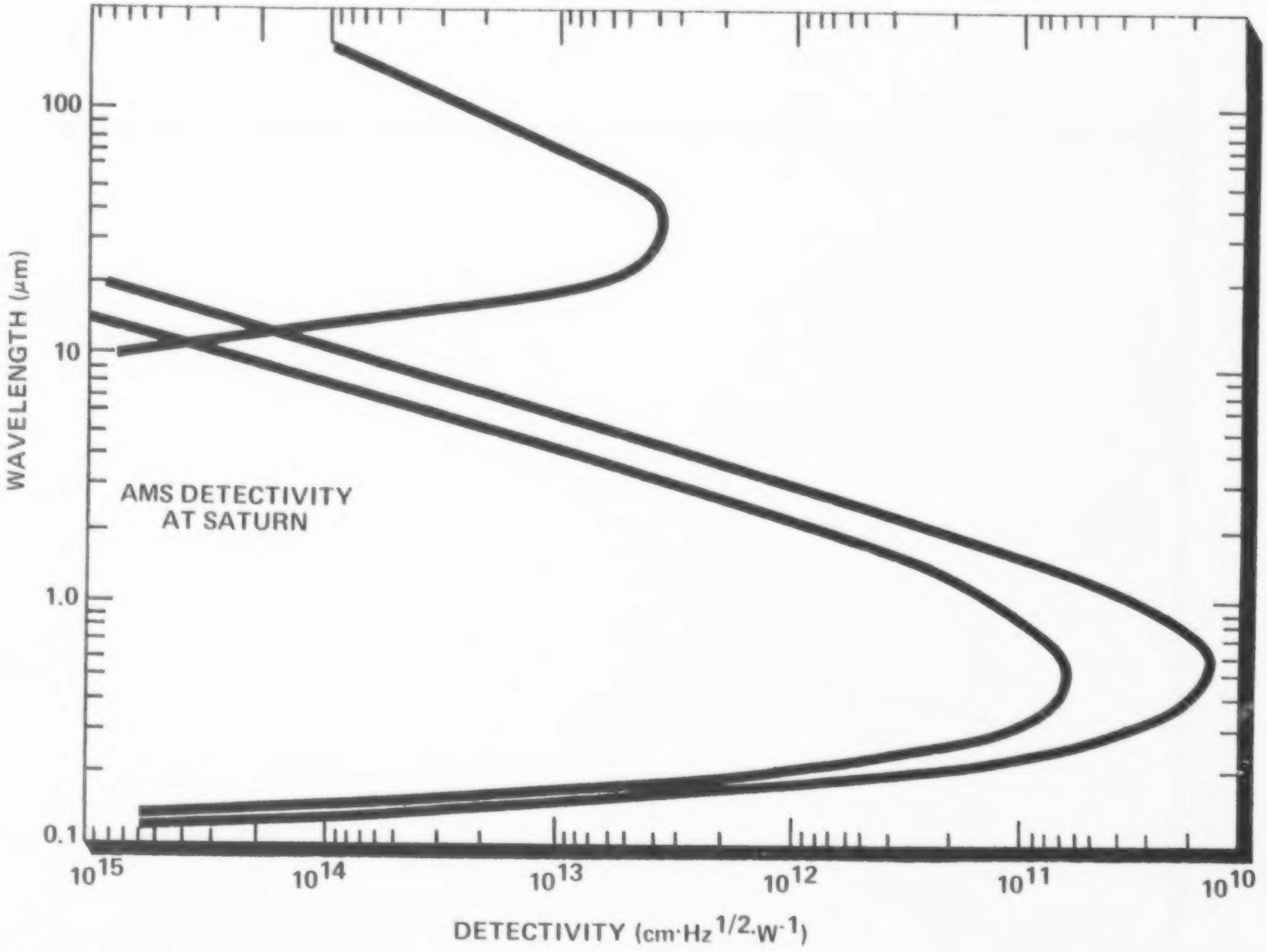

Figure 4.19. Infrared Remote Sensing Required Detectivity as a Function of Wavelength (AMS 1985 Requirements)

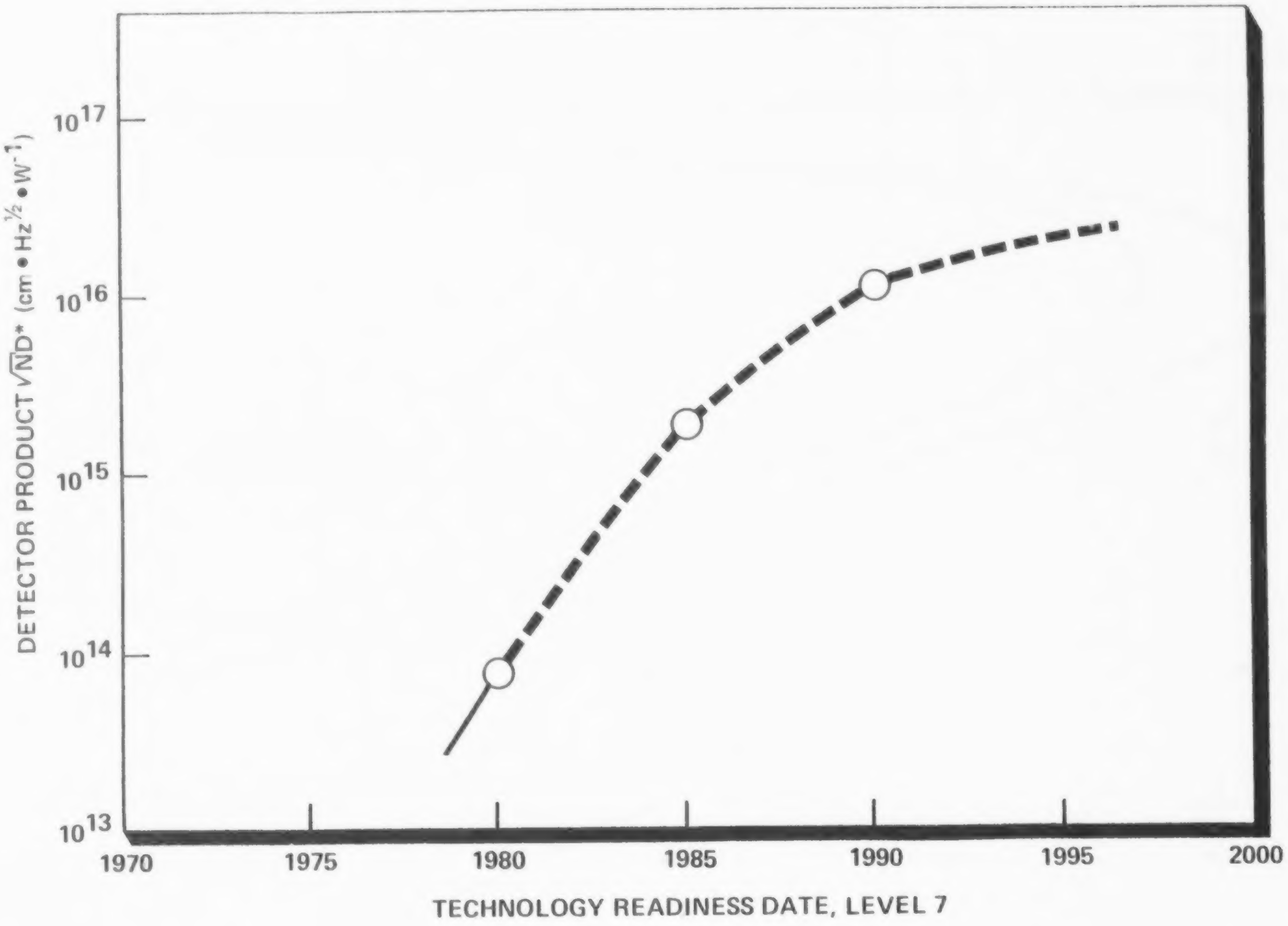

Figure 4.20. Infrared Detector Array Performance

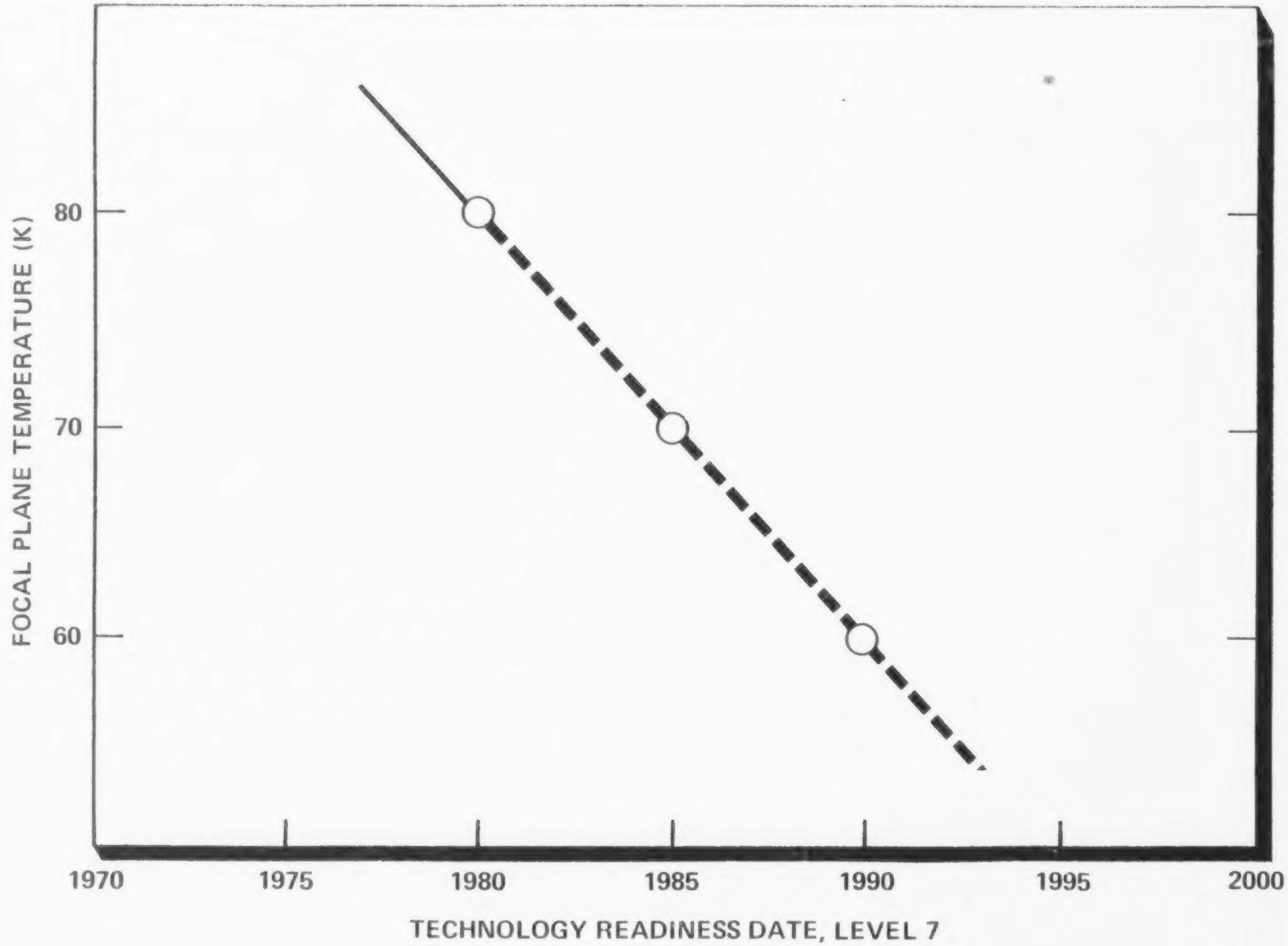

Figure 4.21. Performance of Radiative Cooler

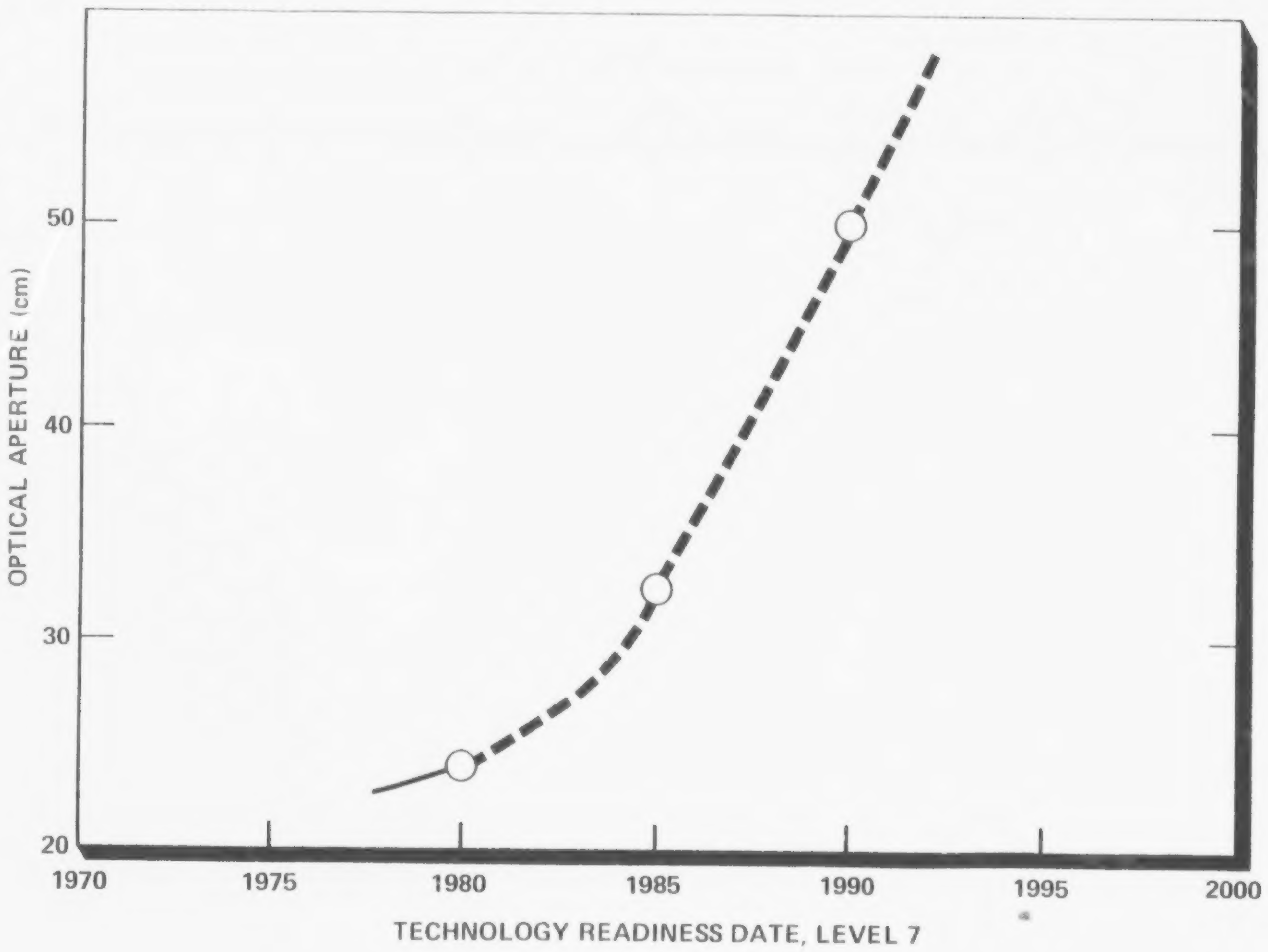

Figure 4.22. Development of Lightweight Optics

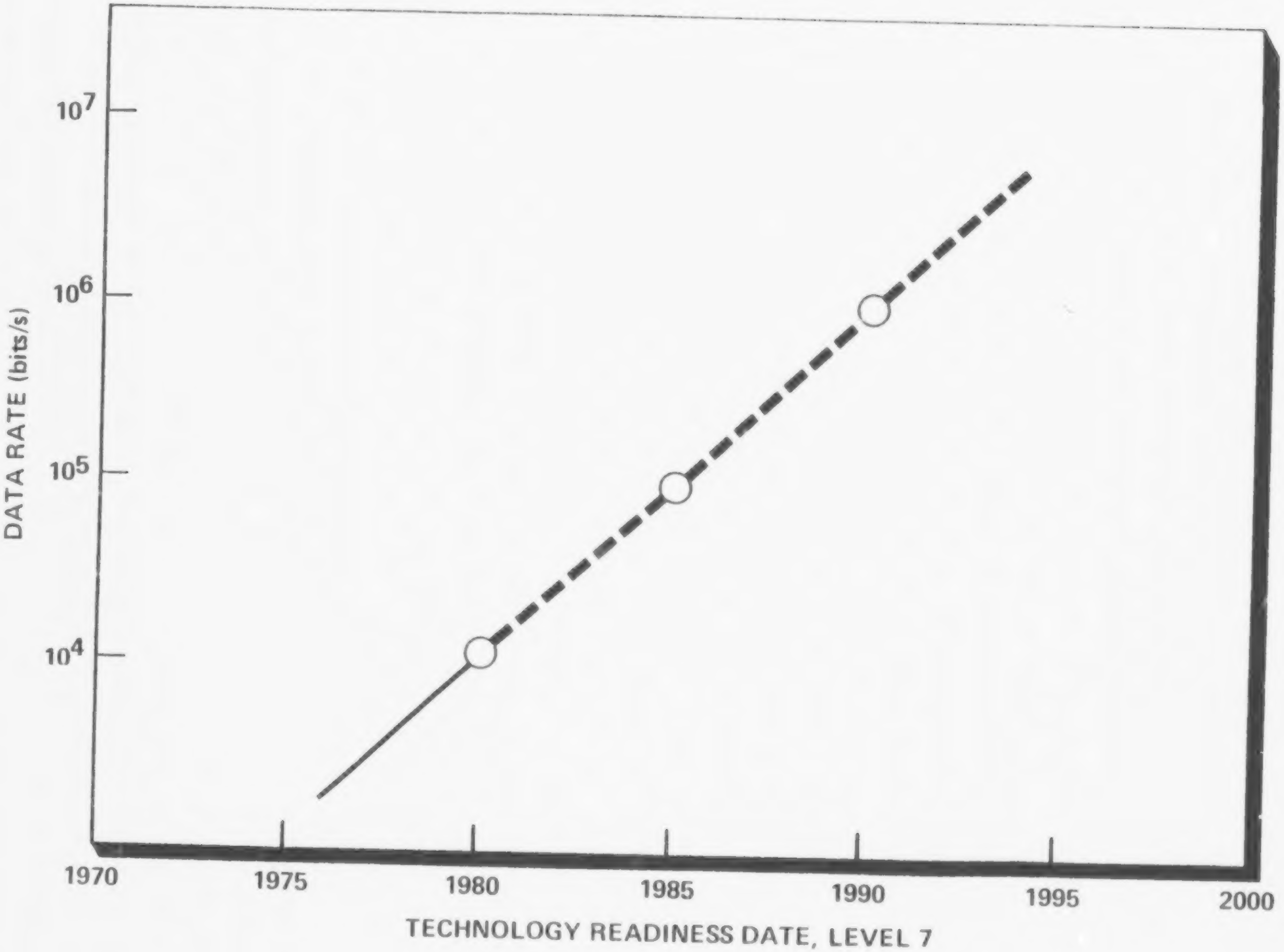

Figure 4.23. Instrument Data Rate for Planetary Spacecraft

4.1.9 Passive Laser Heterodyne Radiometer

Basic research in this area is directed toward improving measurement sensitivity and spectral coverage through development of tunable semiconductor laser local oscillators (LO) and wide-bandwidth HgCdTe photomixers. The data presented show the past evolution and the expected evolution of these subsystems. The specific parameters considered for the laser LO are single-mode power, operating temperature, and spectral coverage; for HgCdTe photomixers, bandwidth, heterodyne efficiency, and spectral coverage.

Infrared heterodyne receivers are characterized by very narrow spectral bandwidths which can improve remote measurements of atmospheric parameters related to global weather forecasting, pollutant measurements, and planetary exploration. A tunable (8-12 μm) laser heterodyne spectrometer (LHS) is currently under development by NASA for measurements of trace species in the 1985 time frame using solar occultation techniques from a Shuttle platform. Improvements in laser LOs and HgCdTe photomixers will expand the range of applications of the LHS technology for future Shuttle missions as well as free flyers. In particular, future nadir and limb viewing applications will require lasers having improved single mode power and higher operating temperatures over the 3 to 30 μm range coupled to photomixers having wider bandwidths and improved heterdyne efficiency with a spectral coverage commensurate with the laser LO.

Lead salt semiconductor lasers have demonstrated the technology for covering the 3 to 30 μm spectral range. Ongoing NASA programs are directed toward improving the characteristics of these lasers for LHS application in the 8 to 12 μm range. Current lead salt lasers in this spectral region are available with single-mode powers in the 300 to 400 μW range at operating temperatures from 15 K to 30 K. Single-mode powers from 700 to 1000 μW with operating temperatures greater than 30 K are required for the LHS. While isolated lasers achieving these requirements have been fabricated, the immediate goals of the current program are to improve the material and fabrication technology in order to reproducibly meet these requirements. Longer ranged NASA programs are directed toward providing single-mode lasers in the 1985 time frame over the 3 to 300 μm spectral range.

Although this forecast provides data only for the expected evolution of the lead-salt laser technology, other tunable laser technologies should be noted. These are technologies which either exhibit limited tunability over certain spectral regions, or which are not expected to be viable candidates before 1985. Microwave tunable laser systems have demonstrated limited tunability (i.e., 8 to 18 GHz) around CO_2 injection laser wavelength in the 9-12 μm region, with single-mode powers from 0.2 to 1 mW and room-temperature operation. Also, high-pressure CW electron-beam-excited CO_2 lasers may provide greater tunability over the 9-12 μm range. Moreover, both laser systems may provide greater tunability in other wavelength regions by using various mixing schemes. A technique using transition metal lasers (MIT, Lincoln Laboratory) may eventually provide tunable LOs in the 3 to 30 μm range with operating temperatures above 77 K. However, this laser system is not expected to be available before the 1984-1985 time frame.

The current HgCdTe photomixer technology in the 8 to 12 μm region is satisfactory for the initial LHS solar occultation mission. However, improvements in photomixer bandwidth, efficiency, and spectral response are required to expand application of LHS technology in the 1985 to 1990 time frame to terrestrial nadir and limb viewing missions as well as planetary applications. Ongoing NASA programs are directed toward improving the yield and reproducibility of 8-12 μm HgCdTe photomixers having bandwidths greater than 2 GHz with effective quantum efficiencies, η_{eff}, greater than 30%. This program is expected to eventually yield devices having bandwidths of 5 GHz with $\eta_{eff} \approx 50\%$. Other NASA programs (GSFC) are directed toward achieving 1 GHz response in HgCdTe devices at wavelengths greater than 25 μm.

Single-Mode Power of Lead Salt Lasers (Fig. 4.24). This figure illustrates the expected improvements in the single-mode power of lead salt lasers. The current and future output power in the 3 to 15 μm range is significantly higher than for the longer wavelength regions. In general, lasers in the 1980 to 1985 time period are expected to exhibit multiple longitudinal modes over portions of their tuning range. Single-mode lasers are expected in the 1985 time frame. Single-mode power in the 0.7 to 1 mW range is required for LHS solar occultation missions. For future missions using nadir and limb scanning, techniques with wide-bandwidth detectors or array powers in the 2 to 10 mW range will be needed. These estimates are for the 10-μm spectral range.

Operating Temperature of Lead Salt Lasers (Fig. 4.25). This figure illustrates the operating temperature for various spectral regions. In general, lower operating temperatures are required for the longer wavelength. However, for wavelengths less than 10 to 12 μm, operating temperatures compatible with free flyer requirements are approached.

Bandwidth and Heterodyne Quantum Efficiency of 8-12 μm HgCdTe Photomixers (Fig. 4.26). This figure shows the expected improvements in HgCdTe photomixers for bandwidth (β) and effective heterodyne quantum efficiency (η_{eff}). These data are for 77 K operation. Some improvement in the long-wavelength spectral response (i.e., to ~15 μm) can be expected by operating at lower temperatures. Improved material and device structure combined with low-temperature operation is being pursued at GSFC (Lincoln Lab) to expand performance to 30 μm.

Spectral Response of HgCdTe Photomixers (Fig. 4.27). This figure shows the expected DC quantum efficiency for various spectral regions and operating temperatures. As noted in the description of Fig. 4.26, longer wavelength devices will require temperatures much lower than 77 K.

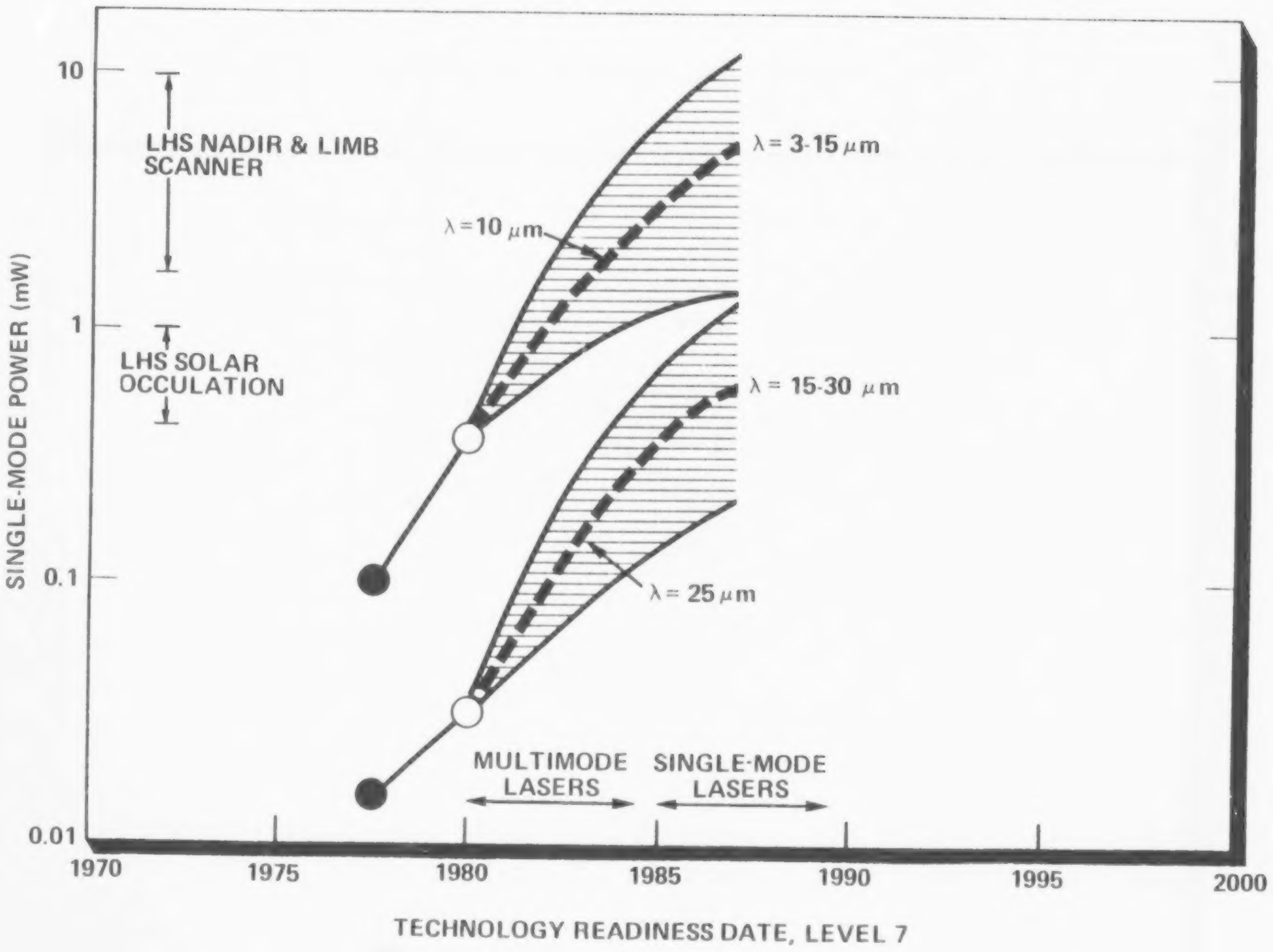

Figure 4.24. Single-Mode Power of Lead Salt Lasers

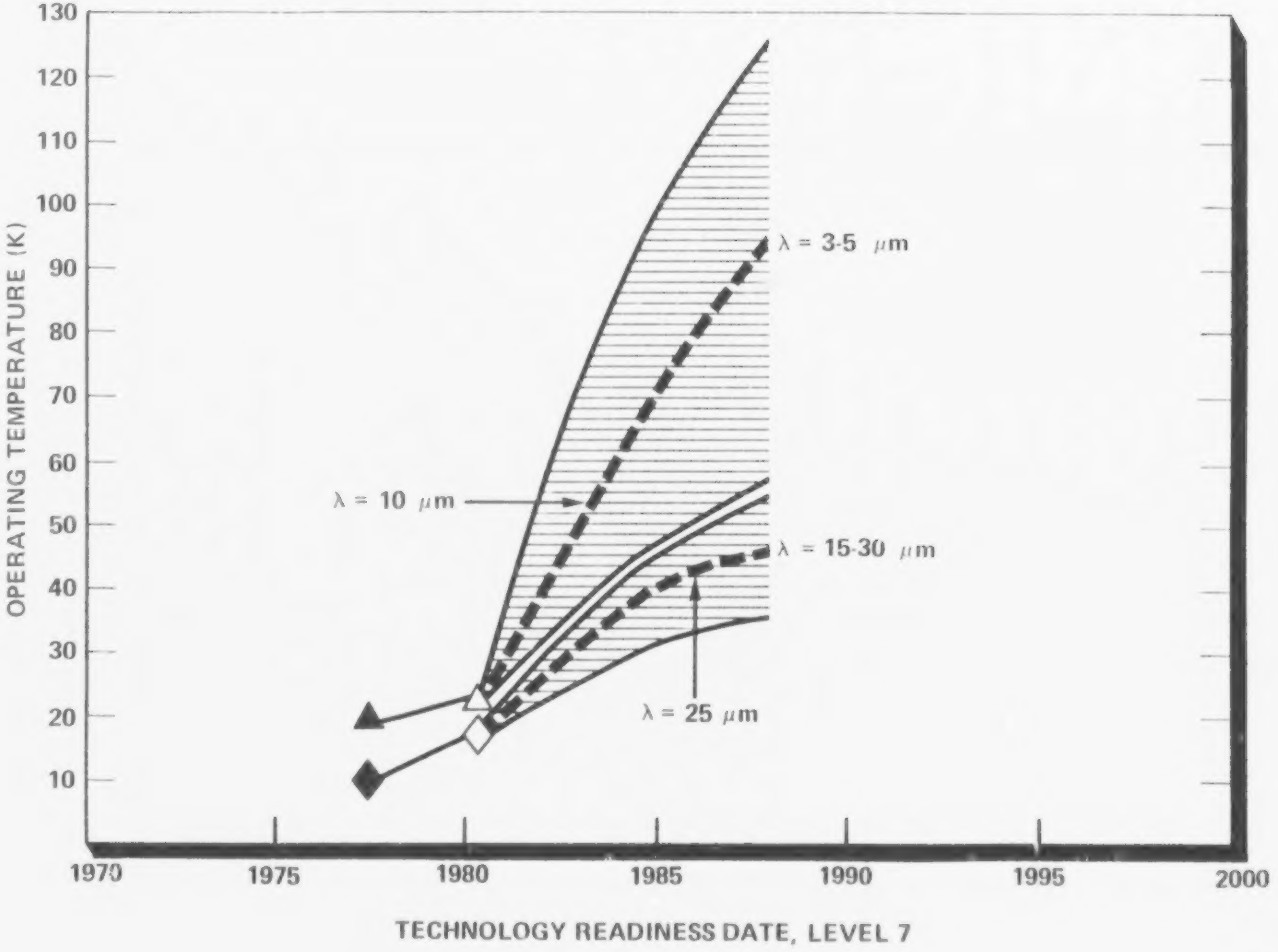

Figure 4.25. Operating Temperature of Lead Salt Lasers

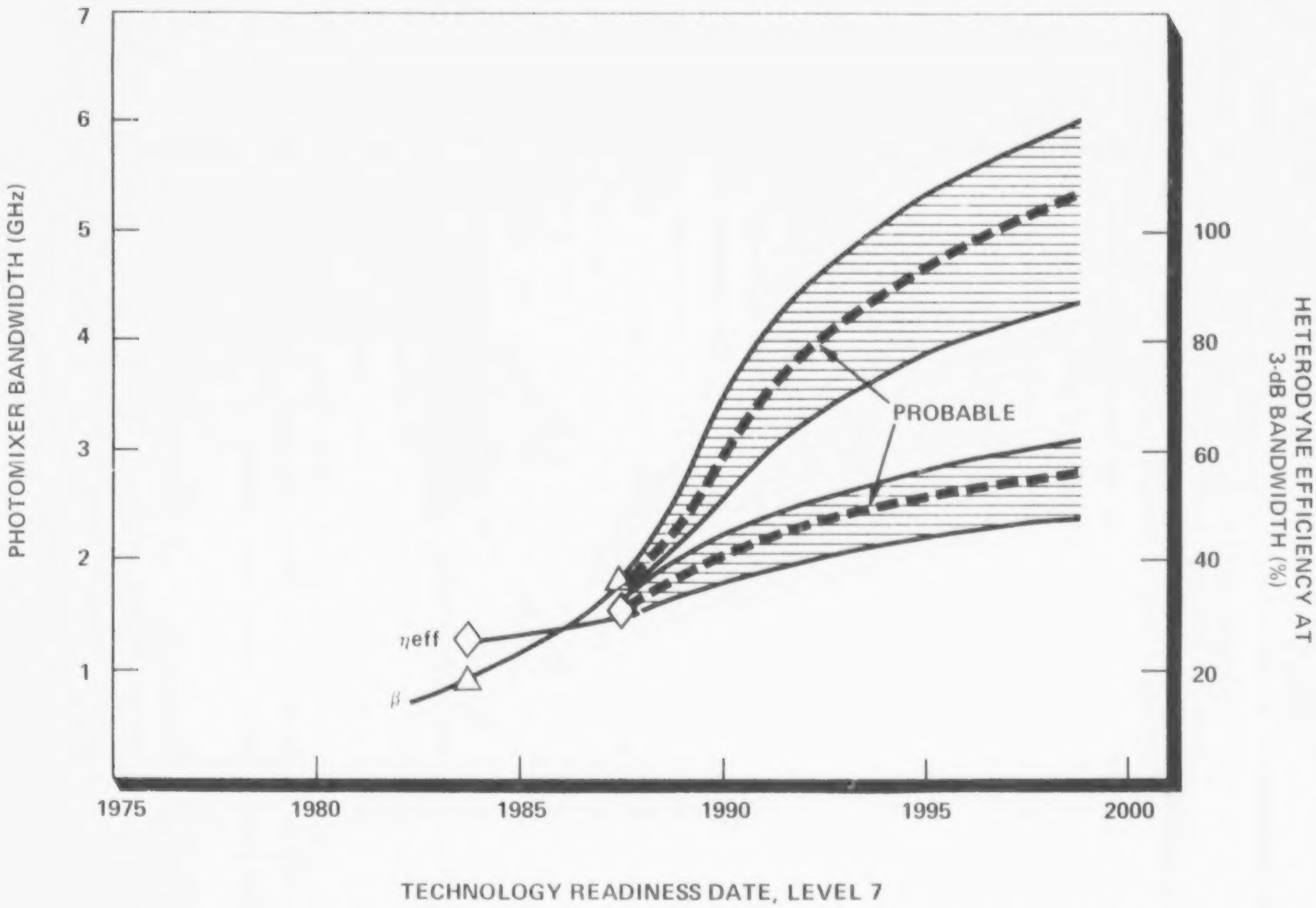

Figure 4.26. Bandwidth and Heterodyne Quantum Efficiency of 8-12 μm HgCdTe Photomixers

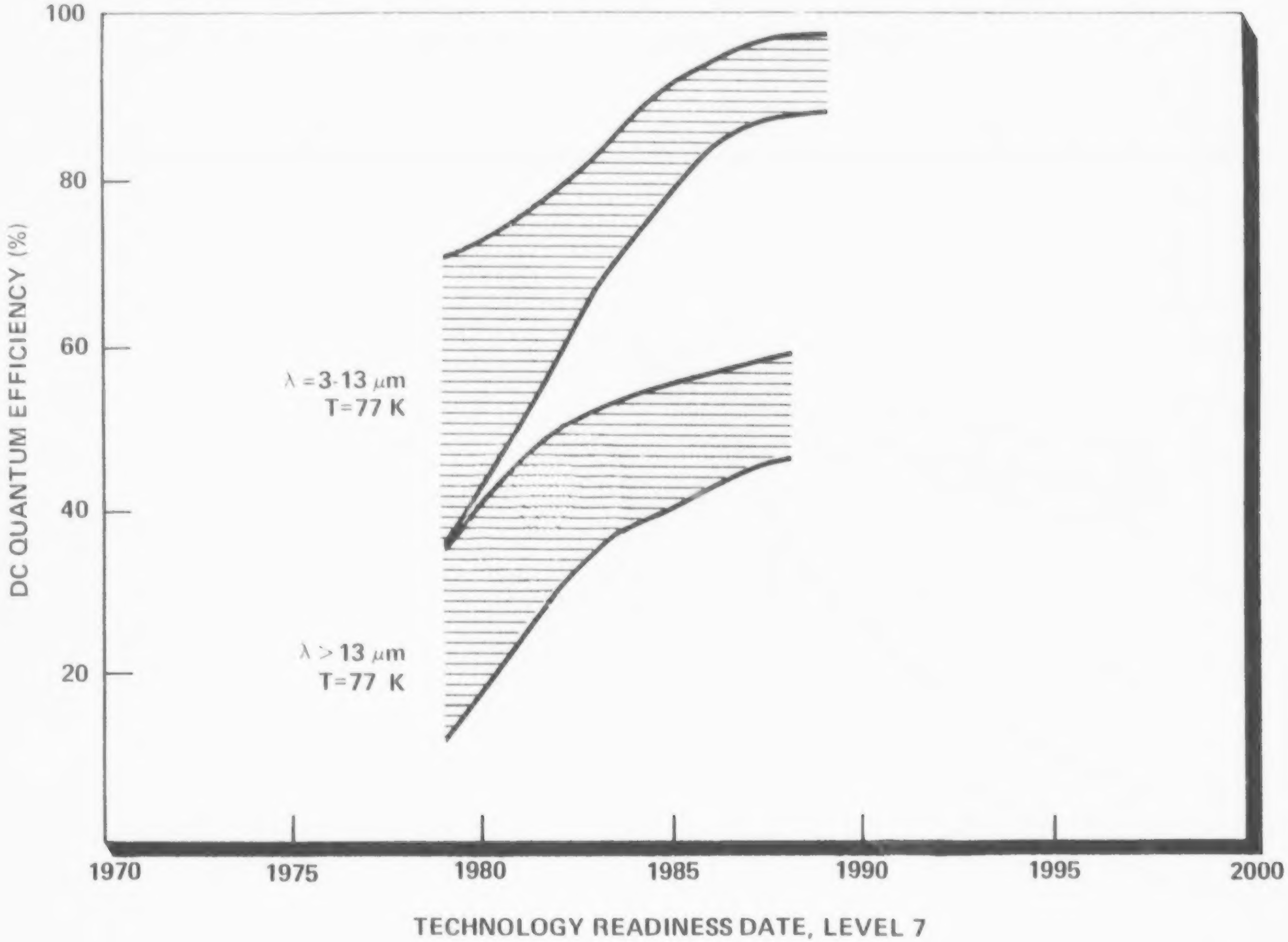

Figure 4.27. Spectral Response of HgCdTe Photomixers

4.1.10 Ultrasensitive Detectors: IR Sensors; Indium Antimonide and Mercury Cadmium Telluride Monolithic Linear Arrays

Basically, research in this area is addressing the development of technology for monolithic linear arrays of infrared detectors (no hybrid array technology) which are read out by a charge coupled technique into an on-chip amplifier performing amplification and other on-chip preprocessing. The data presented shows the past evolution and the expected evolution of the charge coupled infrared imaging device (CCIRID) technology in terms of expected number of detectors in the array, sensitivity in terms of detectivity, and improvements of spectral range in terms of wavelength.

Charge coupled infrared imaging devices (CCIRID) technology has been aimed mainly at development of monolithic InSb and HgCdTe (for 1-30 μm spectral coverage) linear arrays for operation in the pushbroom mode for planetary, atmospheric, astronomical, earth resource, oceanographic, and pollution measurements. Basically, spectral detectivity (in comparison to discrete detectors) is only limited to the noise produced in the CCD transfer device. Resolution capability is limited to the optics technology and detector size which can be tailored to a specific application. The major obstacles lie in achieving wider spectral range (a materials technology and device fabrication problem) and the achievement of fabrication techniques for long (100s to 1000s) arrays and the associated integrated circuit technology for achieving the device and reasonable charge transfer efficiency. Linear array technology is directly transferable to area arrays. The technology now being developed consists of a 100-element linear array and a 20 × 16 time delay and integration (TDI) linear array. For area array considerations the 20 × 16 TDI array can be operated as two 10 × 16 area arrays with 50% coverage.

The major advantages of the monolithic CCIRID development program is that the devices developed will require less power, space, and cooling while providing increased resolution and signal/noise ratio than other infrared devices. In addition, improved data handling capability is achieved along with improvements in signal/noise and overall detector uniformity of response by going to the TDI mode of operation. TDI provides detector signal/noise improvements of $\sqrt{N}$, where N is the number of detectors normal to the linear array detectors (such as the 16 in a 20 × 16 TDI array). Also, preprocessing techniques, using on-chip FETs for amplifiers, multiplexing, and signal manipulation, are being evaluated and developed.

Currently two major areas are being addressed: InSb for 1-5.5 μm spectral range and HgCdTe for 8-12 μm spectral range. Further development plans are dependent on materials technology and device fabrication advances providing spectral coverage from 1-30 μm with state-of-the-art achievable detectivities. (Note that any systems applications of the devices are highly dependent on the mission altitude, optics, design of the system, and required signal processing of the spacecraft.)

Within the spectral range from 1 to 12 μm detectivity requires cooling down to 77 K. Once the temperature is raised to 140 K (as for some passive cooling application), then the detectivity will change and is a strong function of wavelength in which the detector is operated. Out beyond 12 μm, a good photovoltaic device will have to be made in better infrared material than is currently available. This wavelength region is very weak at the present and requires more developmental work.

For longer arrays, two problems arise in the fabrication of longer devices (greater than 100 detector elements): a yield problem and the availability of larger diameter HgCdTe and InSb infrared semiconductor materials. The approach demonstrated with the mosaic arrays is the safe way; we have better yield with 100-element detector arrays than 1000-element detector arrays, and the crystals of semiconductor material are available to provide this capability.

Extension of HgCdTe to longer wavelength response requires greater control of impurities for lower carrier concentration in shorter bandgap material. Infinite melt liquid phase expitaxy seems to be the best way to go for better materials and larger crystals. Figures 4.29 and 4.30 show the best available data, the projection of large mosaic devices in the wavelength region from 1 to 12 μm (with HgCdTe available at higher temperatures in the lower wavelength region) in the early 1980s.

Technology Development--Infrared Imaging InSb and HgCdTe CCIRID-Monolithic Linear Arrays (Fig. 4.28). This figure illustrates the various stages of the evolution of the technology in this category. Basically the projection is that, with current infrared materials, wafer-sized 100-element linear arrays will be available in the early 1980s, with the larger arrays achievable through mosaics formed from the 100-element arrays. Improvements in S/N and detector uniformity will also be achievable in this time frame through the use of TDI arrays. Devices will be available for the missions listed to the far right of the figure. The only constraint is the adaptation of the technology to specific mission detector array configuration requirements. The basic technology through Level 4 will have been demonstrated by the early 1980s. If larger element arrays are required without the use of mosaics, then a materials technology program will have to be funded to provide larger infrared material wafers.

Monolithic InSb and HgCdTe Linear Arrays (Fig. 4.29). This figure is just a graphic representation of Fig. 4.28. It shows the current number of linear detectors which will be available with the current materials technology and the projected size of the mosaics.

Monolithic InSb and HgCdTe Array Sensitivity (Fig. 4.30). This figure shows some expected improvements in array sensitivity through improvements in the reduction in noise of the on-chip CCD devices and associated electronics readout. These data are for 77 K operation of the arrays and would change with operation at other temperatures. These data are also with a field of view (FOV) of 180° and could be improved by just decreasing the FOV. Increased sensitivities in other spectral regions (beyond 12 μm) will be dependent on materials improvements and improved device structures.

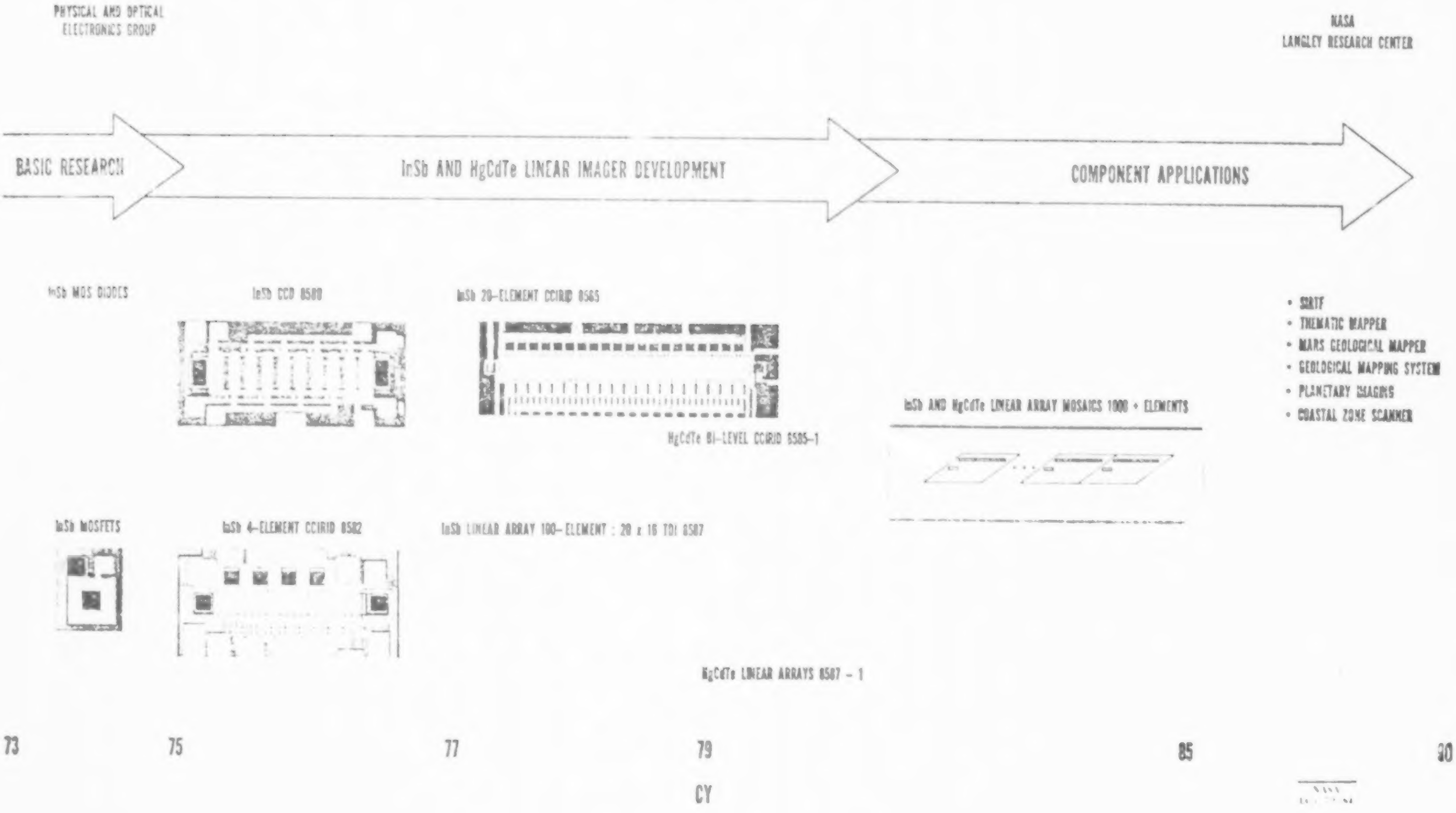
PHYSICAL AND OPTICAL ELECTRONICS GROUP
NASA LANGLEY RESEARCH CENTER
BASIC RESEARCH
InSb AND HgCdTe LINEAR IMAGER DEVELOPMENT
COMPONENT APPLICATIONS
InSb MOS DIODES
InSb CCD 8580
InSb 20-ELEMENT CCIRID 8565
HgCdTe BI-LEVEL CCIRID 8585-1
InSb AND HgCdTe LINEAR ARRAY MOSAICS 1000 + ELEMENTS
• SIRTF
• THEMATIC MAPPER
• MARS GEOLOGICAL MAPPER
• GEOLOGICAL MAPPING SYSTEM
• PLANETARY IMAGING
• COASTAL ZONE SCANNER
InSb MOSFETS
InSb 4-ELEMENT CCIRID 8582
InSb LINEAR ARRAY 100-ELEMENT : 20 x 16 TDI 8587
HgCdTe LINEAR ARRAYS 8587 - 1
73
75
77
79
85
90
CY

Figure 4.28. Technology Development--Infrared Imaging InSb and HgCdTe CCIRID-Monolithic Linear Arrays

]

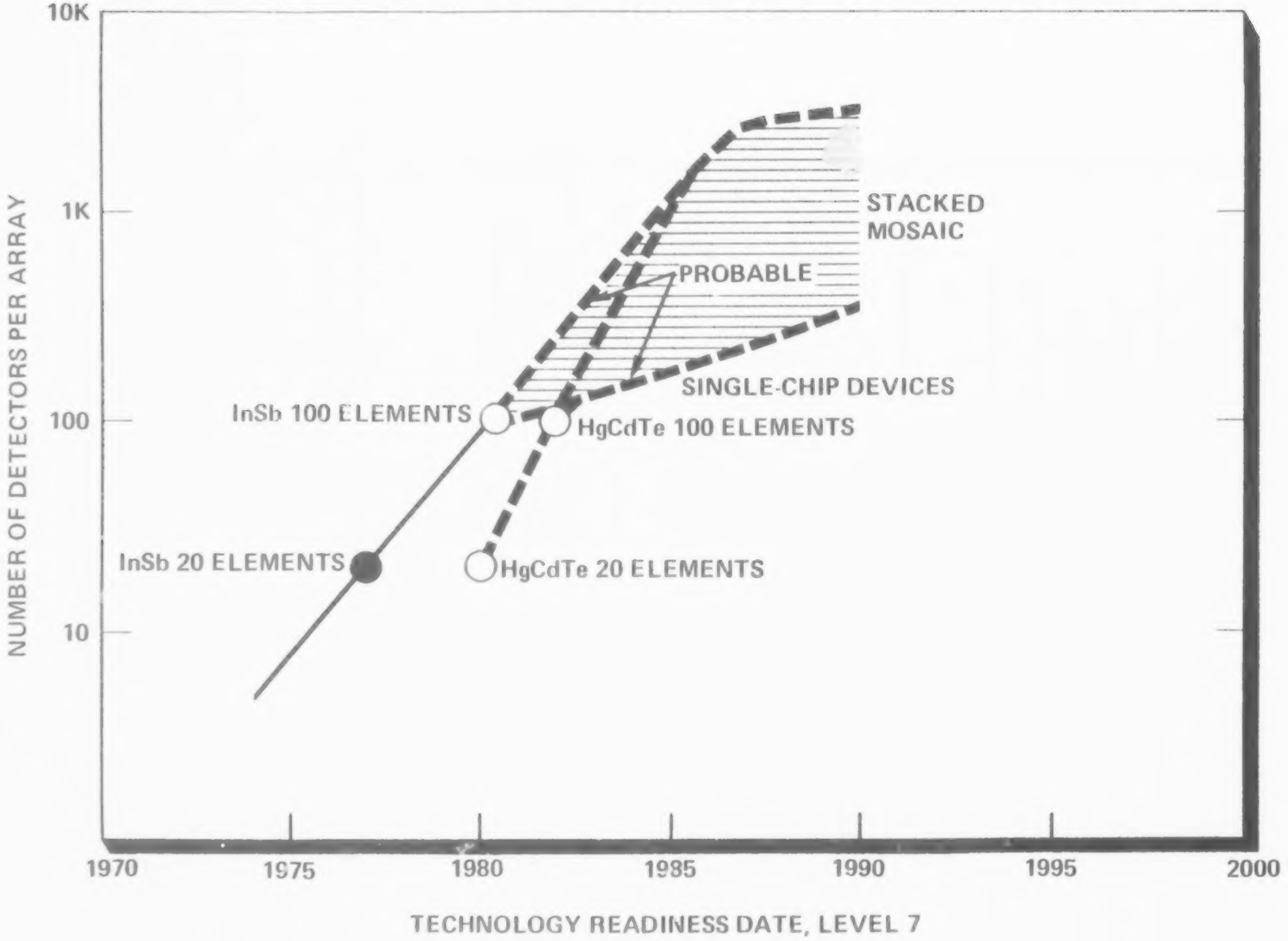

Figure 4.29. Monolithic InSb and HgCdTe Linear Arrays

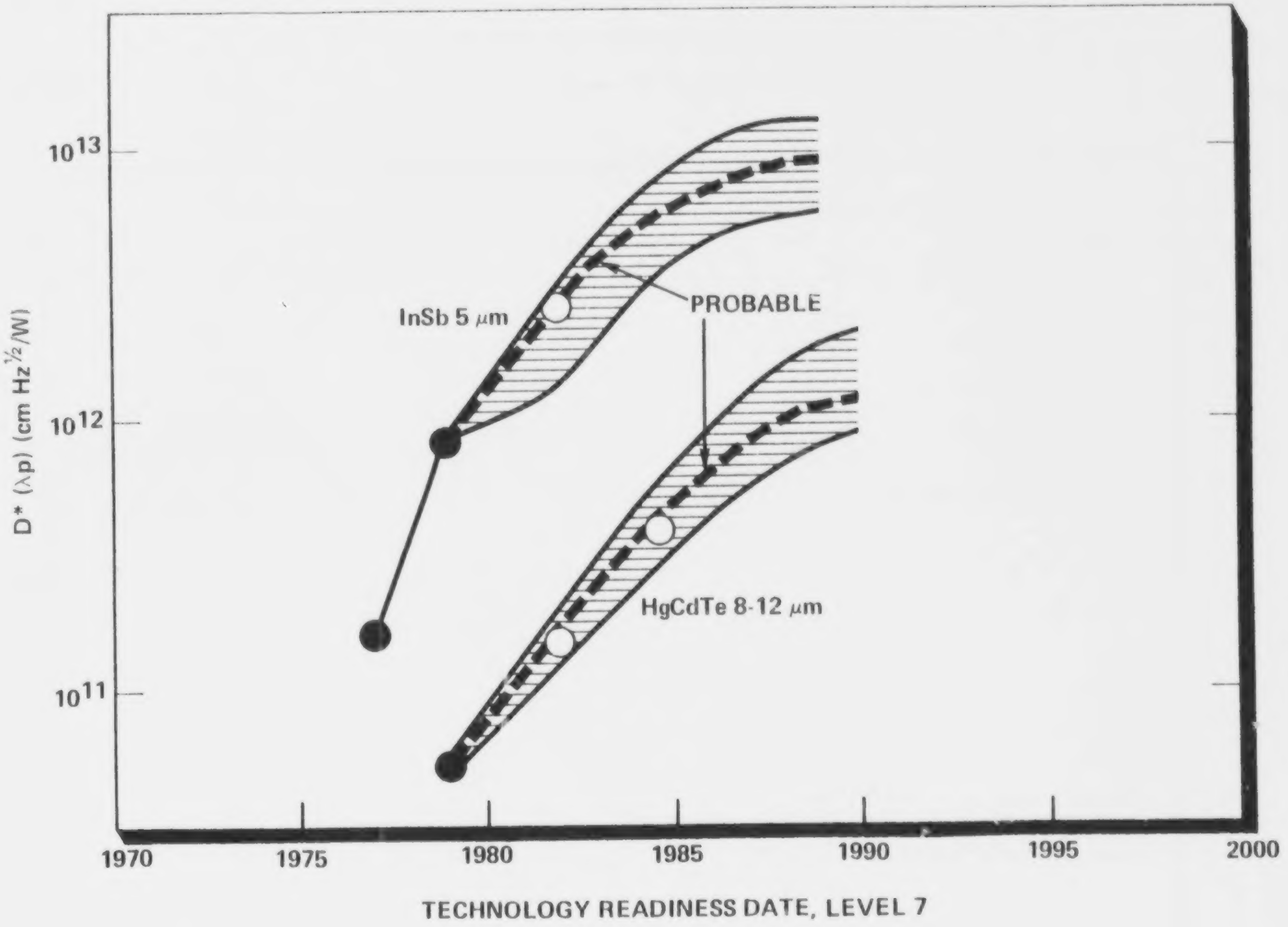

Figure 4.30. Monolithic InSb and HgCdTe Array Sensitivity

Monolithic Linear Arrays--Spectral Range (Fig. 4.31). These data project the current technology development provided that material development and further device technology are addressed. Wavelength regions shorter than 8 μm could be addressed in HgCdTe, but more applications emphasis seems to be in the area of longer wavelength and requires the greater R&D effort. The current technology could be used to develop arrays in HgCdTe all the way down to 1 μm if there is a severe cooling problem where temperatures greater than 77 K must be considered. There is a severe wavelength extension problem beyond 12 μm unless temperatures lower than 77 K are utilized and additional material and device development in this wavelength region is pursued. In the long term, there may have to be a move toward photoconductive (PC) devices in the longer wavelength region. This will present a greater problem where more cooling is required due to greater power dissipation in PC devices.

4.1.11 Laser Systems for Lidar Active Remote Sensing (R. V. Hess, Langley Research Center)

The focus of this technology forecast is the Shuttle Atmospheric Lidar Research Program, recently detailed in the final report of the working group.[1] Several of the seven major science objectives and 26 candidate experiments are addressed in this forecast. Also discussed are some less severe requirements for aircraft experiments. The laser systems requirements are based on measurement simulations and laser systems studies[1] and performed at Langley Research Center.

The technology forecast addresses itself to tunable CO_2 and other infrared gas laser systems, and nonlinear conversion techniques especially advantageous for profile measurements of a wide range of atmospheric species and of wind velocities, and potentially to pressure/temperature throughout the entire troposphere and lower stratosphere and in upper atmospheric species by two-satellite experiments. Rare gas halide, or excimer, lasers have many similarities with pulsed CO_2 and other infrared

---

[1] Final Report of Atmospheric Lidar Working Group, Shuttle Lidar Research Program, NASA SP-433, 1979.

best copy available

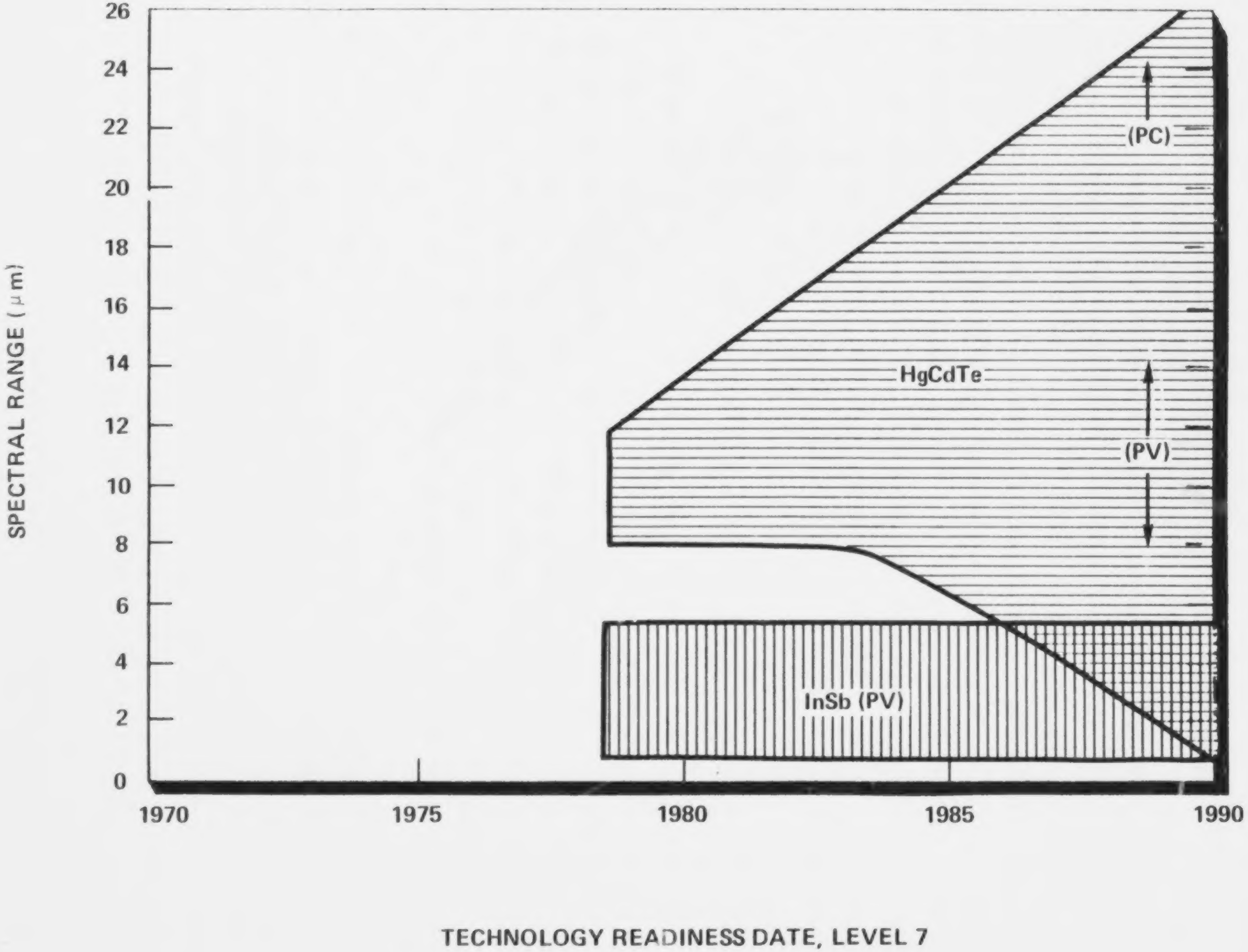

Figure 4.31. Monolithic Linear Arrays – Spectral Range

laser systems, but Langley is not currently involved in their development. Excimer lasers are advantageous for UV atmospheric species measurements above the ozone layer and, by optical pumping of dye lasers, potentially for some select measurements of trace species in the visible-near IR and for pressure/temperature in the atmosphere.

Since tunable infrared lasers and frequency conversion systems for active lidar remote sensing benefit from sensitive heterodyne detection, the present technology forecast overlaps the forecast of laser heterodyne systems for passive remote sensing.

Tunable CO_2 and Other IR Lasers, Nonlinear Conversion. Measurement simulations for differential absorption lidar (DIAL) with tunable 3 to 4 atm CO_2 laser for O_3, NH_3, and H_2O from Shuttle altitudes (~200 km) indicates the need for pulse energies from 1 to 5 J, with repetition rates from ~60 to 300 pps, assuming maximum laser average power of 300 W at 10% conversion efficiency. Long-term frequency stability of $\leq$10 MHz obtained by transient injection locking[1] is required, and closed-cycle operation for CO_2 and rare isotope operation without laser medium degradation.[2] Simulations for aircraft altitudes indicate the need for 0.05 J/pulse and repetition rates of 300 pps.

- Tunable closed-cycle transverse flow CO_2 and rare isotope laser with 0.05 J/pulse, 300 pps and long-term frequency stability of 2 MHz can have aircraft breadboard demonstration in early FY 81. Hardened brassboard for aircraft in FY 82.
- Tunable closed-cycle CO_2 and rare-isotope laser with 1 to 5 J/pulse, 60 to 300 pps and long-term frequency

---

[1] J. S. Levine, M. Guerra, A. Javan, Development of Tunable High Pressure CO_2 Laser for Lidar Measurements of Pollutants and Wind Velocities, Laser Development Corp., NASA Contractor Report, November 1979.

[2] R. B. Gibson, A. Javan, K. Boyer, "Sealed Multiatmospheric CO_2 TEA Laser: Seed Gas Compatible System Using Unheated Oxide Catalyst," Applied Physical Letter 32 (11), 1 June 1978.

stability of ~2 MHz can have Shuttle breadboard demonstration in FY 84.

CW tunable ~3 atm transverse-flow CO_2 laser with mini E-beam preionization[1] for tunable transient injection locking of pulsed laser and for LO in heterodyning DIAL return; and as primary CW source with tuning and power range wider than waveguide laser.

- Mini E-beam "ribbon" ($0.1 \times 0.1 \times 10$ cm^{-3}) for preionization demonstrated in FY 79.
- Demonstration at ~10 mW to 20 mW CW power can be made in FY 81 including long-term frequency stability and wavelength calibration.
- Demonstration for transient injection locking and LO in FY 81; primary tunable CW source in FY 82.

Development of detector array for receiver aperture signal averaging for additional reduction in speckle noise heterodyne detection.

- Detector arrays developed by Spears (Lincoln Laboratory) will be modified for DIAL application in FY 82.

Development of other tunable IR lasers (CO, HF, DF) with frequency stability obtained by transient injection locking and long-time operation.

- Develop transient injection locking for CO, HF, DF lasers in FY 82.
- Develop closed-cycle system with catalysts and make-up flow in FY 83.

Develop frequency doubling of CO_2 lasers from 9-12 μm range to 4.5-6 μm range by non-linear conversion in chalcopyrite crystals such as $CdGeAs_2$. The present optical damage threshold is ~50 mW/cm^2; however, conversion efficiency is currently limited to ~27% by saturation (Lincoln Laboratory). Average power is limited to ~2W. Conversion has been demonstrated with a low-average-power repetitively 1-atm pulsed CO_2 laser without tuning across collision-broadened laser lines and without frequency/bandwidth control. DIAL measurements of CO have been demonstrated by reflection from smooth surfaces at several kilometers' distance (Lincoln Laboratory). Measurement simulations at Langley indicate potential applications for measurements of CO from aircraft (~10-km altitude) through ranging by aerosol scattering.

---

[1] Levine et al., op. cit.

- Increase average power for $CdGeAs_2$ crystals and demonstrate frequency doubling with tunable high pulse repetition rate, frequency stable ~15 W CO_2 laser constructed by Laser Development Corp., in FY 82.
- Perform DIAL measurements of CO, etc., with ranging by aerosol scattering from ground in FY 82 and from aircraft in FY 83.

Develop sum-and-difference frequency mixing of CW CO_2 and CO laser radiation in $CdGeAs_2$ for wide-IR frequency coverage; extend development by Lincoln Laboratory.

- Demonstrate with discrete frequency lasers for 10 mW CW power in FY 82.
- Demonstrate with high-pressure tunable CO_2 laser radiation.

Develop tunable frequency conversion with microwave sideband modulation of CW CO_2 lasers with later CW CO lasers.

- Glen Sachse (Langley) obtained sideband tuning in GaAs waveguide from 8000 to 18,000 MHz of line center from CW CO_2 lasers at low conversion efficiencies in FY 79.

- Increase conversion efficiency by narrower optical confinement in GaAs or CdTe waveguides (R. Chiao, University of California, Berkeley) and reduce 8000-Mhz gap from line center by improved impedance matching in FY 81.
- Demonstrate 10-mW tunable CW power in FY 82.

Develop tunable radiation over wide IR range by non-linear converstion of radiation from transition metal lasers developed at Lincoln Laboratory.

- Tunable transition metal lasers from ~1.6 to 2.2 μm at 77 K were demonstrated with ~9 W average power in FY 79.
- Non-linear conversion with ~10 mW average power through IR in FY 83.

Doppler lidar wind-velocity measurements with ranging by aerosol scattering requires pulsed CO_2 lasers operating on line center, but with sufficient pressure up to ~1 atm to obtain high pulse energies up 10 J/pulse of ~15 pps for operation from Shuttle platforms.[1] For the required 1 m/s wind-velocity measurements, the laser frequency stability and bandwidth must be ~0.2 MHz. As a result, the pulse durations (according to Fourier transform) must be ≳1/frequency bandwidth. To reduce atmospheric attenuation, the laser should operate with rare CO_2 isotopes, which also requires long-duration closed-cycle operation with catalysts or minimal make-up flow as in tunable DIAL measurements.

- In the past, Doppler lidar was performed with amplitude-modulated CW
- Development of pulsed CO_2 laser with required frequency stability and pulse duration with ≥0.1 J/pulse and ~20 pps in FY 81.
- Closed-cycle long-duration CO_2 rare-isotope laser opera-

---

[1] NASA SP-433, op. cit.

tion at ~0.1 J/pulse at ~20 pps for aircraft breadboard in late FY 82.

- Development of 10 J/pulse at ~20 pps with required 0.2-MHz frequency stability, and closed-cycle operation for Shuttle operation in FY 84.

Tunable Rare Base Halide (Excimer). A very good review of excimer lasers in remote sensing is based on extensive studies by Osamu Uchino et al. at Kyushu University, Japan.[1] Tunable excimer lasers operate over a wide-UV frequency range ArF (0.308 μm), KrF (0.244 μm), XeF (0.351 μm), ArCl (0.175 μm), KrCl (0.222 μm), XeCl (0.308 μm), and XeBr (0.282 μm). The tuning range of an individual laser mixture is 0.3 to 1 × 10^{-3} μm. These lasers generally operate at several atmospheres and use simple transverse electric discharge geometries, very similar to high-pressure pulsed CO_2 lasers. Their efficiency is up to ~1%, which is high compared to frequency-doubled tunable dye lasers frequency used for DIAL remote sensing in the near UV (~0.3 μm) for example, for O_3 and SO_2, and fluorescence lidar for OH. Excimer lasers also operate at considerably higher pulse energies, pulse repetition rates, and average powers than dye lasers, in the UV. Excimer lasers with pulse energies of ~1 J and repetition rates up to 2000 pps are under development for Los Alamos.[2]

The approximate coincidences of the XeCl laser with O_3 have resulted in DIAL measurements of stratospheric O_3 from the ground. Use of fluorescence lidar of OH radicals with an XeCl laser shows considerable promise. Excimer lasers, however, promise to play a larger role in remote sensing, since they also provide a comparatively efficient source for tunable dye laser optical pumping; however, long-time operation without dye degradation must be demonstrated. Further, they are potentially important sources for non-linear conversion by stimulated Raman effects, thus considerably widening their tuning range.

---

[1] Osamu Uchino et al., "Applications of Excimer Lasers to Laser-Radar Observations of the Upper Atmosphere," IEEE J. Quantum Electronics, QE-15, No. 10, October 1979.

[2] Personal communication from Keith Boyer.

High-frequency stability/narrow bandwidth of tunable excimer lasers can also be obtained by tunable transient injection locking for tunable CO_2 lasers.[1]

4.1.12 Hybrid Thermal IR/CCD Arrays

Of the several technical approaches to the development of high-density focal plane detector arrays for the thermal IR region (8-14 μm), the hybrid focal plane array represents a pragmatic approach that combines a mature detector technology with a well-developed silicon CCD multiplexer technology. This is the most versatile of the approaches that are available. Its versatility arises from the ability to select and optimize independently the photodetector array and the readout multiplexer.

The separation of the sensing and readout media allows the benefits of CCD readout to be realized in a number of intrinsic detector materials whose MIS properties preclude viable CCD operation. Further, the benefits of intrinsic detectors, i.e., high operating temperatures, high quantum efficiency, and low crosstalk can be realized.

The hybrid approach, however, does introduce a number of critical issues:

- Mechanical and electrical coupling between the detector array and the Si CCD. Differences in the thermal expansion coefficient between the detector material and Si can result in mechanical stress and poor reliability after temperature cycling. Thus thermal expansion mismatch may place a limitation on the hybrid array chip size and require more chips per focal plane.

---

[1] Levine et al., op. cit.

- An efficient input circuit is also needed to inject the detector signal into the CCD multiplexer. Direct injection circuits are simple, but are sensitive to gate threshold non-uniformities. Input circuits have been developed which reduce this effect, but at the expense of increased power dissipation. This latter issue is of particular importance to NASA. The effort to develop the hybrid array is driven in part, by the constraints of radiative cooling capabilities of long-life space missions.

Performance (Fig. 4.32). To indicate the kind of performance growth that may be expected in the future, it is necessary to first establish some form of quantitative relationship or figure of merit which indicates the interrelationship of the sensor parameter. One such figure of merit that can be used is given by:

$$\text{Performance} \propto \left[\frac{(\text{Sensitivity})(\text{Swath Width})^{1/2}}{(\text{Spectral Width})(\text{Linear Resolution})^{2}} \right]$$

Although other figures of merit could be derived, this form has the desirable attribute that is includes most of the major system parameters and the value of the function increases as any of the parameters are made more stringent.

Normalizing the figure to the year 1970, the curve indicates the improvement in relative performance as a function of the number of resolution elements in the detector array. It can be seen that the relative improvement increase is proportional to the square root of the number of elements in the array. Beyond array sizes of roughly 10,000 elements, one of the performance factors, namely, sensitivity, is shown approaching a limit for typical earth-viewing applications. This occurs for integration times in the millisecond region. Other performance factors such as resolution or swath width are not subject to this limitation.

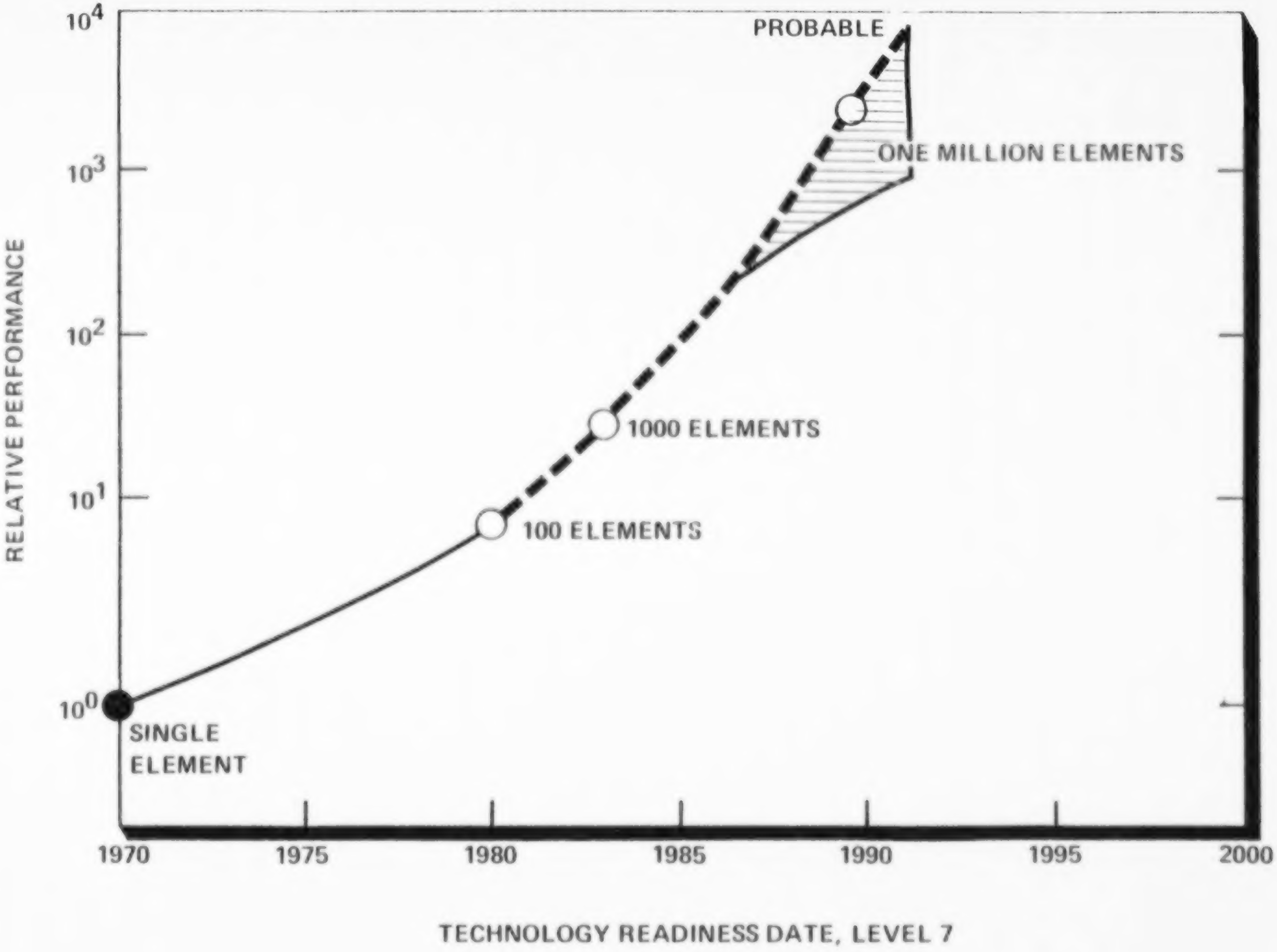

Figure 4.32. Performance Growth

Dates are also shown on the figure to indicate when improvements resulting from OAST support and programs can be expected to be available. Also shown for reference is a high-density (monolithic extrinsic) focal plane array which is being supported by DoD and is expected to be available in the 1980 time frame.

Costs (Fig. 4.33). The costs per detector element are expected to decrease in constant dollars, from a level of $140,000 to roughly $1000 by 1990. The 1970 costs were derived from historical data obtained from flight sensors of that era. It is expected that in the future the detector costs will not significantly depart from present experience but that the test and integration costs will increase by a factor of 5 in 1983 to a factor of 10 in 1990 as the array complexity increases.

Cooling Requirements (Fig. 4.34). As shown in the figure, photovoltaic arrays have an enormous advantage over photoconductor arrays with respect to cooling requirements in the thermal IR region. For long-term missions (years), the current method of cooling is through radiation to space. In earth-orbiting missions, realizable cooling of IR detectors to about 100 K is limited to thermal loads of a few hundred milliwatts.

Some improvement (reduction) in heat dissipation per element is anticipated due to smaller detector element sizes and technological improvements in the CCD circuitry.

The total heat load is projected to show a slow increase to 1990 as the number of detectors increases to the neighborhood of 1 million. The power level at this point is projected to be greater than 1 W for 100 K and, space radiators will undoubtedly require an assist from electromechanical coolers.

Reliability (Fig. 4.35). As electronic equipment becomes more complex, and uses more components, reliability becomes a most important consideration. The development of solid-state electronics, especially its embodiment in integrated electronics, has removed the barriers of

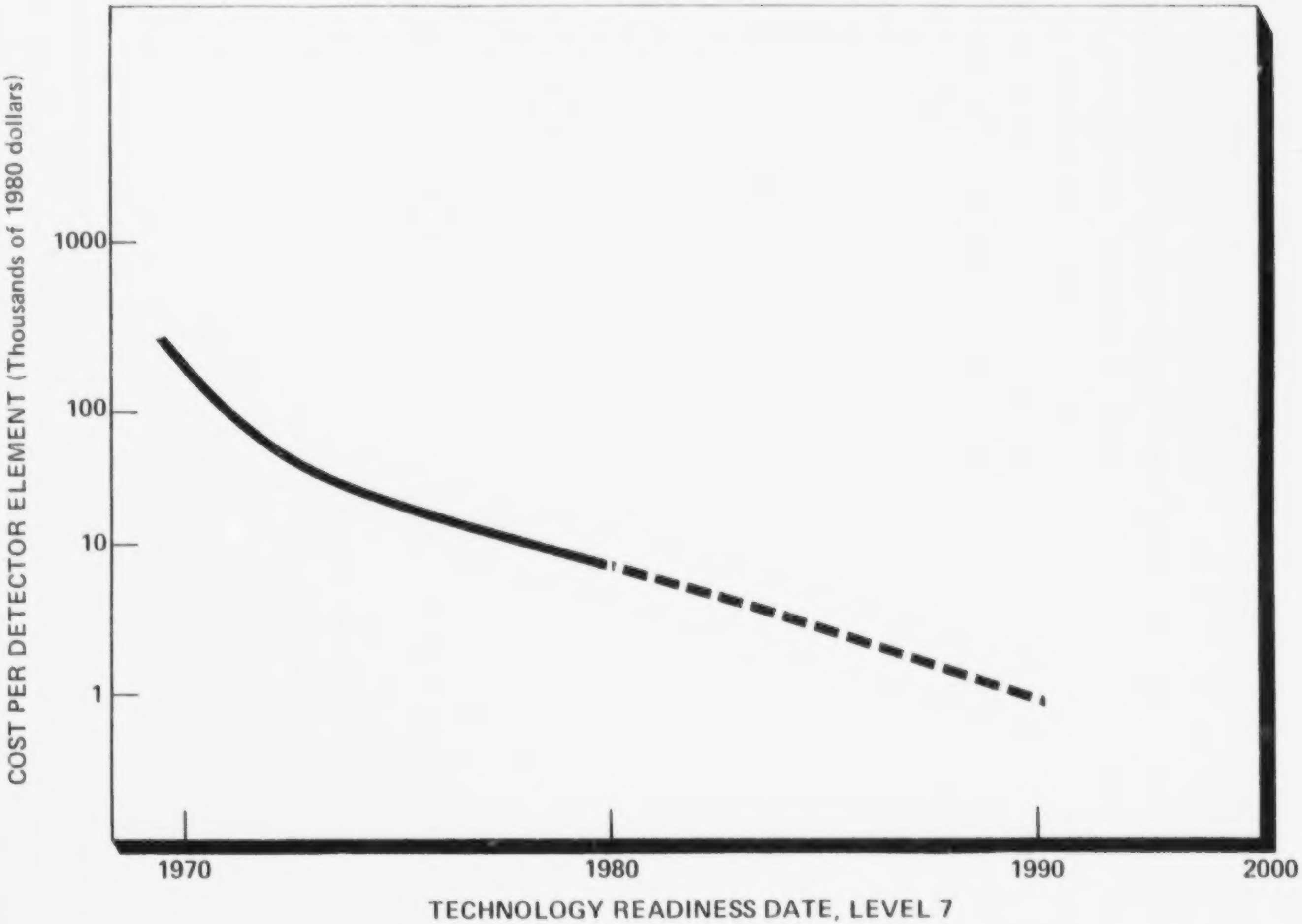

Figure 4.33. Hybrid Thermal IR/CCD Arrays, Cost per Detector Element

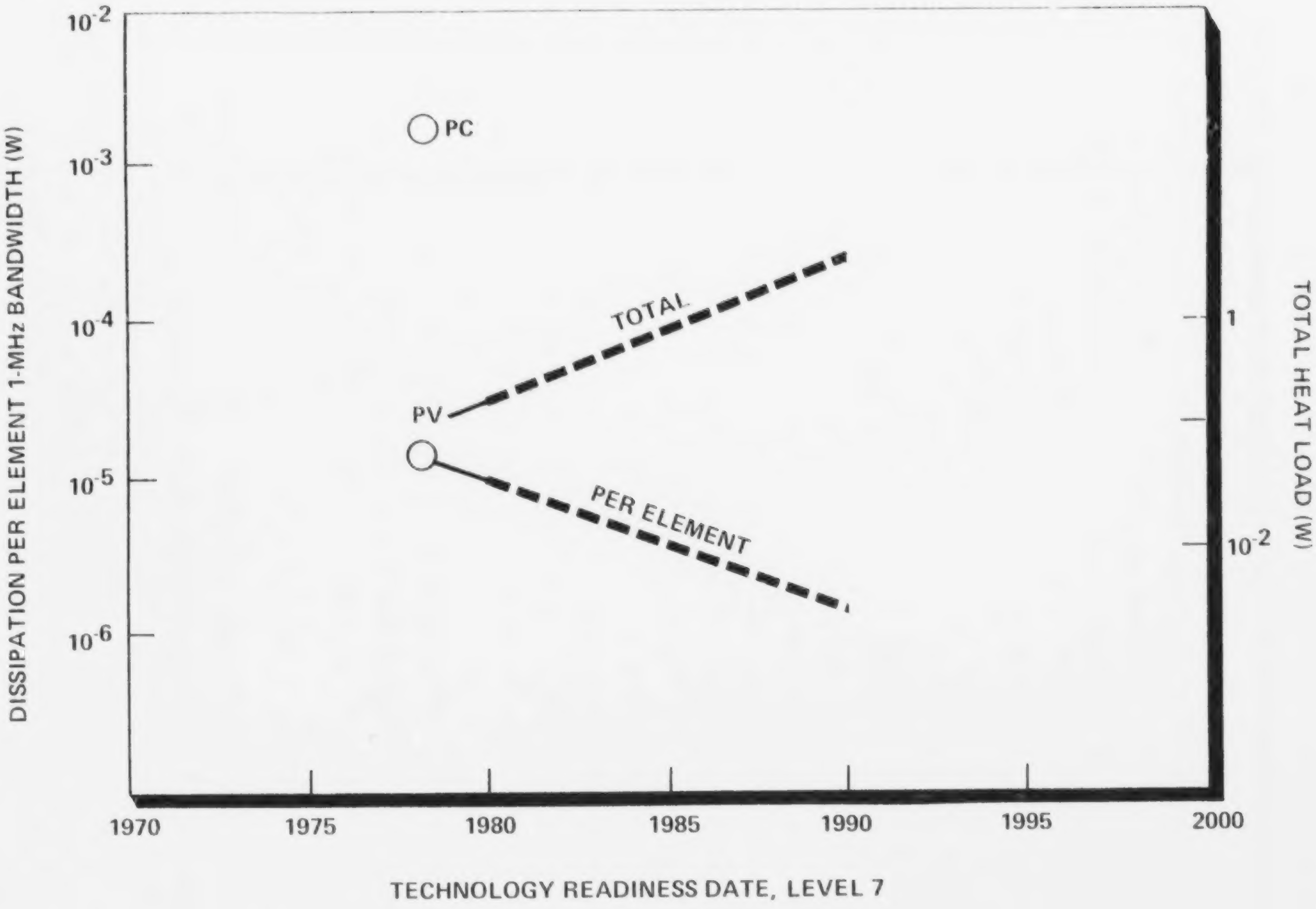

Figure 4.34. Cooling Requirements

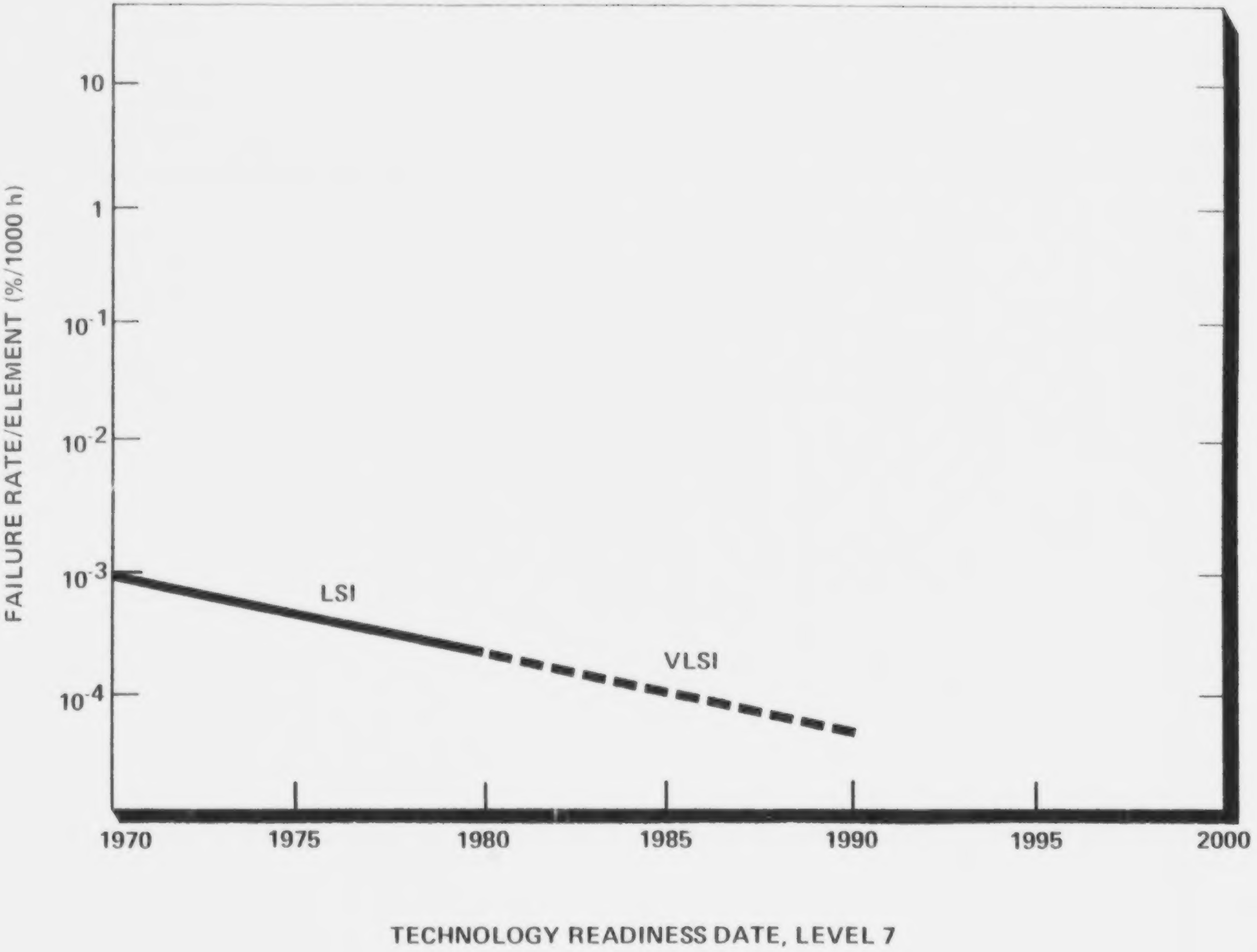

Figure 4.35. Reliability

reliability (and unit cost). Between 1960 and 1970, the curve shows the impact of integrated circuits on reliability in terms of reduced failure rates per element or circuit. From 1970, the development of large scale integration (LSI) and the projection to VLSI continues this growth in reliability. The solid-state self-scanned array will share, in general, this increasing reliability. However, depending upon the type of interconnect that is finally evolved between the detectors and the charge transfer device, thermal hybrid IR arrays may possess significantly less reliability than the projection for 1990. Such arrays, however, will be many orders of magnitude more reliable than the hand-wired, mechanically commutated arrays of the 1960-1975 era.

4.1.13 Millimeter and Submillimeter Heterodyne Radiometers for Atmospheric Measurements from Space (J. W. Waters, Jet Propulsion Laboratory)

The importance of millimeter and submillimeter heterodyne radiometers for atmospheric measurements from space is now well established. The first such radiometers in space operating near 5-mm wavelength were flown on the experimental Nimbus 5 and 6 satellites to determine whether the techniques could provide useful data on atmospheric temperature profiles in cloudy regions. Following the success of the Nimbus experiments, a 5-mm heterodyne radiometer is being used for operational meteorological purposes on the TIROS-N satellites. Extending the operating range of the heterodyne radiometers to the shorter millimeter and submillimeter wavelengths will allow important measurements to be made of upper atmospheric species and physical parameters (e.g., temperature and winds). Because these radiometers can measure atmospheric thermal emission, they can provide data at any time of day or night--an important feature for understanding upper atmospheric processes.

OAST is currently funding programs for the development of submillimeter heterodyne radiometer technology and for a Spacelab technology demonstration experiment. The technology development program has emphasized quasi-optical devices for efficient coupling or radiation into devices and the development of a radiometer at 0.16-mm wavelength for upper atmospheric OH. The Spacelab experiment, being jointly developed with OSTA's Upper Atmospheric Research Program Office, will include radiometers in the wavelength range of 5 to 0.5 mm.

The parameter forecast here is the radiometer noise temperature at the input to the mixer. The noise temperature is the equivalent temperature of a blackbody thermally radiating the same power per unit spectral interval as the radiometer noise power. From the radiometer noise temperature, T_N, the sensitivity ΔT can be calculated from the expression

$$\Delta T = \alpha T_N/(t\Delta f)^{1/2}$$

where α is a constant which describes losses in front of the mixer and any effects due to chopping the input signal, t is the integration time, and Δf is spectral resolution. The spectral resolution of heterodyne radiometers is determined by intermediate-frequency electronics, and can be made arbitrarily fine up to a limit of $\sim t^{-1}$.

The forecast indicates the predicted data at which a radiometer could be tested in space on the Shuttle.

Noise Temperature for 5-mm Wavelength Radiometers (Fig. 4.36). Radiometers at this wavelength have been flown on Nimbus and TIROS satellites. These radiometers used Schottky-barrier diodes and transistor first stage amplifiers. Reduction in noise temperature can be achieved by cooling the mixer, using new devices such as Josephson junctions or quasi-particle mixers, or low-noise (maser) amplification at the signal wavelengths. Local oscillators for these radiometers can be Gunn or IMPATT solid-state devices for which current technology is adequate.

Noise Temperature for 1-mm Wavelength Radiometers (Fig. 4.37). Present technology for 1-mm wavelength radiometers falls into two major categories. Uncooled broad bandwidth mixers using Schottky diodes can achieve noise temperatures of a few thousand kelvins, and narrow-bandwidth mixers using "hot electron" InSb mixing at liquid helium temperatures can achieve noise temperatures of a few hundred kelvins. Both devices

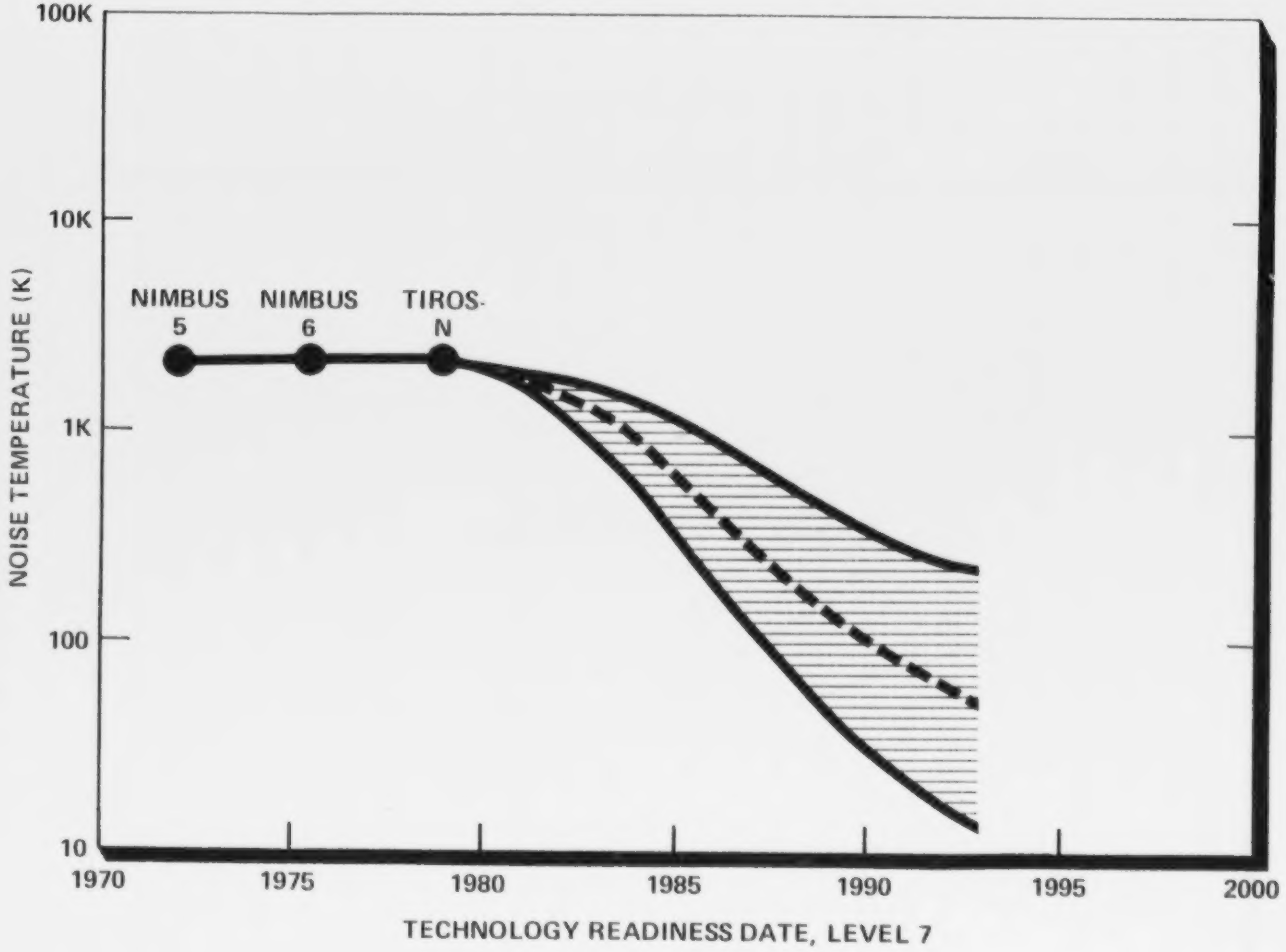

Figure 4.36. 5-m Wavelength Heterodyne Radiometer Noise Temperature

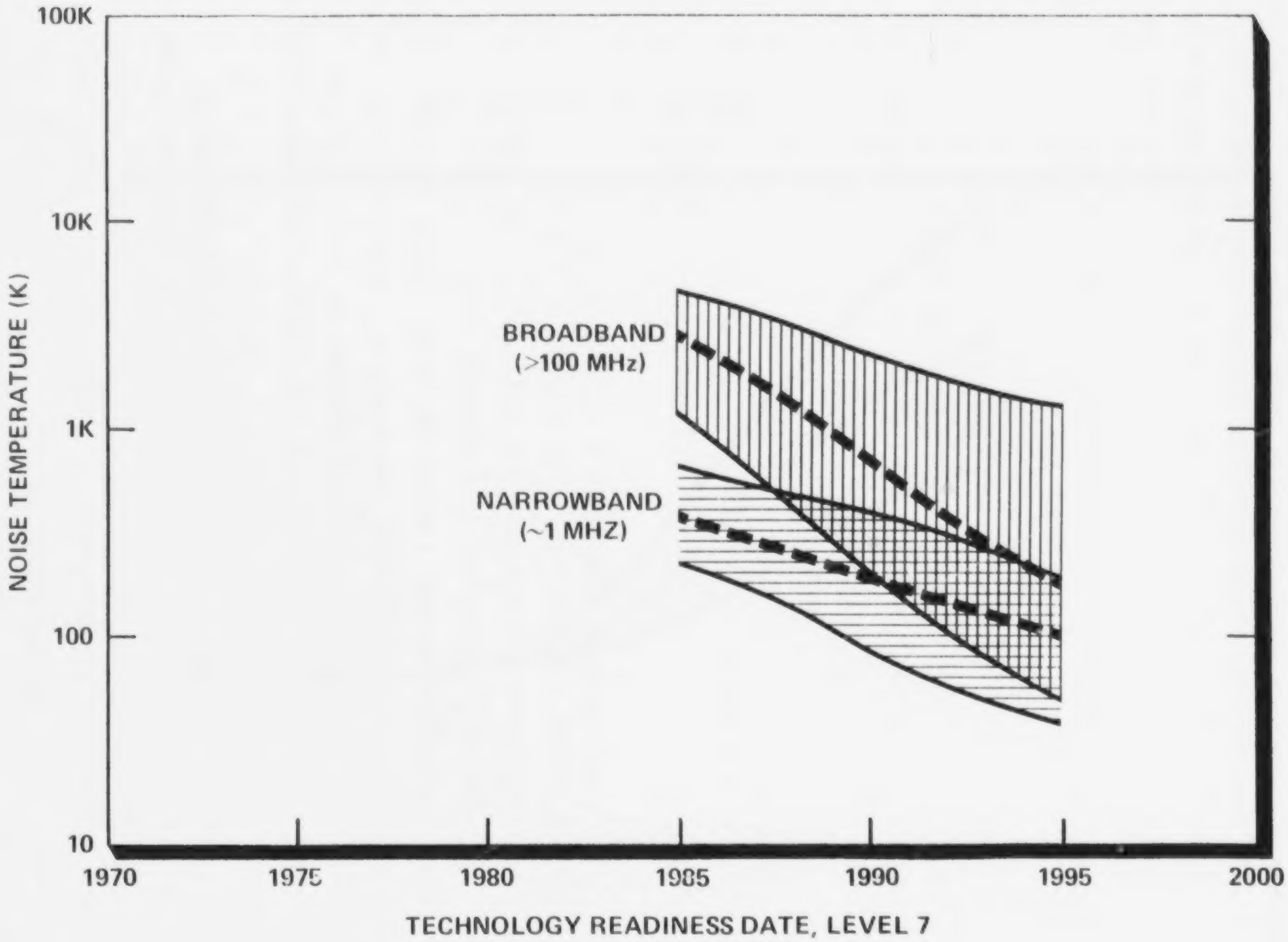

Figure 4.37. 1-mm Wavelength Heterodyne Radiometer Noise Temperature

could be made ready for a space test in the mid-1980s. The local oscillator is a more serious problem for the Schottky mixer (which requires ~10^{-2} W) than for the InSb mixer (which requires ~10^{-5} W), whereas the cooling requirements are more severe for the InSb. For the Schottky mixer, either electron tubes (reflex klystrons or backward-wave oscillators) requiring ~0.5 kW power supply or less-well-developed solid-state systems could be used for the local oscillators. Improvements in noise temperature can be achieved by cooling and improving the coupling and diodes for Schottky mixers and by using Josephson or quasi-particle mixers which are now under development.

Noise Temperatures for 0.5-mm Wavelength Radiometers (Fig. 4.38). Laboratory tests have indicated that uncooled Schottky diode heterodyne radiometers with noise temperatures of a few ten thousands of kelvins and cryogenic InSb hot electron radiometers with noise temperatures of several hundred kelvins are feasible. Such radiometers could be tested in space by the middle 1980s. Local oscillators for the Schottky radiometer and cryogenic coolers for the InSb radiometers which are suitable for space must be developed. Improvements in performance can be achieved by cooling the Schottky diodes and improving the coupling of the radiation to the diodes and the diode performance. The development of quasi-particle and, perhaps, Josephson junction mixers should also improve the performance.

Noise Temperatures for 0.1-mm Wavelength Radiometers (Fig. 4.39). It seems likely that broadband Schottky diode radiometers, with present technology, could achieve noise temperatures of the order of 100,000 K and narrowband photoconductor mixers could achieve noise temperatures of a few thousand kelvins. However, this is very speculative as mixers at these wavelengths are only in the pioneering development stages. The only local oscillators available at these wavelengths are optically pumped gas lasers which will require development for space use. With adequate research and development, however, it should be possible by the mid-1990s to have heterodyne radiometers at 0.1-mm wavelength with the

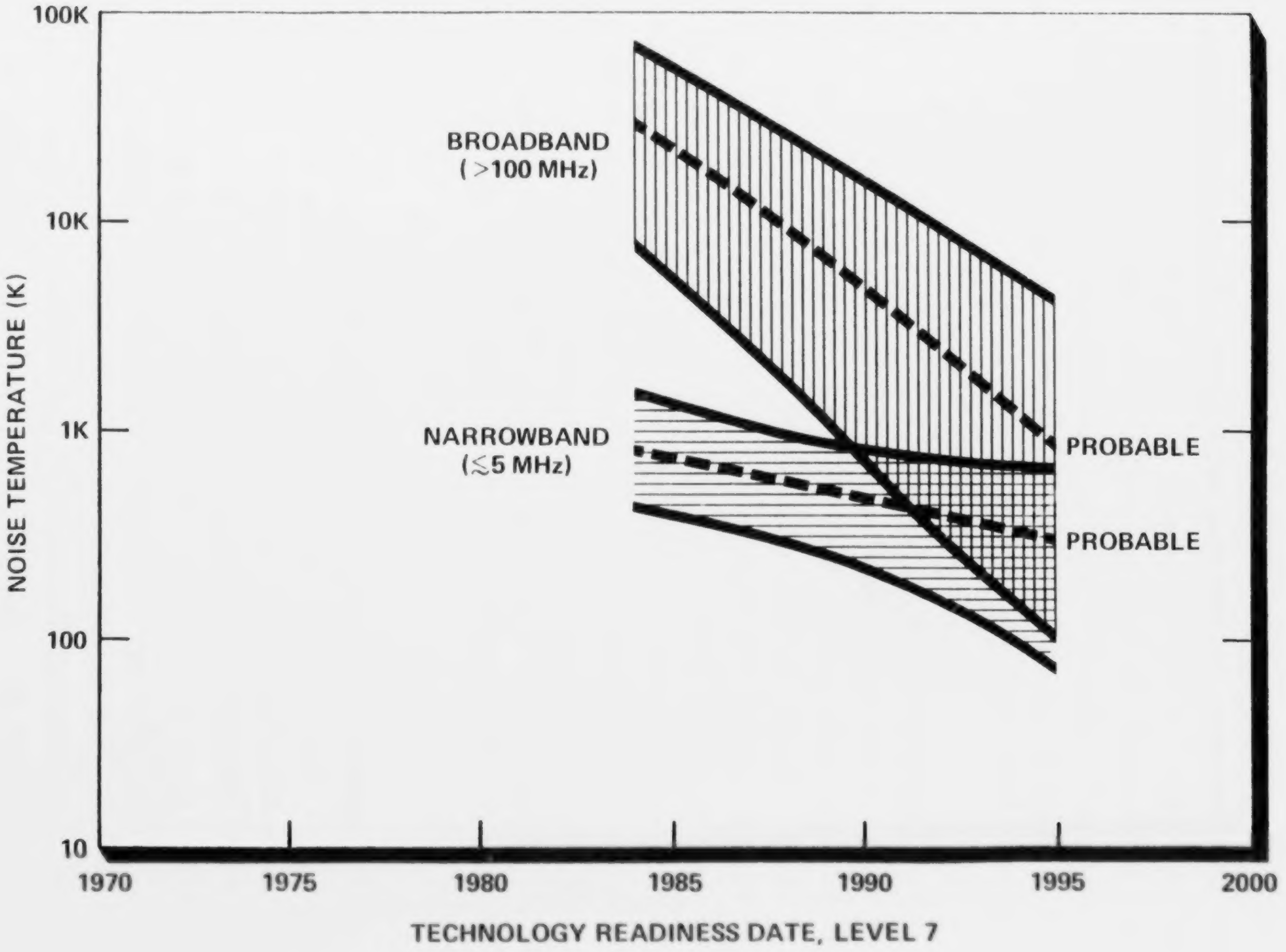

Figure 4.38. 0.5-mm Wavelength Heterodyne Radiometer Noise Temperature

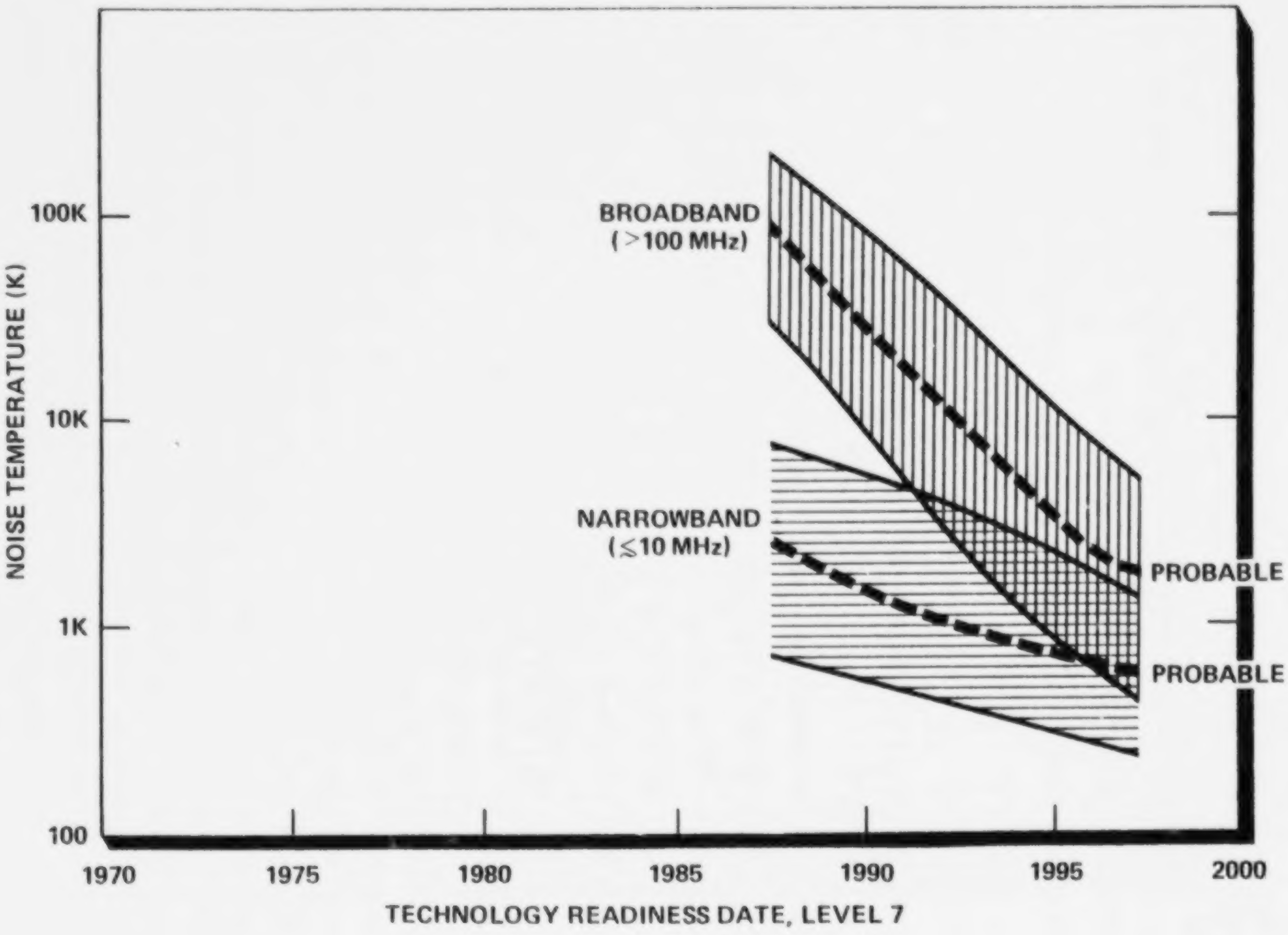

Figure 4.39. 0.1-mm Wavelength Heterodyne Radiometer Noise Temperature

same quantum efficiency (~0.3) as has been achieved in the middle infrared. This corresponds to a few hundred kelvins of noise temperatures.

4.1.14 Synthetic-Aperture Radar Systems and Techniques (K. Krishen, Johnson Space Center)

The design of the synthetic aperture radar (SAR) evolved primarily from the requirements established by military users. Major steps in SAR system development can be summarized as follows:

1951 - Carl Wiley of Goodyear postulates Doppler beam-sharpening concept

1952 - University of Illinois demonstrates beam-sharpening concept

1953 - Project Wolverine (DoD) formulates SAR radar development program

1957 - Project Michigan produces first SAR imagery using optical correlator

Mid 1960s - Analog electronic SAR correlation demonstrated in non-real time

Late 1960s - Digital electronic SAR correlation demonstrated in non-real time

Early 1970s - Real-time digital SAR demonstrated with motion compensation

Most of the early work considered an unfocused synthetic antenna. Fine resolution was demonstrated using focusing techniques, in the late 1950s. In recent years, emphasis has been placed on moving-target detection and the higher resolution for the fixed-target capability within the military community. The potential for SAR in terrestrial and extraterrestrial observations has become evident in the past decade. This has placed unique demands on SAR designs beyond those addressed by the military user community. Some of these requirements become evident by glancing at Table 4.2, which gives the anticipated mission set for the 1980s within NASA. Specific SAR technology development areas for this mission includes: wide-swath, multifrequency, multipolarization, multi-incidence

TABLE 4.2 FUNCTIONAL REQUIREMENTS FOR SAR MISSION SET

MISSION SET	REQUIREMENTS						
	RE-SOLUTION (m)	SWATH WIDTH (km)	NO. OF LOOK	INCIDENT ANGLE (deg)	FRE-QUENCY (MHz)	POLAR-IZATION	AL-TITUDE (km)
Seasat	25	100	4	22.64	1275	S	800
SIR-A & Reflights, L	40	50	7	20-70	1275	S	210-280
X	40	50	7	20-70	9600	S	210-280
NASA Aircraft JPL-L	10-20	18-35	8	0-60	1275	S	3-12
JPL-X	10-20	18-35	8	0-60	9600	S	3-12
JSC-X	10	18	8	0-60	9600	D	13-20
JSC-C	15	7.4	8	10-30	5500	S	12-20
VOIR Hi-Res 52^{o}	50	13	8	52	1275	S	300
Lo-Res 52^{o}	300	50	24	52	1275	S	300
Hi-Res 25^{o}	50	12	6	25	1275	S	300
Lo-Res 25^{o}	300	40	24	25	1275	S	300
Ocean L-Band	25	200	4	25	1275	S	700
ICEX X-Band	150	360	6	36.42	9600	S	700
ERSAR L	10	50	4	75	1275	D	700
X	10	50	4	75	9600	D	700

S = Single; D = Dual

angle, and precise/accurate reflectance data. There are other technology areas for which user requirements are not defined at the present time. These include: pixel elevation mapping, pixel phase mapping, and circular polarization SAR design. These areas will not be addressed at the present time since no requirements have been identified. After a study of the anticipated NASA SAR requirements, OAST has initiated a program for the development of advanced SAR technology aimed at wide-swath, multifrequency, multipolarization, multi-incidence angle, and precise/accurate amplitude calibration.

SAR Swath Width (Fig. 4.40). Wide-swath should be considered from two points of view. In one case, the angle of incidence might be left variable. This is presently the case with the aircraft SAR systems. The pulse repetition rate presents the limit in terms of ambiguity in this case, and the variation of scattering with incidence angle causes calibration problems for applications where constant angle of incidence is required. In the second case, wide swath is to be generated with nearly constant incidence angle. This can be achieved by using multibeam or a scan SAR in the squint mode. Long antennas with specifically shaped elevation beams are needed for wide-swath SARs without the constant-angle-of-incidence requirement. Antenna design for Seasat was successful in achieving a 100-km swath at 20° incidence angle. The Shuttle Imaging Radar A (SIR-A) system design expects a swath of 50 km at 50° incidence angle. The wide-swath SAR development aimed at 200 km from space is currently funded by OAST under Advanced SAR RTOP.

Multifrequency (Fig. 4.41). For multifrequency operation, reliable, space-qualified power sources are needed. Solid-state sources provide better stability and long-operation possibilities. In addition, multifrequency SAR requires calibrated modulators and antennas which will enable establishing accurate image intensity levels for various frequencies. Efficient design approaches for multifrequency SARs call for modular construction, and multimode operation. No such systems are known to exist at this time. The Seasat and SIR-A SARs both operate at L-band. Design approaches are also available for X-band spacecraft SARs. With

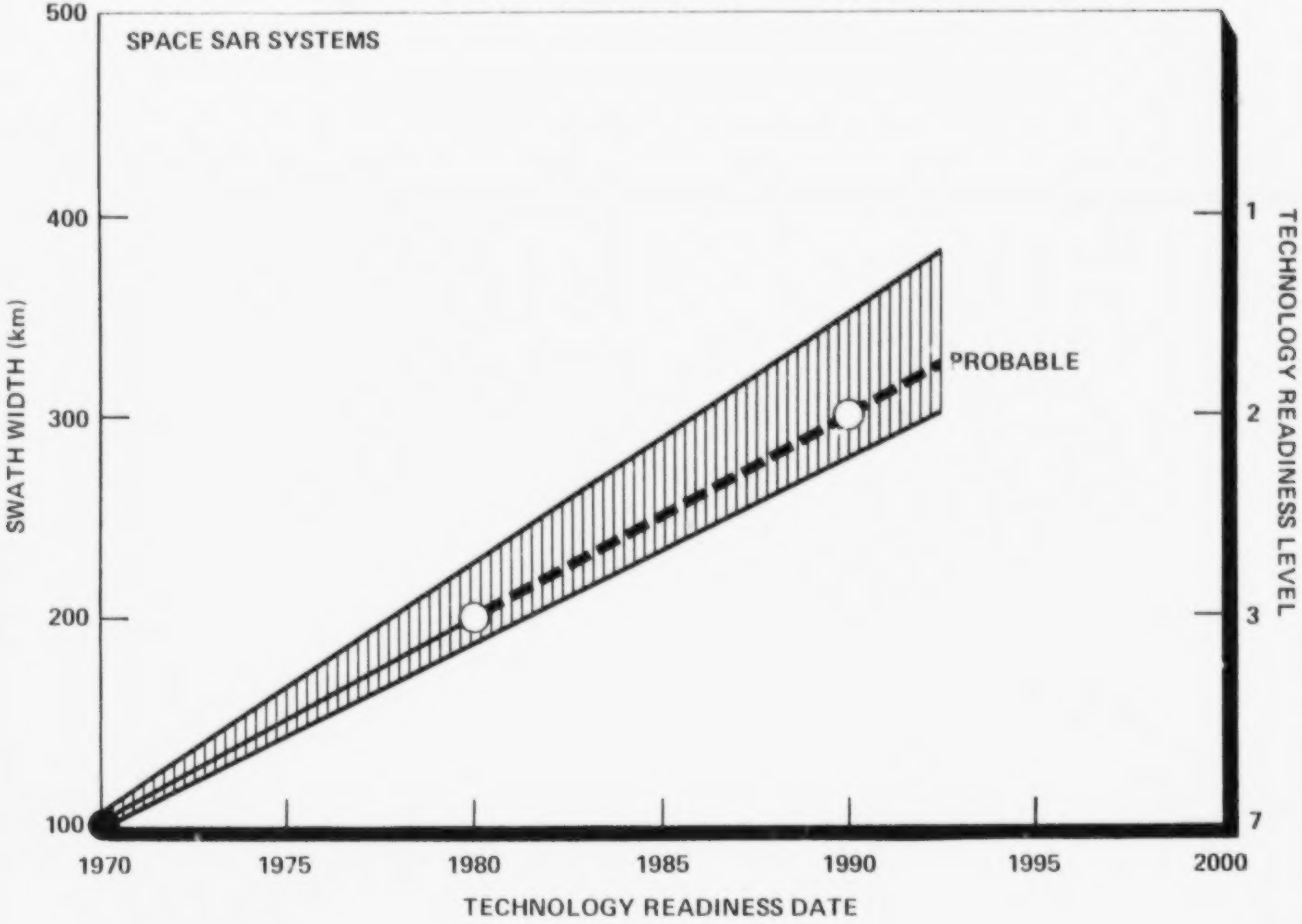

Figure 4.40. Wide Swath Radar Technology

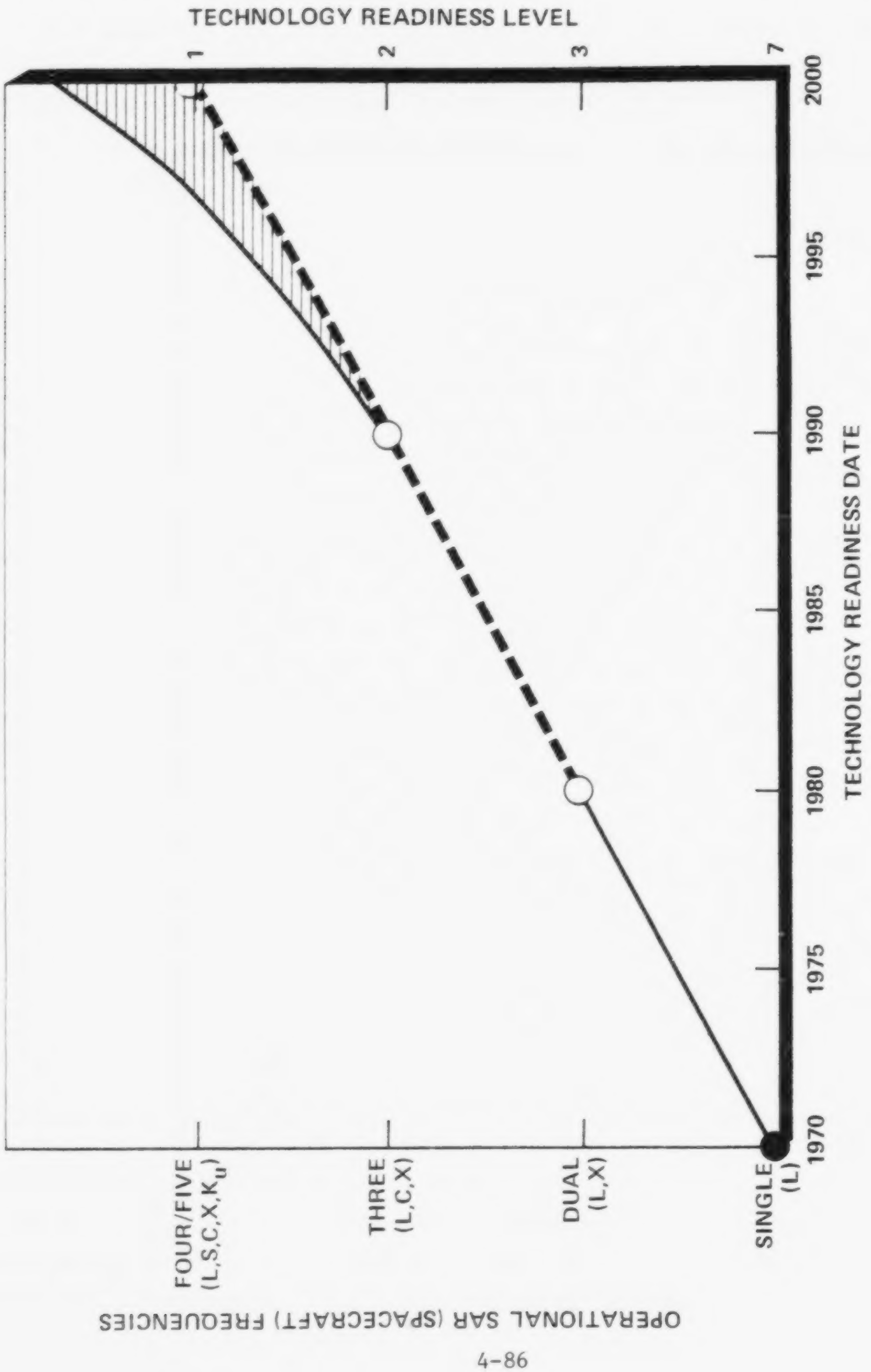

Figure 4.41. Multi-Frequency SAR Operation

the development of the OAST Advanced SAR (ASAR), technology will be available for multifrequency spacecraft SARs. Technology trends in Fig. 4.41 are presented on the basis of the OAST and OSTA (Shuttle Imaging Radar) programs and studies.

Multipolarization and Multi-Incidence Angle. To date, no multipolarization, multi-incidence angle SAR systems have been developed for the spacecraft. The L-band system on Seasat and the one scheduled to fly on the Shuttle operate at one polarization combination (HH). However, the angle of incidence for SIR-A is 50°, whereas Seasat operated at an angle of incidence of 20°. The technology required for multipolarization and multi-incidence angle is available at L- and X-band and has been partially demonstrated on the aircraft. Such technology can be incorporated in spacecraft systems at added cost and complexity. The demonstration of this technology will be undertaken under the OAST ASAR program. A system capable of acquiring data at HH, HV, and VV polarization combinations at two angles of incidence will be developed. The verification of this multimode operation will allow similar design for the spacecraft systems.

Signal Amplitude Precision Accuracy (Fig. 4.42). Quantitative measurements of ground scatter requires knowledge of the absolute calibration of the radar system, including the antenna. The returned signal should be corrected for all system variations and any uncertainty in the antenna gain. Techniques for calibrating SAR system (minus antenna) variations are based on sending samples of the transmitted signal at various power levels through the receiver and the signal processors. This technique has been used for aircraft SARs, but is yet to be adopted for the spacecraft SARs. Antenna gain uncertainties have been accounted for by external calibration using spheres, corner reflectors, and other deterministic reflectors. Calibration of this type has not been demonstrated from spacecraft altitudes. Figure 4.42 is presented on the basis of the aircraft and Seasat SAR experience.

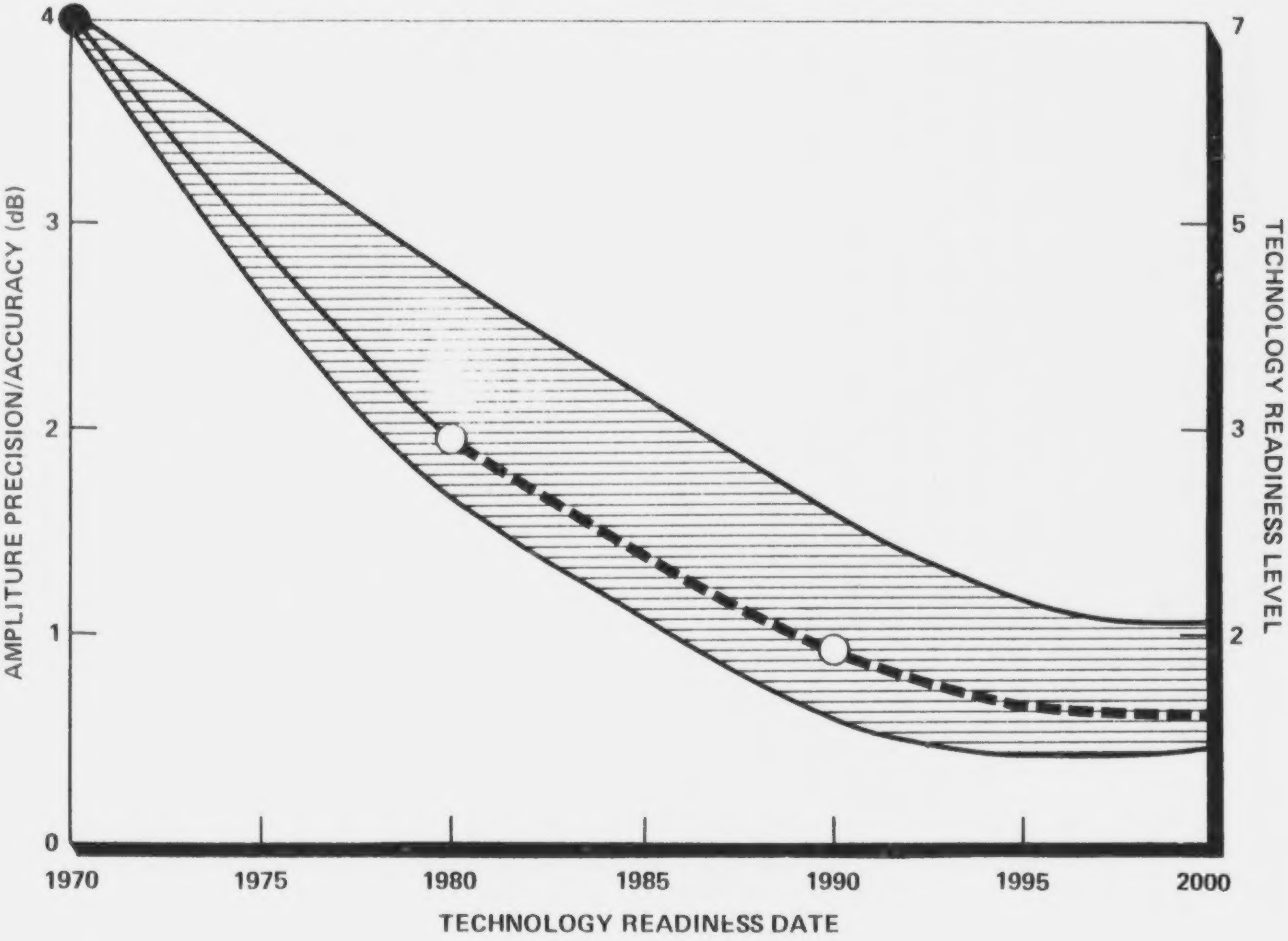

Figure 4.42. SAR Amplitude Precision/Accuracy

4.2 DATA PROCESSING

4.2.1 On-Board Processing (D. Lord, Jet Propulsion Laboratory)

Data are presented to show past, present, and future (expected) on-board processsing capability. Only NASA missions are considered in evaluating past capabilities. Past military missions are not included due to the lack of familiarity with them and the fact that the intent herein is to address the NASA community. Some military and commercially available processors are considered in evaluating current and future capability, but because of the dynamic nature of processor development, the list may not be complete.

The information presented is not intended to be a complete overview of all past, present, and future activities, but rather to present general "trends" and "forecasts."

Processor performance is characterized in three ways:

- Operations (instructions) per second
- Operations (instructions) per second per kilogram
- Operations (instructions) per second per watt

A number of other parameters must be considered when selecting a processor for space application, including:

- Reliability
- Power
- Weight
- Volume
- Cost

These are not thoroughly evaluated in the information presented. Any of the processors shown for either past, present, or future use are considered to be acceptable in these areas.

On-board processing capability is being developed. In the past, most of the emphasis came from within NASA itself. There were no commercially developed processors available that met the reliability, power, weight, and volume requirements of NASA missions, so they were developed separately through NASA-funded projects (a similar approach was taken by the military and DoD to satisfy their requirements). Commercially developed processors were flown in the past in noncritical areas such as science experiments or on low-cost missions. Major space missions went to custom-designed processors for missions critical for high-reliability applications.

With the advent of microprocessors and large scale integration (LSI) technology, the trend within NASA has been to depend more on commercially developed processors for use in space, and less on NASA-sponsored processor development efforts. The trend toward more dependence on commercial development efforts has both good and bad features. In the "good" category are:

- High initial development costs are borne by commercial companies.
- Individual piece parts are less costly to NASA since they are produced in high volume for commercial applications.

In the "bad" category are:

- Difficult to influence the design.
- Difficult to get parts flight qualified.
- Difficult to impose or determine reliability characteristics.

The trend within NASA to do less custom processor development and depend more on commercial development efforts appears justified, given the current fiscal and technology environment.

From a technology standpoint, LSI and microprocessor manufacturing techniques offer the potential for vastly improved on-board processor capabilities. From a cost standpoint the effort can only be justified if a high-volume market exists for the product, such as is the case in a commercial venture. Taking advantage of commercial processor development efforts appears to provide the best near-term solution to the NASA desire for sophisticated on-board processing capabilities.

It should be noted that commercial companies are becoming more receptive to including NASA and DoD desires in some of their commercial development efforts. The trend in industry to more actively solicit NASA and DoD as potential customers of commercially developed processors is expected to make them better suited for space applications.

Processors are not the only components necessary for an on-board computer system. Development of peripheral circuits, memories, etc., are companion efforts that are necessary before a processor is of any use. Commercial development of these required components is being done, but does not always result in an optimum match between commercial and space requirements. NASA (OAST) support in processor-related areas is geared toward developing capabilities required to make maximum use of the commercially developed processors. OAST supported activities include:

- Customer LSI manufacturing and testing capability
- Highly reliable LSI manufacturing and testing capability
- Radiation hardening of LSI devices
- Microprocessor application studies and designs
- System implication of using LSI circuitry

It should be noted that the emergence of a highly reliable radiation-hard testable LSI manufacturing capability is essential for the development of optimum peripheral circuits. Optimum LSI peripheral circuits are required to take maximum advantage of new processors and new computer system architectures.

Once a reliable custom LSI manufacturing capability exists, it is not inconceivable to envision the development of custom microprocessors as well as custom peripheral circuits. The goal of all custom LSI circuits would be to make them more ideally suited to a particular set of requirements and to make them more easily and thoroughly testable.

Performance of Spaceborne Computers (Fig. 4.43), per Kilogram (Fig. 4.44), and per Watt (Fig. 4.45). Performance can be measured in a number of ways. One method involves comparing operations per second, but even that is not too accurate unless the complexity of instructions and certain architecture features are considered. The curves in the figures are determined from the formula

$$\text{Performance} = \frac{1}{0.7t_a + 0.3t_m + 2k_m t_{mc}}$$

where t_a = add execution time

t_m = multiply execution time

t_{mc} = memory cycle time

k_m = degree of look-ahead by the control unit

k_m = 1 indicates no look-ahead

k_m = 0 indicates total transparent memory

The figures, as well as some of the stated conclusions, are taken from A Forecast of Space Technology 1980-2000, NASA SP-387. The three figures assume that some form of distributed computer system architectures will be employed in the future. It becomes more difficult to increase single computer speed as theoretical technological limits are approached. Effective speed is increased by using a number of dedicated processors to provide parallel computational capability.

The massively parallel processor (MPP) NEEDS activity is a form of distributed computer system architecture where each processor element has a dedicated function, and many functions are performed in parallel.

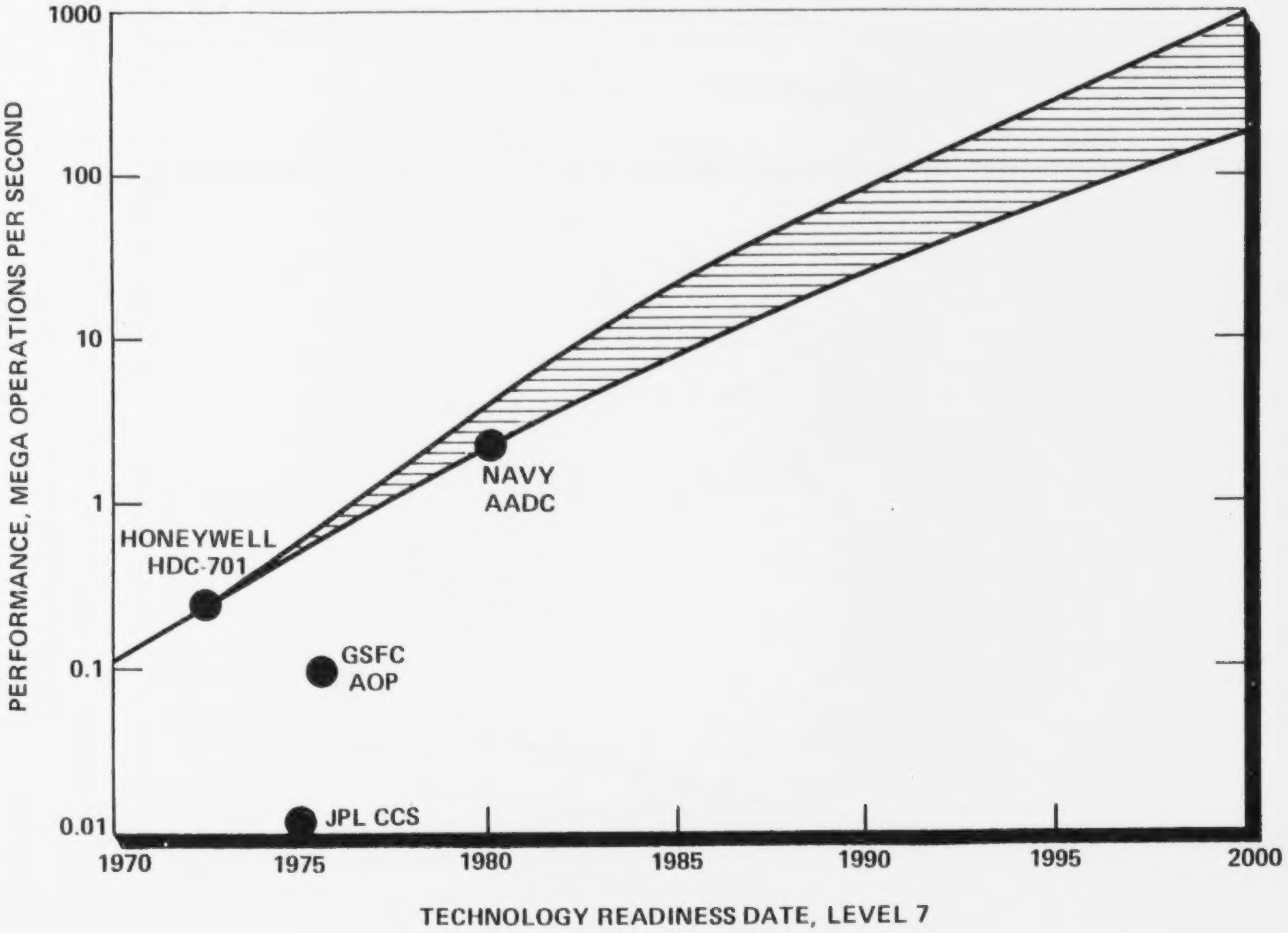

Figure 4.43. Performance of Spaceborne Computers

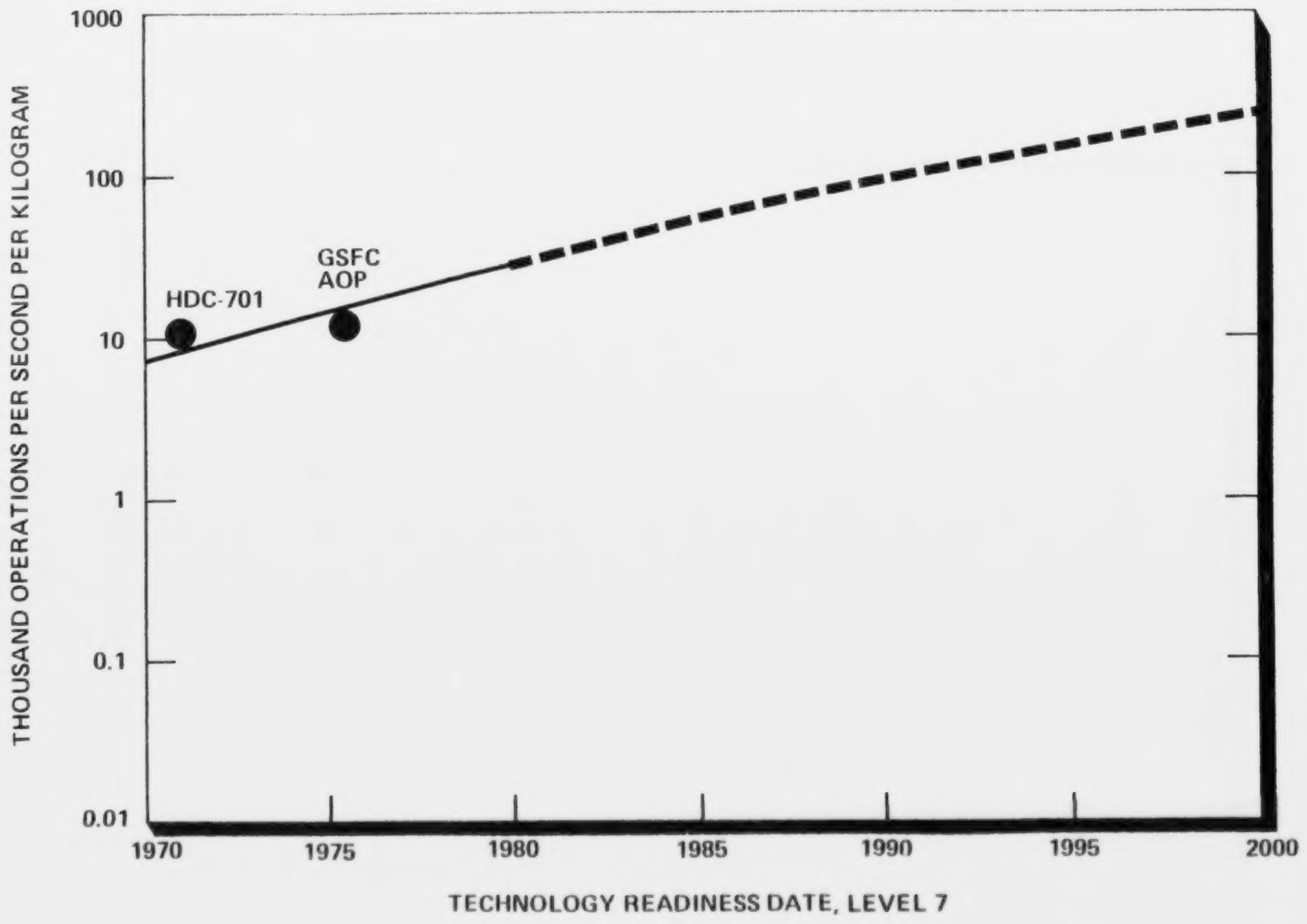

Figure 4.44. Performance of Spaceborne Computers per Kilogram

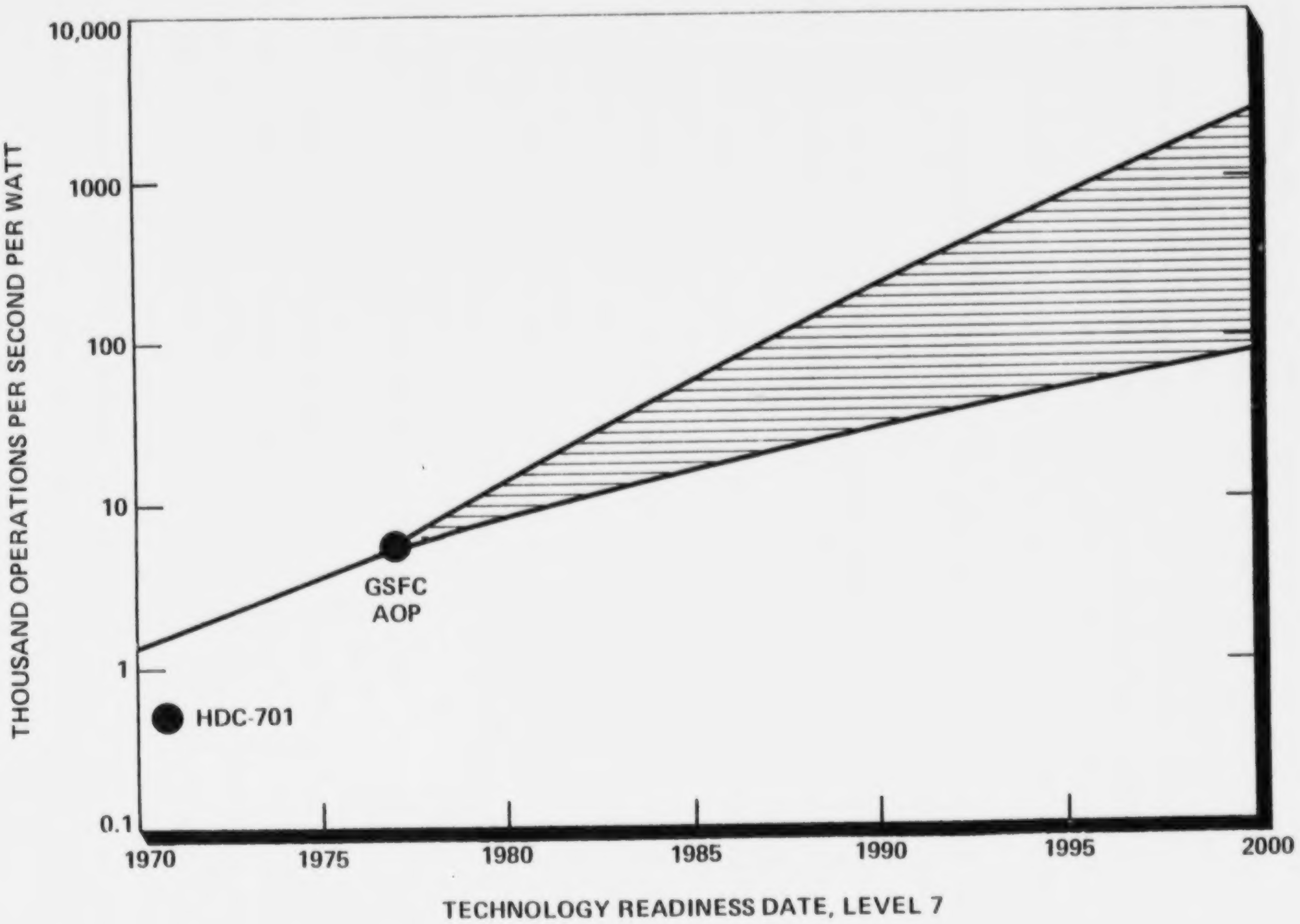

Figure 4.45. Performance of Spaceborne Computers per Watt

The Distributed Data System (DDS) NEEDS activity is another form of distributed computer system architecture where the system interconnects are via a common serial data bus.

Both the MPP and DDS, as well as most on-board computer systems of the future, obtain their performance increases through the use of creative system architectures, and not so much from the characteristics of a particular processor.

Figures 4.44 and 4.45 forecasts are based on an extrapolation of the following data:

	Performance (operations × 1000)	Weight (kg)	Power (W)
Saturn 1 (IBM ASC-15B)	1	34	150
AGC Block 11	30	26	100
HDC-701	200	23	270
GSFC AOP	80	6	14

The following technology readiness status of ongoing tasks (and projections of the future) are presented.

Effort	Technology Readiness Status Level						
	1	2	3	4	5	6	7
MPP				1979	1980	1982	1985
DDS				1977	1978	1981	1985
Radiation Hard Manufacturing Technique					1979	1980	1985
Custom LSI Manufacturing Technique			1979	1980	1980	1981	1985

4.2.2 On-Board Mass Storage

R. Zenore, Jet Propulsion Laboratory

The data presented herein deals primarily with magnetic tape systems and relates past, present, and future on-board mass storage capabilities. Data is not intended to provide a complete overview of on-board mass storage, but rather to furnish general trends and forecasts.

Parameters selected to characterize on-board mass storage are:

- Total storage capacity (Fig. 4.46)
- Data transfer rate per track (Fig. 4.47)

There are a number of other parameters that must be considered when selecting a mass storage tape system for space application. These include: reliability, power, weight, volume, speed range, bit error rate, and cost considerations, which were not thoroughly evaluated in the information presented. Each of or any combination of these parameters can influence the parameters selected for characterization. On-board mass storage magnetic tape systems shown for past, present, and future use are considered to be acceptable in these areas.

Present technology for on-board mass storage using magnetic tape is capable of storing up to 160 kbits/in.^{2} and transfer rates up to 2.0 Mbits/s/track.

Development of on-board mass storage tape systems have been sponsored by NASA and industry in the past; however, recent trend in development has been left largely to commercial industry. Although mass storage technology is being pursued by many commercial firms, only a few are actively involved in mass tape storage for space applications. Technology acquired for ground-based systems are not always applicable for space applications, due to environments and unattended life.

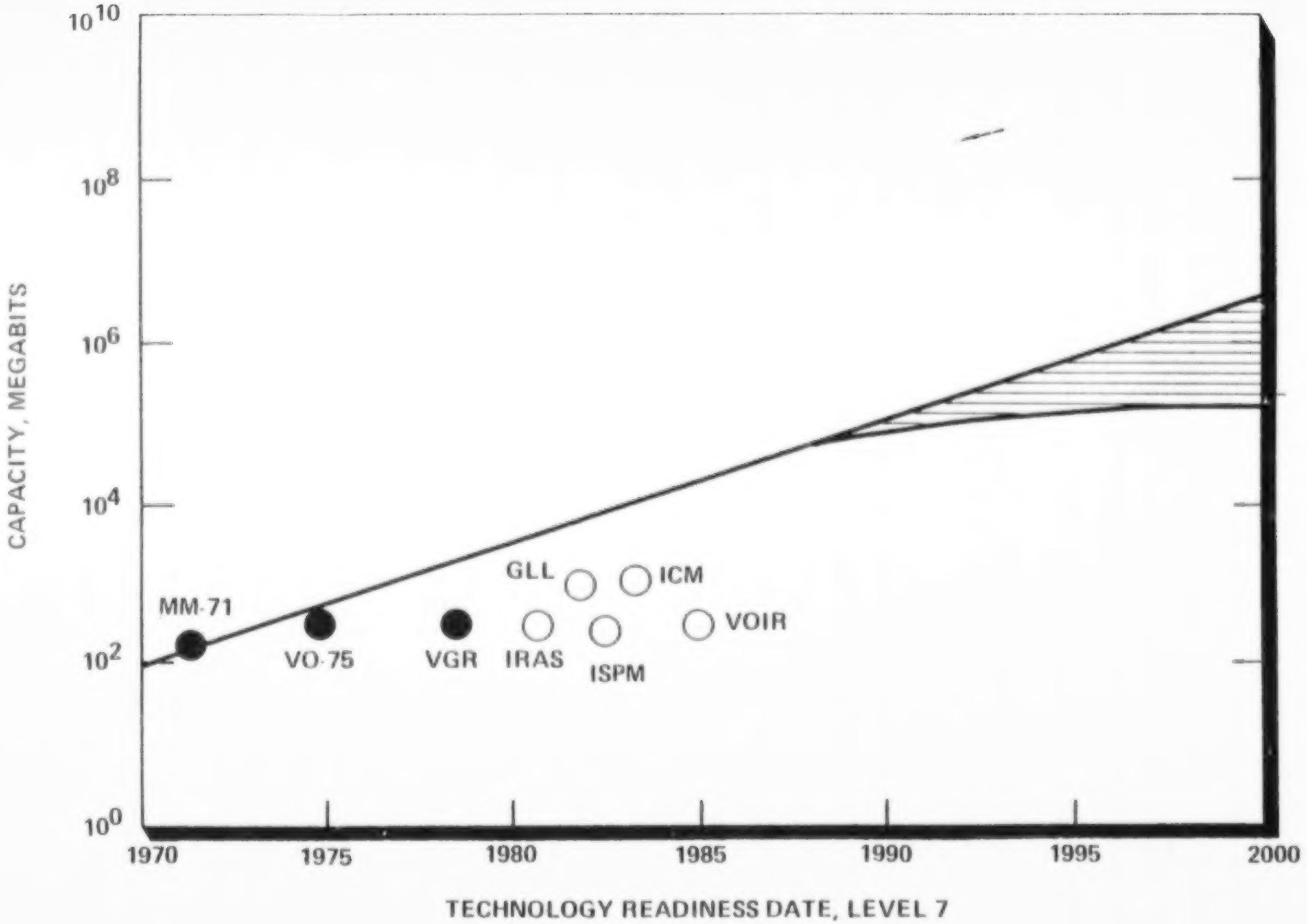

Figure 4.46. Capacity of Spaceborne Mass Storage Systems

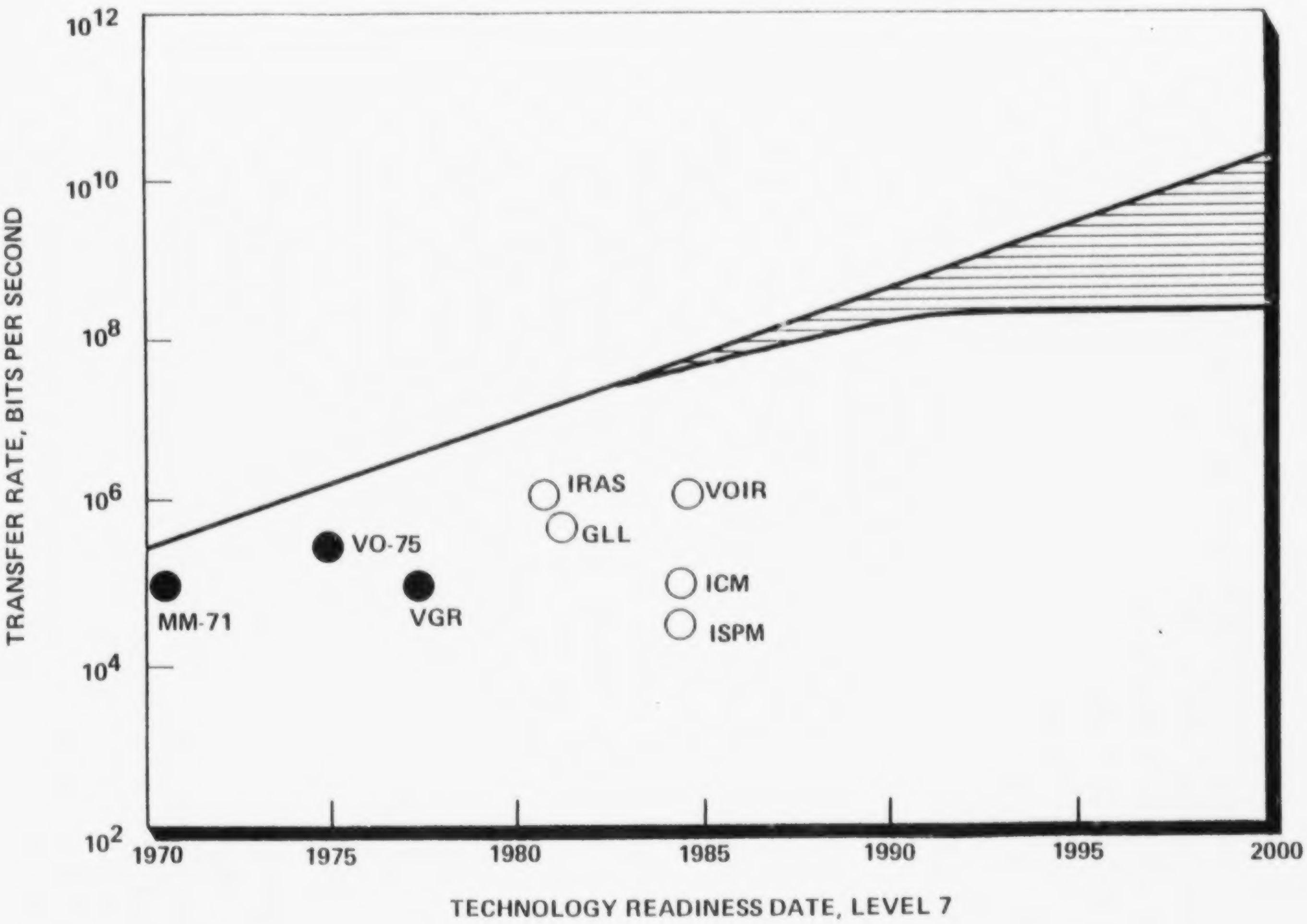

Figure 4.47. Transfer Rate of Spaceborne Mass Storage Systems

Up to the present, magnetic tape systems have been used exclusively for spaceborne mass storage and will probably continue to be used for data storage requirements of 10^9 to 10^{11} bits in the 1980s, but substantial improvements in lifetime and reliability will be necessary for the longer duration missions. Solid-state memories, using magnetic-bubble, CCD, or MNOS technologies, will be available for buffer applications by 1980 but are not expected to compete with magnetic tape systems until about 1990. The bubble memory technology is considered to be the most promising because it offers the advantages of higher bit density, lower power consumption, nonvolatility, nondestructive readout, and radiation resistance.

The continued demand to increase mass storage capacity for on-board processing requirements could result in the same growth rate in capacity as experienced in the past, paralleling the growth rate of earth-based mass storage systems. Magnetic bubble memories are currently emerging as a serious contender for low-capacity tape recorders. Competing technology, such as CCD and MNOS memories, have been clearly overtaken because the bubble technology offers high-bit density, nonvolatility, radiation resistance, and moderate power consumption. While cost is still high, there is potential for dramatic cost reduction during the next decade. In contrast to tape recorders cost per bit will determine the practical storage capacity of bubble memory systems and the course of the competitive battle between bubbles and tape recorders. By 1986 bubble memories with storage capacities up to 5×10^7 bits could be flown in space. 10^8-bit memories should be in space by 1988 and 10^9-bit memory systems by 1990.

Data transfer rates of bubble memories depend on the availabe power. Initial bubble memories will operate at rates below 10^6 bits/s. In time, low-power memories will be developed and the upper limit for data rates can be expected to be around 4×10^6 bits/s by 1990.

4.2.3 Ground Data Processing Technology (J. Sos, E. Connell, and F. McCaleb, Goddard Space Flight Center)

Ground data processing technology is primarily limited by current system architectures rather than basic component operating speeds. The greatest increase in throughput rates and decrease in processing costs for image data will be achieved with special-purpose computer architectures such as the massively parallel processor (MPP) (being developed for NASA by Goodyear) and special-purpose SAR processing machines. These special-purpose processors will allow throughput to be increased from the current rates by at least 2 orders of magnitude and possibly 6 or more orders of magnitude by 1990. The primary constraints limiting throughput in these machines will be input/output functions rather than processing algorithm execution time. Development of VLSI chip technology will allow processing machines such as the MPP to be built within reasonable cost, size, and power consumption constraints.

Memory technology, particularly nonerasable laser memory technologies such as the Phillips and RCA optical disc systems, will be sufficiently developed to allow on-line archival data storage of at least 10^{14} bits and off-line storage (in the same room) of at least another 10^{15} bits. On-line access times for image size (10^7-10^9 bits) files will range from a few milliseconds to a few seconds. Off-line data will be accessible in less than 5 min. Storage densities will be greater than 500 Mbits/in^2. Data transfer rates into and out of such an archival memory system will be in the 50 to 300 Mbit/s range. Writing rates of 100 Mbits/s or higher on an optical disc systems using ablative media will require development of multichannel write heads using laser diodes as light sources.

The successful application of large archival mass memories will require significant advances in data base management systems. Relational and network data base management system designs appear to hold great promise for linear and polygonal data representation, while hierarchical designs appear best suited for point specific and attribute data. Future data base management systems for large data bases encompassing a variety of data types will probably be a hybrid of relational and hierarchical systems.

An increasingly attractive alternative for the data base management system is the data base machine--a highly parallel, pipelined computer. In such a machine, the basic data management functions (insert, delete, retrieve) are built into the hardware, providing functional speed and reducing software complexity.

The higher data rate sensors flown in the late 1980s will generate a requirement for very high speed data buffering at the front end of ground data processing systems. It appears that in the 1990 time frame this need will still primarily be met with magnetic tape recording technology. Technology, such as that used in the Ampex Super HBR, has the potential to operate at recording rates up to 2 Gbits/s.

Processor Performance (Fig. 4.48). Processor performance is depicted in terms of millions of operations per second (MOPS). The solid line shows the trend for general-purpose computers. Special-purpose hardware tends to run about an order of magnitude higher than general-purpose hardware (dashed line). Thus, by 1990, special-purpose processors should be capable of at least 10^4 MOPS. If array sizes on the order of 1000 × 1000 become practical, then MPP-type computing devices will be capable of as much as 10^6 MOPS.

Ground Processing Costs (Fig. 4.49). Ground processing cost per bit is declining rapidly. Current cost for processing image data is about 5×10^{-6} cent/bit. For MPP-type devices in the 1990 time frame, processing costs for image data should be about 10^{-8} cent/bit. Costs for processing nonimage data are two or more orders of magnitude less than for image data.

Processor Throughput (Fig. 4.50). Processor throughput will rise from the current 2×10^6 bits/s (MDP) to 10^{10}-10^{12} bits/s for an MPP-type device in the 1990 time frame.

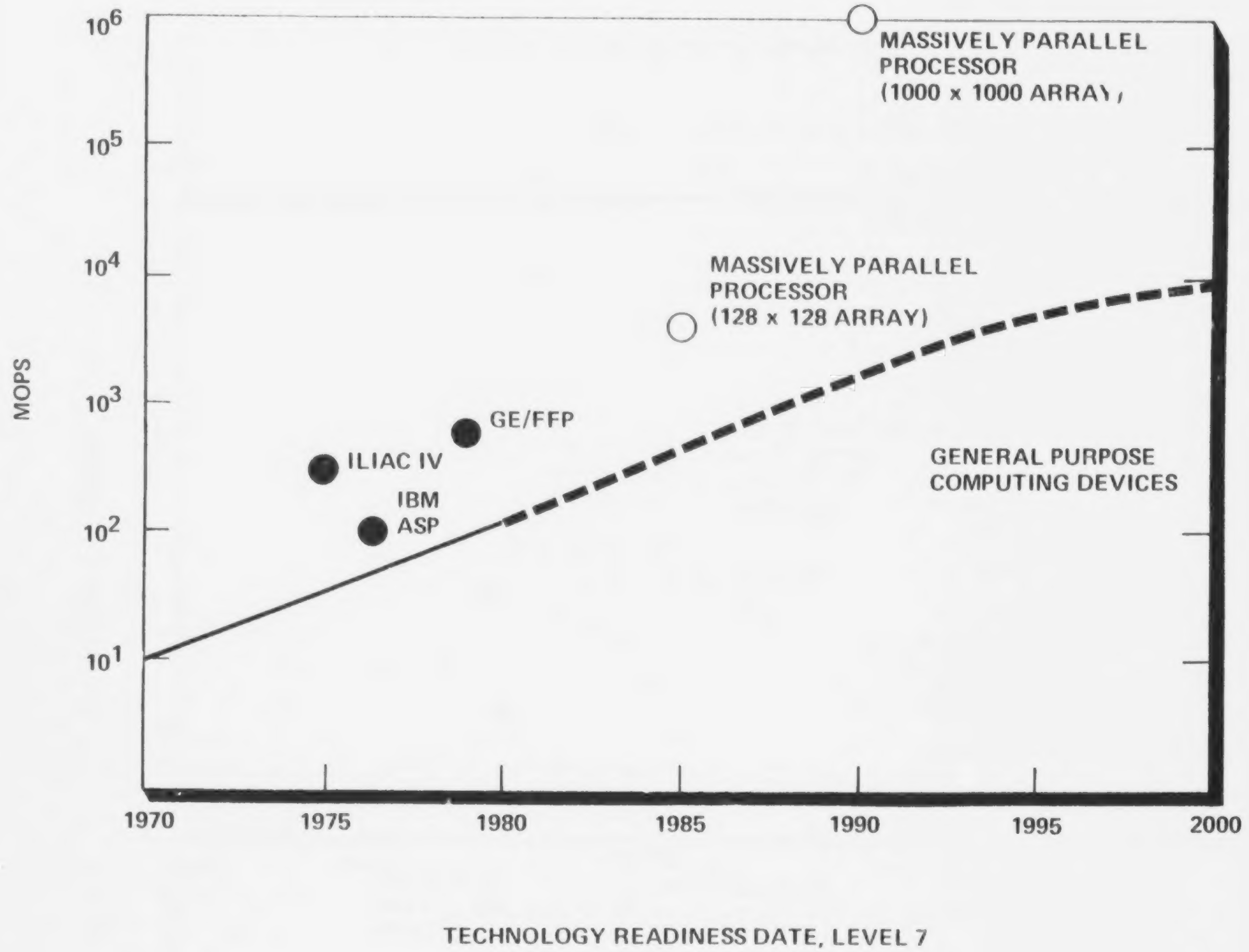

Figure 4.48. Processor Performance

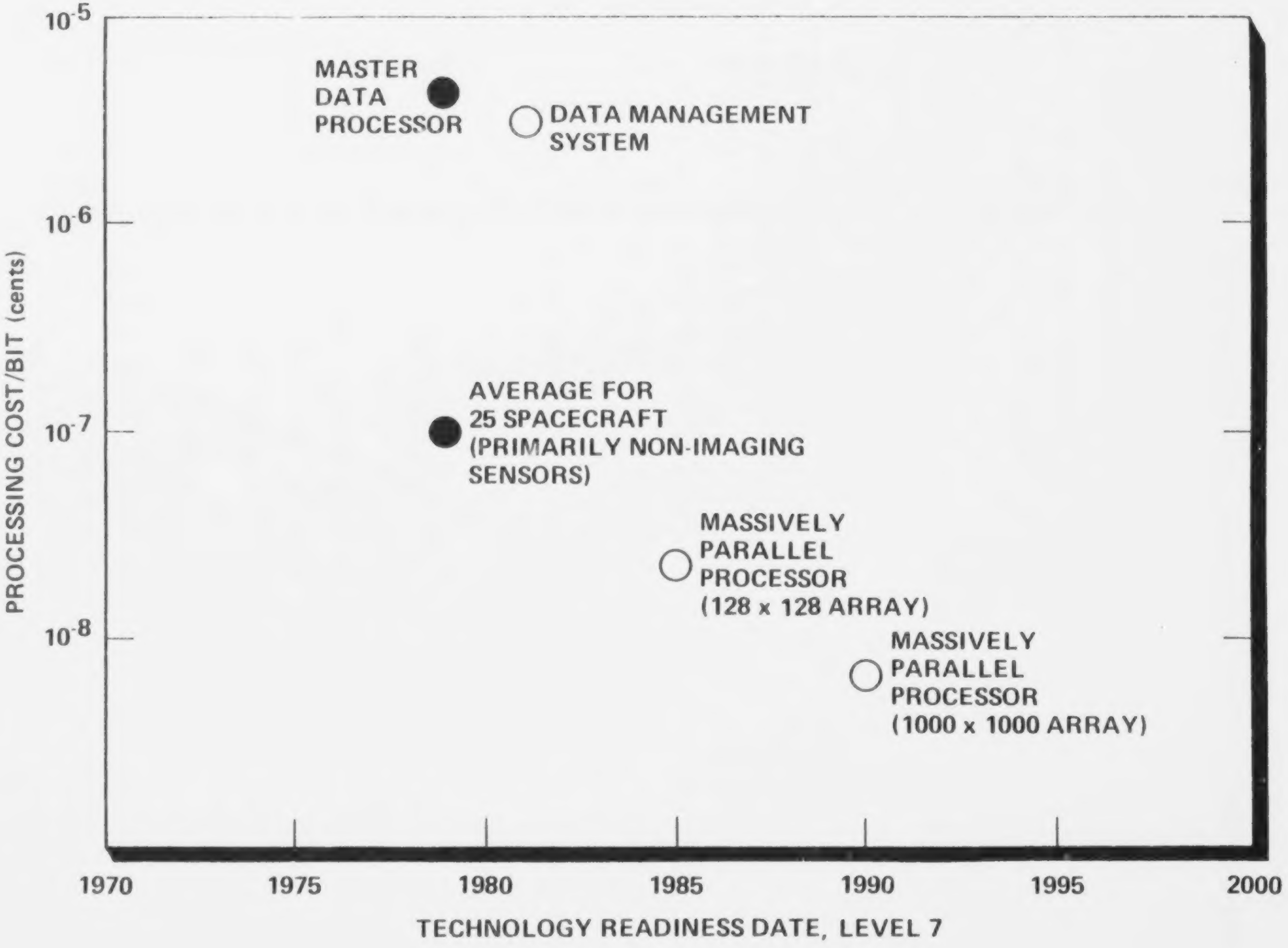

Figure 4.49. Ground Processing Costs

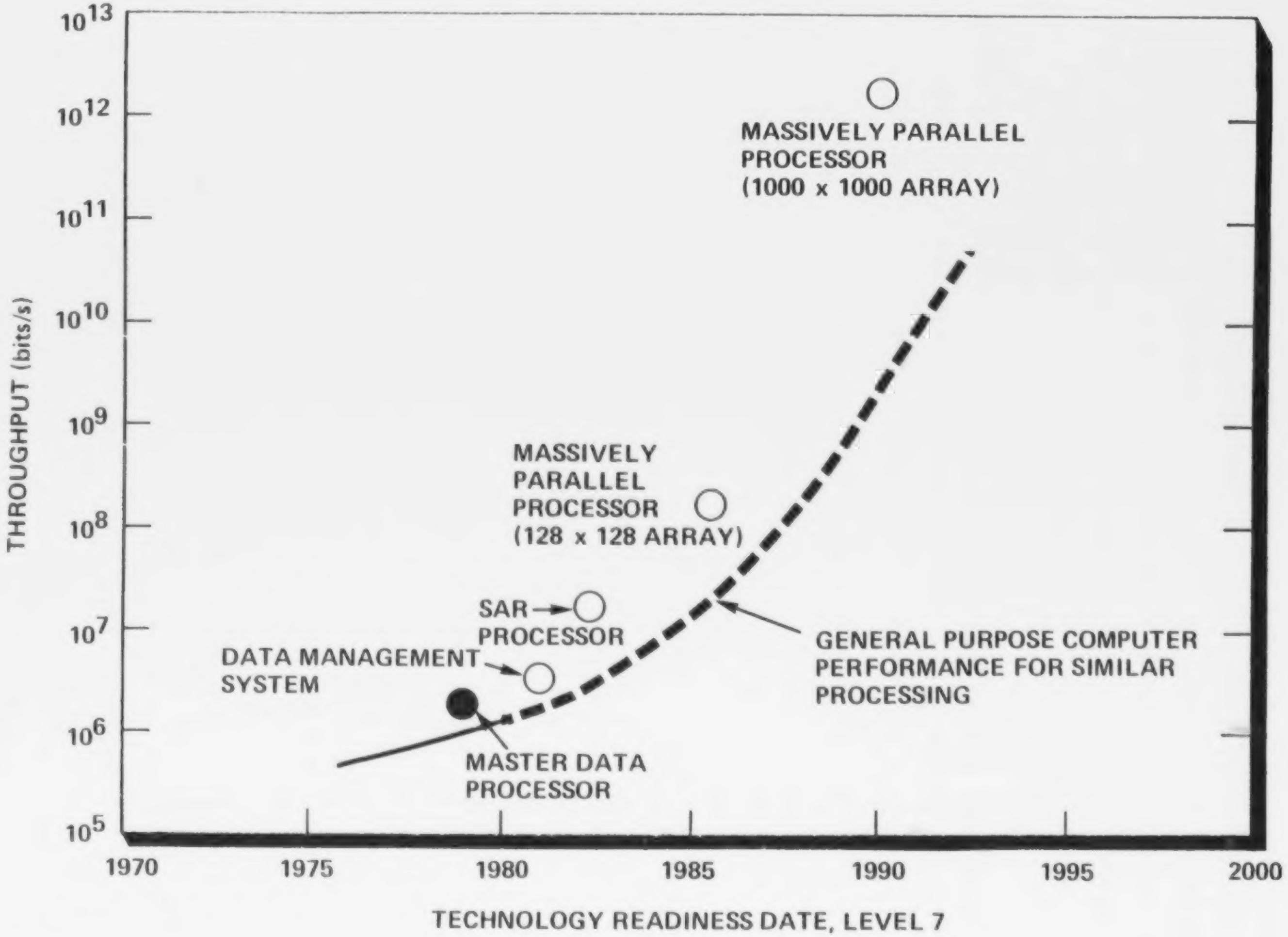

Figure 4.50. Processor Throughput

On-Line Auxiliary Storage Capacity (Fig. 4.51). On-line auxiliary storage capacity depends on access time requirements. On-line optical memories (nonerasable) will be available by 1990 with capacities on the order of 10^{14} to 10^{15} bits; however, access times will range from a few milliseconds to a few seconds. Magnetic-bubble and CCD memories about 10^{9} bits in size with microsecond access times will be available in the early 1990s. Read/write laser memories with submillisecond access time and 10^{12}-bit capacity will not be available before the mid-1990s.

High-Speed Data Buffering (Fig. 4.52). High-speed data buffering will still primarily be accomplished using magnetic tape recording devices. Input data rates will rise from the current maximum rate of 1 or 2×10^{8} bits/s to about 2×10^{9} bits/s.

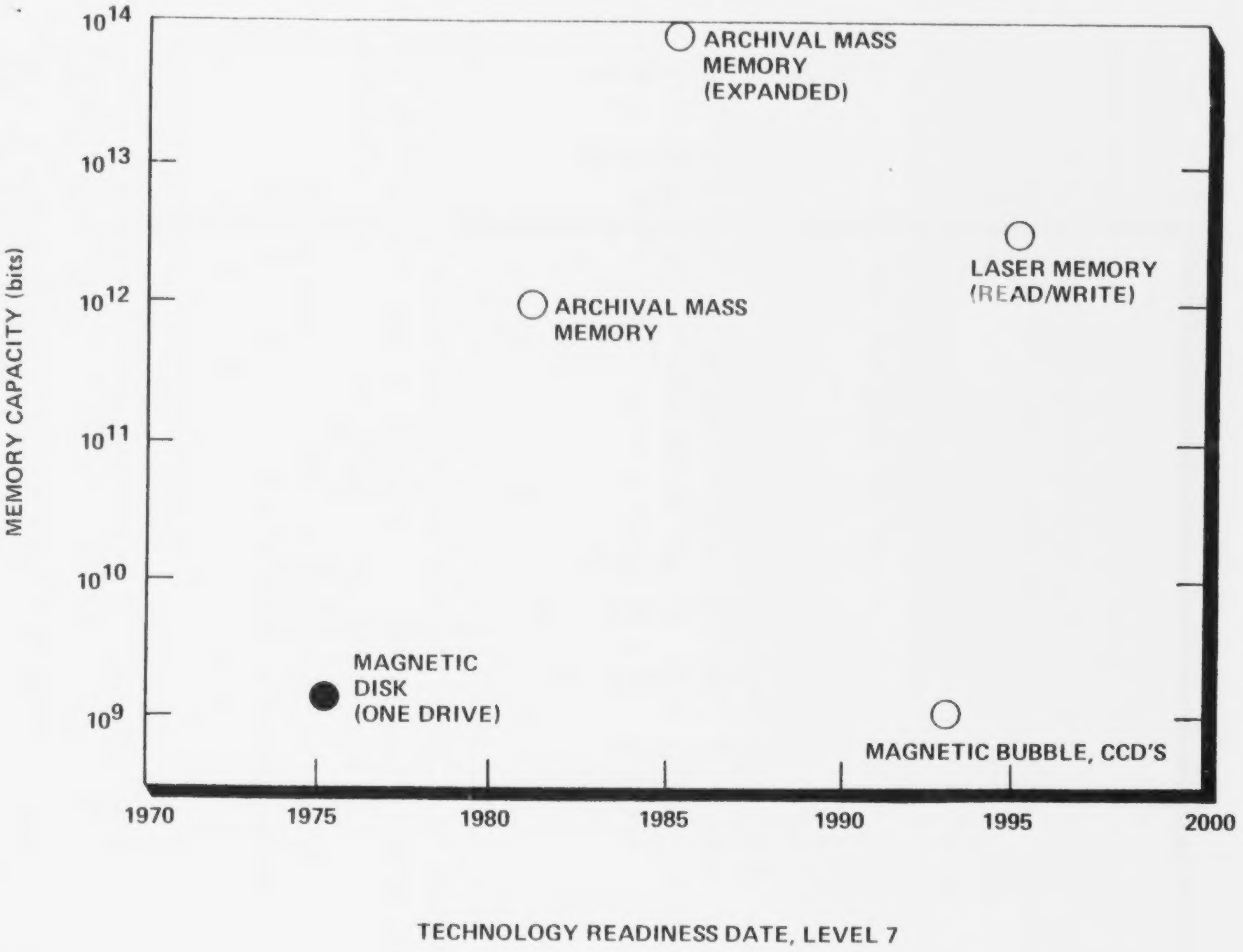

Figure 4.51. On-Line Auxiliary Storage Capacity

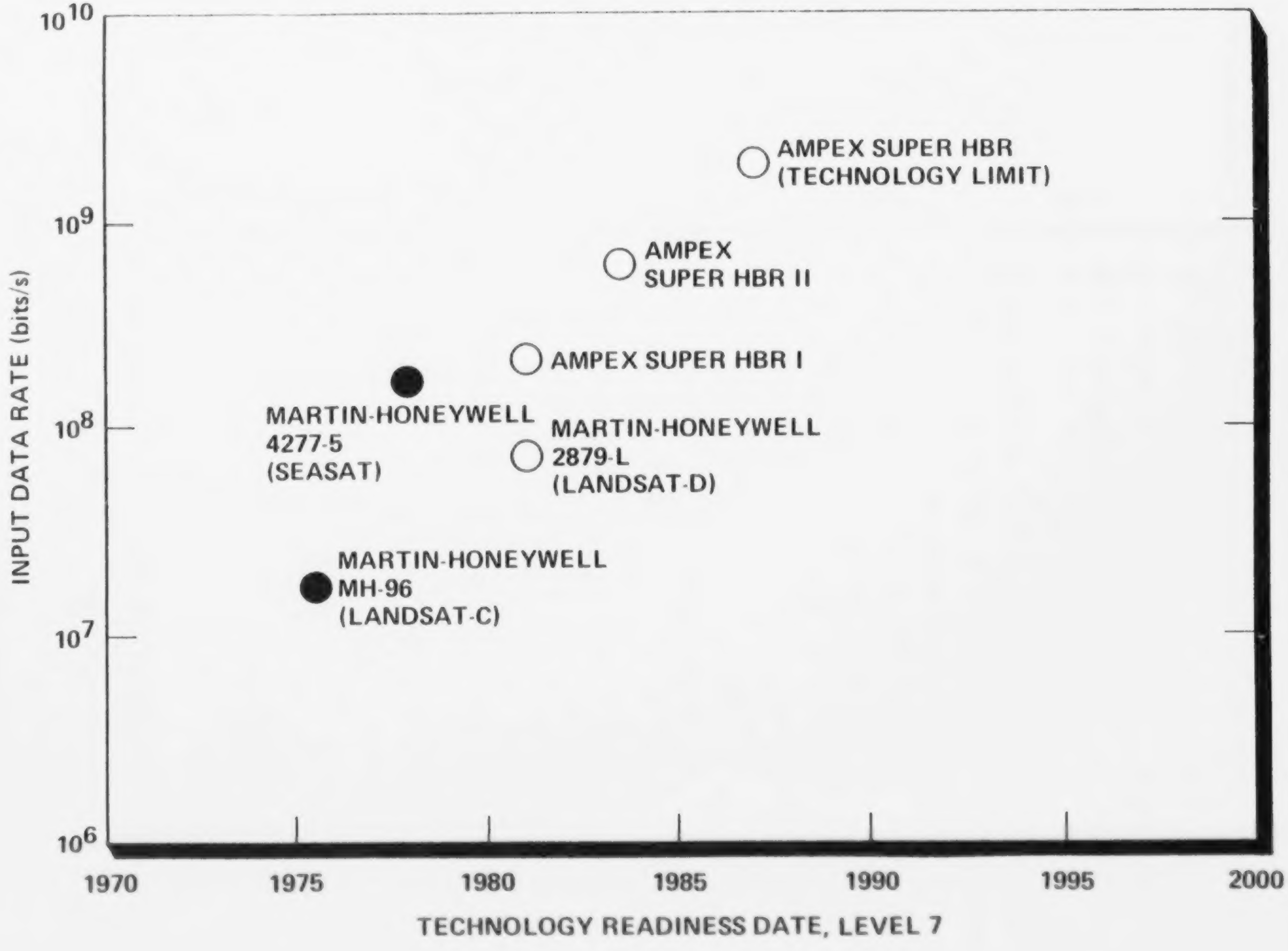

Figure 4.52. High-Speed Data Buffering

4.3 COMMUNICATIONS

R. E. Alexovich, Lewis Research Center

The demand for communications services is at a relatively high growth rate, which is expected to continue. The service demand through the year 2000 was investigated in market studies conducted by ITT and Western Union.[1,2] Projected annual growth rates, during this period, for data, video, and voice services were 17%, 11%, and 10%, respectively. Of this total demand, there is an appreciable fraction which is addressable by satellite communications (Fig. 4.53). These market studies concluded that satellite communications capture of the addressable market would exceed projected C-band (3.7-4.2 GHz downlink; 5.9-6.4 GHz uplink) and K_u-band (11.7-12.2 GHz downlink; 14.0-14.5 GHz uplink) capacity by 1990.

Allocated frequency bands for space communications services, established by international treaty, are given in Table 4.3. In order to provide additional space communications capacity, it will be necessary to develop the use of higher frequency bands about K_u-band. Extension of current communications technology developed for C- and K_u-band fixed services, to K_a-band (17.7-20.2 GHz downlink; 27.5-30.0 GHz uplink), will provide the capacity shown in Fig. 4.53. As can be seen from Fig. 4.53, the development of K_a-band for fixed services, in itself, will be inadequate to meet service demand in the 1990-2000 time period. Therefore, the following technology options exist, in addition to those technologies necessary to implement K_a-band fixed service communications.

1. Development of multibeam antenna technology for 20/30 GHz fixed services. This requires concomitant advances in sidelobe reduction and beam isolation.

---

[1] 18/30 GHz Fixed Communications Systems Services Demand Assessment, U.S. Telephone & Telegraph Corp., Contract NAS 3-21366, 1979. Vol. 1: Executive Summary, CR-159619; Vol. 2: Final Report, CR-159620; Vol. 3: Appendices, CR-159621.

[2] 18/30 GHz Fixed Communications System Service Demand Assessment for 1980-2000, Western Union, Contract NAS 3-21359, 1979. Vol. 1: Executive Summary, CR-159546; Vol. 2: Final Report, CR-159547; Vol. 3: Appendices, CR-159548.

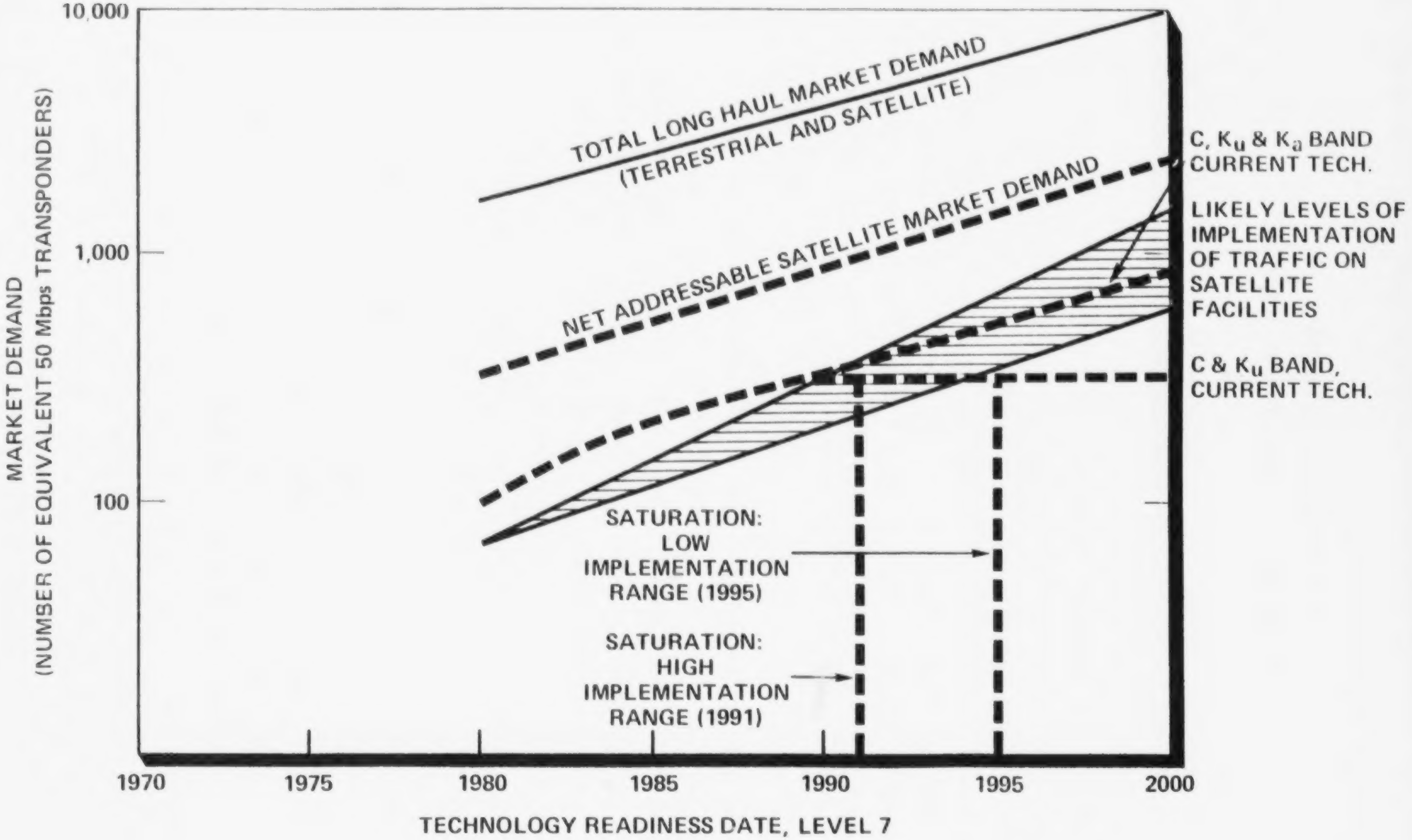

FIGURE 4.53. Protected Communications Market Demand and Satellite Capacity Versus Time

TABLE 4.3

SPACE COMMUNICATIONS ALLOCATED FREQUENCIES
(Principal Bands in Region 2, North and South America)

SERVICE		FREQUENCY (GHZ)	
		DOWNLINK	UPLINK
FIXED		3.7-4.2	5.925-6.425
		11.7-12.2	14.0-14.5
		17.7-20.2	27.5-30.0
		40.0-41.0	50.0-51.0
		102.0-105.0	92.0-95.0
BROADCAST		2.50-2.69	NONE ASSIGNED*
		11.7-12.2	
		41.0-43.0	
		84.0-86.0	
INTERSATELLITE		54.25-58.20	
		59.0-64.0	
		105.0-130.0	
		28000	
		560000	
SATELLITE MOBILE	MILITARY	0.24-0.40	
	AERONAUTICAL MARITIME	1.5350-1.5585	1.6365-1.6600
		43.0-48.0	
		66.0-71.0	
		95.0-101.0	

*WITH THE EXCEPTION OF THE SHARED 14.0-14.5 GHz

2. Development of time division multiple access (TDMA) with on-board matrix switch routing to achieve greater capacity utilization through dynamic allocation based on demand.
3. Development of switched and/or scanned beam antennas.
4. Increases in the bit/Hz utilization of allocated bandwidths from 1 bit/Hz to 3 bits/Hz. This will necessitate higher energy-per-bit/noise power density, and therefore higher output power transmitters and improvements in low-noise receivers.
5. Improvements in orbital arc utilization. Reduction in satellite spacing from 4.5° to 3° between satellites.
6. Development of intersatellite relay technology from 54 GHz to 64 GHz. This technology can be used to enhance frequency reuse. Spatial discrimination between two satellites can be used where adjacent beam isolation is inadequate.
7. Development of technology for 40/50 GHz frequency band.

Each of the above advances in technology will provide increases in satellite capacity for fixed services. This in turn, depending on circuit costs, will determine the fraction of the net addressable satellite market that can be captured by communications satellite service. Comparative costs in 1978 dollars are given in Table 4.4. The costs of C- and K_u-band services are based on utilizing the available orbital arc and current technology. The costs of K_a-band service are based on advances beyond current technology. These advances are part of the OSTA communications program. The technology advances include:

1. Multibeam antennas
2. On-board signal processing and matrix switching
3. Solid-state and TWT power transmitters
4. 30-GHz low-noise receivers

TABLE 4.4

VOICE CIRCUIT COSTS

Year	Terrestrial Path Length (miles)	Terrestrial ($/yr/circuit)	C-Band ($/yr/circuit)	K_u-Band ($/yr/circuit)	K_a-Band ($/yr/circuit)
1980	2000	14,600	5600	8200	--
	1000	10,600	5600	8200	--
	500	6,700	5600	8200	--
1990	2000	13,300	5000	7700	4300
	1000	9,600	5000	7700	4300
	500	6,100	5000	7700	4300
2000	2000	12,000	4600	7300	4300
	1000	8,700	4600	7300	4300
	500	5,500	4600	7300	4300

Technology advances which augment this program and those which address operational needs of the year 1995 and beyond are:

1. Intersatellite relay technology for 54 to 64 GHz bands.
2. Increases in solid-state and TWT power output and efficiencies at 20 and 40 GHz.
3. Large matrix switch technology.
4. Improvements in low-noise amplifiers for 20-60 GHz.

Specific trends and forecasts relevant to communications are presented, grouped under the categories of antennas, solid-state devices, and microwave amplifiers.

Advances in antenna technology are motivated by the need to maximize utilization of both the limited spectrum and limited geostationary arc resources. Technology developments can be categorized in terms of antenna type: reflectors, microwave lenses, phased-arrays, and multibeam systems. Each exhibits advantages which the technology attempts to exploit and disadvantages which the technology attempts to overcome. However, in all cases, operation at higher frequencies provides opportunity for increased frequency and geostationary arc utilization. Parameters which can serve to characterize antenna technology are frequency of operation, number of beams (multibeam antennas), and reflector size.

In the category of solid-state devices, gallium arsenide FETs give evidence of highly desirable potential characteristics in both low-noise and high-power applications. The parameters selected for characterization are the noise figure of LNAs and the single-chip power capability of power amplifier devices. The noise figure of individual devices is not too meaningful unless associated gain is also considered. Therefore the noise figure of a complete amplifier, rather than a single device, is chosen for characterization. Because power FETs can be used in the system in such a variety of ways, the single-chip power output is considered more meaningful than the power that can be achieved by power combining in external circuitry.

Advances in microwave amplifier technology for space communication applications are driven by our growing demand for increased communications capacity. In order to meet the growing demand it has been necessary to develop amplifiers for increasing frequency of operation and with increasing RF output power. Two additional factors of extreme importance to space communications are amplifier efficiency and life. Efficiency and life have direct cost effects in determining total systems costs. The parameters selected to best present microwave amplifiers technology readiness are frequency of operation, overall efficiency, and life. RF output power versus frequency is also presented.

4.3.1 Antennas

Reflector antenna technology is the mostly highly developed in terms of space readiness. Present efforts are focused on the development of multifeed and multireflector systems which have low-sidelobe levels. Major efforts are also being directed toward the development of precision deployable large-structure antennas. Much of this work is being done at Jet Propulsion Laboratory (JPL) and Langley Research Center (LaRC) under the NASA Large Space Systems Technology (LSST) Program. In the future, narrower beams and hence greater gain will be achieved as both frequency and aperture size are increased. However, corresponding improvements must be made in achieving higher reflector surface tolerances in order to avoid increasing sidelobe levels.

Multiple feed clusters used in multibeam antennas result in significant blockage when employed in a center-fed reflector configuration. By using a microwave lens rather than a reflector, the blockage problem is eliminated. Lenses also offer the capability to accomplish scanning over large angles with low distortion as compared to center-feed or offset-fed reflector systems. Lens technology is the least developed of antenna types and future technology emphasis will focus on developing designs which can provide wide bandwidth while maintaining low-sidelobe levels and polarization isolation for scanning beams up to 50 beamwidths from the antenna without excessive beam shape degradation.[1] A lens antenna is a possible candidate for the multibeam system developed for the OSTA SRT 30/20 GHz program at Lewis Research Center (LeRC).

Phased-array antennas have generally excellent performance characteristics and considerable versatility for space communications applications. They can form fixed, low-sidelobe beams; electronically steerable beams; or multiple beams. Because of complexity, size, weight, and cost considerations, phased-array systems will require substantial technology developments in several areas. Beam forming network components technology must be developed to permit operation at higher frequency and integrated system approaches developed to handle the complexity and weight problems associated with the vast number of elements required. Phased-array components include microwave integrated circuit (MIC) power amplifiers and preamplifiers; and phase-control and time-delay networks. The NASA OAST and OSTA have funded phased-array work at JPL at X-band frequencies.

Multiple-beam antennas (MBA) have recently beome the subject of great interest for communication satellite applications.[2] As a category, they represent some of the best opportunities for significant frequency reuse and versatility in service options. Since multiple beams are formed from a single aperture (reflector, lens, or phased-array) by independently controlling the phase and amplitude of individual beams, many advantages are possible. By feeding beams independently, frequency reuse is achieved. As increasingly high frequencies become utilized, the number of realizable independent beams per given area of coverage increases, resulting in even greater reuse factors. By using ground-commandable amplitude and phase control elements, dynamic in-orbit reconfiguration is possible. This leads to a capability for individual beam control in position (beam scanning or steering) or in time (time division multiplexing). Dynamic in-orbit reconfiguration also permits acquisition and tracking for inter-satellite applications and adaptive interference rejection by turning off beams (or placing nulls) pointing in the direction of interfering sources. Finally, power may be conserved by shaping beam contours to cover only defined regions. As in phased-arrays, the use of MBAs will be paced by technology developments in achieving miniature and efficient beam-control devices; integrated system design advancements; well-shaped beams at large scan angles; and desired isolation between independent beams in frequency reuse applications. LeRC is planning to develop a multibeam (10-beam) antenna system for 30/20 GHz under the OSTA SRT program.

---

[1] Communication Satellite Technology: State of the Art and Development Opportunities, Contractor Report, Contract NAS 5-24489, The Aerospace Corporation, 1978.

[2] Technological Priorities for Future Satellite Communications, NASA/Goddard Space Flight Center, 1978.

Antenna Operating Frequency (Fig. 4.54). The curve shows antenna frequency capability moving into the 30/20 GHz band in the early 1980s and into the next higher band 10-15 years later.

The location of each antenna type in time indicates approximately the initial Level 7 technology readiness date for that type. The use of reflectors dates back to pre-1975 communications satellites.

Recognizing the increasing interest in multibeam antennas, it is important to note that parallel technology developments in solid-state devices will be required for components (preamplifiers, power dividers, phase shifters, etc.) in beam forming networks.

Antennas - Number of Beams (Fig. 4.55). The number of individual beams which can be formed is shown. The curves represent forecasts which differ depending on the type of multibeam system. The upper curve, representing fixed beam/frequency division multiplexing (FDM) systems, achieves frequency reuse by switching the signals sequentially between fixed multiple beam locations. The lower curve represents scanning beam/time division multiplexing (TDM) systems technology. For these systems, fewer total beams are generated. Frequency reuse is achieved by a combination of beam scanning and frequency sharing.

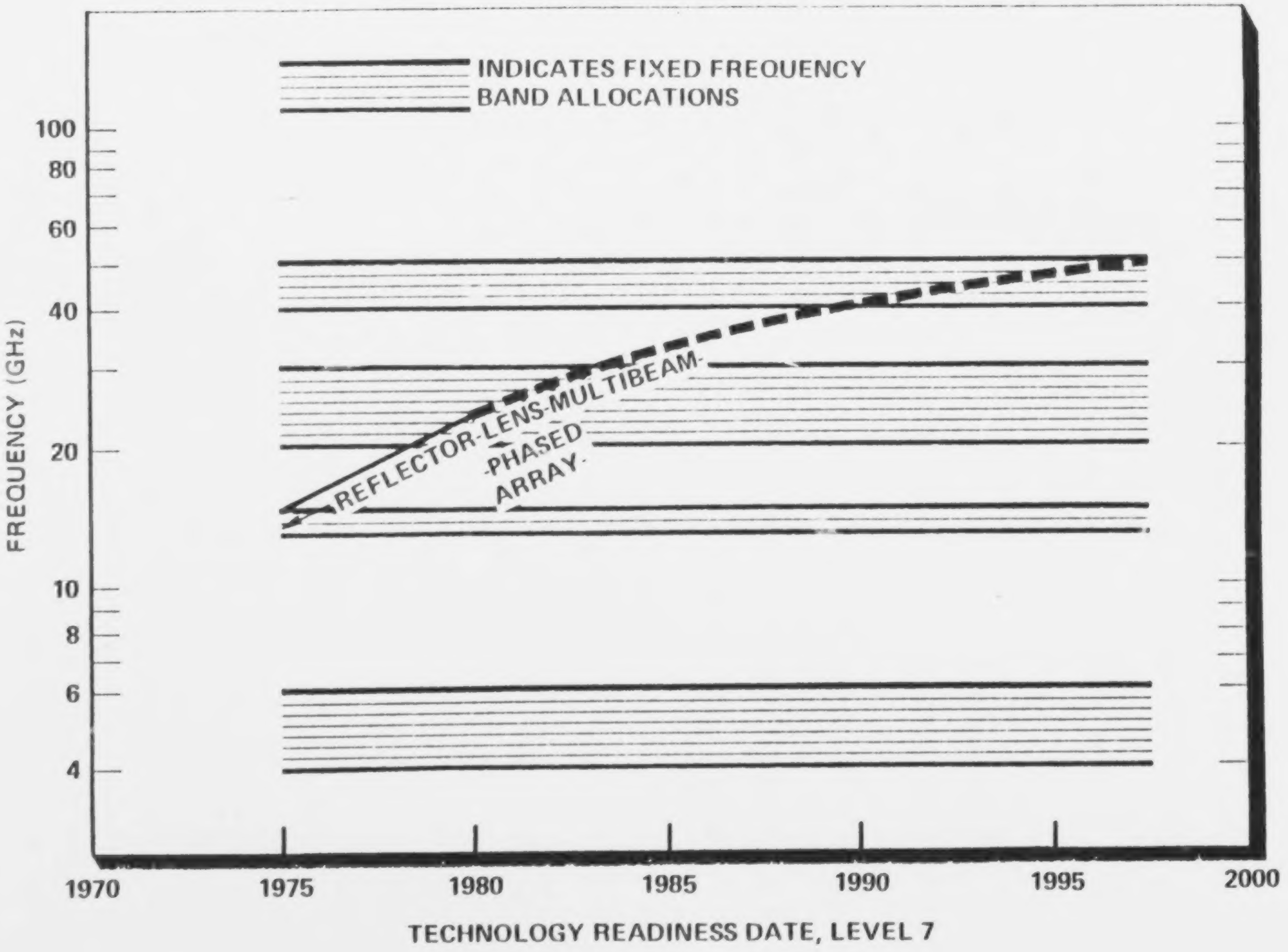

Figure 4.54. Antennas Operating Frequency

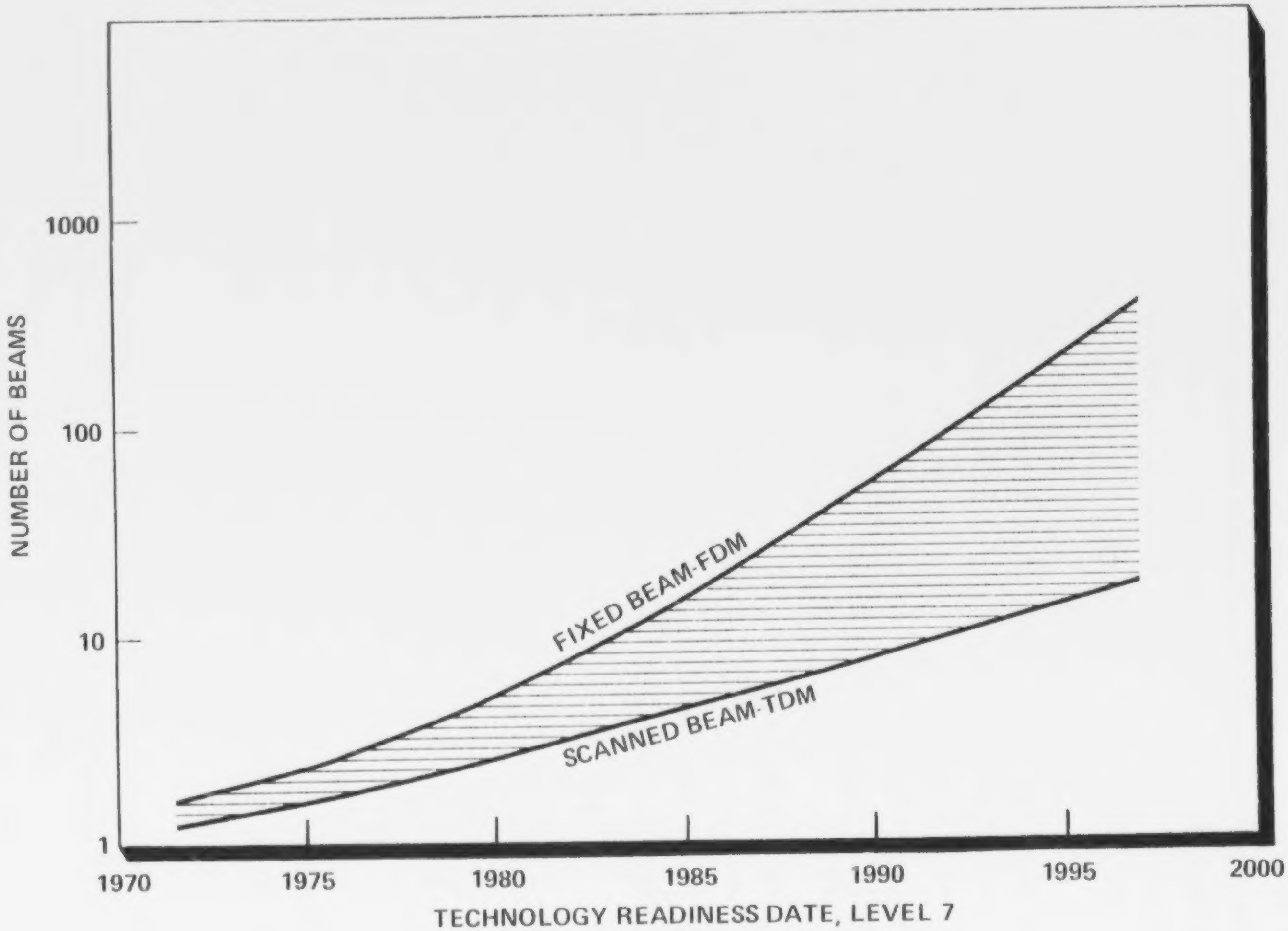

Figure 4.55. Antennas – Number of Beams

Antennas - Reflector Size (Fig. 4.56). To date, the largest reflector antenna in orbit is a 30-ft dish on AST-6 (1974 launch). The upper curve shows the trend anticipated for deployable antennas using the ATS antenna as a base. Various approaches for deployable antennas are being investigated including flex-rib or ridged-rib/mesh, expandable truss/mesh, and segmented, folded rigid surface. Because of surface roughness considerations, the largest are expected to be useful only at frequencies below approximately 6-8 GHz.

The trend for fixed antennas is illustrated in the lower curve. In this case the Shuttle launch envelope is used as an upper size limit. Fixed reflector technology is directed toward the development of techniques for producing precise surfaces which can be used in a space environment at frequencies to 100 GHz.

4.3.2 Solid-State Devices

As presently planned, the NASA communications program is focused on the 30/20 GHz satellite communications requirements. This activity will establish the early 1980s base-line capability for space-qualifiable solid-state microwave amplifiers, both low noise and high power.

At present, microwave GaAs FET amplifier technology appropriate for 30/20 GHz satellite communication applications is mainly in technology readiness Levels 2 and 3. OSTA funded 30/20 GHz project SR&T is expected to produce, at technology readiness Level 5, 6-W, 20-GHz power amplifiers with about 0.75-W output power per device. Expected performance of LNAs developed under the project SR&T is about 6 dB overall amplifier noise figure at 30 GHz. This technology should be brought to Level 5 about the end of 1982.

OAST-funded base R&T maturing beyond 1982 will develop improved devices in the areas of substrate and buffer layer quality, better doping level control and improved doping profiles, more reliable and less loss, metallization, shorter gates, recessed gate structure, improved source

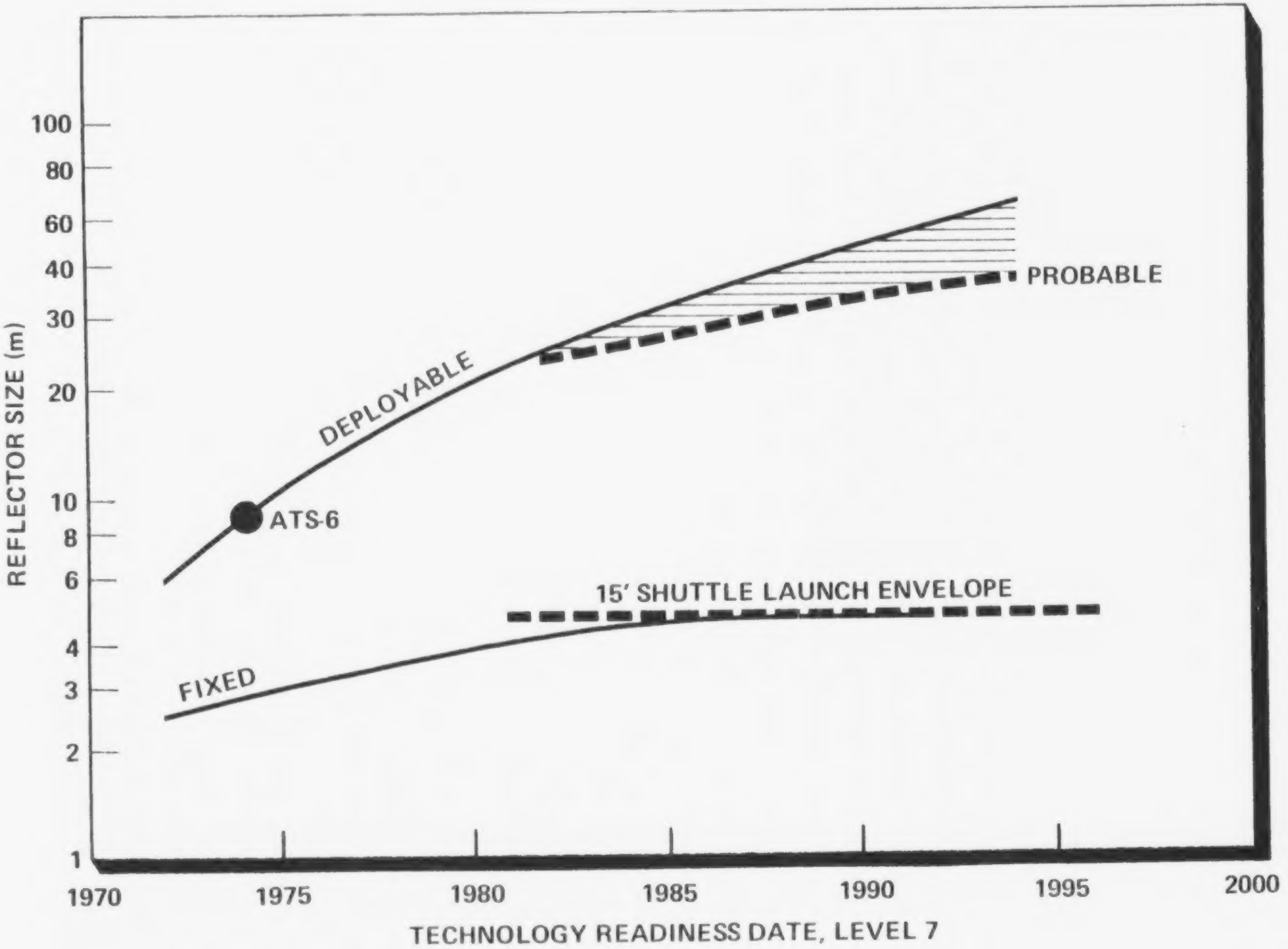

Figure 4.56. Antennas – Reflector Size

grounding, and on-the-chip matching techniques. All of the above should lead to improvement in both low-noise and high-power devices. The development of satellite passive and/or cryogenic cooling should provide substantial further improvement in GaAs FET LNA noise figure. Monolithic integration of many devices on a single chip will produce substantial further improvement in output power per chip.

GaAs FET Output Power at 20 GHz (Fig. 4.57). The expected 20-GHz output power per chip is shown from 1975 to 1990. The dashed curve is considered most probable, and the technology capability required to support this curve is rapidly appearing.[1-5] The development of E-beam defined submicron gate length fabrication technology along with advanced doping profiles and gate recess techniques will lead to power capability near 1 W/mm of gate width in 1981, and reliable 0.75-W devices a year later. The use of improved source grounding techniques and development of advanced on-the-chip impedance matching and power combining methods should easily support the prediction of the dashed curve provided presently planned levels of NASA and DoD support continue. The upper and lower bounds represent extreme assumptions regarding the level of on-the-chip combining and integration development support. A power output of 2 W per device, provided as a pessimistic estimate for 1990, assumes only presently planned single FET technology improvements plus chip level power combining of

---

[1] J. V. DiLorenzo and W. R. Wisseman, "GaAs Power MESFETs: Design, Fabrication, and Performance," IEEE Tran., MTT-27, May 1979.

[2] C. A. Liecht, "GaAs FET Technology: A Look into the Future," Microwaves, October 1978.

[3] "GaAs FETs Market and Technology Review," Microwave Journal, Microwave Journal Staff Report, February 1978.

[4] J. V. DiLorenzo, "GaAs FET Development - Low Noise and High Power," Microwave Journal, February 1978.

[5] Peter Ramin, Henry G. Kosmahl, and Thomas A. Fox, Design and Performance Evaluation of Small, Two- and Four-Stage Depressed Collectors for a 4.8 to 9.6 GHz High-Performance Traveling-Wave Tube, NASA TMX-73486, August 1976.

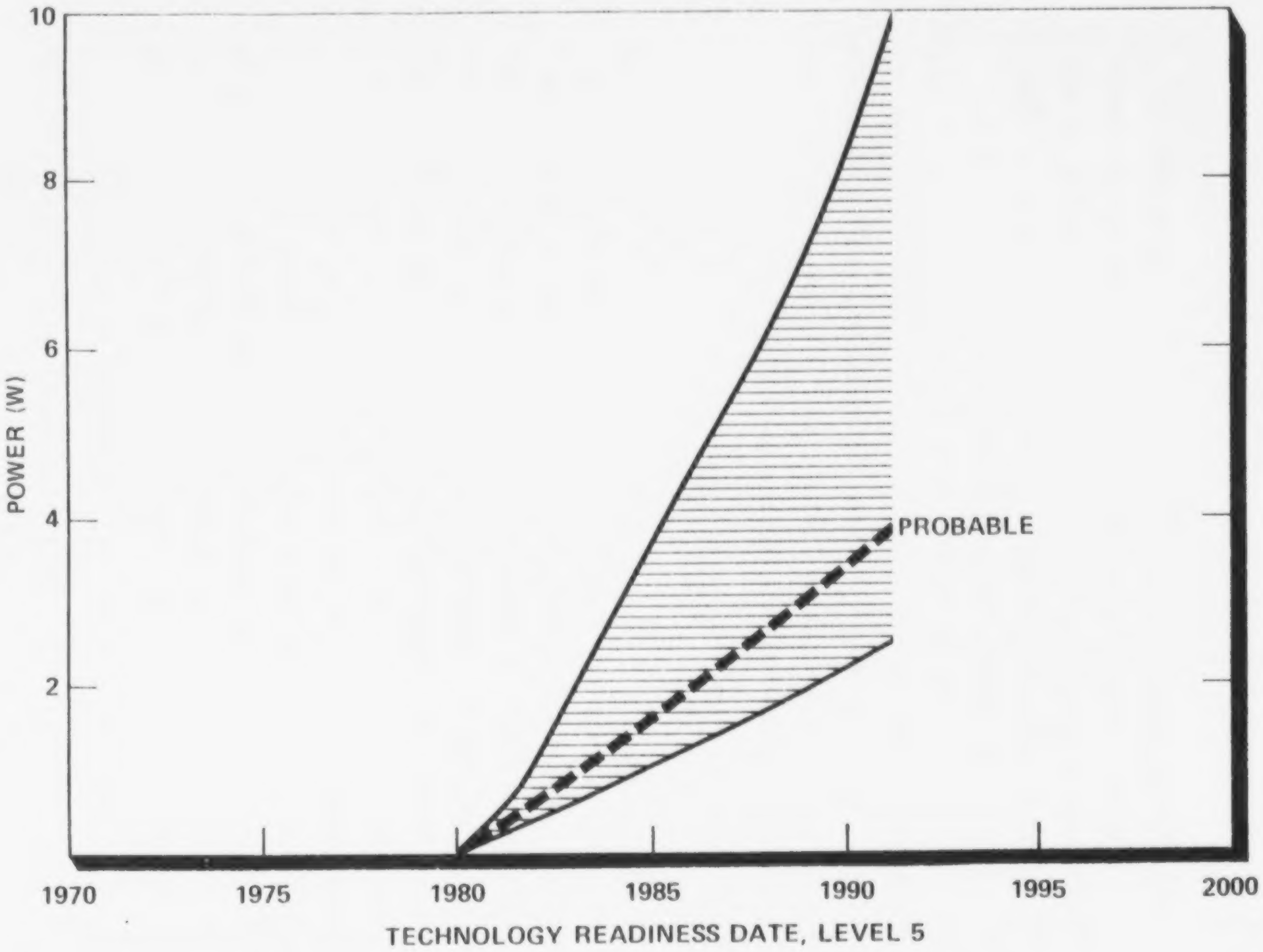

Figure 4.57. 20-GHz GaAs FET Power per Chip

four discrete devices. A power output of 10 W per device by 1990 assumes a substantial effort in developing microwave integrated circuit techniques for power FETs leading to on-chip power combining of more than 20 discrete devices.

GaAs FET LNA Noise Figure at 30 GHz (Fig. 4.58). GaAs FET LNAs at 30 GHz do not presently exist beyond technology readiness Level 3 or 4.[1] However, technology development under NASA programs is expected to produce amplifiers with 6-dB noise figures, in technology readiness Level 5, by the end of 1982. The upper, pessimistic, bound assumes continued evolutionary device and circuit improvements in areas such as gate length, doping profile, and material quality. This should lead to a 4.5-dB noise figure by 1990. The lower bound assumes, in addition, the implementation of passive and/or cryogenic cooling techniques. The development of suitable passive cooling techniques would make amplifier noise figures near 3 dB achievable by 1990.

4.3.3 Microwave Amplifiers

The state of the art and technology of electron beam amplifiers, of which the classic traveling-wave tube is the best known example, is advancing rapidly in power, frequency domain, improved efficiency, linearity and life expectancy. These advances were made possible through introduction of dielectric supporting structures, such as diamond rods, with the result of a tenfold increase in heat removal and reduction of circuit losses; design of an improved depressed collector working above the 90% efficiency level; development and test verification of high-current-density cathodes; and theoretical understanding and experimental progress in the field of cyclotron-resonance fast-wave devices that will extend the frequency and power range into 500 GHz and hundreds of watts CW.

---

[1] DiLorenzo, op. cit.

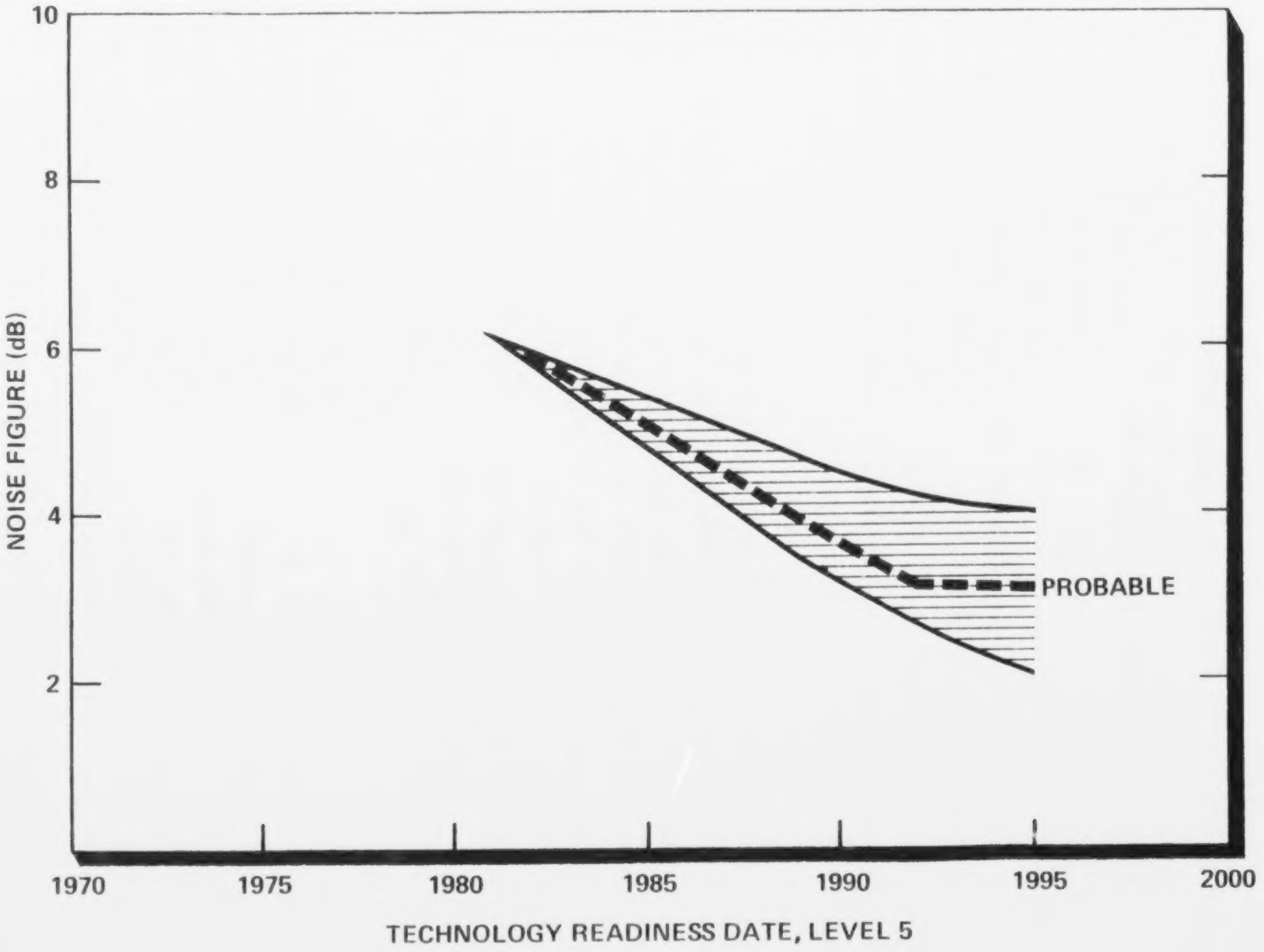

Figure 4.58. GaAs FET LNA Noise Figure at 30 GHz

Introduction of nonconventional slow-wave circuits, for example the Karp structure, promises the availability of inexpensive TWT amplifiers of limited bandwidth (1%) at millimeter-wave frequencies below 100 GHz at power levels up to 200 W CW and high efficiency.

The current NASA communications program is focused on development of the 30/20 GHz frequency for space communications fixed services. A part of the SR&T is directed toward the development of a 75-W, 20-GHz multimode TWT. This effort will provide a space qualifiable amplifier by 1983. This amplifier will incorporate technology advances from a base R&T program, in microwave amplifiers, supported by OAST. This base R&T program in microwave amplifiers is also advancing technology by improving efficiency, increasing life, and extending the technology to make available higher frequency amplifiers.

Microwave Amplifier Operating Frequency (Fig. 4.59). Figure 4.59 shows microwave-amplifier operating frequency versus projected technology readiness date. The band between the lower and upper bound is largely due to the range of RF output power at a given frequency without adversely affecting life, it is projected that advances in cathode life will occur. This, when combined with increased RF output power required to achieve 3 bits/Hz communications, will produce the lower bound. The upper bound is based on technology needs assuming current technology of C- and K_u-band operations are extended to K_a-band and above.

Microwave Amplifier Efficiency (Fig. 4.60). Figure 4.60 shows three curves of microwave-amplifier efficiency versus technology readiness date for C-, K_u-, and K_a-band frequencies. Because higher frequency tubes are inherently less efficient than lower frequency tubes, maximum efficiency achievable will be greater for the lower frequencies. The projections are based on advanced applications of improved multistage depressed collector technology,[1] and incorporating low secondary yield materials.[2]

---

[1] Ramins et al., op. cit.

[2] Ralph Forman, Secondary-Electron-Emission Properties of Conducting Surfaces with Application to Multistage Depressed Collectors for Microwave Amplifiers, NASA Technical Paper 1097, November 1977.

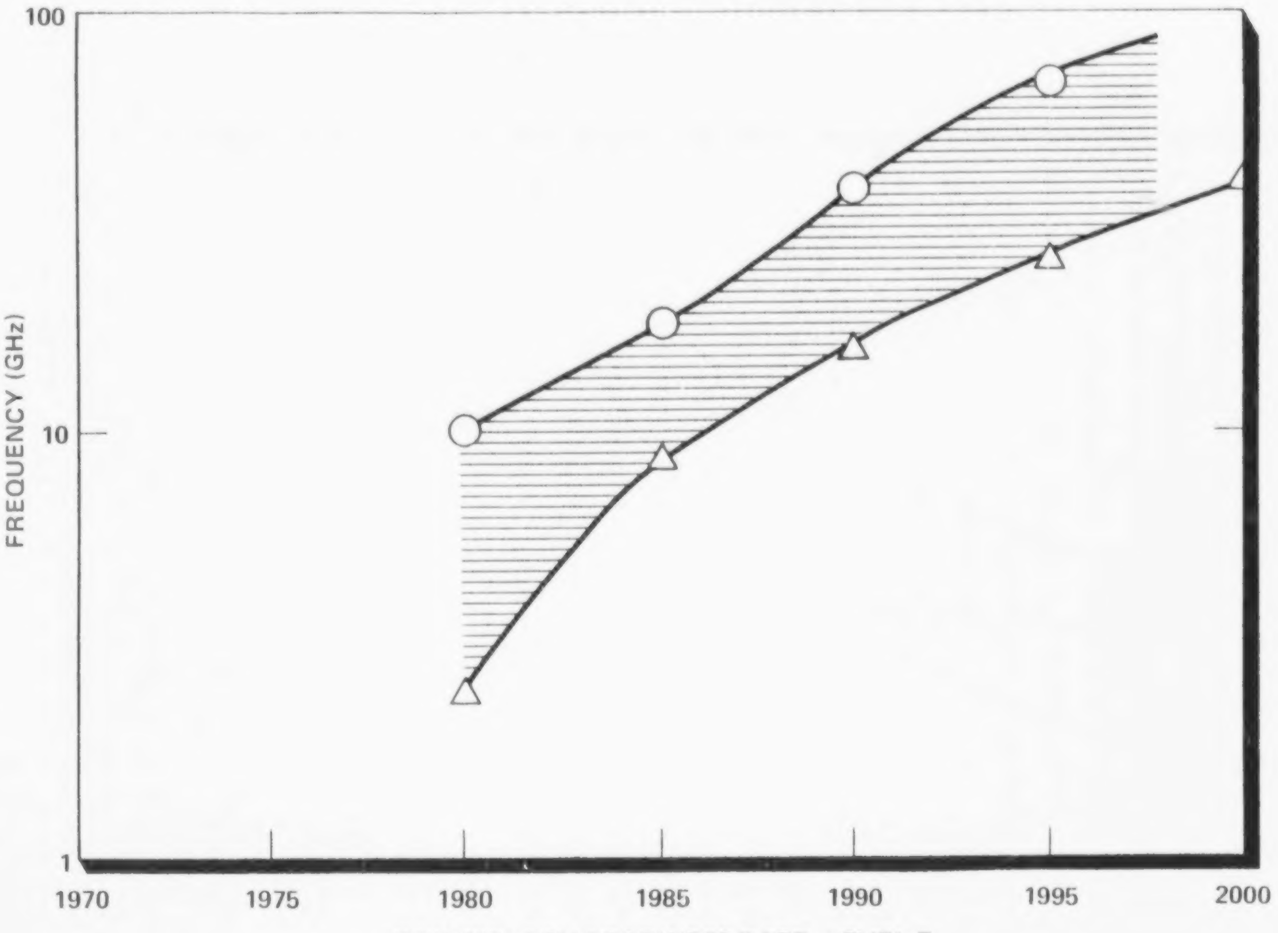

Figure 4.59. Microwave Amplifier Operating Frequency

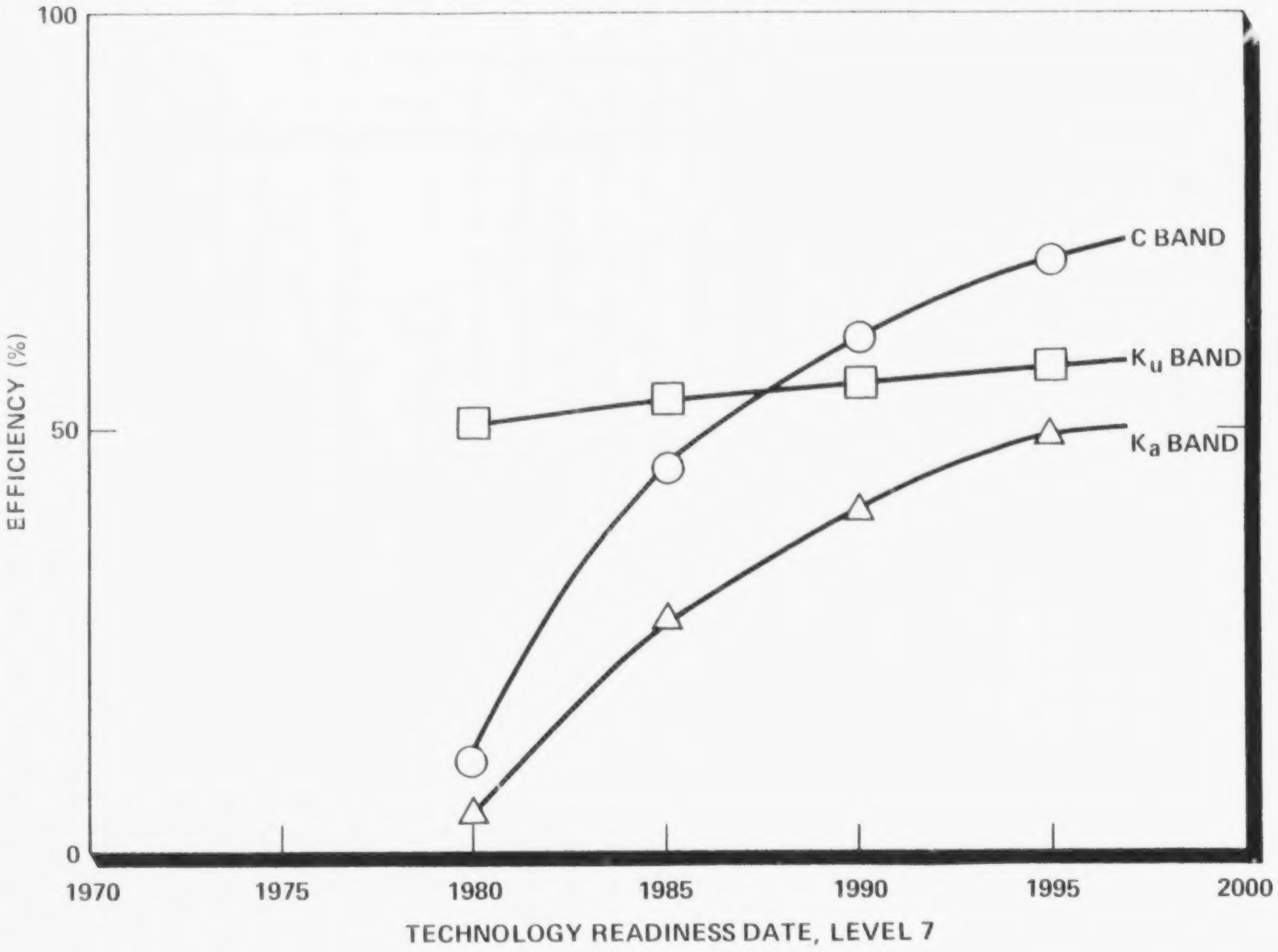

Figure 4.60. Microwave Amplifier Efficiency

The high level of efficiency of 50% for K_u-band at the early technology readiness date of 1980 represents the advanced technology demonstrated by the 200-W, 12-GHz TWT used in the communications technology satellite.[1] Further advances in technology are not expected to significantly increase efficiency, but will result in device simplification.

Microwave Amplifier Life (Fig. 4.61). Figure 4.61 presents the technology readiness of microwave amplifier life. The life of a microwave amplifier is determined predominently by cathode life. Cathode life in turn is a function of operating temperature necessary to produce a given emission current density. As amplifier operating frequency is increased, size becomes smaller in proportion to wavelength. For a given power, emission current density increases with frequency. In addition, at a given frequency, emission current density also increases with RF output power. Hence, the life of a microwave amplifier using a thermionic cathode is determined by emission current density. The operating life of microwave amplifier, thermionic cathodes having emission current densities of 2 A/cm^2, is shown as the lower bound. This is based on the use of type B cathodes in the near term, and the introduction of the M-type cathodes by 1985.[2] The upper bound represents the successful development of the Field Emission Cathode, which expected to achieve a technology readiness date of 1990.[3] This development is expected to make dramatic increases in life even at much higher current desnities.

Microwave Amplifier Output Power (Fig. 4.62). Figure 4.62 shows two curves representing the power output versus frequency in the frequency range from 10 to 100 GHz. Curve A describes either the already

---

[1] Denis J. Connolly et al., Communication Technology Satellite Output - Tube Design and Development, NASA TMX-3480, April 1977.

[2] Ralph Forman and David H. Smith, "Thermionic Cathode Life Test Studies," IEEE Transactions on Electron Devices, October 1979.

[3] C. A. Spindt, Development Program on a Cold Cathode Electron Gun, Final Report NASA CR 159751, April 1979.

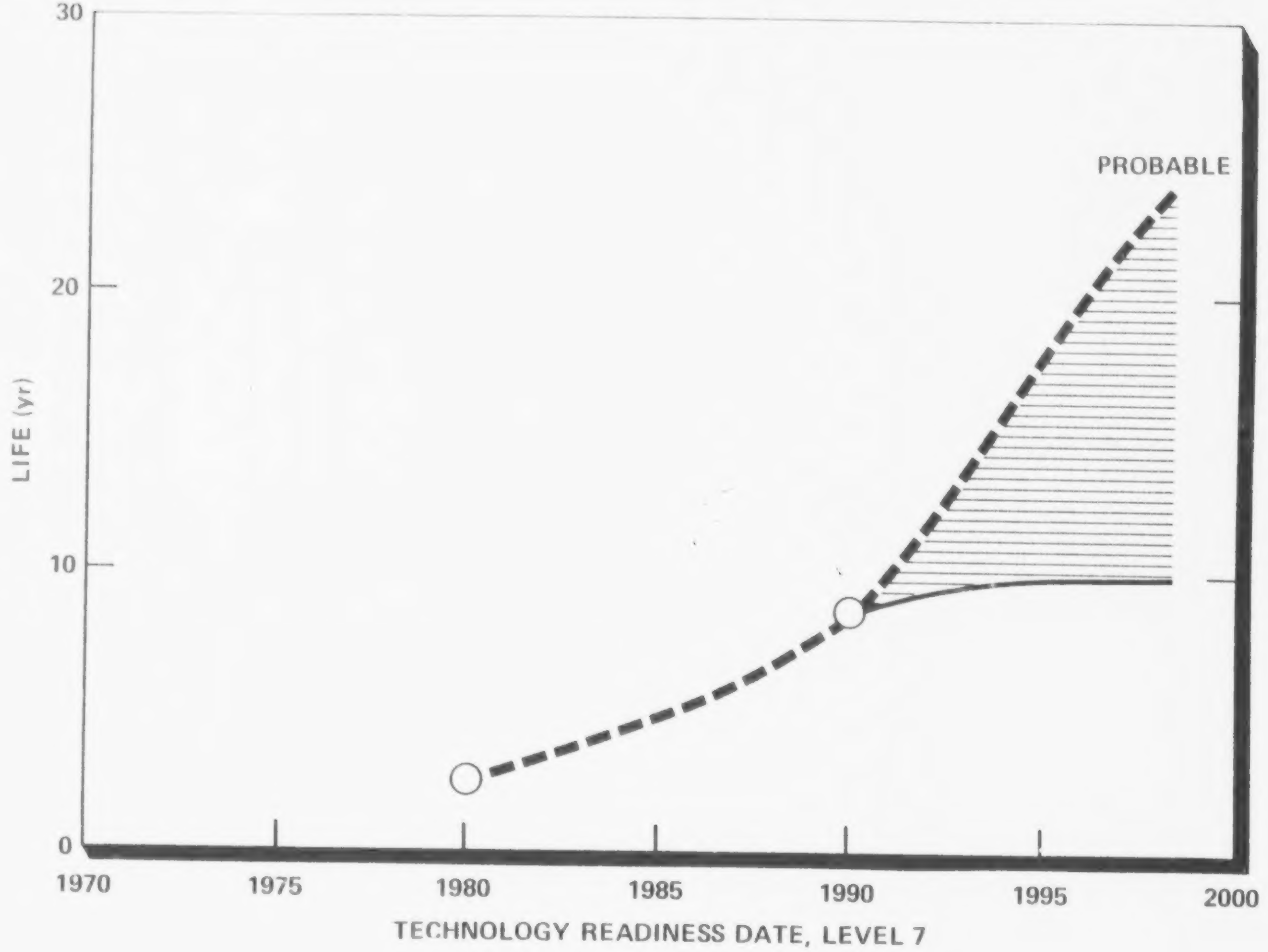

Figure 4.61. Microwave Amplifier Life

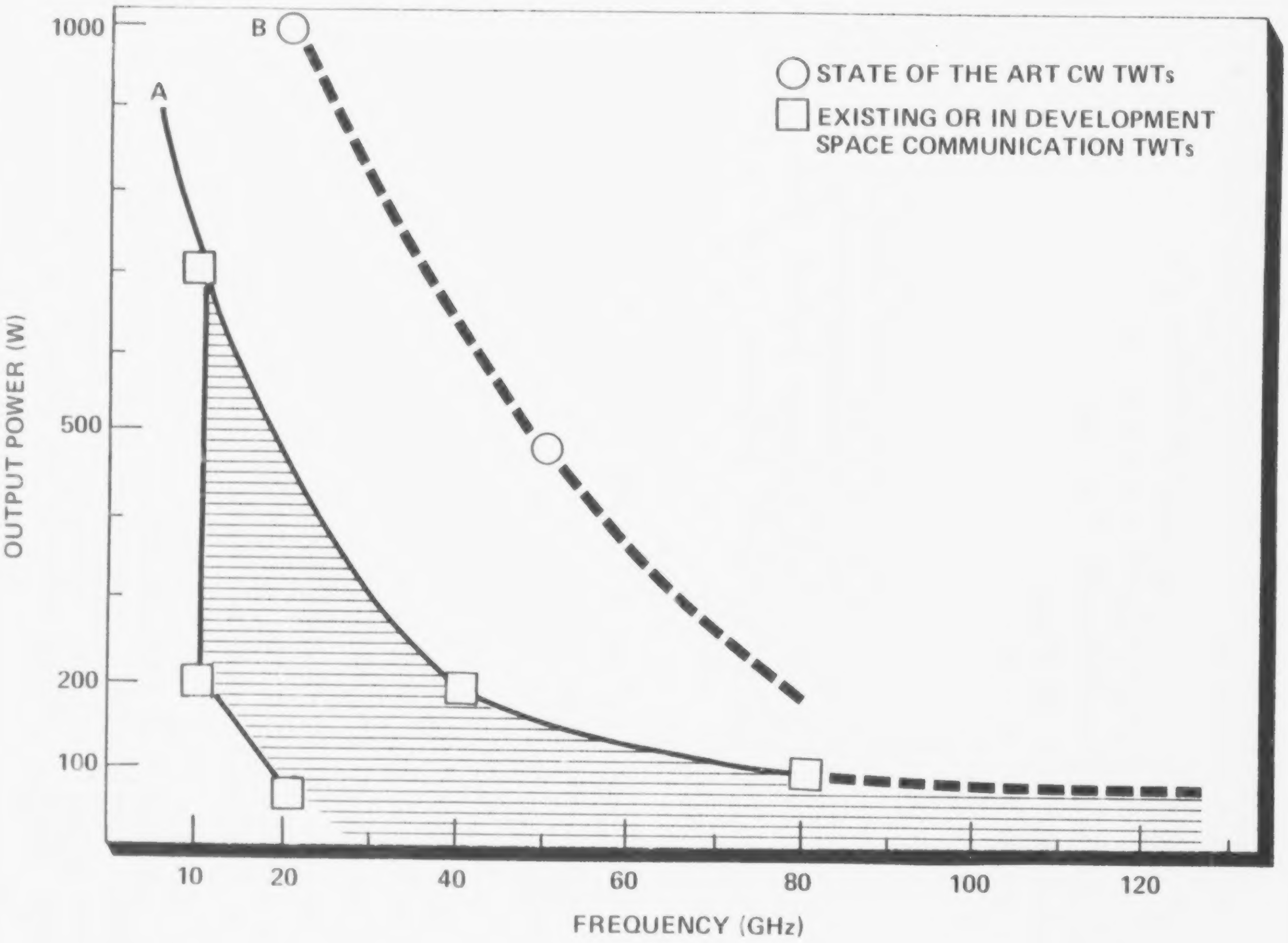

Figure 4.62. Microwave Amplifier Output Power Versus Frequency

established or near realization state of the art of long-life power amplifiers with an instantaneous bandwidth of 1% to 10%. Curve B is an estimate of power-handling ability of wideband amplifiers that indicates the potential rather than a long-life, reliable power source.

Gyrotron amplifiers exceed the state of the art of classic TWT in power-handling ability by 2 orders of magnitude.

4.3.4 Electron Guns, Cathodes, and Materials

Improvements in the efficiency and reliability of high-power microwave amplifiers are the goals of several OAST R&T development programs on cathodes and electron guns and on low secondary yield materials for the electrodes of multistage depressed collectors.

The technology of high-power microwave amplifiers is being pushed by anticipated usage of the C and K_u satellite frequency bands to operation at higher frequencies and in some cases higher power levels.[1,2] Because higher frequency tubes are inherently less efficient and smaller in size, both of these trends produce a need for electron guns capable of delivering higher current density beams. Present electron gun design already approaches the practical limit of beam compression imposed by the statistical distribution of transverse electron emission velocities; therefore, the required increases in beam current density must be obtained primarily by increases in emission current density at the cathode. The problem of obtaining higher beam current density is being approached in several ways, which include life tests of various cathodes installed in simulated amplifying tubes, research on the basic surface physics of cathodes, development of new electron beam measurement techniques, research on novel field emission cathodes, and the analysis and testing of new gun designs.

---

[1] "18/30 GHz Fixed Communications Systems Services Demand Assessment," US Telephone and Telegraph Corporation, Contract NAS3-21366, Vol. 1, Executive Summary, CR-159619; Vol. 2, Final Report, CR-159620; Vol. 3, Appendices, CR-159621, 1979.

[2] "18/30 GHz Fixed Communications System Service Demand Assessment for 1980-2000," Western Union, Contract NAS3-21359, Vol. 1, Executive Summary, CR-159546; Vol. 2, Final Report, CR-159547; Vol. 3, Appendices, CR-159548, 1979.

For some applications it may be necessary to produce, from the same electron gun, different beams for different modes of tube operation. This multimode problem is being addressed both as a gun design problem using conventional cathodes and as a possible application for a gun employing a field emission cathode.

To maximize efficiency in the multistage depressed collector (MDC) it is necessary to suppress secondary emission from the surfaces of the collecting electrodes.[1] This can be accomplished in part by good MDC design, but it is inevitable that secondary emission will result in some current being collected at a less depressed potential. Furthermore, electrons that are elastically reflected from the collecting surface have the possibility of returning to the tube body. In addition, the thermal conductivity and thermal emissivity of these materials is also of fundamental importance. This problem is being approached by studying the basic physical properties of materials that might be used in collectors, and by constructing collectors from various promising materials for tests on operating tubes.

Cathode Emission (Fig. 4.63). At the time of the design of the amplifying tube for CTS in the early 1970s, conservative engineering practice dictated the use of a "B-type" cathode[2] with an emission current density of 0.5 A/cm^2. Subsequent life tests on various commercially available cathodes have indicated that "M-type" cathodes can be operated at current densities of at least 2 A/cm^2,[3] and it is expected that further tests now just beginning will confirm in the early 1980s that these can be operated safely at 4 A/cm^2. Further advances in the cathode emission current density for conventional thermionic cathodes are expected to

---

[1] Peter Ramins, Henry G. Kosmahl, and Thomas A. Fox, Design and Performance Evaluation of Small, Two- and Four-Stage Depressed Collectors for a 4.8 to 9.6 GHz High-Performance Traveling Wave Tube, NASA TMX-73486, August 1976.

[2] Denis J. Connolly, Ralph Forman, C. L. Jones, Henry G. Kosmahl, and G. Richard Sharp, Communication Technology Satellite Output - Tube Design and Development, NASA TMS-3480, April 1977.

[3] D. H. Smith, Design, Construction, and Long-Life Endurance Testing of Cathode Assemblies for Use in Microwave High-Power Transmitting Tubes, NASA CR-135371, December 1977.

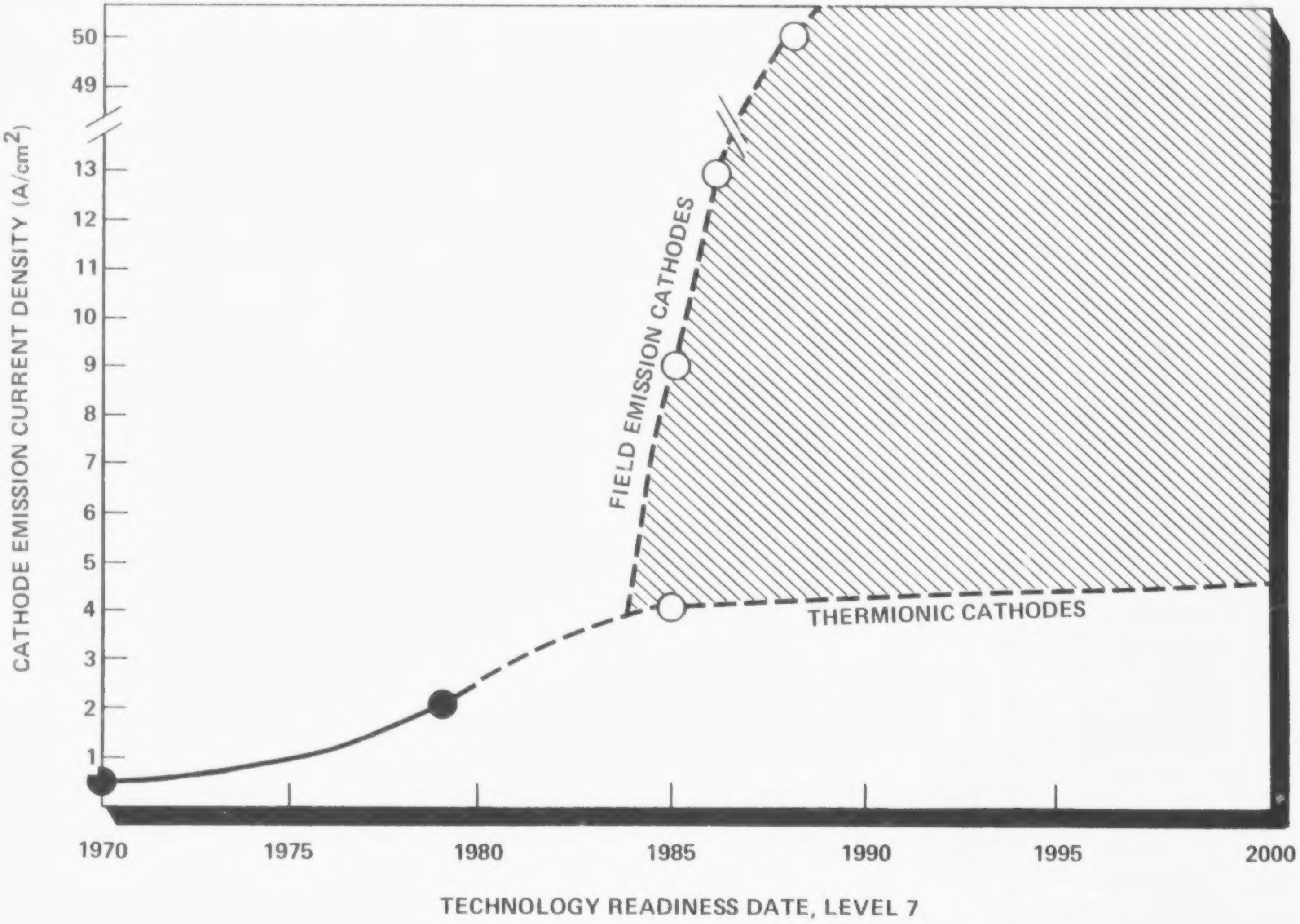

Figure 4.63. Electron Guns – Cathode Emission

require intensive research into emission processes and the development of new emissive surfaces. The more optimistic forecast shown by the upper curve allows for the successful development of the field emission electron gun. Tests are presently being conducted on a field emission electron gun designed for a cathode loading of 9 A/cm^2. Field emission cathodes now available have been tested at current densities up to 13 A/cm^2, but these tests have not been performed in a practical electron gun. It is predicted that fabrication techniques are available that would permit the fabrication of field emission cathodes capable of current densities of 50 A/cm^2.

Cathode Lifetime (Fig. 4.64). It is nearly impossible to separate predictions of cathode lifetime from the emission current density. In typical thermionic cathodes, if a higher emission current density is required, it is achieved by raising the cathode temperature at the expense of shortening the cathode lifetime. The emission current densities presented in Fig. 4.63 are those that are considered to be consistent with the extended lifetimes required for NASA missions. The very great potential improvements in cathode lifetime shown in Fig. 4.64 are dependent on the successful development of the field emission gun.

Secondary Emission Field (Fig. 4.65). The secondary emission yield is the ratio of the number of secondary electrons emitted from a surface to the number of primary electrons incident on the surface. The yield is a function of the energy and angle of incidence of the primary electrons and is also dependent on the material comprising the target, the cleanliness of the target surface, and the roughness of the surface. The ideal collector electrode would be fabricated from a material with zero yield, that is one that absorbed completely all incident electrons. Such a material has not yet been found in nature, but some materials, for example, pyrolytic graphite, have yields of about 5 in the range of primary electron energy of interest for MDC designs.[1] This yield can be reduced to approxi-

---

[1] Ralph Forman, Secondary-Electron-Emission Properties of Conducting Surfaces with Application to Multistate Depressed Collectors for Microwave Amplifiers, NASA Technical Paper 1097, November 1977.

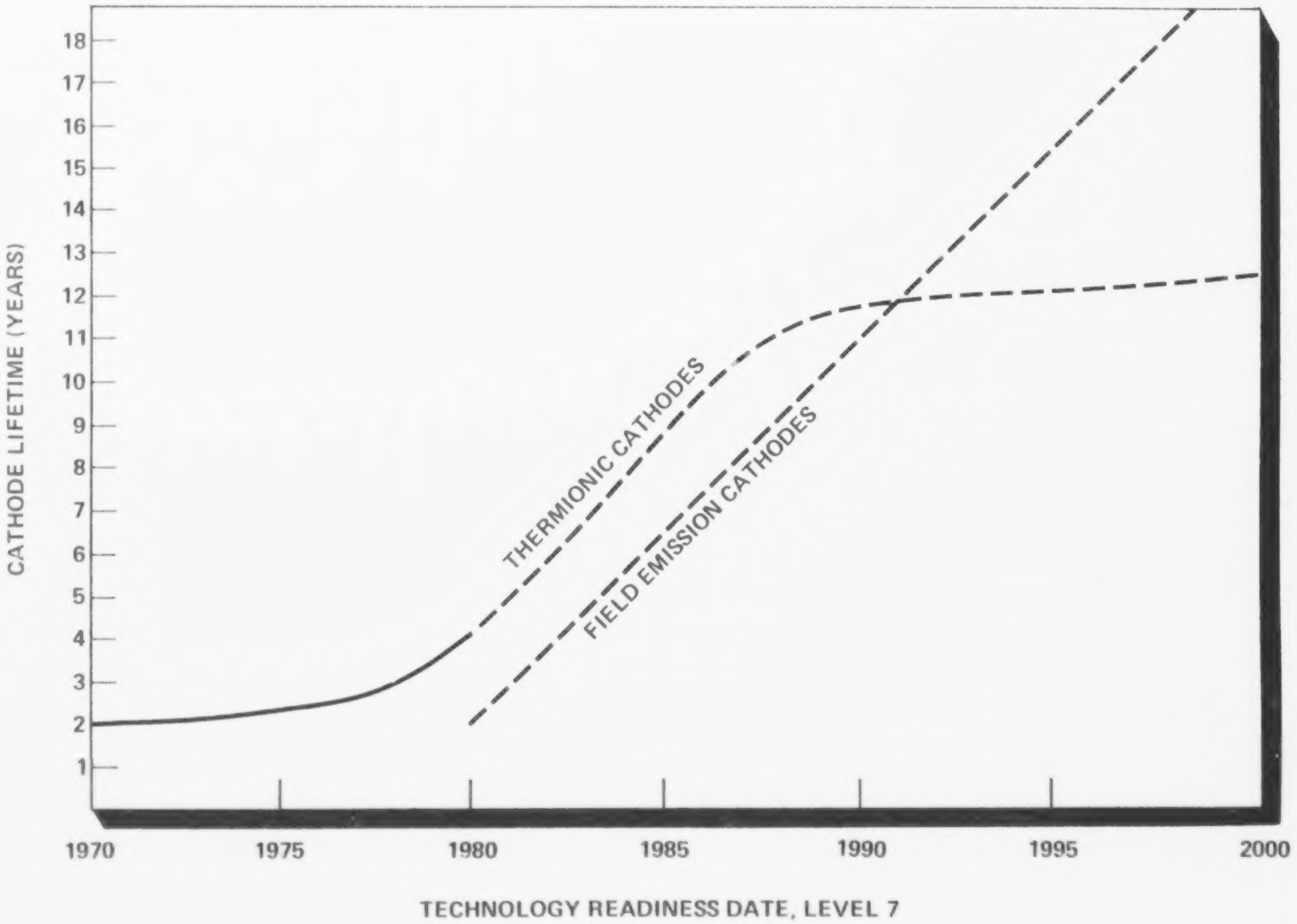

Figure 4.64. Cathode Lifetime

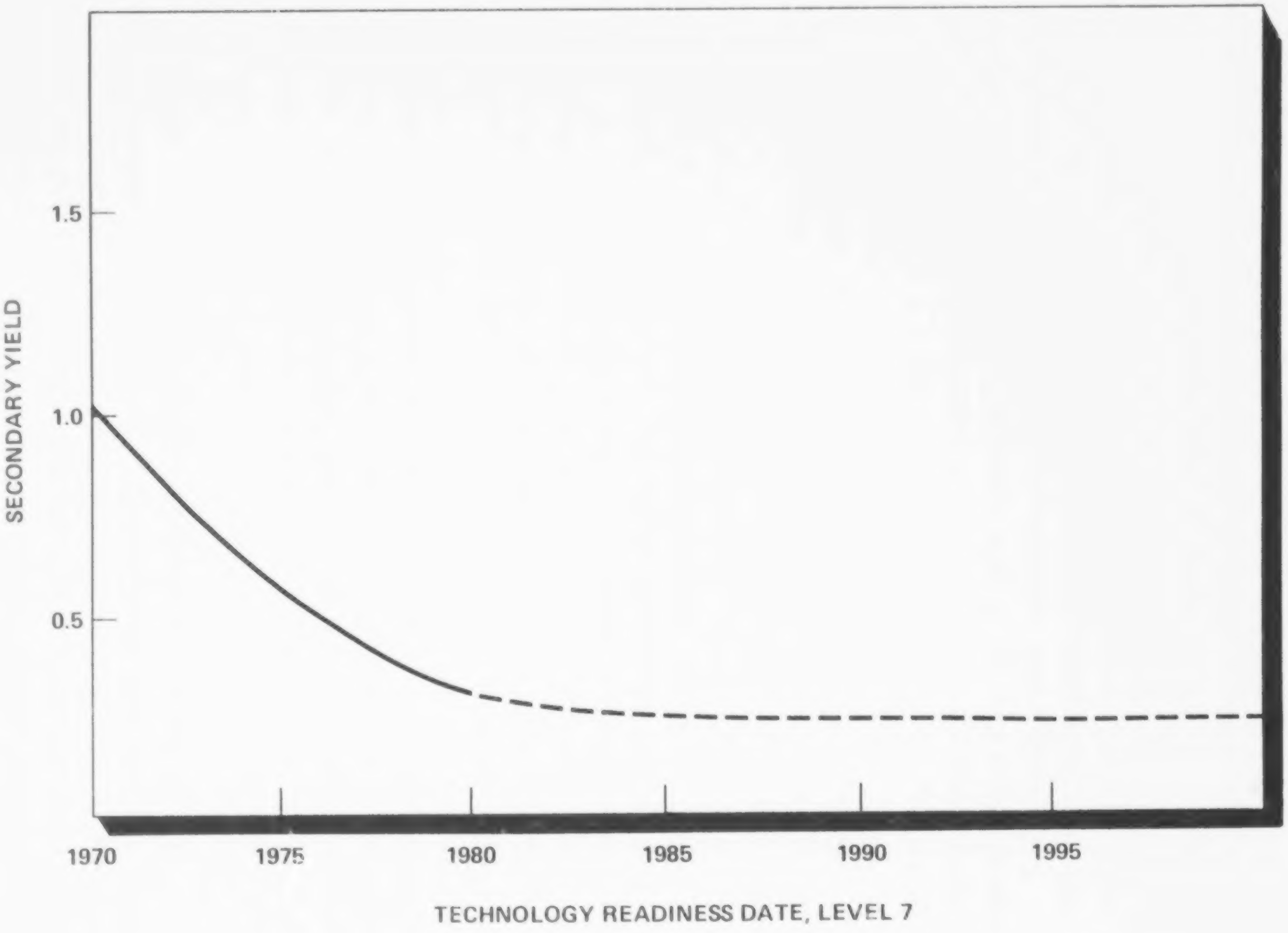

Figure 4.65. Secondary Yield

mately 0.25 by roughening the surface by etching. This and other materials are currently being studied. Figure 4.65 shows the yield of 1.0 for copper collectors as used in CTS in the early 1970s. A prediction is made that materials with a yield of 0.25 will be available for use in the mid 1980s.

4.3.5 Planetary Spacecraft Communications

Spacecraft communication capability from planetary distances has been increased by OAST, by developments in transmitter components at higher frequencies, by larger more efficient antennas, and by more efficient coding of the communication channels.

The companion technology for the ground-based antennas and receivers has been developed by OSTDS. The systems are very much driven by the types of missions planned.

A measure of the planetary spacecraft communication system performance is the equivalent data rate at Jupiter distance. Currently, the 115 kbps achieved by Voyager and the existing DSN can return approximately one Jupiter encounter picture per minute. Ten years ago, only 64 bps could have been achieved. The probable forecast for 1990 is that 100 Mbps could be the equivalent data rate from Jupiter distance at the future time.

The projected 40 dB increase in performance could be achieved by arraying DSN ground receiving antennas, and a combination of higher frequency, higher spacecraft transmitter power, a larger diameter spacecraft antenna that has a more efficient aperture utilization, and more efficient data encoding.

OAST is currently funding the development of more efficient semiconductors for spacecraft RF power conversion, the development of solid-state array feeds that are power combined in a large aperture-shaped reflector antenna, and with the capability for electronically steered fine beam pointing. Coding developments for more efficient channel utilization are not currently funded.

Equivalent Data Rate at Jupiter Distance (Fig. 4.66). The increases in data rate for Jupiter distance is shown from 1960 with a forecast through 1990. A gradual increase is shown in the prediction, although the improvements will be discrete jumps in capability as in the past. For example, there could be an eventual 7-dB increase in DSN receiving antenna array gain, a 20- to 40-W increase in spacecraft transmitter output power (3 dB), and a 10-dB increase in spacecraft antenna gain in going from 3.6 to 10 m diameter. This possible combination of technology improvements could account for a total 20-dB increase in system performance by 1980. Alternatively or additionally, a change in the operating frequency capability of all the system components from 8.4 to 31 GHz could provide up to 12-dB change during fair weather at the receiving site. Improvements in concatenated coding could yield an additional 2 to 3 dB of system performance improvement.

Antenna larger in diameter than the 3.7 m Voyager high-gain antenna, and projected performance at K-band frequencies near 31 GHz are assumed, particularly in the post-1990 era. At the higher RF frequencies and particularly for larger diameter spacecraft antennas, the pointing requirements become severe. Therefore, antenna-mounted electronics must be employed to aid in earth pointing. Either monopulse or conical-scan pointing error signals must be developed and supplied to a spacecraft reaction wheel or mass expulsion attitude control system for rigid antennas; or alternatively the antenna beam must be capable of electronic beam steering or an active retrodirective array feed employed in lighter weight structures. OAST technology developments for RF phase shifters currently under examination could provide a portion of the capability for permitting improved spacecraft antenna gains.

The Air Force space-based radar technology component developments may yield applicable technology to assess in improved data rates for planetary spacecraft communications.

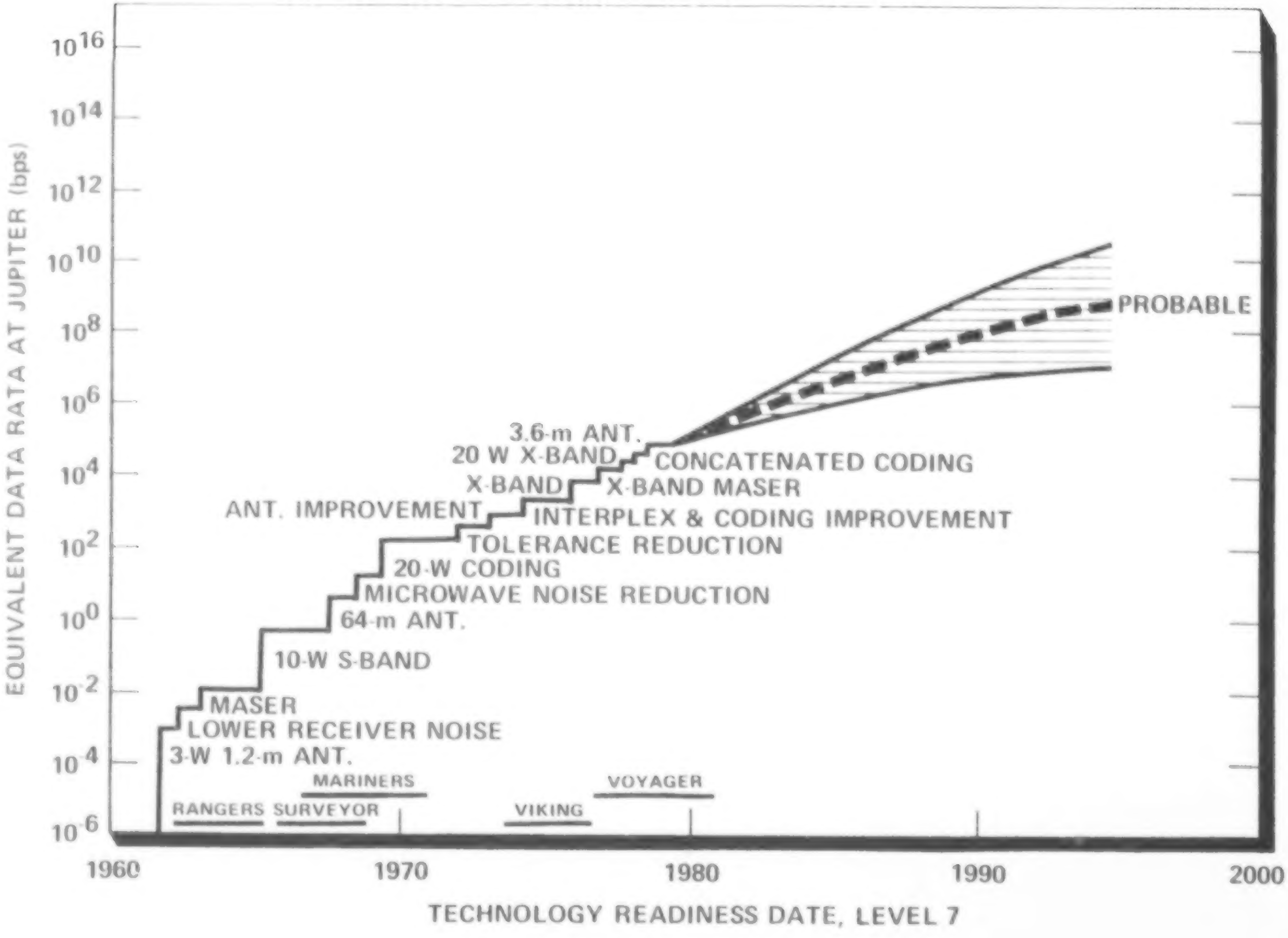

Figure 4.66. Equivalent Data Rate at Jupiter

With respect to solid-state high-power semiconductors, without a significant, fundamental breakthrough in individual device technology, the overall DC to RF conversion efficiency is expected to remain in the 30% range, for flight-qualified power amplifiers below 100-W RF output. (High-power capability missions will probably still employ tube-type RF amplifiers.) Higher efficiency solid-state devices for the same power output will have longer life times that are necessary for the very long range missions.

The pessimistic projection for 1990 assumes only modest increases in transmitter power (3 dB), antenna gain (10 dB), coding (2 dB), and ground-based arrays (7 dB). The optimistic data rate upper bound is based upon definitely upgrading the system to K-band. There is the promise of orbiting antennas for the earth end of the link and of optical frequency links in the wings for the long-term era. Specific performance parameters in the July 1975 Outlook For Space volume[1] are, for the most part, still applicable.

4.3.6 Space-to-Space Communications

Present space-to-space communication systems utilize frequencies that are limited both in availability and data transmission capability. In addition, the problem of mutual interference between ground-based and space-based systems has proved to be a significant design driver.

Specific examples of known application areas for a new communications system technology are listed below with some of the reasons for the need for a new capability.

A. Comsat to Comsat--would make worldwide communications more efficient due to increased bandwidth.

---

[1] Outlook For Space, Reference Volume, A Forecast of Space Technology 1980-2000, NASA, 15 July 1975.

B. Next-generation TDRS

   1. Data rates of future TDRS users will exceed present TDRS capability

   2. Higher frequency TDRS system can be designed with a much smaller structure

C. High-data-rate requirements of future space programs

   1. SPS controls and monitoring

   2. Space construction

   3. Expanded video requirements

D. Spacecraft requiring secure communications

   1. A frequency can be chosen such that atmospheric absorption precludes ground interference to spacecraft

   2. Interference with ground systems would be eliminated

While laser approaches to these applicational areas offer potential, a more beneficial solution is the exploitation of the frequency band between 100 and 200 GHz. Since this band has several designations, the term ultramicrowave is used to cover the band between 100 and 200 GHz. This band offers the advantage that it is above that region which the military has been assigned and which will eventually become congested.

Overall ultramicrowave communications techniques and hardware are being advanced in a number of different areas. Present development programs are directed toward advancing the state of the art in power generation and reception techniques and hardware. This effort is primarily device-oriented and conducted by DoD organizations. Recently NASA has undertaken overall system[1] design and integration studies. Special emphasis is being placed on techniques and hardware considerations that are unique to space-related applications. The basic system model that is being used as a design goal is a two-way communications system capable of transmitting information to and from synchronous altitude with a data rate of at least 1 Gbit/s. This communications system would operate on any frequency between 100 and 200 GHz and would have a tuning range of at least 10%.

---

[1] Ultramicorwave Communications System, NASA Contract NAS 9-15617, 1978.

In order to accomplish the necessary acceleration of technology for the higher frequency system, certain development areas will be selected for special emphasis. These development areas, along with key criteria in each area, are listed below. The range of frequency will be 100 to 200 GHz.

A. Source Development

  1. All solid-state--increase range of choices
     - Impatt
     - Gunn effect
     - Etc.
  2. Increase power out
  3. Increase efficiency
  4. Frequency stability
  5. Tuning bandwidth
  6. Packaging flexibility

B. Modulator Development

  1. Increase modulation technique flexibility (FM, digital, etc.)
  2. Increase tuning bandwidth, data rates
  3. Decrease insertion losses
  4. Decrease phase errors, etc.
  5. Increase center frequencies of several types to get greater device choices

C. Amplifier Development

   1. Increase efficiency

   2. Increase gain bandwidth product

D. Antenna Development

   1. Improve paraboloids to reduce sidelobes and coupling

   2. Increase beamwidth for a given gain

E. Mixer Development

   1. Decrease noise figure and conversion loss

   2. Increase bandwidths

F. Communications Signal Processor Improvement--increase throughput rates for multiplexers, source, and channel coders

The parameters that have been chosen for the figures are output power and power conversion efficiency. Technology readiness dates shown represent Level 7 state of development. Since system performance is highly affected by the atmosphere, spacecraft demonstrations are required.

Output Power (Fig. 4.67). A gradual increase in output power capability throughout the remainder of this century is shown. Present capabilities are in general below 100 mW except for certain controlled experiments. The major advancements indicated are based on a continued support of solid-state devices such as the double drift silicon impatt diode. A number of different companies[1,2,3] are currently working in this area, and it seems likely that with sufficient support a power output of 100 W is very realistic.

---

[1] M. Kramer, "Solid-State Technology for Millimeter Waves," Microwave Journal, August 1978.

[2] K. Weller and R. Wing, "Millimeter Impatt Sources for the 130-170 GHz Range," IEEE T-MTT, November 1976.

[3] T. Ishibashi and M. Ohmort, "200 GHz 50 mW CW Oscillation with Silicon SRD Impatt Diodes," IEEE T-MTT, November 1976.

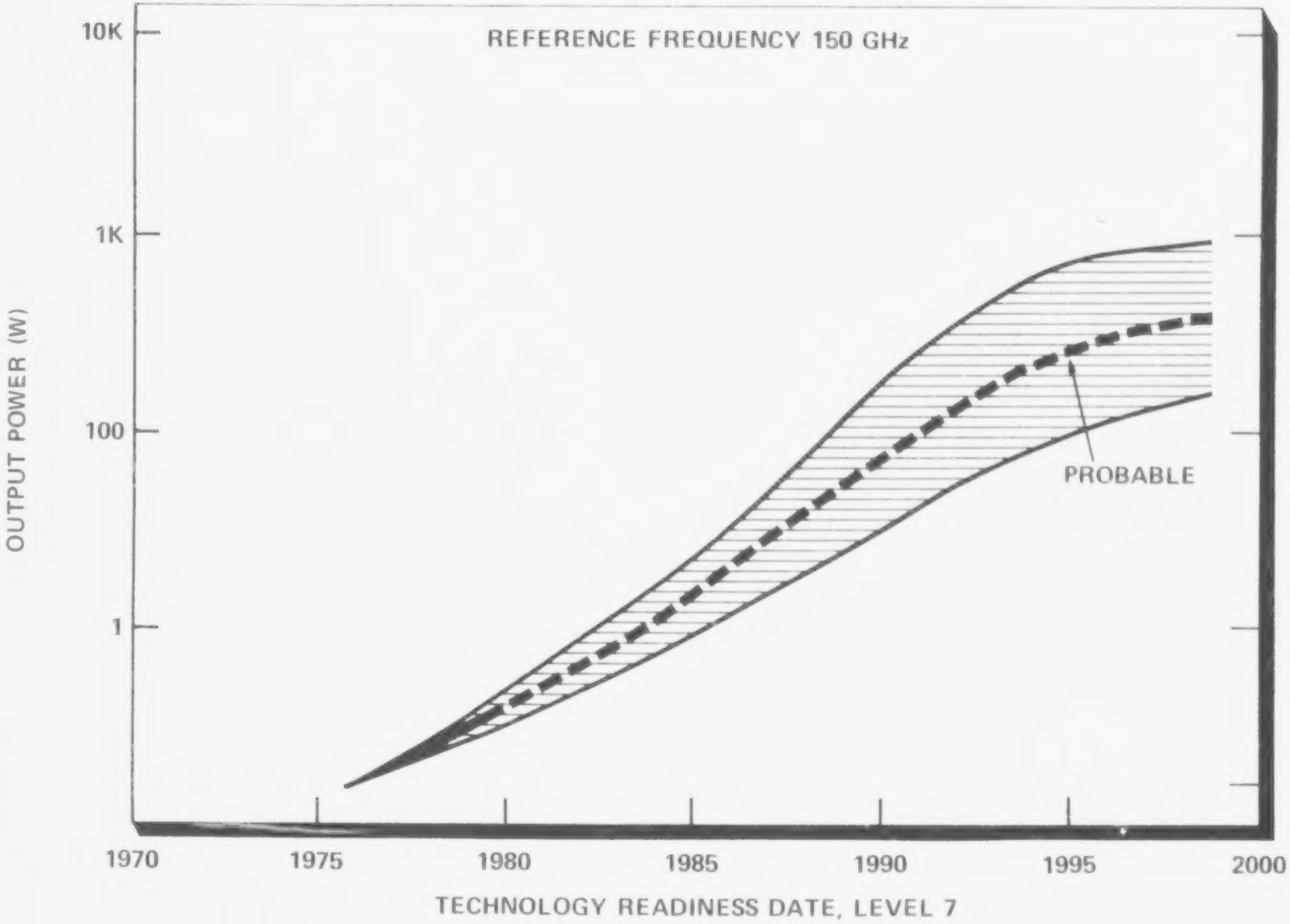

Figure 4.67. Output Power in Space-to-Space Communications

A more optimistic projection based on new discoveries in either the solid-state technology or possibly some combination of solid-state and tube technology could result in power outputs of several hundred watts by 1990. The major factor that will determine the available power output will be new developments in the basic material technology.

Power Conversion Efficiency (Fig. 4.68). Power conversion efficiency is presently very low for the sources being used to generate RF in the range of 100 to 200 GHz. Efficiencies of 1-2% are common, with a few companies reporting results as good as 10%.[1] Continued support of the key development companies in this field will likely yield efficiencies of 20% by 1990. However, an all-out effort to improve efficiency could likely increase this to 30% in the same time frame. The importance of this parameter should not be overlooked since it will dictate the power source size for any satellite application.

---

[1] Weller and Wing, op. cit.

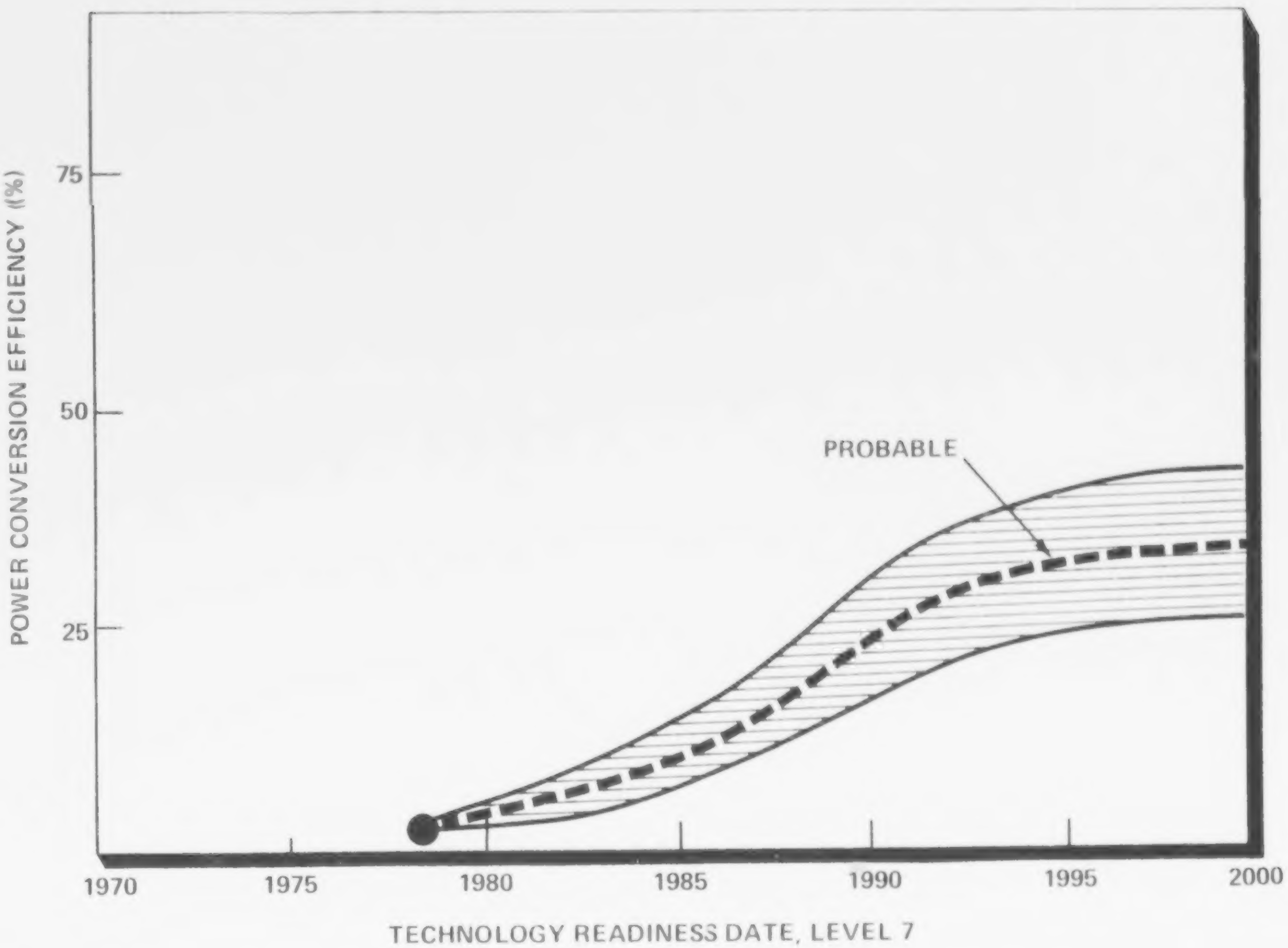

Figure 4.68. Power Conversion Efficiency in Space-to-Space Communications

blank page

5 NAVIGATION, GUIDANCE, AND CONTROL

W. G. Gevarter, NASA Headquarters

5.1 GYROSCOPE

Gyroscopes are used to determine or maintain attitude or attitude rate in space applications for experiment or spacecraft pointing, control, or navigation applications. Major characteristics of interest are drift rate and reliability as characterized by lifetime.

Two major types of gyros of current interest are the spun mass gyro, which uses the resistance to rotation of its angular momentum vector as a reference, and gyros which use the change in the path length due to rotation of a light beam as it transverses a closed path. The latter may be implemented directly by using a fiber optics coil and measuring the difference in phase of a light beam split to circulate in opposite directions around the coil, or may be implemented as changes in the laser resonance frequency of a closed path in a laser gyro.

Spun mass gyros have been in use for over 50 years and are asymtotically approaching the limits of their capability due to refinements (Fig. 5.1). Laser gyros are newly entering use as a result of DoD support and have considerable room for improvement. Fiber optics gyros are still in the research stage, but appear to have considerable potential and long expected lifetimes due to lack of moving parts. These trends are shown in Figs. 5.1 and 5.2.

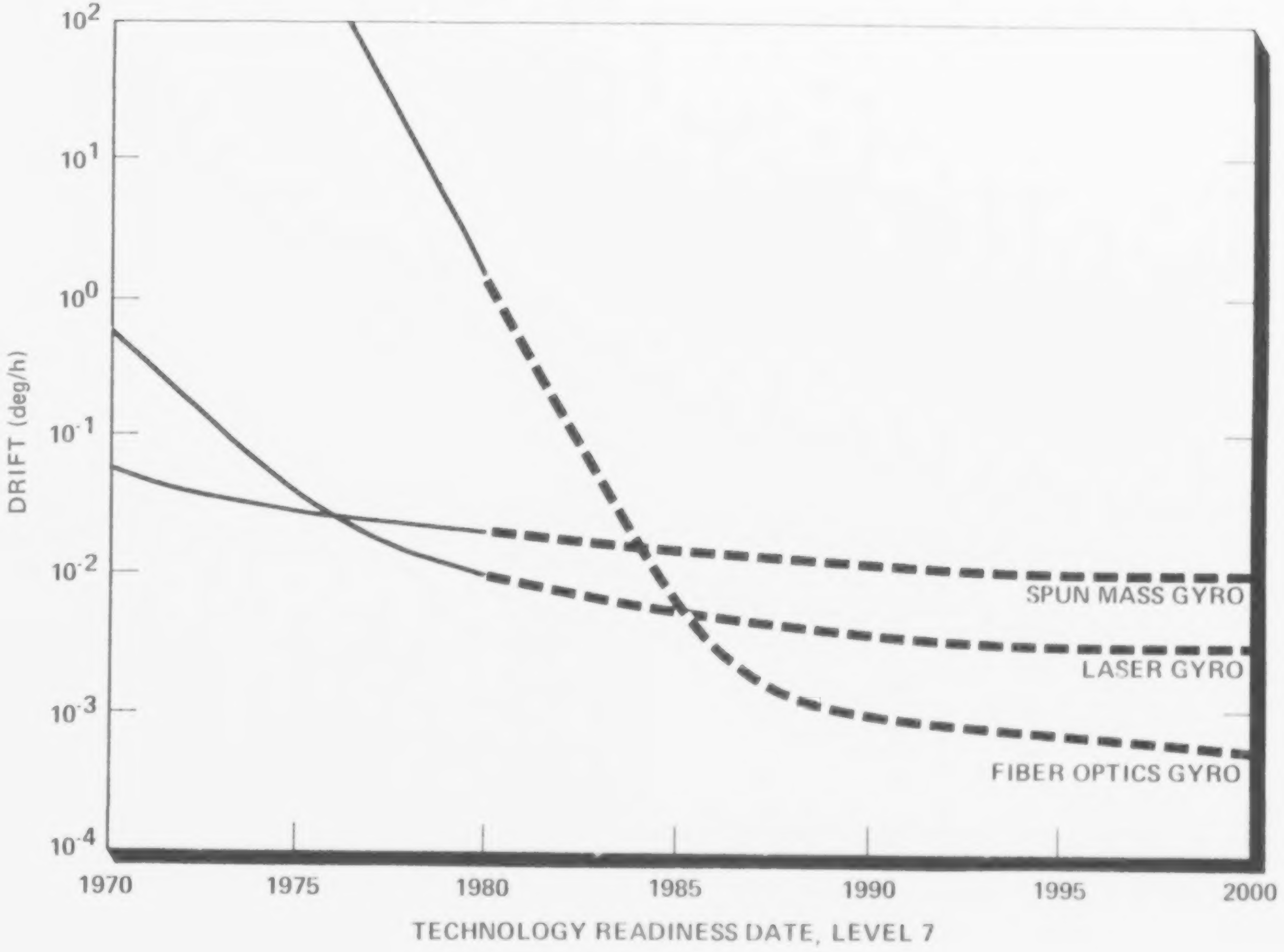

Figure 5.1. Gyro Drift

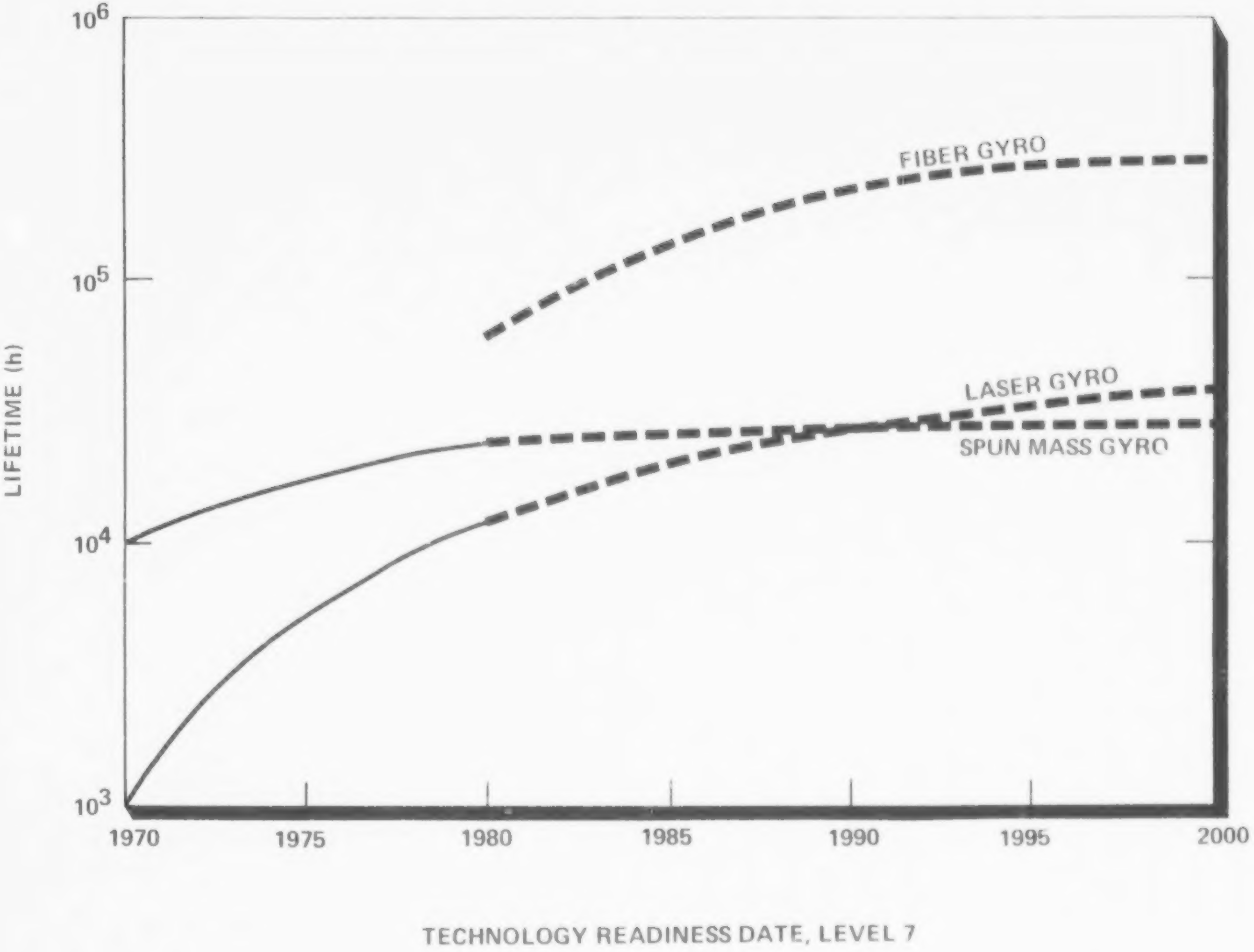

Figure 5.2. Gyro Lifetime

5.2 STAR TRACKERS

Star trackers are utilized to determine inertial attitude for printing or for navigation in space. The angular discrimination and therefore pointing accuracy is a function of the field of view (FOV), which in turn is a function of the optics. The FOV is chosen so that the star desired will reside in the initial FOV or can be easily found by using a search strategy. The accuracy can thus be specified as a fraction of the FOV.

Star trackers have traditionally used image dissection tubes as the sensing element. However, due to their nonlinearities and other problems with tube devices, newer star trackers are opting for solid-state sensors such as charge transfer devices (CTD). NASA has produced a solid-state CCD star tracker (STELLAR) which, though tested successfully in the atmosphere, has not been qualified for space. NASA is currently following the DoD effort to produce a space-qualified solid-state tracker.

Figure 5.3 presents trends for conventional and solid-state star trackers.

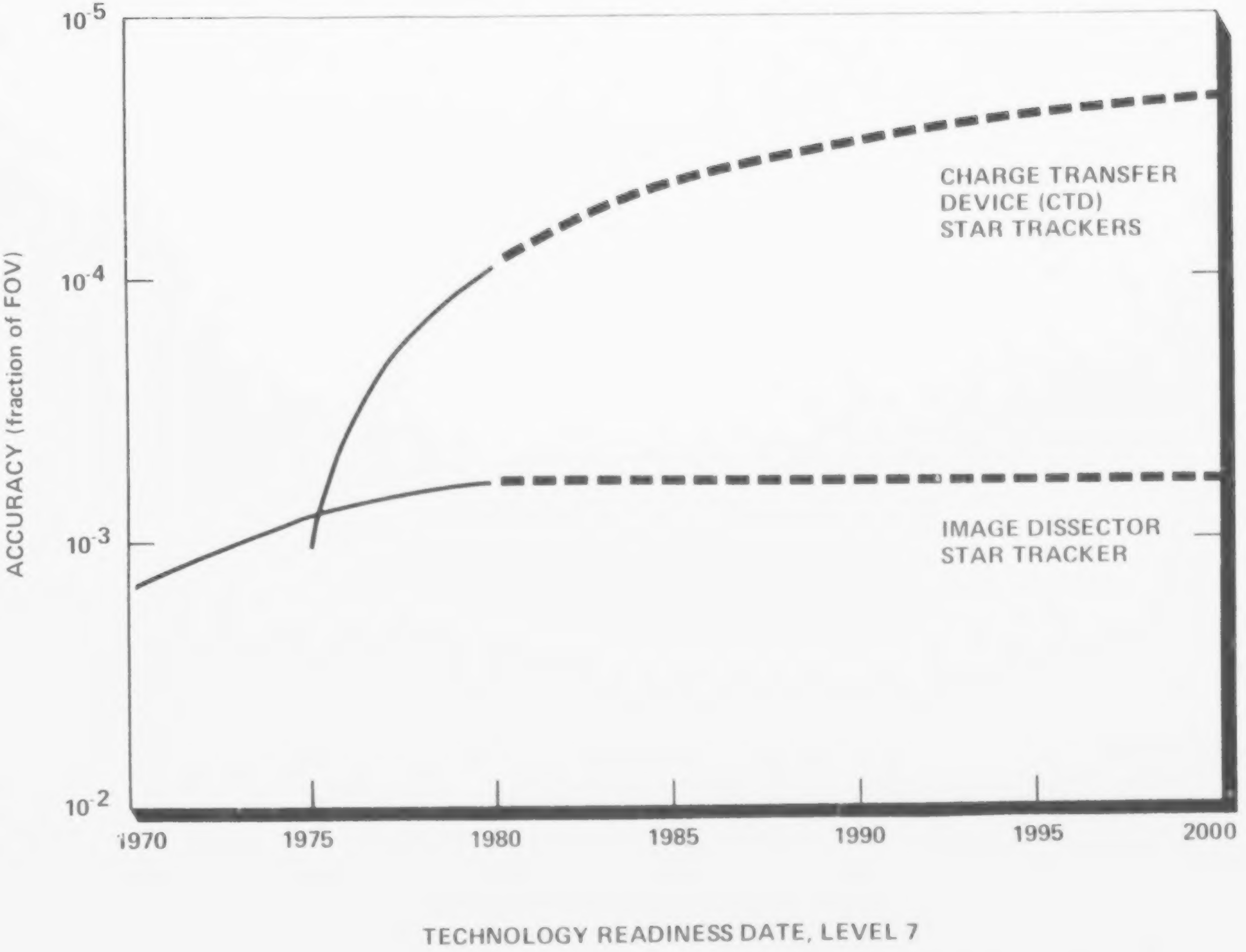

Figure 5.3. Star Tracker Pointing Accuracy

5.3 HORIZON SENSORS

Horizon sensors are used to determine the local vertical to a planetary body by scanning the limb. The resultant vertical is used primarily for attitude determination. An appropriate measure is the angular accuracy of determination of the local vertical as a function of spacecraft altitude.

Horizon sensors have been in use for two decades and in general are quite reliable. Problems arise when the signal is distorted by glint, stray particles, or sun or moon inputs, though proper filtering should alleviate this problem in the future.

The accuracy of these sensors is limited by the natural imperfection of the limb of the planetary body and by atmospheric distortion, so that only minor improvements in accuracy of these devices can be expected in the future. This trend is reflected in Fig. 5.4, which shows angular error as a function of altitude and year.

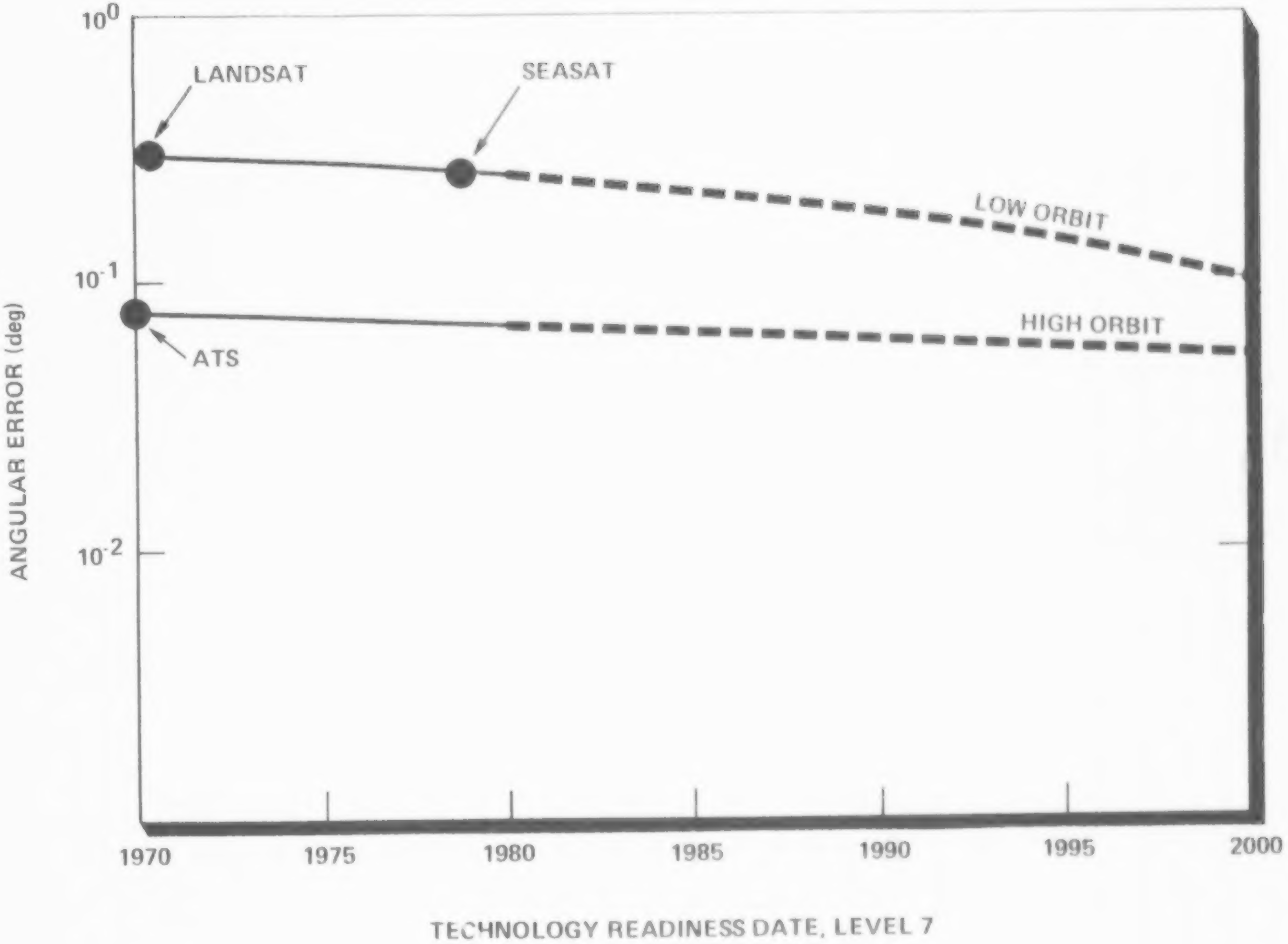

Figure 5.4. Horizon Sensor Angular Error

5.4 INSTRUMENT POINTING ACCURACY AND STABILITY

For many years sounding rockets and planetary spacecraft have utilized systems to point their experiments at desired targets. Traditionally, these have used ball-bearing gimbals and accuracy has been limited by bearings, the control system, and the reference system. The accuracy is specified in terms of angular error from the desired pointing direction and the pointing stability (the maximum excursions about the nominal pointing direction).

Spacecraft experiment pointing systems have been relatively small and simple and in general open-loop controlled rather than target referenced. NASA has been pursuing a ball-bearing two-axis pointing system (precision pointing and tracking system, PPTS) that can incorporate a correlation tracker for tracking features on planetary surfaces. NASA is also developing annular suspension and pointing system (ASPS) for pointing Shuttle-attached experiments. This latter system consists of a ball-bearing two-axis coarse system and a vernier three-axis magnetically suspended fine system. This latter system has the potential capability for fractional arc-second pointing and stability even in the presence of minor Shuttle disturbances. It is anticipated that performance beyond this will be referenced to the experiment sensor and probably will employ image motion compensation (IMC) internal to the experiment.

Figures 5.5 and 5.6 indicate the 3σ instrument pointing accuracies and stabilities anticipated for the future without IMC.

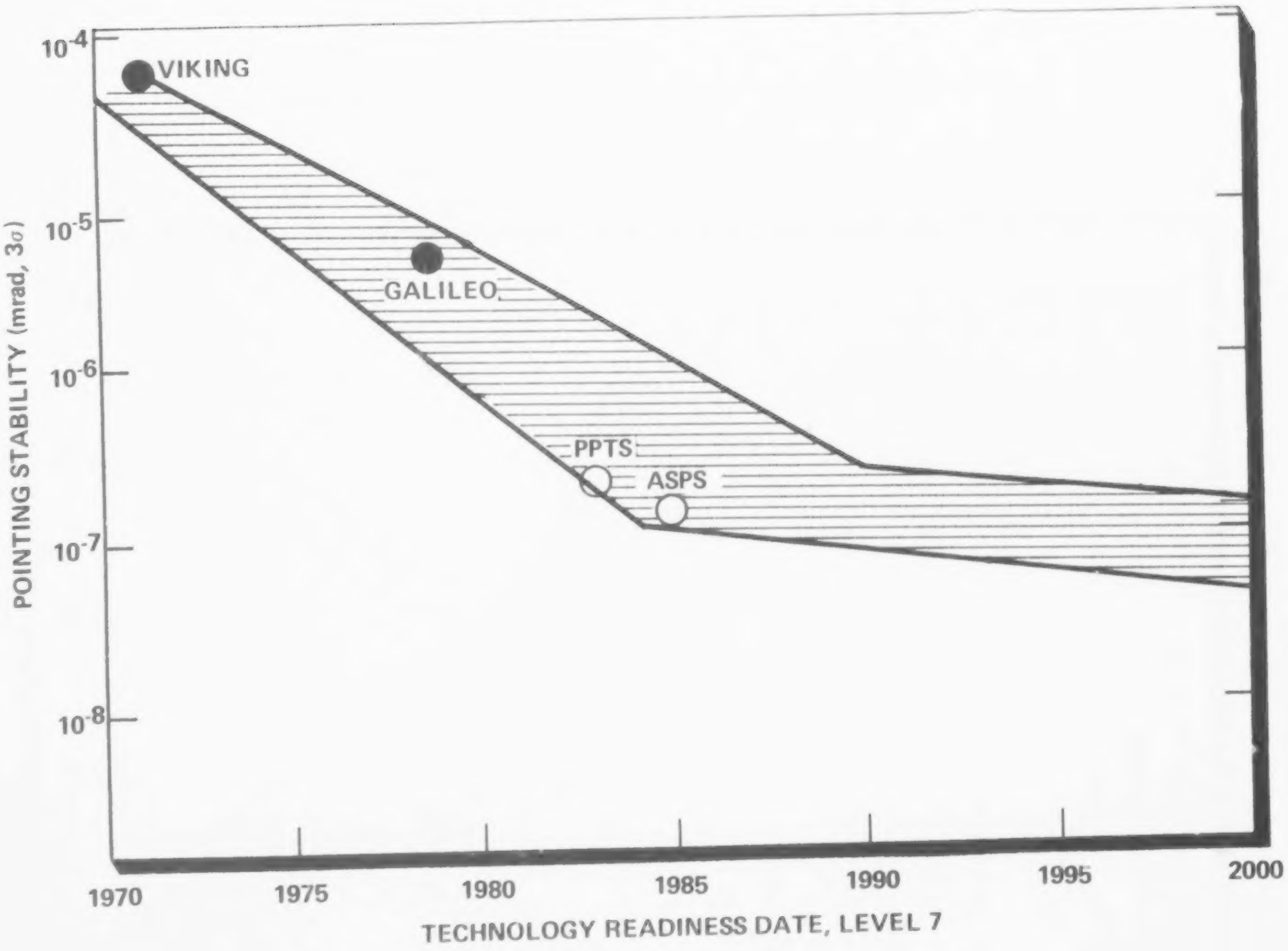

Figure 5.5. Instrument Pointing Stability

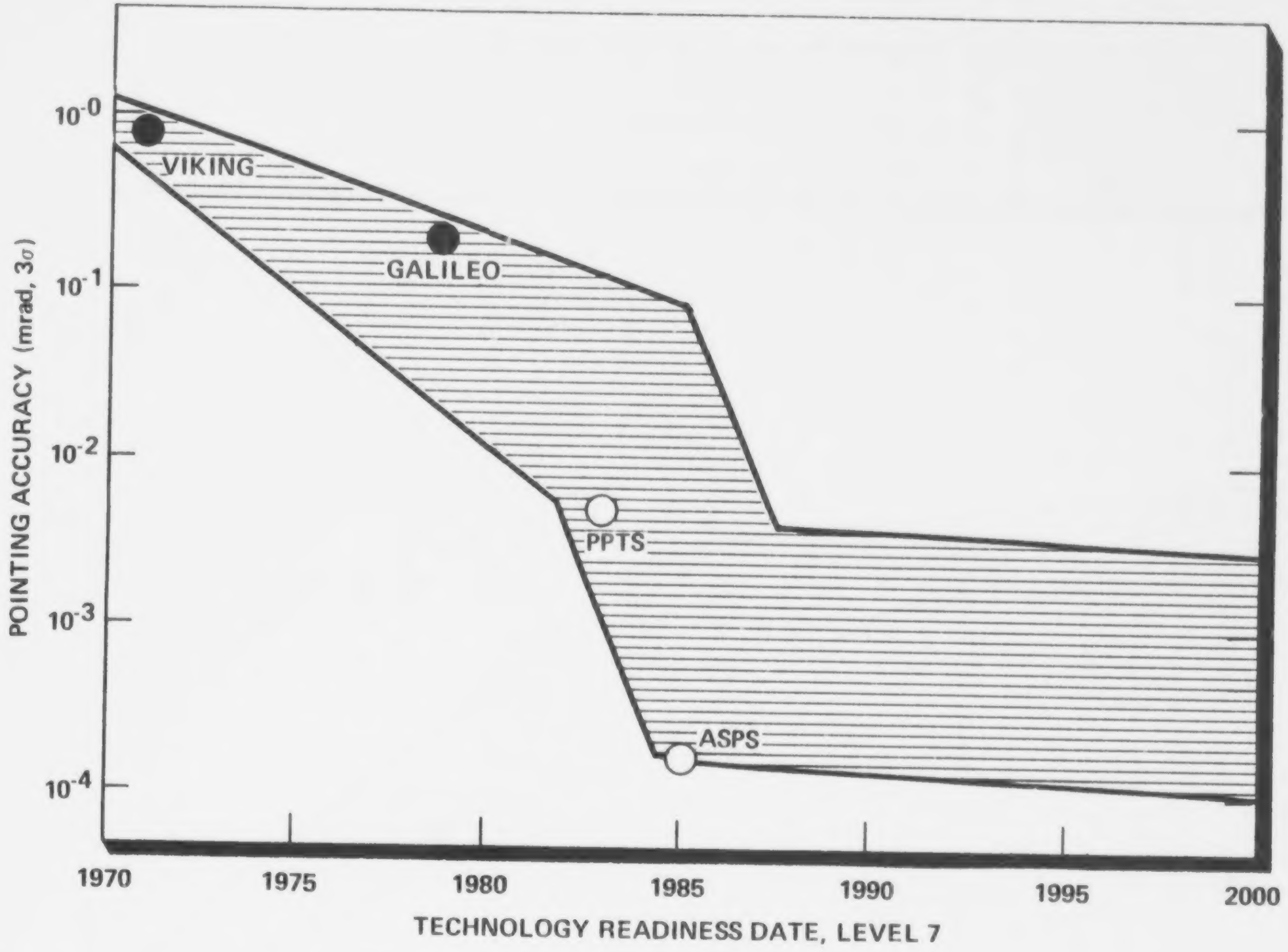

Figure 5.6. Instrument Pointing Control Accuracy (Stellar Referenced)

5.5 ON-BOARD ESTIMATION

Because of noise in the system and inadequate information, it is usually not possible to accurately determine the complete state of a complex system from observations or measurements at one time. Instead, filtering and predictive devices are used such as Kalman Filter to estimate the state or other characteristics of the systems based upon observations over a period of time.

This estimation has become an important part of spacecraft navigation, attitude determination, and other aspects of spacecraft state determination. It is expected in the future that estimations will also be used to determine the state of large flexible space systems.

Figure 5.7 shows the trends of on-board estimator capability over time with state estimation having in the order of 50 variables being possible by the 1990s.

best copy available

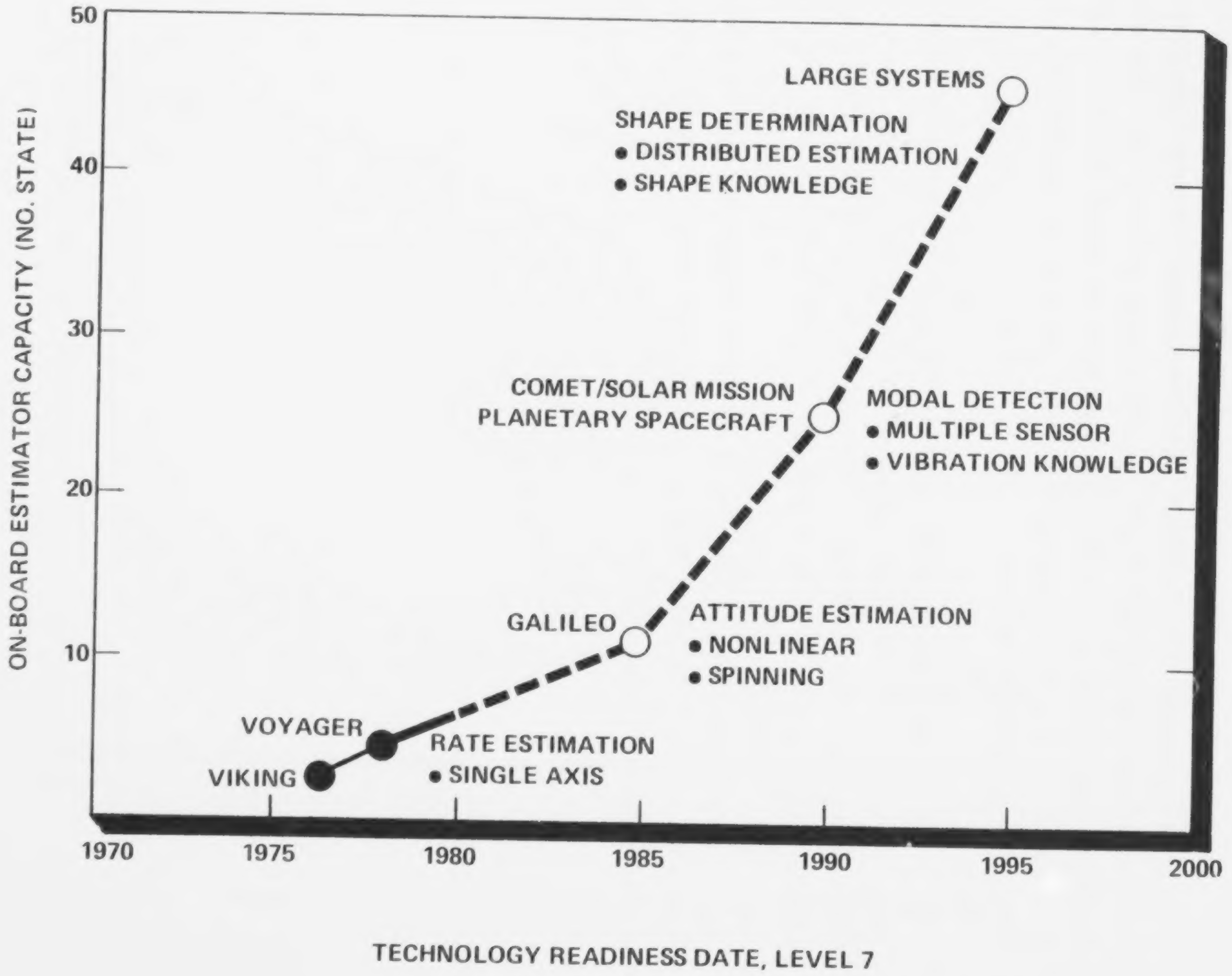

Figure 5.7. On-Board Estimator Capacity

6 AUTOMATED OPERATIONS

6.1 ON-BOARD AUTOMATION

To provide new capability, be able to perform in real time, and relieve ground support requirements and associated costs, on-board spacecraft automation is expected to rapidly increase. This can be characterized by the number of on-board processors, their speed, and the associated core memory present.

Though on-board computer capability has lagged considerably behind that of ground computers, because of space qualification requirements, this lag should be substantially reduced with the advent of routine Shuttle flights that can provide easy access to space for new computer hardware testing and qualification purposes.

Figures 6.1 to 6.4 provide a forecast of number of on-board processors, their speed, and memory that can be expected on future spacecraft--with Galileo being used as a reference. This increased capability will be a function of advances in computation and future automation requirements.

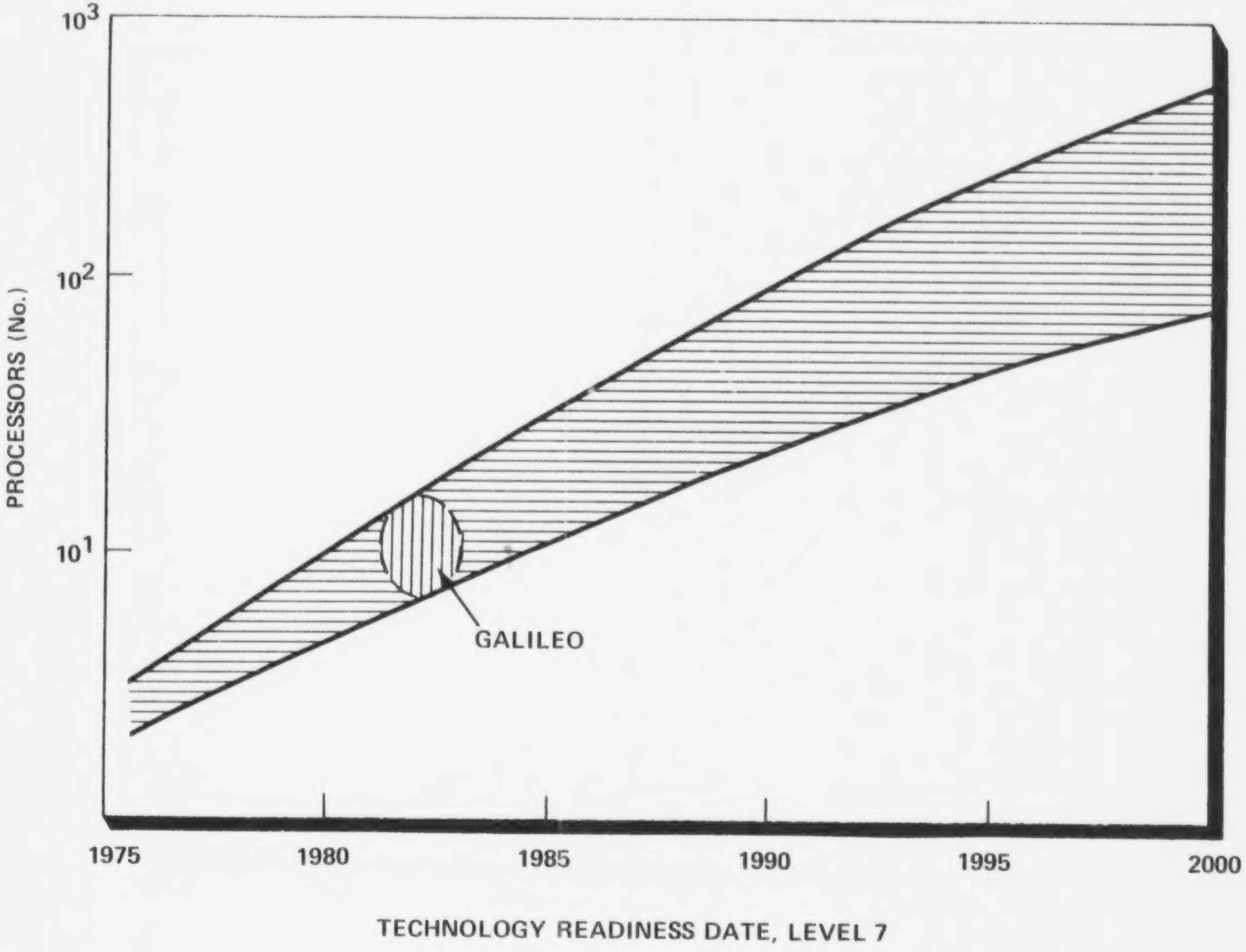

Figure 6.1. Number of Processors On-Board Spacecraft

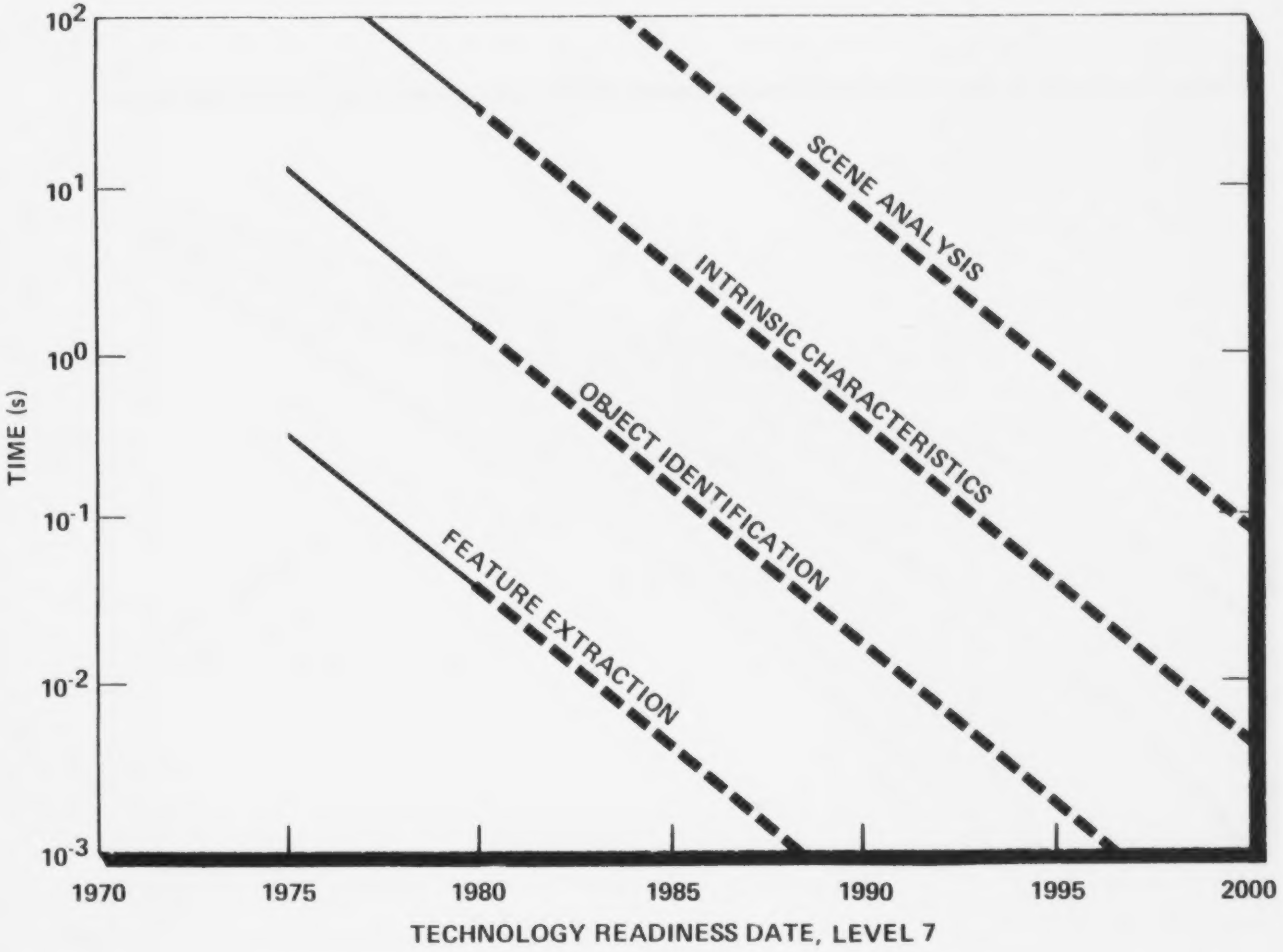

Figure 6.2. Image Processing Speed for 400 x 400 Pixels

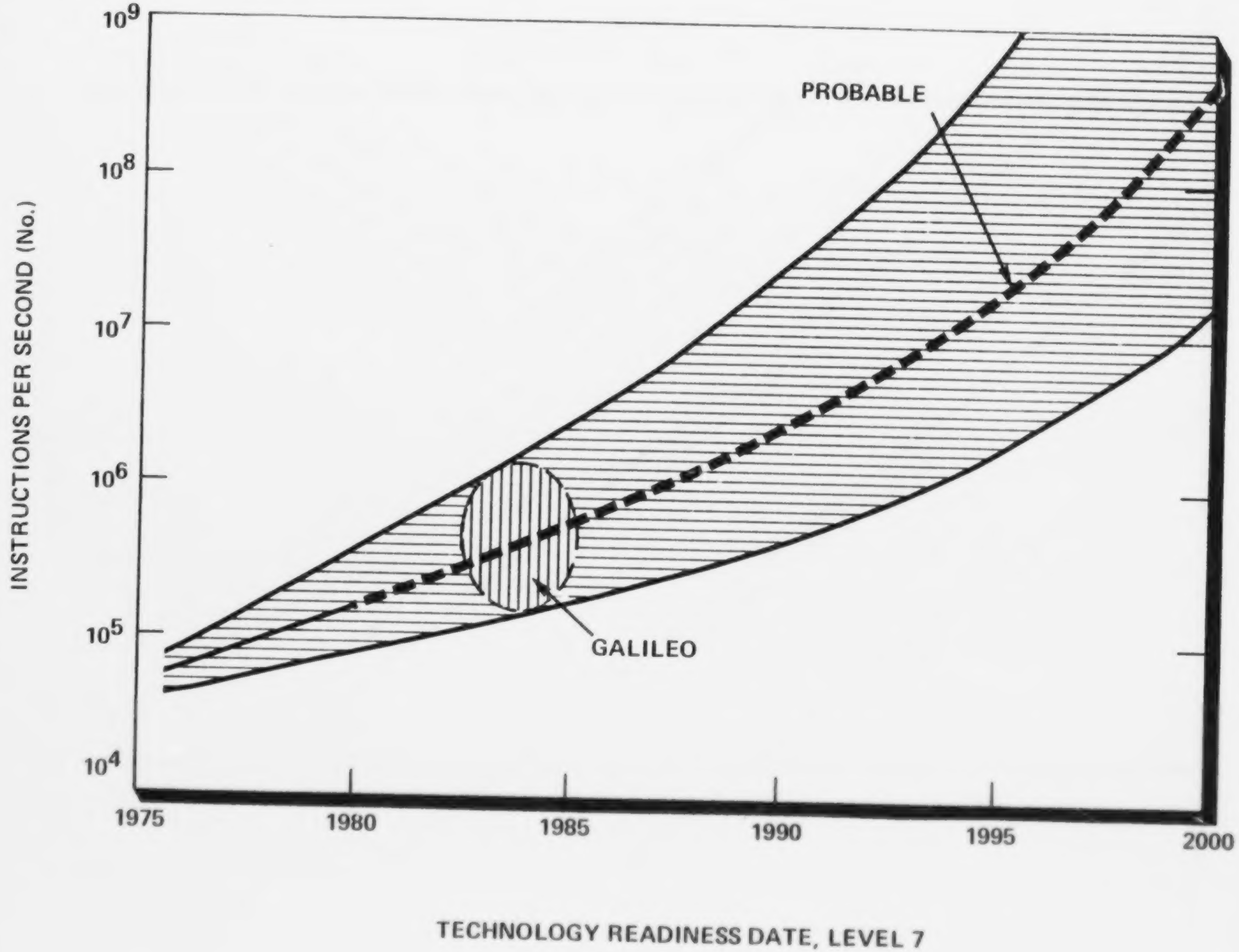

Figure 6.3. On-Board Processor Speed of Operation

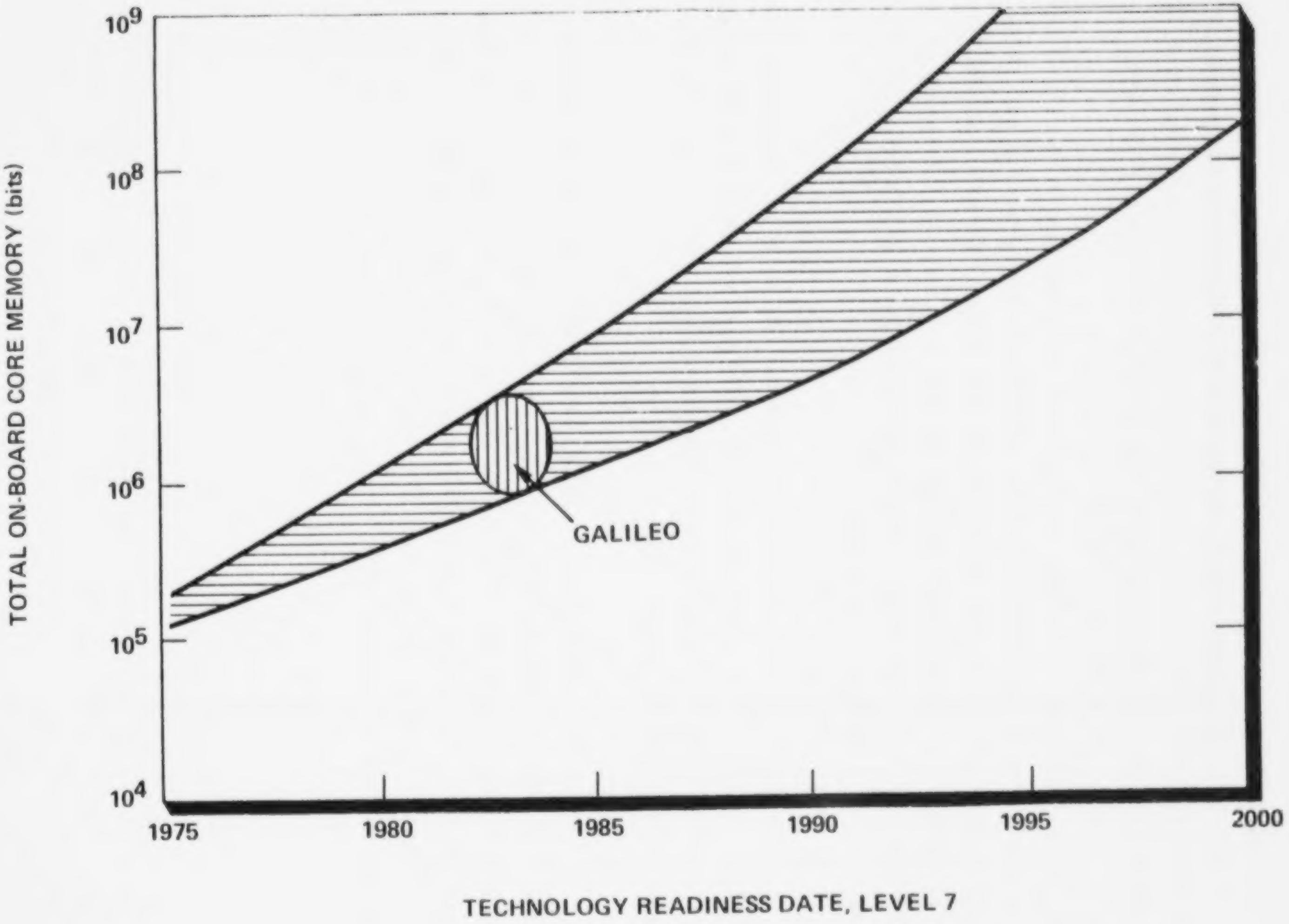

Figure 6.4. Total On-Board Core Memory

6.2 AUTOMATED PROBLEM SOLVING

Increasingly, computer programs are being relied upon to aid in solving problems of a nature previously solved by humans. Contributions to this area come from the disciplines of artificial intelligence, operations research, and control theory. One rough way to characterize the complexity of the problems is by the number of variables involved.

At present, real-time solutions of problems are primarily limited to control where the problem has a relatively fixed structure. Planning and scheduling fall into the areas of operations research and artificial intelligence. Intelligent systems to assist human decision-making tends to fall into the artificial intelligence area and are currently under development, rather than operational.

DoD and NSF have provided the primary funding in these more advanced areas. NASA is now trying to harvest this technology and build an integrated automation program to fit NASA needs, but that is well coordinated with other federal agencies.

Figure 6.5 provides an indication of future trends in automated decision making showing that solution times are dropping, so that relatively complex problems may be solvable in near real time within the next decade. This improvement is based upon not only expected increases in computer capability but expected advances in problem-solving theory and data base structure.

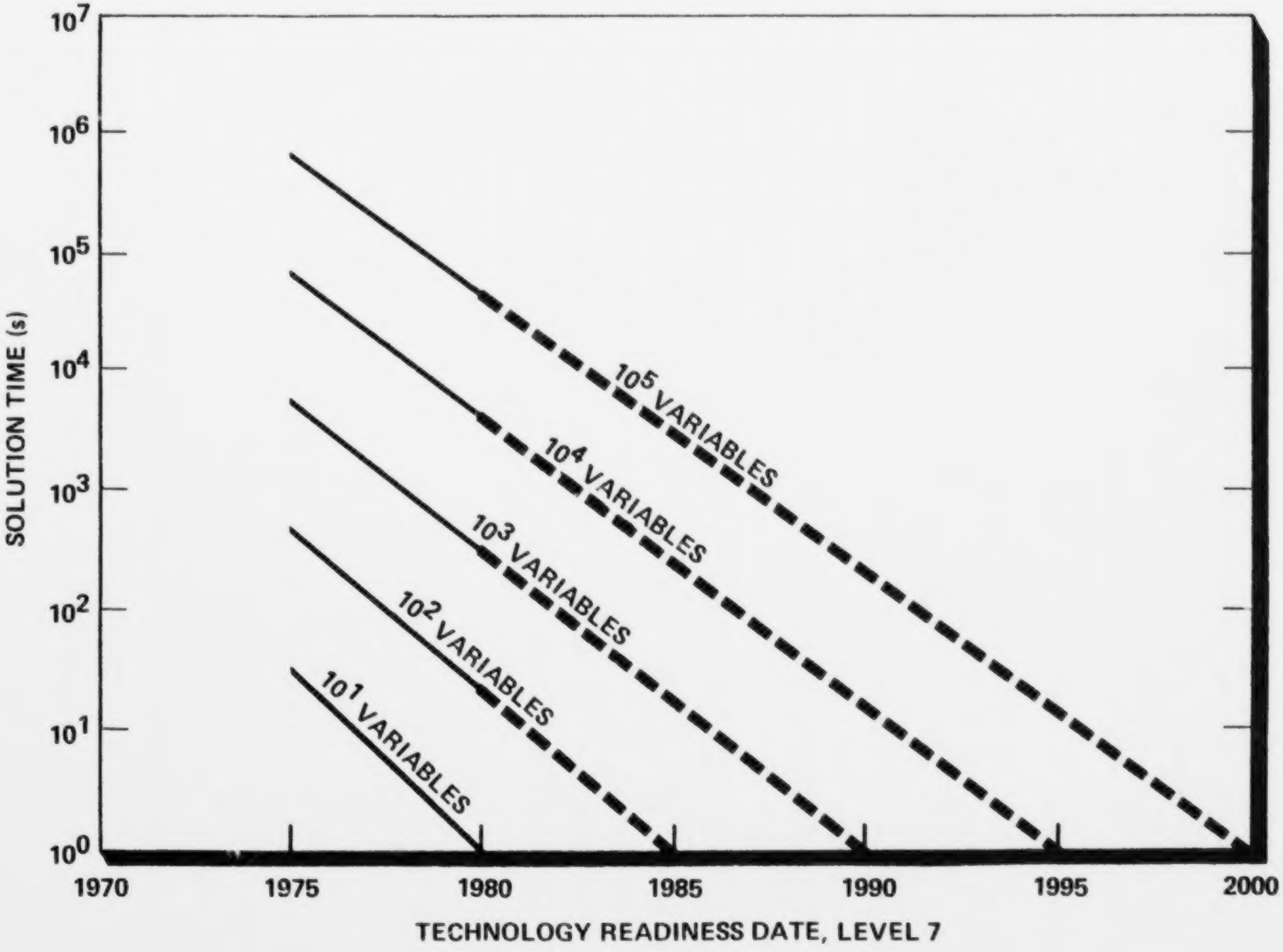

Figure 6.5. Problem Complexity vs. Solution Time

6.3 MACHINE VISION

Machine vision is becoming increasingly important in manufacturing, robotics, and machine intelligence. Areas of interest include feature extraction, object identification, and scene interpretation. To aid in scene interpretation, determination of the intrinsic characteristics of the objects in the scene such as object location, surface orientiation, texture, and reflectivity are very useful.

Machine vision is important to image interpretation, surface exploration, and navigation in space. At the present time, humans are far superior to machines in visual object identification and scene interpretation. The methods and rules that human beings automatically use for doing this are now being explored by DoD, NSF, and NASA so that programs can be generated to duplicate these approaches on a computer to complement the human approaches currently in vogue.

Figure 6.2 presents the trend in time requirements for processing to do the various machine vision tasks. The time required for these tasks are expected to rapidly decline as shown due to advances in computers, system architecture, special-purpose hardware and firmware, and advances in machine vision concepts and algorithms.

ACKNOWLEDGMENT OF CONTRIBUTORS

The contents of Volumes I, II, and III were developed with the cooperation of several offices in NASA Headquarters: OAST (Office of Aeronautics and Space Technology), OSTA (Office of Space and Terrestrial Applications), OSS (Office of Space Sciences), OSTS (Office of Space Transportation Systems), and OSTDS (Office of Space Tracking and Data Systems). NASA field Centers contributed in response to direction provided by the NASA Headquarters offices.

OAST was responsible for Volume II and Volume III, Parts B and C. OAST provided guidance and administrative support for the compilation of Volume I and Volume III, Part A. Most of this data was provided by the other offices.

General Research, under contract to OAST, assembled the many system and program contributions, prepared system and program descriptions, where contributions were lacking, extracted the summaries from the whole, and prepared the final manuscript. Mr. Terry Reese led the GRC effort.

Science Applications Incorporated assembled the system and program descriptions for the Office of Space Sciences and prepared the associated parts of the manuscript. Dr. William Wells led the SAI effort.

Planning Research Corporation reduced the voting data required to complete Volume III, Part B.

Many individuals contributed to the creation of the Model in its present form. A significant number are acknowledged on the following page, not to imply their universal agreement, but to give credit and to identify individuals familar with at least parts of the Model. OAST/RS hopes that the product adequately reflects their efforts and will promote the efficient and deliberate accomplishment of their high goals.

NASA HQ

A. Timothy
T. Chappelle
J. Rosendhal
S. Morgan
D. Herman
M. Helton
A. Diaz
G. Newton
M. Sander
J. Disher
M. Savage
W. Kisko
M. Nolan
E. Brazill
S. Keller
W. Piotrowski
G. Essenwein
J. McElroy
J. Carruthers
F. Wulff
W. Schneider
R. Stephens
H. Fosque
D. Serice
D. Williams
G. Deutsch
R. Riebling
W. Olstad
S. Tilford
S. Wilson
W. Townsend
W. Whitley
B. Tarner
L. Edwards
L. Thompson
E. Gabris
B. Rubin
L. Holcomb
R. Carlisle
J. Lundholm
F. Stephenson
W. Brainard
J. Winblade
W. Gevarter
H. Rediess
C. Schwenk
P. Compton
W. Hudson
J. Mullin
F. Povinelli
L. Randolph
M. Sokoloski
R. Gualdoni
R. Kennedy
J. DiBattista
G. Knouse
S. Fordyce
D. Dement
J. Murphy
H. Mannheimer
T. Fichetti
M. Calabrese
R. Diller
A. Cervenka
D. Broome
R. Seals
R. Schiffer
W. Bishop
E. Prior
R. Arnold
J. Dodge
J. Lehman
I. Rasool
R. Aller
T. McGunigal
J. Heuser
H. Roseman
P. Goozh
P. Eaton
J. Salmanson
F. Schmidt
B. Lam
J. Wild
M. McDonald
L. Fero
W. Smith
R. Johnson
M. Kitchens
R. Freitag
E. James
I. Bekey
T. Hagler
B. Schardt
R. McCullar
F. Kochendorfer
R. Mills
M. Stull
D. Lilly
J. Molinder
P. Cerreta
E. Whiting
D. Schultz
L. Harris
J. Harrington
J. Mahon
R. Sheridan
J. Von Puttkamer
C. Lee

JPL

W. Hasbach
I. Stein
J. Mondt
J. Laundenslager
J. Wellman
J. Waters
D. Lord
R. Zenore
R. M. Jones
A. Gupta
F. Anderson
T. Auslander
B. Morrison
R. Richter
F. Vote
L. Friedman
C. Ruoff
H. Frank
L. Rudolph
R. Nixon
L. McGlinchley
C. Elachi
A. Goetz
L. Simmons
D. Flower
R. Manzies
J. Hunter
K. Atkins
D. Pivirotto
J. French
R. Wallace
R. Boain
J. Burke
C. Uphoff
P. Roberts
H. Aumann
R. Preston
P. Swanson
H. Norris
J. Randolph

GSFC

R. Hartenstein
J. Sos
R. Pinamonti
T. Anderson
A. McCulloch
J. Mather
S. Paddack
D. Kniffen
T. Stecher
E. Boldt
J. Ormes
P. Burr
G. Hogan
T. Buckler
G. Ousley
J. Longanecker
B. Hibbard
R. Benson
D. Suddeth

MSFC

C. Jones
G. von Tiesenhausen
R. Decher
M. Page
W. Fowlis
F. Speer
E. Field
S. Willis
R. Potter
M. Weisskopf
M. Nein
J. Warner
L. Richards
R. Chappell
J. Dabbs

LeRC

J. Fordyce
J. Dayton
R. Alexovich
S. Gorland

LaRC

C. Swift
R. Hess
C. Eldred
J. Johnson
J. Harris
P. Lebel

ARC

C. McCreight
J. Murphy
F. Whitteborn

JSC

R. Williams
K. Krishen

General Research Corporation

T. Reese
C. Gartrell
T. Zakrzewski
M. Hord
N. Sprinkel
W. Davis
M. Tollin
C. Chrisp
F. Kabat
W. Hill
D. Moran
G. Choma
M. Farrelly
A. Johnson

Science Applications, Inc.

W. Wells
J. Niehoff
L. Graff

Planning Research Corporation

R. Shepperson